Tesis de Doctorado en Ciencias Biológicas
PEDECIBA Biología - Neurociencias
Universidad de la República

Activación glial y precursores de mastocitos asociados a la neuroinflamación en la Esclerosis Lateral Amiotrófica

Estudiante: Lic. Mariángeles Kovacs
Orientador: Dr. Luis Barbeito
Co-orientador: Dr. Emiliano Trias

Comité evaluador:
Dra. Natalia Lago
Dra. Silvia Olivera
Dr. Pablo Oppezzo

Agradecimientos

Gracias a todos los que estuvieron presentes durante estos años…

…en primer lugar a mis turores, a Luis y a Emi.

…a mis compañeros del Laboratorio de Neurodegeneración, Vale, Sofi, Cata, Ceci y Lucas.

…a Silvia Olivera, Natalia Lago y Pablo Oppezzo por acompañarme en su rol de CAS durante estos años y por aceptar corregir este trabajo como integrantes del comité evaluador.

…a los integrantes de los otros laboratorios que de alguna u otra manera participaron del día a día, en especial a los integrantes de la Unidad de Biotecnología en Animales Transgénicos, de la Unidad de Bioimagenología Avanzada, y la Unidad de Biología Celular.

…finalmente y en especial, a Flo, a mi familia y a mis amigos, por su apoyo incondicional, siempre.

¡Gracias!

Índice

Publicaciones y manuscritos durante el proyecto de Doctorado

Publicaciones que hacen al proyecto de la tesis:

1. **Kovacs M**, Alamón C., *et al*, Barbeito, L, Trias, E. The pathogenic role of c-Kit+ mast cells in the spinal motor neuron-vascular niche in ALS**.** Acta Neuropathologica Communications, 2021**.** DOI: 10.1186/s40478-021-01241-3.

2. Trias E, **Kovacs M**, King PH, Ying S, Kwon Y, Varela V, Ibarburu S, *et al*, Barbeito L. Schwann cells orchestrate peripheral nerve inflammation through the expression of CSF1, IL-34 and SCF in amyotrophic lateral sclerosis. GLIA, 2019. DOI: doi: 10.1002/glia.23768

3. **Kovacs M**, Trias E, Varela V, Ibarburu S, *et al*, Barbeito L. CD34 Identifies a Subset of Proliferating Microglial Cells Associated with Degenerating Motor Neurons in ALS. International journal of molecular sciences (IJMS), 2019. DOI: https://doi.org/10.3390/ijms20163880.

Publicaciones de co-autoría:

1. Ibarburu S, **Kovacs M**, Varela V, *et al* Barbeito L , Trias, E. A Nitroalkene Benzoic Acid Derivative Targets Reactive Microglia and Prolongs Survival in an Inherited Model of ALS via NF-κB Inhibition. Neurotherapeutics, 2020. DOI: 10.1007/s13311-020-00953-z

2. Alamón C, Davila B, García, (…) **Kovacs M**, Trias, E, Barbeito L, *et al*. Sunitinib-Containing Carborane Pharmacophore with the Ability to Inhibit Tyrosine Kinases Receptors FLT3, KIT and PDGFR-β, Exhibits Powerful In Vivo Anti-Glioblastoma Activity. Cancers, 2020. DOI: https://doi.org/10.3390/cancers12113423

3. Couto M, Alamón C, García MF, **Kovacs M**, Trias E, et al. Cells, 2020. Closo-Carboranyl- and Metallacarboranyl [1,2,3] triazolyl-Decorated Lapatinib-Scaffold for Cancer Therapy Combining Tyrosine Kinase Inhibition and Boron Neutron Capture Therapy. DOI: https://doi.org/10.3390/cells9061408

4. Trias E, Beilby PR, **Kovacs M**, Ibarburu S, Varela, V, *et al*, Barbeito L. Emergence of Microglia Bearing Senescence Markers During Paralysis Progression in a Rat Model of Inherited ALS. Frontiers in Neuroscience, 2019. DOI: https://doi.org/10.3389/fnagi.2019.00042

5. Trias E, King PH, Si Y, Kwon Y, Varela V, Ibarburu S, **Kovacs M**, *et al*, Barbeito L. Mast cells and neutrophils mediate peripheral motor pathway degeneration in ALS. Journal of Clinical Investigation Insight, 2018. DOI: https://doi.org/10.1172/jci.insight.123249

Resumen

Las enfermedades neurodegenerativas constituyen uno de los grupos de enfermedades de mayor relevancia en la sociedad moderna. En primer lugar, por su impacto socioeconómico debido a su creciente prevalencia, lo cual puede ser explicado por el aumento de la expectativa de vida de la población. En segundo lugar, son enfermedades que a pesar de décadas de investigación biomédica, no cuentan con estrategias terapéuticas efectivas para su tratamiento. Un informe de la OMS/OPS en 2020, estima que a nivel mundial se acumulan 35 millones de personas con Enfermedad de Alzheimer (EA), 23 millones con Enfermedad de Parkinson y 2 millones con Esclerosis Múltiple. En Uruguay se estimó en 2010 que existían 54.000 pacientes con EA, cifra que se proyecta a 77.000 personas en el año 2030 y a 112.000 personas en el 2050, lo que implicará un incremento del 107%.

La principal característica de las enfermedades neurodegenerativas es la muerte selectiva de neuronas y la pérdida de sinapsis, lo que se acompaña típicamente de neuroinflamación crónica, caracterizada por la activación de células gliales y por la infiltración de células del sistema inmune, incluyendo linfocitos, monocitos y mastocitos. Estas células se organizan alrededor de las neuronas en degeneración, constituyendo un microambiente celular neurodegenerativo que contribuye a acelerar la progresión lesional. Nuestro grupo de investigación ha contribuido a la comprensión de los mecanismos moleculares y celulares que subyacen a la progresión de la Esclerosis Lateral Amiotrófica (ELA), una enfermedad neurodegenerativa paradigmática que afecta a las motoneuronas superiores e inferiores y produce axonopatía periférica y parálisis muscular.

El objetivo general de este proyecto de doctorado fue estudiar con mayor profundidad cómo se constituye el microambiente celular neuroinflamatorio en la ELA. Focalizamos la investigación en la emergencia de fenotipos gliales aberrantes y de precursores hematopoyéticos tanto de microglia como de mastocitos a lo largo de la vía motora. En la médula espinal degenerante de pacientes con ELA y de un modelo animal $SOD1^{G93A}$, analizamos la posible emergencia de precursores hematopoyéticos $CD34^{+}$ y c-Kit^{+}, los que luego de infiltrar el Sistema Nervioso Central (SNC) podrían diferenciarse en células macrofágicas o microglías, así como también en mastocitos. También nos propusimos estudiar los efectos del fármaco masitinib, un inhibidor de receptores de tirosina quinasa como c-Kit y CSF-1R, cuyo mecanismo de acción en la ELA podría estar asociado a la modulación de células gliales e inmunitarias.

En la **Publicación 1** de la Tesis logramos identificar una subpoblación, hasta ahora desconocida, de precursores microgliales que expresan el receptor CD34 tanto en la médula espinal post-mortem de pacientes, como en el modelo murino de ELA que expresa la mutación $hSOD1^{G93A}$. El receptor CD34 se expresa comunmente en precursores hematopoyéticos, sugiriendo la infiltración de estos precursores al microambiente celular degenerativo en la ELA. Se demostró que las células $CD34^{+}$ proliferan activamente y forman "*clusters*" en las cercanías de las motoneuronas en degeneración en la médula espinal. Además, por primera vez, las células $CD34^{+}$ fueron aisladas en la fase no-adherente de

cultivos celulares primarios de la médula espinal sintomática, dando lugar a microglías diferenciadas en la fase adherente luego de sucesivos pasajes. Este hallazgo sostiene el concepto de que células inmaduras o precursores provenientes de la periferia, son capaces de infiltrar el SNC en la ELA, adoptando luego un fenotipo diferenciado regulado por factores locales. Este estudio fue publicado en 2019 bajo el título *"CD34 Identifies a Subset of Proliferating Microglial Cells Associated with Degenerating Motor Neurons in ALS"* en la revista *International Journal of Molecular Sciences* (1).

En las **Publicaciones 2 y 3** nos propusimos desafiar la hipótesis de que precursores de mastocitos derivados de precursores $CD34^+$/c-Kit^+ podían infiltrar las vías motoras en degeneración, tanto a nivel central como periférico, orquestando así la inflamación crónica. Existen muy pocos datos en la literatura sobre el papel patogénico de los mastocitos en neurodegeneración y particularmente en la ELA. Los mastocitos son células poco numerosas en los tejidos pero tienen un enorme potencial proinflamatorio, de forma que podrían orquestar la cronicidad de la neuroinflamación y alterar la integridad de la barrera-hemato encefálica (BHE) en la ELA. Nuestros resultados en tejido post-mortem de pacientes, así como también en modelos animales de ELA, muestran que los precursores de mastocitos c-Kit^+ y mastocitos diferenciados infiltran las vías motoras del Sistema Nervioso Periférico (SNP). Pudimos identificar mecanismos quimiotácticos y de diferenciación de mastocitos que implican a la expresión de factores tróficos como *Stem Cell Factor* (SCF), que es el ligando del receptor c-Kit, en las células de Schwann denervadas y macrófagos. De la misma forma, demostramos que en la médula espinal en la ELA se acumulan precursores de mastocitos c-Kit^+ asociados a alteraciones microvasculares de la BHE y motoneuronas espinales afectadas. Por primera vez, pudimos aislar estos precursores de mastocitos c-Kit^+ en cultivo y demostrar su diferenciación en mastocitos maduros *ex vivo*. También mostramos la asociación espacial entre precursores de mastocitos con astrocitos reactivos que expresan SCF, aportando un mecanismo novedoso que explica la quimiotaxis y diferenciación de los precursores de mastocitos en la médula espinal de la ELA. Finalmente, mostramos evidencia de que los mastocitos de la médula espinal pueden ser un blanco terapéutico de masitinib, un fármaco en estado avanzado de desarrollo en la ELA. Este estudio sostiene el concepto de que los mastocitos son células inmunes que contribuyen a la neuroinflamación y remodelación tisular en la ELA, y fueron publicados bajo los títulos "*Schwann cells orchestrate peripheral nerve inflammation through the expression of CSF1, IL-34, and SCF in amyotrophic lateral sclerosis*" en la revista GLIA (Trías *et al*, 2020) y *"The pathogenic role of c-Kit^+ mast cells in the spinal motor neuron-vascular niche in ALS"* en la revista *Acta Neuropathologica Communications* (2).

En conclusión, nuestro trabajo de tesis ha permitido avanzar significativamente en la comprensión de la neuroinflamación en la ELA, tanto a nivel del SNC como del SNP, permitiendo identificar nuevos tipos celulares de origen hematopoyético y con un claro potencial patogénico en la ELA, además de ser blancos terapéuticos de novedosos fármacos.

Abstract

Neurodegenerative diseases are one of the most important groups of diseases in modern society. First, there is a strong socioeconomic impact associated to them due to its increasing prevalence, which can be explained by the population's life expectancy increase. Secondly, despite decades of biomedical research, no effective therapeutic strategies exist to treat neurodegenerative diseases. A WHO/PAHO report in 2020 estimates that there are 35 million people worldwide with Alzheimer's disease (AD), 23 million with Parkinson's disease, and 2 million with Multiple Sclerosis. In Uruguay, it was estimated that in 2010, that there were 54,000 patients with AD, a number that is projected to reach 77,000 people by the year 2030 and 112,000 people by 2050, which implies a 107% increase.

The main pathological characteristic of neurodegenerative diseases is the selective loss of neurons and synapses, which is typically accompanied by chronic neuroinflammation, characterized by the activation of glial cells, as well as the infiltration of immune system cells, including lymphocytes, monocytes, and mast cells. These cells are organized surrounding degenerating neurons, constituting a neurodegenerative cellular microenvironment, which contributes to accelerating disease progression. Our research group has contributed to the understanding of the molecular and cellular mechanisms underlying the progression of Amyotrophic Lateral Sclerosis (ALS), a paradigmatic neurodegenerative disease that affects upper and lower motor neurons and produces peripheral axonopathy and muscle paralysis.

The general aim of this doctoral thesis was to study in greater depth how the neuroinflammatory cellular microenvironment is constituted in ALS. We have focused our research on the emergence of aberrant glial phenotypes and hematopoietic precursors of both microglia and mast cells along the motor pathway. In the degenerating spinal cord of patients with ALS and in a $SOD1^{G93A}$ animal model, we analyzed the emergence of $CD34^{+}$ and c-Kit^{+} hematopoietic precursors, which after infiltrating the Central Nervous System (CNS) could differentiate into phagocytic cells or microglia, as well as into mast cells. We also set out to study the effects of a drug, masitinib, a receptor tyrosine kinase inhibitor targeting c-Kit and CSF-1R, whose mechanism of action in ALS could be associated with the modulation of glial and immune cells.

In the **first publication** of this thesis, we identified a yet unknown population of microglial precursors that express the CD34 receptor, both in the postmortem spinal cord of patients and in the mouse model of ALS that expresses the $hSOD1^{G93A}$ mutation. The CD34 receptor is commonly expressed in hematopoietic precursors, suggesting the infiltration of these precursors into the degenerative ALS cellular microenvironment. $CD34^{+}$ cells were shown to actively proliferate and form clusters in the surroundings of degenerating motoneurons in the spinal cord. Furthermore, for the first time, $CD34^{+}$ cells were isolated in the non-adherent phase of primary cell cultures obtained from the symptomatic spinal cord, giving rise to differentiated microglia in the adherent phase after successive passages. This finding

supports the concept that immature cells or precursors from the periphery can infiltrate the CNS are capable of infiltrating the CNS in ALS and later adopt a differentiated phenotype as regulated by local factors. This study was published in 2019 under the title “CD34 Identifies a Subset of Proliferating Microglial Cells Associated with Degenerating Motor Neurons in ALS” in the International Journal of Molecular Sciences (Kovacs *et al.,* 2019).

During the **second, and third publications**, we set out to challenge the hypothesis that mast cell precursors derived from $CD34^+$/c-Kit^+ precursors could infiltrate degenerating motor pathways, both in the CNS and Peripheral Nervous System (PNS), thereby orchestrating chronic inflammation. There are very little data in the literature on the pathogenic role of mast cells in neurodegeneration and particularly in ALS. Mast cells occur in low numbers in the tissues but have enormous pro-inflammatory potential, so they could orchestrate the chronicity of neuroinflammation and alter the integrity of the blood-brain barrier (BBB) in ALS. Our results in postmortem tissue from patients and animal models of ALS showed that c-Kit^+ mast cell precursors and differentiated mast cells infiltrate the motor pathways of the PNS. We were able to identify chemotactic and mast cell differentiation mechanisms, which involve the expression of trophic factors such as Stem Cell Factor (SCF), the c-Kit ligand, in denervated Schwann cells and macrophages. In the same way, we demonstrated that in the spinal cord in ALS, c-Kit^+ mast cell precursors accumulate in association with microvascular alterations of the BBB and affected spinal motoneurons. For the first time, we were able to isolate these c-Kit^+ mast cell precursors in cell culture and demonstrate their differentiation into mature mast cells *ex vivo*. We were also able to show the spatial association between mast cell precursors with reactive astrocytes expressing SCF, providing a potential mechanism explaining the chemotaxis and differentiation of mast cell precursors in the ALS spinal cord. Finally, we show evidence that spinal cord mast cells may be therapeutic targets of masitinib, a drug in advanced development in ALS. This study supports the concept that mast cells are immune cells that contribute to neuroinflammation and tissue remodeling in ALS and was published under the titles "Schwann cells orchestrate peripheral nerve inflammation through the expression of CSF1, IL-34, and SCF in amyotrophic lateral sclerosis" in the journal GLIA (Trías *et al*, 2020) and "The pathogenic role of c- Kit^+ mast cells in the spinal motor neuron-vascular niche in ALS” in the journal Acta Neuropathologica Communications (Kovacs *et al*, 2021).

In conclusion, our thesis work has made it possible to make significant progress in the understanding of neuroinflammation in ALS, both at the CNS and PNS, making it possible to identify new cell types of hematopoietic origin and with clear pathogenic potential in ALS, making them potential therapeutic targets of novel drugs.

Introducción

En las sociedades modernas la esperanza de vida aumenta anualmente a nivel global, pero también lo hacen la incidencia y la prevalencia de las enfermedades neurodegenerativas asociadas al envejecimiento, adquiriendo un carácter "epidémico" (3). La prevalencia se sitúa entre 1,5 y 2,5 % en la población general, pudiendo elevarse hasta el 50% en personas mayores de 85 años. Las enfermedades neurodegenerativas conforman un grupo de enfermedades caracterizadas por la degeneración y la muerte selectiva de poblaciones neuronales, llevando a un deterioro funcional progresivo de las diferentes funciones neurológicas, con síntomas que varían dependiendo de las regiones del sistema nervioso afectadas (4,5). La Enfermedad de Alzheimer (EA), la Enfermedad de Parkinson, la Esclerosis Lateral Amiotrófica (ELA) y la Enfermedad de Huntington son las enfermedades neurodegenerativas más comunes, pero también se conocen muchas otras de menor prevalencia. La Esclerosis Múltiple tiene un componente degenerativo crónico y algunos autores la incluyen como degenerativa (6). En la mayoría de los casos, las enfermedades neurodegenerativas son progresivas y el deterioro puede resultar en condiciones inhabilitantes, con pérdida de autonomía y muerte prematura (7), con un impacto socioeconómico muy significativo. Estas enfermedades se caracterizan por ser crónicas y de progresión ineluctable. Pese a décadas de investigación biomédica, aún no existen tratamientos efectivos que logren prevenir, enlentecer de manera significativa o detener la progresión de estas enfermedades (8). Por estas razones, desde hace décadas se realizan enormes esfuerzos de investigación médica y en neurociencia para comprender los mecanismos patogénicos que subyacen a la neurodegeneración, con el objetivo final de identificar nuevas formas de prevención o tratamiento.

Durante mucho tiempo, el foco de estudio se puso casi exclusivamente en las poblaciones neuronales que degeneran en estas enfermedades, sin considerar el ambiente celular que las rodea. Sin embargo, en los últimos 20 años comenzó a comprenderse que la neurodegeneración involucra otros tipos celulares que interactúan con las neuronas, así como otras poblaciones celulares del sistema inmune. Estos tipos celulares, que hoy se conoce que participan activamente de los procesos de neurodegeneración, conforman el microambiente celular neurodegenerativo. Este microambiente está constituido principalmente por células gliales que adquieren fenotipos activados y por células provenientes del sistema inmune. En este contexto, se acepta que la neuroinflamación crónica es un mecanismo patogénico determinante que subyace a todas las enfermedades neurodegenerativas (9,10). Se puede definir a la neuroinflamación como el conjunto de respuestas celulares que se desencadena en el Sistema Nervioso Central (SNC) frente a estímulos nocivos, como traumas, infecciones, envejecimiento o en condiciones neurodegenerativas (11). La neuroinflamación involucra la activación de células gliales, principalmente astrocitos y microglías, que interactúan tanto con células provenientes del sistema inmune (monocitos, neutrófilos, linfocitos, mastocitos, etc.) como con elementos microvasculares (9,12–14). La activación inflamatoria lleva a la liberación de diversos mediadores que subyacen a la inflamación, incluyendo citoquinas, quimioquinas, factores tróficos, prostaglandinas y eicosanoides, óxido nítrico, etc. A su vez, estos tienen el

potencial de producir profundos cambios fenotípicos y transcripcionales en el entorno celular, en la actividad neuronal y sináptica, así como en la unidad neurovascular. En condiciones de neurodegeneración, la neuroinflamación se vuelve crónica y constituye un mecanismo patogénico auto-perpetuado que lleva a la degeneración y muerte neuronal (12–17). De esta manera, la patología neuronal y sináptica, así como la neuroinflamación crónica, son los principales constituyentes de lo que se ha denominado el microambiente celular neurodegenerativo (15).

Nuestro grupo de investigación ha realizado aportes significativos a la descripción de los mecanismos patogénicos que subyacen a la progresión de la ELA (18–21). La ELA es una enfermedad neurodegenerativa paradigmática, que se caracteriza por la degeneración y pérdida selectiva de motoneuronas, tanto superiores, localizadas en la corteza cerebral, como inferiores, localizadas en el tronco cerebral y la médula espinal (22,23). Durante las últimas dos décadas, nuestro grupo ha profundizado en el estudio del microambiente celular neurodegenerativo que se orquesta durante la progresión de la ELA, con foco en astrocitos y microglías activadas o aberrantes, las cuales adquieren un fenotipo inflamatorio, proliferativo y neurotóxico (15,24,25). Más recientemente, nuestro grupo ha realizado aportes significativos sobre el papel de la inflamación a lo largo de la vía motora periférica. Se estudió la relación entre la infiltración de células del sistema inmune, asociada a los axones motores en degeneración, y las células de Schwann denervadas (con sus componentes mielínicos en degeneración) durante la progresión de la enfermedad (26–28). Sin embargo, poco se conocía sobre los mecanismos por los cuales un daño primario de las motoneuronas lleva a la constitución progresiva de la neuroinflamación, la proliferación celular, la aparición de células inmunes, a los defectos vasculares que caracterizan al microambiente celular degenerativo y a su efecto en la muerte de motoneuronas.

La hipótesis al comienzo del presente trabajo de tesis, era que la neuroinflamación y la neurotoxicidad asociada en la ELA estaban determinadas por la emergencia de células anormales o con fenotipo aberrante en el microambiente celular neurodegenerativo (24,25,29). Esta hipótesis involucraba a células del sistema inmune y sus precursores provenientes de la sangre, cuyo pasaje podría estar mediado por el aumento de factores quimiotácticos y de diferenciación producidos en exceso por las células gliales activadas y/o por defectos en la barrera hemato-encefálica (BHE) o barrera hemato-espinal. Esta hipótesis unificaba los mecanismos inflamatorios y sus consecuencias neurotóxicas a lo largo de la vía motora, tanto en el SNC como en el Sistema Nervioso Periférico (SNP), ya que la infiltración de células inmunes y su interacción con células neurales es una característica de la patología en la ELA (30). La microgliosis es un hallazgo patológico sistemático en las áreas afectadas del SNC en la ELA, incluso, mostrando fenotipos activados aberrantes (25). Sin embargo, era desconocido si la microglía neurotóxica aberrante tenía su origen en precursores mieloides específicos que infiltran la médula espinal a partir del torrente sanguíneo durante el proceso neurodegenerativo, o bien, si se originaba a partir de una población endógena a través de un proceso de indiferenciación y proliferación. De manera similar, al comienzo de nuestro trabajo de tesis, se mostraron evidencias de que en el SNP en la ELA, hay una sorprendente infiltración de mastocitos que interaccionan con

axones motores a lo largo de las raíces ventrales, nervios periféricos y terminales axónicas del músculo (26,27). Los mastocitos son células inmunes residentes en los tejidos periféricos, que derivan de precursores hematopoyéticos y alcanzan su diferenciación a nivel local (27). Por lo tanto, este hallazgo anticipaba la producción de mediadores quimiotácticos y de diferenciación de mastocitos, como es el caso del factor de células madre - *Stem Cell Factor (SCF)* - a partir de elementos neurales afectados en la ELA. Por otra parte, los mastocitos poseen un gran potencial inflamatorio gracias a la liberación inmediata de una variedad de mediadores inflamatorios y vasoactivos, los que podrían perpetuar la inflamación crónica. En este contexto, nos propusimos estudiar los mecanismos que subyacen a la infiltración de mastocitos en el SNC y SNP en la ELA, e identificar células neurales que expresaran SCF. El estudio de precursores sanguíneos que dan origen a células macrofágicas o mastocitos en la ELA, anticipaba el estudio de marcadores considerados específicos de estos tipos celulares, incluyendo el receptor CD34 (marcador de células hematopoyéticas inmaduras) (31,32) y el receptor c-Kit (expresado por precursores de células mieloides en la médula ósea y mastocitos) (33,34). Los mastocitos c-Kit^{+} eran los candidatos más importantes a explorar, puesto que son reconocidos por orquestar procesos inflamatorios crónicos y por activar fuertemente a las microglías (35,36). En la ELA, se había observado la presencia de estas células en la médula espinal de pacientes (37), sin embargo, su papel patogénico dentro del microambiente celular neurodegenerativo era desconocido.

Durante mis estudios de postgrado, me he enfocado en caracterizar con mayor profundidad la infiltración de células precursoras de microglías y mastocitos, así como a sus fenotipos neurotóxicos (tanto *in vivo* como *in vitro*), y su interacción con células gliales y elementos microvasculares. Los principales estudios los he realizado en la médula espinal de pacientes con ELA y de modelos animales. Observamos una subpoblación de microglías que expresa CD34 y que se acumula en las cercanías de las motoneuronas. Las mismas pueden ser aisladas a partir de un cultivo primario de ratas SOD1^{G93A} en la fase no-adherente, y dar lugar a microglías en cultivo. Por otro lado, encontramos que los mastocitos y sus precursores CD34^{+}/c-Kit^{+}, infiltran las vías motoras tanto central como periférica. A partir de los hallazgos generados durante este proyecto, también surge la pregunta de cuáles son los mecanismos celulares y moleculares que guían la infiltración de estos fenotipos celulares inflamatorios a los sitios de lesión. De esta manera, observamos que los mastocitos y sus precursores en el nervio ciático en degeneración, interactúan con células de Schwann y macrófagos SCF^{+}. A nivel central, se observó que los mastocitos y sus precursores c-Kit^{+} se acumulan en el microambiente que rodea a las motoneuronas, en estrecha relación con elementos microvasculares y astrocitos reactivos SCF^{+}. Los mastocitos y sus precursores pueden ser modulados farmacológicamente con el inhibidor de tirosina quinasa, masitinib.

En este trabajo de tesis, se compilan los 3 principales artículos en los que me he desempeñado como autora principal o he tenido una participación significativa en su desarrollo. Para brindar un marco teórico a la tesis, continúa un capítulo en donde se detallan los antecedentes que llevaron a la producción de esos trabajos. Cada artículo consta de una breve introducción y un resumen de los resultados, así como de una breve

conclusión. Para finalizar, se desarrolla un capítulo de discusión y conclusiones que busca integrar de forma crítica los resultados y conocimientos generados en las 3 publicaciones acerca del aporte realizado al campo del conocimiento.

Antecedentes

La Esclerosis Lateral Amiotrófica (ELA)

Las enfermedades neurodegenerativas están caracterizadas por la degeneración y muerte selectiva de poblaciones neuronales, llevando a un deterioro funcional progresivo de las diferentes funciones neurológicas, en donde los síntomas que se presentan son dependientes de las regiones del sistema nervioso afectadas (4,5).

La ELA, también conocida como enfermedad de Lou Gehrig en los Estados Unidos y enfermedad de la motoneurona en el Reino Unido, es una enfermedad neurodegenerativa relativamente rara, incurable e implacablemente progresiva, caracterizada por la pérdida de motoneuronas en el cerebro y en la médula espinal (22,23). La ELA comienza de manera insidiosa con síntomas motores focales, pero se propaga rápidamente afectando a la mayoría de los músculos esqueléticos, los cuales sufren la denervación de las terminales neuronales, lo que finalmente conduce a la muerte comúnmente debido a insuficiencia respiratoria (22). Aunque alrededor del 10 % de los pacientes con ELA sobreviven 10 años o más, la mayoría fallecen en aproximadamente 3 años desde el inicio de los síntomas (38). Las motoneuronas se agrupan en superiores o corticoespinales (localizadas en la corteza motora) e inferiores (localizadas en el bulbo y en la médula espinal). Las motoneuronas superiores establecen conexiones directas o indirectas con las inferiores, que posteriormente inervan los músculos esqueléticos y controlan los movimientos. La presentación clínica de la ELA en los pacientes es heterogénea, dependiendo de las motoneuronas primariamente afectadas (39). Puede presentarse con debilidad y atrofia muscular progresiva por compromiso de las motoneuronas inferiores, predominio de hiperreflexia y espasticidad, que denota afectación de las motoneuronas superiores, o bien predominio de disartria y/o disfagia con atrofia de la lengua, lo que denota una ELA bulbar por compromiso de las motoneuronas del tronco encefálico (39,40).

Aproximadamente la mitad de los pacientes con ELA tienen deterioro cognitivo y conductual, y un 13 % puede tener demencia frontotemporal (40)Actualmente, el diagnóstico de la ELA sigue estando basado en los hallazgos clínicos y la exclusión de diagnósticos diferenciales. Por este motivo, existe un retraso en el diagnóstico definitivo de aproximadamente un año, lo que puede implica para los pacientes una pérdida de tiempo vital de potencial intervención terapéutica con el objetivo de enlentecer la progresión de la enfermedad.

La incidencia de la ELA a nivel global se estima en 1,75 casos cada 100.000 personas, con diferencias discretas entre sexos y razas (41). En Uruguay, la tendencia es similar a la observada globalmente, con una incidencia de 1.42 pacientes cada 100.000 habitantes/año (42). La incidencia parece estar aumentando a nivel mundial, probablemente debido al diagnóstico más certero, pero también podría explicarse por el envejecimiento general de la población (43). Debido a su rápida progresión, la prevalencia de la ELA sigue siendo baja,

estimándose en 4-5 por cada 100.000 personas (44). Paulatinamente los distintos factores de riesgo están siendo aclarados (45,46), y algunos de los aceptados hasta la fecha incluyen edad avanzada, sexo masculino, antecedentes familiares y mutaciones genéticas. Además, varios factores ambientales podrían aumentar el riesgo de desarrollar ELA (47).

Al igual que ocurre en otras enfermedades neurodegenerativas, el tratamiento farmacológico de la ELA es muy limitado. Ningún medicamento ofrece un efecto curativo o beneficio clínico significativo para los pacientes. El Riluzol, el primer medicamento aprobado para el tratamiento de la ELA, actúa suprimiendo la activación excesiva de las motoneuronas mediante la reducción de la neurotransmisión glutamatérgica en las neuronas presinápticas (48), logrando prolongar la supervivencia de los pacientes en un promedio de 2 a 3 meses. Más recientemente fue aprobado un fármaco antioxidante, Edaravona, que ralentiza moderadamente la progresión de la enfermedad en un reducido número de pacientes en etapa temprana, diagnosticados con una ELA definitiva o probable (49). Existen otros fármacos para el tratamiento sintomático de la ELA, incluyendo relajantes musculares como baclofeno y tizanidina, anticolinérgicos para control de la sialorrea y analgésicos para el control del dolor neuropático, como la gabapentina y pregabalina (45). En general, el tratamiento de un paciente con ELA incluye muchas otras aproximaciones no- farmacológicas basadas en la atención multidisciplinaria, lo que incluye neurólogos, psicólogos, nutricionistas, fisioterapeutas, logopedas y enfermeras especializadas. Esta aproximación ha demostrado prolongar la supervivencia y mejorar la calidad de vida de los pacientes (50).

Un gran número de riesgos genéticos de la ELA han sido aclarados en las últimas décadas. Aproximadamente el 90% de los casos de la enfermedad son esporádicos (ELA esporádica), ya que carecen de antecedentes familiares, mientras que el 10% restante se conocen como familiares (ELA familiar) (51), ya que pueden ser causados por distintas mutaciones heredadas en diversos genes (45,52). Se han descrito más de 25 genes con mutaciones puntuales asociados a un aumento en la probabilidad de desarrollar ELA, siendo los más prevalentes el gen que codifica para la proteína TAR 43 de unión al ADN (TDP-43) (53,54), el gen que codifica para la proteína FUS de unión al ARN (55–57), el gen que codifica para la proteína C9Orf72 (58) y el gen que codifica para la enzima citosólica Cu/Zn superóxido dismutasa 1 (SOD1) (59). Dentro de los casos familiares de ELA, el 10-20% es causado por mutaciones en este último. Se han identificado más de 100 mutaciones en el gen que codifica para la SOD1 capaces de desencadenar la enfermedad (60–62). El desarrollo de la ELA en estos pacientes no está asociado a una pérdida de la función catalítica de la enzima, sino por el contrario, a una ganancia de función que la vuelve neurotóxica a nivel celular, promoviendo la formación de agregados proteicos, la inhibición del proteasoma, disfunción del retículo endoplásmico y las mitocondrias, entre otros mecanismos (51,63).

La identificación de estas mutaciones asociadas a la ELA hizo posible el desarrollo de modelos murinos que recapitulan varios de los fenómenos fisiopatológicos de la enfermedad en humanos, como la muerte de motoneuronas, la degeneración muscular y la neuroinflamación crónica (64–67). Durante las últimas décadas, estos modelos animales

permitieron elucidar diversos mecanismos celulares y moleculares patogénicos que subyacen a la neurodegeneración y a la progresión de la enfermedad, así como también realizar numerosos estudios preclínicos (68).

Neuroinflamación y microambiente celular neurodegenerativo

La neuroinflamación es un proceso complejo y multifactorial que implica la activación de células gliales e inmunitarias en el SNC en respuesta a una lesión, infección u otras formas de daño (13,69,70). La activación de estas células lleva a la producción y liberación de una variedad de mediadores inflamatorios, incluyendo citoquinas y quimioquinas, que pueden contribuir a la reparación y regeneración del sistema, pero también pueden impedir la capacidad del SNC para repararse a sí mismo. La neuroinflamación crónica se ha relacionado con varias afecciones neurodegenerativas, como la EA, la Enfermedad de Parkinson, la enfermedad de Huntington y la ELA (10).

Durante el proceso de neuroinflamación, el microambiente celular que rodea a las neuronas del SNC se remodela a través de varios mecanismos moleculares y celulares. Las células gliales activadas adquieren un fenotipo inflamatorio y potencialmente neurotóxico, cambiando su morfología y perfil secretorio (11,14). Numerosos tipos de células inmunes de la circulación sanguínea, o precursores mieloides, son atraídos hacia el parénquima del SNC en las áreas afectadas, lugar en donde alcanzan una diferenciación específica y contribuyen significativamente al diálogo intercelular, modificando el microambiente (69,70). Esta remodelación del microambiente celular neurodegenerativo también implica cambios en la composición de la matriz extracelular, formación de tejido cicatricial, remodelación de vasos sanguíneos y cambios en la permeabilidad de la BHE o hemato-espinal (71). Durante los últimos años, nuestro grupo ha contribuido de manera significativa a la caracterización de distintos componentes de la neuroinflamación crónica, emergiendo paulatinamente el concepto de microambiente celular neurodegenerativo en el contexto de la ELA (24,25,29). Esta concepción comparte semejanzas con el microambiente celular característico de los tumores malignos, así como también en otras enfermedades inflamatorias crónicas, como la artritis reumatoidea o incluso la obesidad, en donde el microambiente celular inflamatorio promueve el crecimiento, mantenimiento e invasividad de células tumorales, inflamatorias, productoras de matriz, etc. (72–74).

En general, es ampliamente aceptado que la muerte de motoneuronas en la ELA ocurre por mecanismos no-autónomos celulares (75), es decir, que involucran un diálogo anormal de las motoneuronas afectadas con su entorno celular. Por ejemplo, estudios recientes han mostrado que la expresión en astrocitos o microglías de proteínas mutantes causantes de la ELA, como la SOD1 mutada o TDP43, puede hacer que estas células se vuelvan tóxicas para motoneuronas en condiciones de cultivo celular (76,77). También hay evidencias en ratones que sobre-expresan formas humanas mutantes de la SOD1 ($SOD1^{G93A}$), que muestran que las microglías y los astrocitos contribuyen a la muerte de motoneuronas (24,78,79) a través de cambios funcionales, ganancia o pérdida de distintas funciones que contribuyen a la homeostasis y/o del perfil de secreción de factores tróficos e inflamatorios

(80). Otras células gliales activadas en el contexto de la ELA, como oligodendrocitos y sus precursores $NG2^+$, así como las células de Schwann, también pueden tener un rol activo en la sobrevida o muerte de motoneuronas y en el daño axonal, a través de la liberación de factores proinflamatorios, entre otras alteraciones (81,82).

Más allá del rol significativo que tiene la neuroinflamación crónica en la progresión de la ELA, la hipótesis predominante es que esta neuroinflamación es un evento secundario a un daño primario de las motoneuronas, los axones motores y el músculo esquelético en la periferia. En su intento regenerativo y reparador, la neuroinflamación va generando cambios progresivos en la constitución del microambiente celular y en las interacciones entre los distintos componentes del mismo. Cuando la remodelación tisular llega a un punto crítico, se pierde la capacidad de sostener el trofismo de las motoneuronas y sus conexiones sinápticas.

Astrocitos y astrocitosis

Los tipos celulares no-neuronales que contribuyen mayoritariamente a la neuroinflamación en el SNC son los astrocitos y las microglías. Los astrocitos son las células gliales más numerosas del SNC, poseen un alto grado de especialización y cumplen funciones claves para el correcto funcionamiento neuronal y el mantenimiento de la homeostasis (83). Los astrocitos se encuentran en contacto directo con las neuronas, formando lo que se conoce como sinapsis tripartita, le proveen soporte estructural, metabólico y trófico, además de participar activamente en la modulación de la excitabilidad neuronal y la neurotransmisión (83,84). Además, sus prolongaciones, llamadas pies terminales, están en estrecho contacto con los vasos sanguíneos y cumplen funciones importantes en el control vascular del flujo sanguíneo y de la circulación gliofática, formando una parte fundamental de la BHE y hemato-espinal (85,86). Los astrocitos son capaces de proveer soporte trófico a las motoneuronas en cultivo, produciendo y liberando una gran cantidad de factores tróficos y moléculas pequeñas (87–89). En respuesta al daño, pueden sufrir cambios significativos, tanto morfológicos como fisiológicos, por un proceso conocido como astrogliosis reactiva o astrocitosis, que se caracteriza por un aumento en la proliferación y la aparición de astrocitos “reactivos” (90). Morfológicamente, estos astrocitos se caracterizan por la prolongación de procesos cortos y gruesos, debido a una redistribución de la expresión de la proteína glial fibrilar acídica (GFAP) (91). Además, los astrocitos sufren cambios a nivel de la respiración mitocondrial y la producción de radicales libres, y son capaces de liberar factores de crecimiento, así como también una serie de citoquinas, tanto pro como anti-inflamatorias (92–94).

Durante los últimos 20 años, nuestro grupo de investigación ha realizado contribuciones significativas a la comprensión del rol de los astrocitos en la ELA, principalmente estudiando los diferentes mecanismos moleculares patogénicos a través de los cuáles estas células gliales modifican su fenotipo y se vuelven tóxicas para las motoneuronas (79,95–98). En el año 2002, Cassina y colaboradores, así como Pehar y colaboradores, demostraron que los astrocitos espinales en cultivo responden a la exposición con peroxinitrito (un compuesto

nitro-oxidativo), sufriendo una transformación fenotípica que se mantiene en el tiempo y que se caracteriza por la expresión de iNOS y por la acumulación de daño nitro-oxidativo (99). Cuando se cultivan motoneuronas embrionarias sobre estos astrocitos reactivos, se produce una muerte significativa de las mismas por apoptosis, un fenómeno que puede ser prevenido cuando se realizan los ensayos utilizando inhibidores específicos de iNOS o "*scavengers*" de superóxido y peroxinitrito (89). Estos resultados se apoyan en estudios previos donde se demostró una correlación positiva entre el estrés oxidativo mediado por el óxido nítrico y su metabolito más tóxico, el peroxinitrito, y la degeneración de las motoneuronas en la ELA (100,101). Estos trabajos fueron pioneros en demostrar que las células gliales pueden sufrir transformaciones fenotípicas duraderas en el tiempo, que convierten a estas células en tóxicas para las motoneuronas. Posteriormente, en el año 2005, Cassina, Pehar y colaboradores profundizaron en estos estudios e identificaron nuevos mecanismos patogénicos a través de los cuales las motoneuronas mueren por apoptosis en la ELA, inducida por la activación aberrante de astrocitos. Observaron que estas células gliales pueden sufrir un proceso de activación crónica cuando son expuestas al factor de crecimiento de fibroblastos 1 (FGF1) (97). Este factor es producido por las motoneuronas y liberado durante el proceso degenerativo, y actúa sobre el receptor FGF-R1 en los astrocitos, produciendo una activación glial significativa que lleva a la liberación del factor de crecimiento nervioso (NGF) y produce la muerte de las motoneuronas a través del receptor p75NTR, el cual es re-expresado por las motoneuronas durante el proceso degenerativo (97). Estos mecanismos celulares de muerte neuronal, así como otros mecanismos aportados por otros autores, evidencian que los astrocitos juegan un rol fundamental en la neurodegeneración en la ELA (98,102–104). La evidencia experimental acumulada durante las últimas dos décadas, demuestran que las células gliales, así como el ambiente que rodea a las neuronas en degeneración, juegan un papel clave, contribuyendo a los mecanismos patogénicos y a la progresión ineluctable de las enfermedades neurodegenerativas.

Células microgliales y microgliosis

La microglía es la célula efectora inmune del SNC (105). Se origina a partir de progenitores primitivos hematopoyéticos que ingresan al sistema nervioso durante el desarrollo embrionario temprano (106,107). En condiciones de reposo, son células pequeñas con finos procesos en continuo movimiento de expansión-retracción y de gran capacidad migratoria (108). Por su capacidad fagocítica, se consideran los "macrófagos" del SNC. Sin embargo, a diferencia de los macrófagos residentes de los diferentes tejidos periféricos, la microglía también participa en múltiples funciones del sistema nervioso, incluyendo la sobrevida neuronal, el control de las sinapsis y de la eficiencia sináptica, la mielinización, la integridad de la BHE, la vigilancia inmunológica, etc (109). Sin embargo, en respuesta al daño tisular (infección, trauma, irradiación, etc.), o bien frente al daño neuronal primario o condiciones de neurodegeneración (110), las microglías sufren cambios fenotípicos considerables y adquieren diversos estados de activación (108). Esta activación puede darse en respuesta a estímulos nocivos de diversos orígenes, gracias a la presencia de receptores tipo Toll (TLR), "*scavenger*" o receptores de citoquinas o quimioquinas, con el fin de contener el daño (111–

114). Tras la activación, la respuesta microglial depende de la naturaleza, magnitud y duración del estímulo. Generalmente incluye una morfología hipertrófica, con retracción parcial de sus procesos, proliferación celular y aumento de la capacidad fagocítica (115). Cuando la activación microglial se vuelve crónica, adquieren la capacidad de liberar neurotransmisores, citoquinas proinflamatorias, de las cuales destacan el factor de necrosis tumoral alfa (TNF-α), IL-6 e IL-1β, especies reactivas de oxígeno (ROS, en inglés "*reactive oxigen species*"), y sustancias excitotóxicas como el glutamato, así como citoquinas anti-inflamatorias y factores neurotróficos (109,116).

En las enfermedades neurodegenerativas, la microglía es uno de los actores principales que contribuye al establecimiento de la neuroinflamación crónica (117). En presencia de diferentes estímulos, como patógenos, restos celulares, agregados proteicos, o proteínas mal plegadas (ej. β-amiloide), la microglía responde internalizando las especies patogénicas para su degradación, así como también activando la expresión de genes de citoquinas y quimioquinas que componen procesos neuroinflamatorios (118).

Microglía en la ELA. El estado de activación de la microglía en el contexto de las enfermedades neurodegenerativas ha sido ampliamente estudiado (117). Cuando se desencadena la neurodegeneración en el SNC, ocurre la proliferación y transformación fenotípica de la microglía, adquiriendo como estadio final un fenotipo fagocítico (119). Entre el estado de reposo y este fenotipo de células fagocíticas, existe un abanico de estados activados. Estos dependen de la región y del estadio de la enfermedad, por lo tanto, dependen del ambiente en el que se encuentren. En el contexto de la ELA, la activación microglial se ha documentado, por un lado, a partir de tejidos post-mortem de pacientes e implica un aumento en la proliferación y los cambios morfológicos, así como cambios a nivel de la expresión génica y a nivel proteico en la ELA (120). Por ejemplo, se observa una regulación positiva de las moléculas de la superficie celular, como el receptor del complemento 3 (CR3), los antígenos del complejo mayor de histocompatibilidad (MHC) I y II, integrinas y reactividad a inmunoglobulinas (121). En este sentido, al igual que ocurre en otras enfermedades neurodegenerativas (122,123), en la ELA la microglía sufre cambios en la expresión génica de TREM2 y TYROBP (124). En particular, estos son eventos que ocurren tempranamente en la enfermedad y anticipan posteriores cambios en la expresión génica en las motoneuronas (124). Por otro lado, otros cambios ocurren de forma más tardía y, potencialmente, podrían ser blancos terapéuticos relevantes. A destacar, la activación de NF-κB es un evento que ocurre en la microglía en etapas tardías en la ELA (125). Las evidencias muestran que la modulación genética o farmacológica de esta vía proinflamatoria, tiene efectos beneficiosos enlenteciendo la progresión de la enfermedad (125,126).

La mayor parte del conocimiento sobre la activación de la microglía en la ELA, proviene de modelos animales en donde las microglías activadas se observan en las primeras etapas de la enfermedad y su número aumenta a medida que la misma progresa (127–133). En la ELA experimental, también se han reportado diversos estados de activación dependientes del ambiente y del estadio de la progresión de la enfermedad. Por ejemplo, en la etapa

asintomática, así como en la fase terminal de la ELA, se han descrito "*clusters*" de microglías proliferantes en estado fagocítico adyacentes a motoneuronas (134). En el año 2006, Boillée y colaboradores utilizaron un modelo transgénico de ELA (ratón hSOD1^{G37R}) para demostrar que la microglía juega un rol preponderante en el microambiente celular neurodegenerativo que rodea a las motoneuronas durante la progresión de la enfermedad. Los ratones ELA con reducción en la expresión de la proteína SOD1 mutada en la microglía, tuvieron una progresión más lenta de la enfermedad (135). Otros estudios han mostrado que las microglías activadas en la ELA promueven la muerte de las motoneuronas de manera significativa (136). En otros estudios, Beers y colaboradores demostraron que el trasplante de microglía "*wild-type*" en ratones SOD1^{G93A} logra modificar el curso de la enfermedad, disminuyendo de manera significativa la gliosis y enlenteciendo la progresión de la ELA (137). Además, se observó que la microglía que sobre-expresa la proteína SOD1 humana mutada, produce y libera ROS y factores nitro-oxidativos con actividad neurotóxica para motoneuronas (137–139). Estos experimentos sugieren que la disfunción de las microglías o la adopción de un fenotipo alterado, es potencialmente neurotóxico en el ambiente que rodea a las motoneuronas y que, por lo tanto, representa un blanco celular relevante para el desarrollo de estrategias terapéuticas.

Transformación fenotípica de microglías en "células gliales aberrantes". En 2011, Díaz-Amarilla y colaboradores (24), y posteriormente Trías y colaboradores (25), aislaron y caracterizaron una subpoblación de células gliales a las que denominaron primero "astrocitos aberrantes" y luego "células gliales aberrantes", respectivamente. Estas células tienen un fenotipo similar a astrocitos y marcadores astrocitarios, tanto en médula espinal de animales de ELA (ratas SOD1^{G93A}), como luego de su aislamiento en cultivo celular (24). Las células gliales aberrantes se caracterizan por su marcado poder neurotóxico para motoneuronas y por inducir microgliosis luego del trasplante en la médula espinal de ratas no transgénicas (24,140). En un trabajo posterior de Trías y colaboradores, la subpoblación de células gliales aberrantes fue caracterizada en profundidad y se pudo demostrar su origen a partir del linaje mieloide o microglial (25). Se considera que este fenotipo aberrante surge por una transformación fenotípica asociada a una respuesta inmunitaria descontrolada que ocurre en el entorno de las motoneuronas espinales en degeneración (25).

Contribución de precursores mieloides a la microgliosis en la ELA

Si bien las células microgliales residentes se originan a partir de progenitores primitivos generados en tejidos hematopoyéticos que ingresan al SNC durante el desarrollo embrionario temprano (141), se reconoce que, en condiciones de lesión o daño de la BHE, el SNC puede ser infiltrado por monocitos o precursores mieloides (fagocitos mononucleares), que adoptan un fenotipo macrofágico característico (142,143) y la gran mayoría de estas células son eliminadas luego de la resolución de la lesión. Sin embargo, el origen de las células que dan lugar a la microgliosis en la ELA ha sido objeto de varios estudios y, aún actualmente, la importancia patogénica de la entrada de células mieloides al SNC en el contexto de la ELA es un tema de debate (144,145).

Se han utilizado ratones $SOD1^{G93A}$ para determinar si la microgliosis observada en la ELA estaba determinada por la proliferación de microglías residentes, o bien por infiltración de monocitos, fagocitos mononucleares o precursores mieloides de origen sanguíneo (146). Los resultados permiten concluir que la expansión microglial proviene principalmente de la proliferación de células residentes y, en menor medida, del reclutamiento periférico de precursores sanguíneos (146). La mayor proporción de microglías provenientes de la periferia, presentan una localización perineuronal y perivascular, sugiriendo sitios discretos de permeabilización como consecuencia del daño que sufren las barreras durante la etapa sintomática de la enfermedad (146). En otro estudio, usando un modelo de parabiosis (unión de los sistemas circulatorios de dos animales que conduce al intercambio de sangre periférica para obtener un 50% de quimerismo) entre un ratón $SOD1^{G93A}$ y un ratón no transgénico que expresaba GFP en células de la médula ósea, se demostró que solamente un bajo número de microglías provenían del torrente sanguíneo en quimeras parabióticas (141).

Más recientemente, se ha demostrado que los monocitos circulantes pueden invadir el SNC en la ELA con potenciales efectos neuroprotectores (145). En la ELA, estas células podrían penetrar al parénquima a través de los plexos coroideos (147). Otro tipo de células mieloides que también infiltran el SNC en la ELA son las células dendríticas (148) que al presentar antígenos en su superficie a otras células del sistema inmune, se caracterizan por estimular la respuesta inmunitaria. Es interesante destacar que las células dendríticas también se acumulan alrededor de los somas de las motoneuronas (149).

CD34 y microglías. CD34 es una proteína transmembrana que pertenece a la superfamilia de las inmunoglobulinas y que es usada ampliamente como un marcador de superficie de células hematopoyéticas (150,151). También se reconoce una subpoblación de células $CD34^{+}$ en la circulación sanguínea que también son consideradas como células madre de estirpe hematopoyético (152), y que tienen el potencial de diferenciarse en varios tipos de células sanguíneas, incluyendo células mieloides (32). En ciertas condiciones patológicas, CD34 también parece expresarse en células con fenotipo microglial (153). Sin embargo, el rol que desempeñan las células $CD34^{+}$ durante la fase sintomática de la ELA permanecía desconocido al momento de comenzar este proyecto de postgrado.

Factores tróficos y quimiotácticos de microglías en la ELA. Diversos factores tróficos y quimiotácticos de microglias han sido estudiados en la ELA. Por ejemplo, la proteína quimioatrayente de monocitos-1 (MCP-1, un factor quimiotáctico para macrófagos y microglía), se encuentra aumentada en el líquido cefalorraquídeo (LCR) y en el suero de pacientes con ELA, y se expresa principalmente en células gliales (149,154). También se encontró que MCP-1 está elevado en modelos animales de ELA con una expresión predominante en células neuronales y gliales (149,155).

De interés en este trabajo de tesis, tanto el factor 1 estimulante de colonias (CSF-1) como la interleuquina-34 (IL-34), son citoquinas implicadas en la producción de células mieloides,

incluyendo macrófagos y células microgliales (156). Ambas son ligandos del receptor de CSF-1 (CSF-1R) (157), se expresan en el SNC de manera diferencial y son secretadas por neuronas y células gliales (156,158). La evidencia muestra que la administración intraperitoneal de CSF-1 a ratones con ELA, tiene un efecto detrimental para la enfermedad, acelerando la progresión al inducir un aumento en la proliferación de la microglía, la cual adopta un fenotipo fagocítico, con aumento en la expresión de citoquinas proinflamatorias como TNF-α e IL-1β (133).

Modulación farmacológica de microglías por mastitinib. CSF-1R forma parte de una familia de receptores de tirosina quinasa de clase III (159). La señalización intracelular de los receptores de tirosina quinasa de clase III y sus ligandos, contribuye en la hematopoyesis y también está implicada en el desarrollo de la inflamación en una gran variedad de enfermedades, así como también en cáncer (159). La clase III de estos receptores también incluye al receptor KIT y PDGF-Rα y PDGF-Rβ. Como mencionamos, CSF-1R es un receptor clave implicado en la quimioatracción, maduración y diferenciación de macrófagos y microglías (157). En la ELA, se demostró que la inhibición farmacológica de CSF-1R con inhibidores de receptores de tirosina quinasa en modelos murinos, produce un enlentecimiento de la progresión de la enfermedad (21,160). En particular, nuestro grupo utilizó el fármaco masitinib y observó una disminución de la microgliosis y de la neuroinflamación, así como una preservación de las motoneuronas espinales, llevando al enlentencimiento de la enfermedad (21).

Infiltración de células inmunes en el SNC en pacientes y modelos de ELA.

Linfocitos. Además de la microglía y los astrocitos, otras células participan en el proceso inflamatorio que ocurre en la ELA. En los últimos años se ha acumulado evidencia sobre la infiltración y el rol patogénico de los linfocitos T, tanto en modos murinos como en el tejido post-mortem de pacientes con ELA (128,161–165). En los pacientes con ELA, se describió la infiltración linfocítica de las clases T colaboradoras ($CD4^+$) y citotóxicas ($CD8^+$) en los tractos corticoespinales y en las astas anteriores de la médula espinal (161–163). Esta infiltración parece desempeñar un rol detrimental, ya que, por ejemplo, la eliminación selectiva de los linfocitos T $CD8^+$ en un modelo murino de ELA, previene la muerte neuronal (166). Por otra parte, algunas poblaciones de linfocitos que infiltran la médula espinal de los ratones con ELA -como los linfocitos $CD4^+$ y T reguladores (T-reg)- cumplen un rol protector, ralentizando la progresión de la enfermedad (167,168) probablemente a través de la secreción local de factores tróficos como el IGF-1, el control inhibitorio de la microgliosis y la estimulación de la expresión de transportadores de glutamato (GLT-1 y GLAST) (167). También se ha mostrado evidencia de que la cinética de infiltración de células T podría estar determinada por alteraciones en la permeabilidad de la BHE descrita en ratones con ELA (169).

Tabla 1. Células inmunes infiltrantes en la ELA. Modificado de McCombe y colaboradores, 2020 (170)

Tipo celular	Cambio observado y efecto en la ELA	Referencias
Leucocitos totales	Se observa un aumento que se correlaciona con una mayor progresión. El bloqueo de la extravasación de leucocitos genera efectos protectores.	(171)
Granulocitos/neutrófilos	Aumento de granulocitos, neutrófilos y ratio neutrófilos relativo a monocitos. Tratamiento con masitinib reduce la degeneración axonal en modelo animal.	(27,172–174)
Linfocitos T CD4	En la mayoría de los estudios se reporta un aumento con efectos protectores en modelos animales.	(174–178)
Linfocitos T CD8	T CD8 citotóxicos en modelo SOD1 promueve la muerte de motoneuronas espinales.	(166,174,175,177,179,180)
Células T Natural Killer	Aumento, y su bloqueo lleva a un aumento en la sobrevida en un modelo animal.	(179,181,182)
Células T- reg	Disminución y disfuncionales. Se observa una correlación inversa entre el número y la progresión.	(164,175,179,183,184)
Monocitos	Evidencia de activación y aumento en el ratio monocitos clásicos/no-clásicos, que se correlaciona con la progresión de la enfermedad.	(145,175,176,185–187)

Mastocitos. Los mastocitos constituyen uno de los tipos celulares con mayor potencial inflamatorio del sistema inmune. Derivan de precursores hematopoyéticos $CD34^{+}$/c-Kit^{+} que se originan en la médula ósea y migran a los diferentes tejidos periféricos, donde maduran y completan su diferenciación gracias a factores locales (188,189), principalmente

mediante la influencia del ligando de c-Kit, el factor de células madre (SCF, del inglés "*stem cell factor*"). Los progenitores de mastocitos inmaduros son liberados al sistema circulatorio para luego residir en las diferentes áreas vascularizadas del organismo, donde cumplen un rol clave en censar el ambiente y en el inicio de la respuesta inflamatoria (190,191). Estas células tienen una gran capacidad proinflamatoria debido a que poseen gránulos preformados, los cuales pueden ser inmediatamente liberados frente a determinados estímulos, en un proceso controlado llamado desgranulación (192–195). Durante este proceso, los mastocitos tienen la capacidad de liberar una gran variedad de sustancias, como histamina, heparina, TNF-α y proteasas, como la triptasa y la quimasa, entre otras. Además, generan una respuesta sostenida en el tiempo, debido a la síntesis *de novo* de mediadores lipídicos como prostaglandinas, citoquinas y quimioquinas, factores de crecimiento como NGF y VEGF, etc (196). Esta gran variedad de mediadores permite a los mastocitos participar en diversos procesos implicados en el establecimiento de la inflamación crónica, entre ellos el reclutamiento y activación de otras células del sistema inmune (35). En el SNC, actúan como centinelas y efectores, comunicando los sistemas nervioso, vascular e inmune (197–200), al ubicarse en las cercanías de la BHE, en plexos coroideos, meninges, bulbo olfatorio, mesencéfalo y en el parénquima, en el tálamo e hipotálamo (201). A través de la gran variedad de mediadores liberados por estas células, los mastocitos surgen como actores importantes en el establecimiento de la neuroinflamación crónica, a través de su comunicación con las células gliales (36,199,202), así como también, afectando activamente la integridad y permeabilidad de la BHE y hemato-espinal (203–205). Por otra parte, son capaces de liberar vesículas, trampas extracelulares y formar nanotubos (206,207) que permiten interacciones con células y estructuras cercanas, como vasos sanguíneos y fibras nerviosas (200). En otras condiciones actúan como mediadores de la respuesta inmune adaptativa, actuando como células presentadoras de antígenos y liberando sustancias quimioatrayentes que reclutan y activan linfocitos (208,209). Sin embargo, en lo que respecta a patologías del sistema nervioso, es menos lo que se conoce acerca del rol de los mastocitos y son pocas las evidencias que en los últimos años han postulado un rol activo de los mastocitos como actores preponderantes en el desarrollo de la neurodegeneración (210). Por ejemplo, se ha observado que en la Esclerosis Múltiple (EM), existe un aumento significativo en el número de mastocitos en los sitios de lesión (211). Por otro lado, una referencia que podría indicar un rol importante de estas células mediando la inflamación en el SNC, es que los pacientes con enfermedades sistémicas donde los mastocitos son clave (como la mastocitosis o la fibromialgia), se caracterizan por tener disfunciones cognitivas o depresión crónica (212,213).

Los mastocitos como "orquestadores" de la neuroinflamación. El foco principal en el componente neuroinflamatorio en las enfermedades neurodegenerativas refiere a cambios morfológicos en astrocitos y microglía. Sin embargo, en estas condiciones de inflamación crónica, poco se ha considerado a los mastocitos, independientemente del rol que estas células pueden desempeñar en el mantenimiento en el tiempo de los procesos inflamatorios (198). En este sentido, un pequeño número de mastocitos es capaz de generar cambios relevantes en su microambiente, además de participar en la comunicación celular

con las células gliales y neuronas, a través de la gran variedad de mediadores que son capaces de liberar rápidamente, estando implicados de esta manera en la neuroinflamación. No solamente participan censando y modificando el microambiente, sino que también pueden tener un efecto directo sobre el aumento en la permeabilidad de la BHE, por ejemplo, a través de la liberación de citoquinas como TNF-α e IL-6 que pueden afectar la expresión y función de las proteínas de las uniones estrechas, permitiendo la entrada de otros componentes del sistema inmune y exacerbando así el microambiente neuroinflamatorio (204). Vale destacar que el rol de las citoquinas mencionadas, así como también mediadores como la histamina, puede ser protector o detrimental, un efecto que es dependiente de la concentración y duración en la que son expresadas y liberadas (214,215).

En la EA, se ha reportado la infiltración y acumulación de mastocitos caracterizados por la expresión de triptasa rodeando las placas β- amiloides en tejido post-mortem de pacientes (216). Se ha reportado que los mastocitos podrían actuar como detectores tempranos de péptidos amiloides en esta enfermedad (217). Además, la liberación de mediadores de mastocitos como histamina y prostaglandina D2, pueden exacerbar la respuesta de los procesos inflamatorios locales, incluyendo la activación microglial (218).

Los mastocitos en la ELA. Uno de los primeros hallazgos importantes acerca del rol de los mastocitos en la patogenia de la ELA, fue el trabajo realizado por Graves y colaboradores, donde se reportó la infiltración de mastocitos en el parénquima de la médula espinal en degeneración en pacientes con ELA, acompañado también por otras células del sistema inmune, como macrófagos y linfocitos, tanto en la sustancia gris como a lo largo de los tractos corticoespinales (37). Estos mastocitos se caracterizaban por la expresión de Cox-2, triptasa, IgE e IL-4, formando "*clusters*" o de manera aislada (37). De igual manera, en trabajos posteriores realizados por Fiala y colaboradores, observaron la presencia de mastocitos que se caracterizaban por la expresión de IL-17A en la médula espinal post-mortem de pacientes con ELA, pero no en los controles (219). Otros autores evidenciaron un aumento en la concentración de IL-15 en el suero y LCR de pacientes con ELA, un mediador que participa en la quimio-atracción de mastocitos (220).

Como se mencionó anteriormente, la infiltración de mastocitos al parénquima de la médula espinal podría producirse gracias a la disrupción de la BHE durante la fase sintomática de la ELA (221–223). En este sentido, los mastocitos pueden desempeñar un rol activo afectando la integridad de las barreras, gracias a la secreción de mediadores vasoactivos pre-sintetizados (204) y factores que promueven el daño en las células endoteliales (224–226). En la ELA, los precursores circulantes de mastocitos podrían ser capaces de atravesar la BHE, posicionarse en el espacio peri-vascular, adquirir un fenotipo secretorio y liberar localmente neuropéptidos, proteasas, citoquinas e histamina, entre otros factores, potenciando los procesos inflamatorios en el microambiente celular neurodegenerativo.

Tabla 2. Mastocitos en enfermedades neurodegenerativas.

Patología	Reportes	Referencia
Enfermedad de Alzheimer	Mastocitos se acumulan rodeando placas de β-amiloide en tejido de pacientes.	(216)
	Los mastocitos se acumulan en depósitos amiloides gracias a la quimioatracción por la proteína amiloide A liberada por la glía local.	(227)
	Los péptidos amiloides son detectados por mastocitos y promueven su desgranulación de manera temprana. Los mastocitos se acumulan en hipocampo y corteza en modelos murinos.	(202,217)
	Los mastocitos liberan mediadores incluyendo histamina y prostaglandina D2, provocando la activación de la microglía local.	(218)
	El tratamiento con masitinib reduce la disfunción cognitiva en pacientes con EA moderado.	(228)
Enfermedad de Parkinson	La exposición de mastocitos derivados de médula ósea a MPP^+ promueve la liberación de MCP-1 y MMP-3.	(229,230)
	Los mastocitos son reclutados vía MCP-1 liberado por microglía y astrocitos en un modelo animal. Estos mastocitos expresan TG2 y pueden liberar mediadores proinflamatorios como histamina, leucotrienos y TNF-α	(231)

ELA	Mastocitos, expresando Cox2, triptasa, IgE e IL-4, fueron observados en pequeños "*clusters*" o de manera aislada en la médula espinal de pacientes.	(37)
	El quimioatrayente para mastocitos IL-15, se encuentra aumentado en el LCR y suero de pacientes con ELA.	(220)
	Mastocitos que expresan IL-17A se encontraron en la médula espinal de pacientes con ELA.	(219)
	Mastocitos desgranulantes asociados a macrófagos, se acumulan en las NMJs en un modelo animal y se correlacionan con denervación. El tratamiento con masitinib reduce el número de mastocitos infiltrantes.	(26)
	Los mastocitos liberan componentes vasoactivos capaces de afectar la permeabilidad e integridad de la BHE.	(204)

Factores tróficos y quimiotácticos de mastocitos en la ELA. La vía de señalización SCF/c-Kit está implicada en la migración de los precursores de mastocitos hacia los tejidos periféricos, así como también en su diferenciación en mastocitos maduros y posterior activación y desgranulación (189,232,233). En el SNC, su localización celular está restringida a neuronas y se observó su presencia en astrocitos en cultivo (234). El SCF cumple un rol importante en la migración de progenitores neurales (235) y, en condiciones de daño oxidativo, puede ser expresado de manera significativa por astrocitos (236,237). La expresión de SCF también se encuentra aumentada en varias condiciones inflamatorias, y la inhibición de la vía SCF/c-Kit llevaría a disminuir los niveles de histamina, así como también modular la infiltración y activación de mastocitos (238). Al igual que CSF-1R, c-Kit es un receptor de tirosina quinasa, y su inhibición surge como posible estrategia terapéutica novedosa para modular la neuroinflamación (239).

Por otro lado, la interleuquina-3 (IL-3) es un factor de crecimiento que promueve la diferenciación de varias células del linaje hematopoyético (240) y una de las citoquinas más importantes en la regulación del crecimiento y diferenciación de mastocitos (241,242). Esta citoquina juega un rol fundamental al exacerbar vías y procesos inflamatorios (243). El trabajo realizado por Chavany y colaboradores mostró que la sobre-expresión de IL-3 en un animal transgénico, lleva a la degeneración de motoneuronas con varias características fenotípicas similares a la ELA (244).

Tabla 3. Factores tróficos y quimiotácticos con efectos sobre mastocitos y microglias producidas por células neurales y no-neurales en el SNC y SNP. Modificado de Skaper y colaboradores, 2018 (197)**.**

		Acciones biológicas sobre:		
Factor-efector	**Factor liberado por:**	**Microglía**	**Mastocitos**	**Referencias**
C5a- C5aR	Astrocitos, microglía, mastocitos	C5aR está aumentado en la microglía activada. Liberado en condiciones neuroinflamatorias. Comunicación entre C5a y TLR-4	C5a es una fuerte señal quimioatrayente vía C5aR. Comunicación entre C5a y TLR-4	(245–248)
C3- C3R	Astrocitos	Expresan C3aR que interactúa con C3 mediando la patología β-amiloide y la neuroinflamación.		(249,250)
ATP-receptores de ATP/P2	Neuronas y células gliales	ATP estimula la liberación de IL-33 en microglía pre-activada por reconocimiento de PAMPs vía TLRs	IL-33 se une a su receptor en mastocitos e induce la liberación de IL-6, IL-13 y MCP-1 que modula la actividad microglial	(251,252)
Receptores PAR2	Mastocitos	La triptasa activa PAR2 en microglía, lo cual resulta en un aumento en la expresión del	IL-6 y TNF-α liberado por microglía regula la expresión de PAR2 en	(252–254)

		receptor P2X4 y la liberación de factores neurotróficos.	mastocitos, que promueve la activación de los mismos y la liberación de TNF-α	
CXCL12-CXCR4	Astrocitos, neuronas.	CXCL12 promueve su migración y activación. La vía se encuentra aumentada en varias condiciones neuroinflamatorias.	CXCR4 se expresa en mastocitos y actúa como receptor quimiotáctico vía su interacción con CXCL12.	(255–257)
CD40/CD40L	Mastocitos	Los astrocitos reactivos tienen aumentada la expresión de CD40. La interacción con CD40L lleva a la producción de citoquinas proinflamatorias que llevan a la desgranulacón de mastocitos.	Mastocitos activados aumentan su expresión de CD40L, que lleva a la producción de citoquinas proinflamatorias cuando interactúa con CD40	(258)
MCP1- CCR2	Microglía activada, astrocitos, monocitos infiltrantes y neuronas.	La microglía activada libera MCP-1, que recluta monocitos $CCR2^{+}$, promoviendo la neuroinflamación.	MCP-1 es un factor quimiotáctico para mastocitos.	(259,260)
IL-17A- IL-17R	Astrocitos, oligodendrocitos, mastocitos.	Actúa sinérgicamente con otras citoquinas proinflamatorias, promoviendo la activación de microglía.	Los mastocitos, así como también linfocitos Th17, producen IL-17A.	(219,261,262)
IL-15- IL-15Rs.	Astrocitos, neuronas y células gliales activadas.	Promueve la reactividad glial vía activación de NF-κB.	Es un factor quimiotáctico de mastocitos.	(263–265)

Mastocitos y defectos de la barrera hemato-encefálica y hemato-espinal. Muchos autores consideran al SNC como un sitio de inmuno-privilegio, en donde el ingreso de células inmunes periféricas está regulado por la BHE y hemato-espinal (266). Estas barreras son barreras físicas que separan el SNC de la periferia y están compuestas por células endoteliales que se mantienen unidas gracias a uniones estrechas, evitando que el parénquima sea invadido masivamente por moléculas, patógenos, células y otros elementos o sustancias potencialmente neurotóxicas. Sin embargo, durante el establecimiento y la progresión de las enfermedades neurodegenerativas, las barreras se dañan y aumentan su permeabilidad (71,221,267). Se ha reportado en pacientes con ELA la presencia de albúmina en el LCR, sugiriendo una pérdida en la integridad de la BHE (222), así como también depósito de componentes del sistema inmune como IgG y C3 en la médula espinal y en la corteza motora en tejido post-mortem de pacientes (268).

Los mastocitos se ubican estratégicamente en las cercanías de los vasos sanguíneos y tienen un potencial de modular la BHE gracias a la liberación de mediadores capaces de aumentar la permeabilidad vascular. Los mecanismos que llevan a la disrupción de la BHE involucran factores vasoactivos y componentes con capacidad de degradar elementos de la matriz, como heparina, histamina, serotonina, óxido nítrico, VEGF, así como también citoquinas como TNF-α o proteasas como triptasa (269). TNF-α induce la expresión de ICAM-1, lo que permite la entrada de leucocitos al parénquima (270). Además, algunas metaloproteasas, como MMP-2 y MMP-9, tienen la capacidad de degradar componentes de la lámina basal como colágeno IV, así como también proteínas de las uniones estrechas (271–273). Los mastocitos regulan la actividad de estas metaloproteasas y las producen (274). Por otro lado, se ha reportado que los mastocitos aportan el 50% de la histamina cerebral y varios reportes indican que la permeabilidad de la BHE está regulada, en gran parte, por la histamina cerebral (275).

Modulación farmacológica de mastocitos por masitinib. c-Kit también forma parte de la familia de receptores de tirosina quinasa de clase III (159). Como ya mencionamos, c-Kit es el receptor clave que media la migración, diferenciación, maduración e incluso la desgranulación en mastocitos, vía su interacción con SCF (233,276)**.** Masitinib es un inhibidor potente de c-Kit (277) y evidencias muestran el efecto de este fármaco previniendo la infiltración de mastocitos en diversas patologías (278,279). Por ejemplo, Georgin- Lavialle y colaboradores, reportaron los efectos de masitinib en un paciente con leucemia de mastocitos, una enfermedad rara que se caracteriza por una rápida expansión de mastocitos en la médula ósea, sangre y otros órganos, que además poseía el gen que codifica para c-Kit mutado (279). Observaron que luego de 3 meses de tratamiento, el paciente mejoraba significativamente sus síntomas y reportaron una disminución en la infiltración de mastocitos en la médula ósea (279). Particularmente en la ELA, nuestro grupo reportó la acumulación y desgranulación de mastocitos en el músculo en degeneración, observando una prevención de la patología periférica observada luego del tratamiento con masitinib (27).

Neurodegeneración e inflamación del SNP en la ELA

La ELA tiene como particularidad que la afectación de la motoneurona inferior se acompaña de una afectación del SNP, incluyendo axonopatía motora periférica y denervación de las placas motoras del músculo esquelético. La hipótesis de degeneración anterógrada en la ELA, establece que el daño primario ocurre en el soma neuronal y consecuentemente continúa hacia compartimientos periféricos (280). Sin embargo, la hipótesis de degeneración retrógrada comenzó a desafiar a la primera y muchos autores consideran a la ELA como una axonopatía distal (281,282), con un patrón de daño distal-proximal, típicamente observado en algunas neuropatías (283). Este concepto se basa en observaciones de que la degeneración axonal, la pérdida de axones periféricos y la denervación y degeneración de las uniones neuromusculares en el músculo esquelético (NMJs, del inglés "*NeuroMuscular Junctions*"), son eventos que ocurren tempranamente en la ELA, que anticipan la degeneración de los somas neuronales y el inicio de los síntomas clínicos (281,284). En 1996, Kennel y colaboradores mostraron que en los ratones $SOD1^{G93A}$ la pérdida de función en las placas motoras comienza semanas antes de que se hagan presentes los síntomas clínicos y ocurra la pérdida de motoneuronas en la médula espinal (284). Lo que sugieren estos autores, es que la pérdida de función e integridad de las NMJs en los modelos animales se condice con la degeneración retrógrada. Esto significa que sería un fenómeno de comienzo distal donde se pierde la integridad de los axones, provocando una denervación temprana de las placas motoras en los músculos esqueléticos, y no una consecuencia de la degeneración primaria de los somas neuronales centrales (284). Años más tarde, Fischer y colaboradores mostraron fuerte evidencia que sostenía el patrón de degeneración retrógrada a partir de estudios realizados en ratones $SOD1^{G93A}$ así como también en tejido post mortem de un paciente con ELA esporádica. Observaron que la axonopatía precedía a la degeneración de motoneuronas espinales y al inicio de los síntomas (281). En este estudio, también reportaron en un paciente recientemente diagnosticado con ELA, que falleció tempranamente por otras causas, la presencia de denervación y reinervación de las placas motoras en el músculo pero sin afectación de los somas de las motoneuronas espinales, lo que sugiere un comienzo distal de la enfermedad (281). Otros autores sugieren que el fenotipo motor observado en modelos animales, en parte es a causa del daño al SNP, ya que a medida que progresa la enfermedad se observa también una axonopatía más severa (285,286). Este concepto también fue apoyado por los trabajos de Gould y colaboradores, en donde generaron un animal doble transgénico al cruzar un ratón deficiente en la proteína proapoptótica Bax con el modelo murino de ELA, $SOD1^{G93A}$. Como resultado, este animal tenía duplicado el número de motoneuronas a nivel de la médula espinal. Sin embargo, esta restitución del número de motoneuronas no fue suficiente para contrarrestar el daño axonal y el fenotipo motor de los animales $SOD1^{G93A}$ (285), sugiriendo que los mecanismos patogénicos centrales y los periféricos son, al menos en parte, independientes (285,287,288).

Sin embargo, aún siguen sin conocerse cuáles son las causas que llevan inicialmente a la degeneración axonal. Una de estas podría ser un transporte axonal deficiente a lo largo de la vía motora en las etapas tempranas de la ELA (289). En este sentido, Williamson y

Cleaveland observaron que el transporte de algunas proteínas se ve enlentecido de manera significativa meses antes del inicio de los síntomas clínicos (290). Estas observaciones fueron también realizadas por otros grupos (291), sugiriendo que el transporte enlentecido podría dar lugar a la agregación tóxica de proteínas a lo largo de la vía motora, induciendo así procesos neurotóxicos que promuevan la degeneración temprana de los axones motores. El transporte axonal de mitocondrias a lo largo de la vía motora también se ve afectado en modelos murinos de ELA, contribuyendo así a la degeneración distal (292). Estos mecanismos de degeneración retrógrada podrían estar explicando, en parte, la muerte que ocurre a nivel central y el proceso neurodegenerativo progresivo en la ELA (293).

Por otro lado, el rol de las células de Schwann en la degeneración de los nervios periféricos en la ELA permanece parcialmente desconocido. En la última década han habido avances al respecto y se ha evidenciado que éstas podrían tener un rol dual durante la progresión de la enfermedad (82,294). El transporte axonal deficiente en etapas tempranas de la enfermedad, anteriormente mencionado, podría ser inicialmente compensado por la transferencia de polirribosomas por parte de las células de Schwann al compartimiento axonal, impulsando así la síntesis local de proteínas (295). Por otro lado, a diferencia de lo que ocurre en el SNC, donde la sobreexpresión de la SOD1 humana mutada en las células gliales desempeña una función principalmente neurotóxica (75,132), Lobsiger y colaboradores demostraron que la sobreexpresión de la SOD1 humana mutada en las células de Schwann podría ejercer una protección parcial contra el aumento en la producción de ROS asociadas a la degeneración de los axones (82). Cuando se bloquea la expresión de la SOD1 mutada con actividad dismutasa, se produce una degeneración acelerada en los ratones SOD1 (82). Por otro lado, si se bloquea la SOD1 mutada, pero sin actividad dismutasa en células de Schwann en un modelo murino de ELA, se extiende la sobrevida y se retrasa la patología (296). Por otro lado, Keller y colaboradores han reportado un aumento significativo y progresivo de GFAP en las células de Schwann en el nervio ciático de ratones $SOD1^{G93A}$ (294). Sin embargo, este aumento podría ser consecuencia del daño axonal y se desconoce su rol patogénico.

La respuesta neuroinflamatoria a lo largo de la vía motora y las alteraciones de la barrera hemato-nerviosa, podrían ofrecer mecanismos de acción adicionales para entender la patogénesis en la ELA. Sin embargo, aún se desconoce si estas alteraciones de las estructuras neuronales periféricas pueden constituir una causa o, por el contrario, son consecuencia del proceso degenerativo de la motoneurona central. Los estudios llevados a cabo por Kano y claboradores, mostraron que la denervación de las placas motoras, así como la degeneración axonal, que como mencionamos preceden al inicio de los síntomas, ocurren antes de la inifiltración de células inmunitarias y del establecimiento de la inflamación crónica en el SNP (297). Sin embargo, luego de desencadenarse el proceso neurodegenerativo, se ha demostrado que el microambiente celular que se constituye alrededor de los axones motores y las NMJs, contribuye a la progresión de la enfermedad y podría ser modulado tanto genética como farmacológicamente como estrategia terapéutica válida para enlentecer la progresión (298). Es importante destacar que sigue

siendo controversial el rol de la inflamación en la ELA (299–301). Finalmente, también se ha reportado que la denervación de la NMJs en la ELA se acompaña de un infiltrado de macrófagos (298), aunque aún se investiga si la infiltración de células hematopoyéticas proinflamatoria depende de la axonopatía distal o si es una respuesta adaptativa orquestada por las células de Schwann. Por lo tanto, comprender cómo dialogan las células inflamatorias que infiltran el SNP con las células de Schwann y las NMJs, podría elucidar nuevos mecanismos que permitan comprender de forma más global los procesos celulares y moleculares que contribuyen a la progresión ineluctable característica de la ELA, y así poder avanzar en el desarrollo de nuevas y mejores estrategias terapéuticas.

El conocimiento que existe acerca del rol de los mastocitos en el SNP, se relaciona principalmente con los nervios sensoriales. Los mastocitos se ubican en la cercanía de las fibras nerviosas en el tejido conectivo periférico y, debido a la gran variedad de mediadores que son capaces de liberar, actúan amplificando las señales de inflamación (302). Por otro lado, mediadores liberados por mastocitos como histamina, triptasa, serotonina, TNF-α y NGF pueden modular los nervios sensoriales a través de la activación de receptores en las terminales nerviosas (303,304). Además, se ha reportado un rol importante de los mastocitos y sus mediadores, en particular, histamina y serotonina, en la patogénesis del dolor neuropático de diverso origen (305–307).

En la ELA, nuestro grupo ha realizado aportes significativos, mostrando que los mastocitos se acumulan significativamente a lo largo de los axones motores periféricos, así como en el músculo esquelético y en las NMJs denervadas (26,27). Específicamente, se observó que los mastocitos infiltran masivamente el músculo extensor de ratas transgénicas y se acumulan en el microambiente que rodea a las NMJs denervadas (26). Además, se observó que los mastocitos son abundantes en el músculo de pacientes con ELA y que se acumulan también en el nervio ciático y en las raíces ventrales de los modelos murinos (27). Sin embargo, durante mis estudios de doctorado nos preguntamos si la activación sobresaliente de las células de Schwann en respuesta a la axonopatía y retracción de axones motores, estaría vinculada a la respuesta neuroinflamatoria local, incluyendo la acumulación de mastocitos.

Visión integrada sobre la interacción causal neuroinflamación-mastocitos-células gliales y neurodegeneración

La Figura 1 resume en forma esquemática la hipotética interacción causal entre neuroinflamación y degeneración de las motoneuronas, con énfasis en mecanismos depedientes de células gliales y mastocitos. Es reconocido que la neuroinflamación crónica forma parte de la fisiopatología de la ELA y que las células gliales e inmunes participan de manera compleja en la progresión de la enfermedad. La disfunción primaria y temprana de las motoneuronas y de sus axones periféricos parece ser el principal desencadenante de la neuroinflamación en la ELA. Los factores provenientes de las motoneuronas dañadas estarían en el origen de la activación astrocitaria y microglial (98), lo que conduciría a la remodelación del microambiente celular y a un aumento de la neurotoxicidad mediada por

las células gliales crónicamente activadas, en contraposición con su acción neuroprotectora normal. Llegado a un punto crítico, se altera la permeabilidad vascular y de las barreras, y aumenta la expresión de factores quimiotácticos y tróficos para células inmunes de origen sanguíneo, incluyendo monocitos, linfocitos y células precursoras hematopoyéticas indiferenciadas $CD34^+$ o $c\text{-}Kit^+$, incluyendo precursores de mastocitos. Cuando el proceso degenerativo local se vuelve autosostenido y descontrolado, daría lugar a la afectación de regiones vecinas a las motoneuronas afectadas, extendiendo el proceso de neurodegeneración.

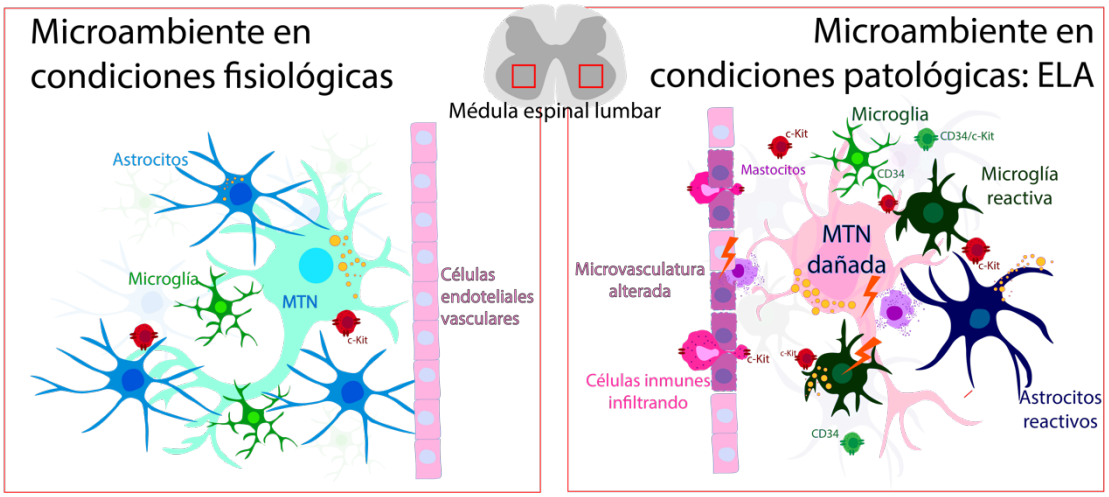

Figura 1. Visión integrada de la interacción causal neuroinflamación-mastocitos-células gliales y neurodegeneración.

Hipótesis

Nuestra hipótesis establece que el microambiente celular neurodegenerativo de la ELA se compone en parte de precursores hematopoyéticos que pueden ser identificados por marcadores específicos como CD34 o c-Kit. A su vez, éstos deberían dar orígen a una variedad de fenotipos más diferenciados, incluyendo células macrofágicas similares a la microglia endógena o con fenotipos aberrantes y/o mastocitos. En su conjunto, estos precursores deberían contribuir al aumento de densidad y heterogeneidad celular que caracteriza a la neuroinflamación y, en última instancia, a la muerte neuronal. La hipótesis también predice mecanismos que alteran la permeabilidad de las barreras vasculares, así como mecanismos quimiotácticos y de diferenciación local expresados por células neurales o inflamatorias afectadas en la ELA. Por tanto, si estas células pudieran ser aisladas en cultivo utilizando, por ejemplo, marcadores de superficie como CD34 y c-Kit, se podría demostrar su capacidad de generar células diferenciadas utilizando factores tróficos específicos. Finalmente, en el caso de los precursores c-Kit^{+}, la hipótesis predice que la inhibición farmacológica de este receptor por fármacos como el masitinib, podría reducir la capacidad proliferativa y la activación de los precursores o bien inhibir su diferenciación, lo que podría resultar en el control terapéutico de la neuroinflamación y de la neurotoxicidad.

Objetivo

El objetivo general de este proyecto fue estudiar con mayor profundidad cómo se constituye el microambiente celular neurodegenerativo en la ELA. Focalizamos la investigación en la emergencia de fenotipos celulares que hasta ahora no habían sido formalmente reconocidos en la neuroinflamación asociada a la ELA. En particular, nos enfocamos en la emergencia de precursores hematopoyéticos identificados con marcadores como CD34 y c-Kit y que infiltran el SNC o SNP en a lo largo de la vía motora, para contribuir a la neuroinflamación y muerte neuronal. La demostración formal de estos precursores conlleva caracterizar los fenotipos celulares en base a estudios histopatológicos en tejido de pacientes con ELA y de un modelo animal SOD1^{G93A}, la realización de cultivos celulares para aislar los precursores y demostrar su capacidad para generar células diferenciadas similares a microglia o mastocitos, así como demostrar su pasaje a través de la barrera hematoespinal y su potencial sensibilidad a fármacos inhibidores de c-Kit.

Objetivos específicos

1. Estudiar la asociación de la microgliosis en la ELA con la emergencia de células que expresan la proteína CD34, que es considerada como un marcador de células madre y precursores hematopoyéticos.

    - Caracterizar su fenotipo y su ubicación dentro del microambiente celular en la médula espinal de pacientes afectados con ELA y en un modelo animal de la enfermedad, utilizando técnicas de inmunohistología seguida de análisis por técnincas de microscopía confocal.
    - Realizar estudios cuantitativos mediante técnicas de citometría de flujo.
    - Demostrar formalmente la capacidad progenitora de las células CD34 aisladas de la médula espinal en cultivo celular, analizando su diferenciación en células macrofágicas similares a microglías.

2. Estudiar los mecanismos quimiotácticos mediados por SCF que regulan la infiltración de mastocitos derivados de precursores c-Kit$^+$ en el nervio ciático y raíces ventrales en degeneración en tejido de pacientes y en modelos murinos de ELA.

    - Identificar los tipos celulares que expresan SCF en la ELA, incluyendo las células de Schwann denervadas.
    - Determinar si la inhibición farmacológica de la vía SCF/c-Kit se asocia a una disminución en la infiltración de mastocitos y en una reducción de la axonopatía distal en la ELA.

3. Caracterizar en profundidad la infiltración de mastocitos derivados de precursores c-Kit$^+$ y su significación patológica, tanto en la médula espinal de pacientes con ELA como en modelos murinos de la enfermedad.

- Describir su fenotipo y su ubicación dentro del microambiente celular, utilizando técnicas de inmunohistología seguida de análisis en microscopio confocal.
- Realizar estudios cuantitativos mediante técnicas de citometría de flujo.
- Demostrar formalmente la capacidad progenitora de las células c-Kit$^+$ aisladas de la médula espinal en cultivo celular, analizando su diferenciación en mastocitos convencionales.
- Aportar evidencias sobre el origen hemático de los mastocitos espinales en la ELA, utilizando técnica de inyección intravenosa de precursores obtenidos de la médula ósea.
- Analizar la asociación espacial de los precursores de mastocitos espinales con alteraciones de la microvasculatura.
- Determinar la potencial regulación farmacológica de mastocitos espinales c-kit$^+$ en animales ELA tratados con masitinib.

Resultados

Publicación 1

CD34 identifies a subset of proliferating microglial cells associated with degenerating motor neurons in ALS

(La proteína CD34 identifica una subpoblación de células microgliales proliferantes asociadas con la degeneración de motoneuronas en la ELA)

Mariángeles Kovacs, Emiliano Trias, Valentina Varela, Sofia Ibarburu, Joseph S. Beckman, Ivan C. Moura, Olivier Hermine, Peter H. King, Ying Si, Yuri Kwon and Luis Barbeito.

Resumen

Es ampliamente aceptado que la activación exacerbada de la microglía en la ELA es un mecanismo patogénico significativo asociado a la degeneración de las motoneuronas. Además, la proliferación de microglías (microgliosis) en la ELA se asocia a la emergencia de fenotipos gliales aberrantes, sugiriendo procesos de transformación fenotípica que podrían involucrar a microglías indiferenciadas con características de precursores mieloides. En este contexto, el primer artículo publicado durante mi doctorado tuvo por objetivo estudiar la asociación de la microgliosis en la ELA con la emergencia de células que expresan la proteína CD34, que es considerada como un marcador de células madre y precursores hematopoyéticos. Reportes previos habían estudiado la expresión de CD34 en microglía o en otras células del microambiente celular neurodegenerativo en otras enfermedades, pero no así en la ELA.

En este trabajo se logró identificar una subpoblación de células microgliales que expresa la proteína CD34 en las zonas de degeneración de motoneuronas en la fase sintomática de la ELA, tanto en el tejido post-mortem de pacientes como en el modelo animal de ratas que expresan la mutación $SOD1^{G93A}$.

Se aportó evidencia en cultivo celular de que estas células $CD34^{+}$ aisladas de la médula espinal de ratas $SOD1^{G93A}$, se comportan como células hematopoyéticas precursoras de microglía, sugiriendo que las mismas pueden explicar al menos en parte el crecimiento explosivo en el número de microglías en la fase sintomática de la ELA.

Resultados

- En la médula espinal, observamos un aumento progresivo en la expresión de la proteína CD34 principalmente en células microgliales, la cual estaba restringida al asta ventral lumbar en ratas $SOD1^{G93A}$. La aparición de esta población $CD34^{+}$ se encontraba directamente relacionada con la progresión de la enfermedad, aumentando significativamente desde el inicio de los síntomas hasta 15 días posteriores al inicio de la parálisis. Mientras que en animales no transgénicos la

expresión de CD34 se encontraba limitada a capilares, en los animales sintomáticos se observó que las células $CD34^+$ proliferan activamente y que forman "*clusters*" en las cercanías de las motoneuronas espinales en degeneración, las cuales expresan altas concentraciones de la proteína SOD1 humana mal plegada. El mismo patrón de expresión de CD34 fue observado en la médula espinal de pacientes con ELA, en comparación con una expresión restringida a capilares en tejido de sujetos control. Las células $CD34^+$ se encontraron en las cercanías de motoneuronas, aunque en menor número en comparación a lo observado en el modelo animal.

- Las células CD34 co-expresan marcadores microgliales. Analizamos la expresión de CD34 junto con diferentes marcadores microgliales típicos, como CD11b, Iba1 y CD68. Observamos que el 80% de las células $CD34^+$ co-expresan el marcador CD11b, mientras que el 60% y el 15% expresan Iba1 y CD68, respectivamente. Las células que se organizaban formando grandes "*clusters*", que expresaban CD34 en el centro, y marcadores como CD11b e Iba1 en la periferia. En pacientes con ELA, se observó solamente una subpoblación de las células CD34 que co-expresan Iba1.
- En el cultivo primario obtenido a partir de la médula espinal de ratas $SOD1^{G93A}$ en la fase terminal de la enfermedad, se pueden observar dos fases: una fase de células no-adherentes y una fase de células adherentes con fenotipo activado, fagocítico, que expresan CD11b, CD68 e Iba1 (24). En este cultivo, las células $CD34^+$ no fueron observadas en la fase adherente, pero sí en la fase no-adherente y en gran número debido a la alta tasa proliferativa. Observamos también que estas células que no se adhieren se organizan formando "*clusters*", donde predomina la expresión de CD34 en el centro y CD11b en la periferia, un efecto similar a lo observado previamente en la médula espinal. Finalmente, además de lograr aislar las células CD34 en la fase no-adherente del cultivo primario de médula espinal sintomática, cuando las mismas son subcultivadas en sucesivos pasajes, se siguen obteniendo numerosas microglías diferenciadas en la fase adherente, así como una subpoblación que se mantiene no adherida durante numerosos pasajes.

Conclusiones

Se logró identificar una población de células caracterizadas por la expresión del marcador de células precursoras hematopoyéticas, CD34, que emergen en la médula espinal durante la fase sintomática de la ELA, tanto en pacientes con ELA como en ratas $SOD1^{G93A}$. Estas células, que co-expresan marcadores de microglía como CD11b e Iba1, amplían el abanico heterogéneo de fenotipos gliales aberrantes característicos del microambiente celular neurodegenerativo que rodea a los somas de las motoneuronas en degeneración.

Sin embargo, el origen de esta población de células $CD34^+$ no es del todo claro y podría corresponder a la invasión de precursores hematopoyéticos circulantes. Además, nuestros resultados sugieren que son células precursoras mieloides que pueden dar origen a microglías en condiciones de cultivo celular. Una limitación de este trabajo, es que no se pudo identificar otros posibles fenotipos de células mieloides que podrían originarse a partir de los precursores $CD34^+$, incluyendo monocitos, células dendríticas y mastocitos. Como se

expuso más arriba, estas células ya han sido identificadas en la médula espinal de la ELA y podrían representar blancos terapéuticos novedosos para el desarrollo de tratamientos efectivos.

International Journal of
Molecular Sciences

MDPI

Article

CD34 Identifies a Subset of Proliferating Microglial Cells Associated with Degenerating Motor Neurons in ALS

Mariángeles Kovacs [1,†], Emiliano Trias [1,†], Valentina Varela [1], Sofia Ibarburu [1], Joseph S. Beckman [2], Ivan C. Moura [3,4,5,6,7,8], Olivier Hermine [3,4,5,6,7,8,9,10,11], Peter H. King [12,13], Ying Si [12,13], Yuri Kwon [12] and Luis Barbeito [1,*]

1 Institut Pasteur de Montevideo, Montevideo 11400, Uruguay
2 Linus Pauling Institute, Department of Biochemistry and Biophysics, Environmental Health Sciences Center, Oregon State University, Corvallis, OR 97331, USA
3 Imagine Institute, Hôpital Necker, 75015 Paris, France
4 INSERM UMR 1163, Laboratory of Cellular and Molecular Mechanisms of Hematological Disorders and Therapeutic Implications, 75015 Paris, France
5 Paris Descartes–Sorbonne Paris Cité University, Imagine Institute, 75006 Paris, France
6 CNRS ERL 8254, INSERM U1163, Université Paris Descartes, 75006 Paris, France
7 Laboratory of Excellence GR-Ex, 75015 Paris, France
8 Equipe Labélisée par la Ligue Nationale contre le cancer, 75013 Paris, France
9 AB Science, 75008 Paris, France
10 Department of Hematology, Hôpital Necker, 75015 Paris, France
11 Centre national de référence des mastocytoses (CEREMAST), 75743 Paris, France
12 Department of Neurology, University of Alabama at Birmingham, Birmingham, AL 35294, USA
13 Birmingham Veterans Affairs Medical Center, Birmingham, AL 35294, USA
* Correspondence: barbeito@pasteur.edu.uy
† These authors contributed equally to this work.

Received: 31 May 2019; Accepted: 16 July 2019; Published: 9 August 2019

Abstract: Amyotrophic lateral sclerosis (ALS) is characterized by degeneration of upper and lower motor neurons accompanied by proliferation of reactive microglia in affected regions. However, it is unknown whether the hematopoietic marker CD34 can identify a subpopulation of proliferating microglial cells in the ALS degenerating spinal cord. Immunohistochemistry for CD34 and microglia markers was performed in lumbar spinal cords of ALS rats bearing the $SOD1^{G93A}$ mutation and autopsied ALS and control human subjects. Characterization of CD34-positive cells was also performed in primary cell cultures of the rat spinal cords. CD34 was expressed in a large number of cells that closely interacted with degenerating lumbar spinal cord motor neurons in symptomatic $SOD1^{G93A}$ rats, but not in controls. Most $CD34^+$ cells co-expressed the myeloid marker CD11b, while only a subpopulation was stained for Iba1 or CD68. Notably, $CD34^+$ cells actively proliferated and formed clusters adjacent to damaged motor neurons bearing misfolded SOD1. $CD34^+$ cells were identified in the proximity of motor neurons in autopsied spinal cord from sporadic ALS subjects but not in controls. Cell culture of symptomatic $SOD1^{G93A}$ rat spinal cords yielded a large number of $CD34^+$ cells exclusively in the non-adherent phase, which generated microglia after successive passaging. A yet unrecognized $CD34^+$ cells, expressing or not the microglial marker Iba1, proliferate and accumulate adjacent to degenerating spinal motor neurons, representing an intriguing cell target for approaching ALS pathogenesis and therapeutics.

Keywords: microglia; CD34; amyotrophic lateral sclerosis; misfolded SOD1; motor neurons

1. Introduction

Neuroinflammation is a pathological hallmark of amyotrophic lateral sclerosis (ALS), causally associated with the progressive degeneration of upper and lower motor neurons [1,2]. At sites of motor neuron and axonal damage, reactive glial and infiltrating immune cells orchestrate a characteristic inflammatory microenvironment [3,4]. In particular, microglia display active proliferation and profound phenotypic changes in ALS subjects and ALS animal models [5,6]. A large body of evidence indicates that microglia play a crucial pathogenic role in accelerating motor neuron degeneration [7,8]. However, the complete understanding of different microglia cell phenotypes in ALS pathogenesis remains elusive.

In particular, the ALS rat model expressing the SOD1^{G93A} mutation shows extensive microglia pathology concurrent with paralysis onset and progression [9–11], with extensive proliferation and development of aberrant or senescent phenotypes and formation of multinucleated giant cells [10,12]. Activated microglia bearing SOD1 mutations in rodents also exert toxicity to motor neurons [7] and contribute to accelerated progression of motor neuron disease in a non-cell autonomous manner [13]. In SOD1^{G93A} rats, microglia can transform into a distinct population of cells exhibiting an aberrant phenotype [9] and a potent neurotoxic effect on cultured motor neurons [14,15]. Notably, aberrant microglia are localized in the vicinity of spinal motor neurons after paralysis onset. Downregulation of aberrant glia through pharmacological inhibition of the receptor CSF-1R results in an extension of post-paralysis survival in rat and mouse models of ALS [16,17], suggesting their potential as drug targets to halt or slow disease progression. Given these facts, we aimed to identify different and as yet unknown microglia-related phenotypes that may also emerge and interact with degenerating motor neurons during disease progression in ALS.

CD34 is a transmembrane highly glycosylated protein, which has been extensively used as a marker of hematopoietic stem cells [18] and non-hematopoietic progenitor cells [19,20]. CD34 can regulate trafficking and migration of hematopoietic progenitor cells [20], which eventually may migrate to the CNS and differentiate into microglia [21]. Following CNS damage, CD34-expressing microglia have been found in affected regions [21–23], which are also characterized by microgliosis and blood–brain barrier damage. Because the identification of CD34^{+} cells in ALS remains elusive, we reasoned that this marker may allow the identification of a proliferating subset of microglia in the spinal cord of SOD1^{G93A} rats and autopsied ALS patients.

SOD1^{G93A} rats are characterized by the development of an adult-onset rapid progressing paralysis accompanied by dramatic microgliosis [9–11]. We took advantage of this particular SOD1^{G93A} model to analyze CD34 expression along the course of paralysis progression. Here, we report a massive increase of cells expressing CD34 after paralysis onset, which proliferate and co-express myeloid markers. Notably, numerous CD34^{+} cells were associated with motor neurons in sporadic ALS and SOD1^{G93A} rat spinal cords. In cell culture, CD34^{+} cells yielded microglia upon successive passages, suggesting that this marker identifies a population of proliferating microglia involved in ALS pathogenesis.

2. Results

2.1. Increased Number and Proliferation of CD34^{+} Cells in SOD1^{G93A} Rat Spinal Cord during Paralysis Progression

First, we examined the expression of CD34 in the ventral horn of the lumbar cord at paralysis onset and 15d of paralysis progression in SOD1^{G93A} rats as compared with non-transgenic rats, as shown in Figure 1A. Immunohistochemistry analysis revealed a progressive increase in CD34 expression in SOD1^{G93A} restricted to the ventral horn of the spinal cord, as shown in Figure 1A. CD34 immunoreactivity was significantly increased by 6-fold and 14-fold at paralysis onset and 15d of paralysis progression, respectively, when compared to non-transgenic rats, as shown in Figure 1B.

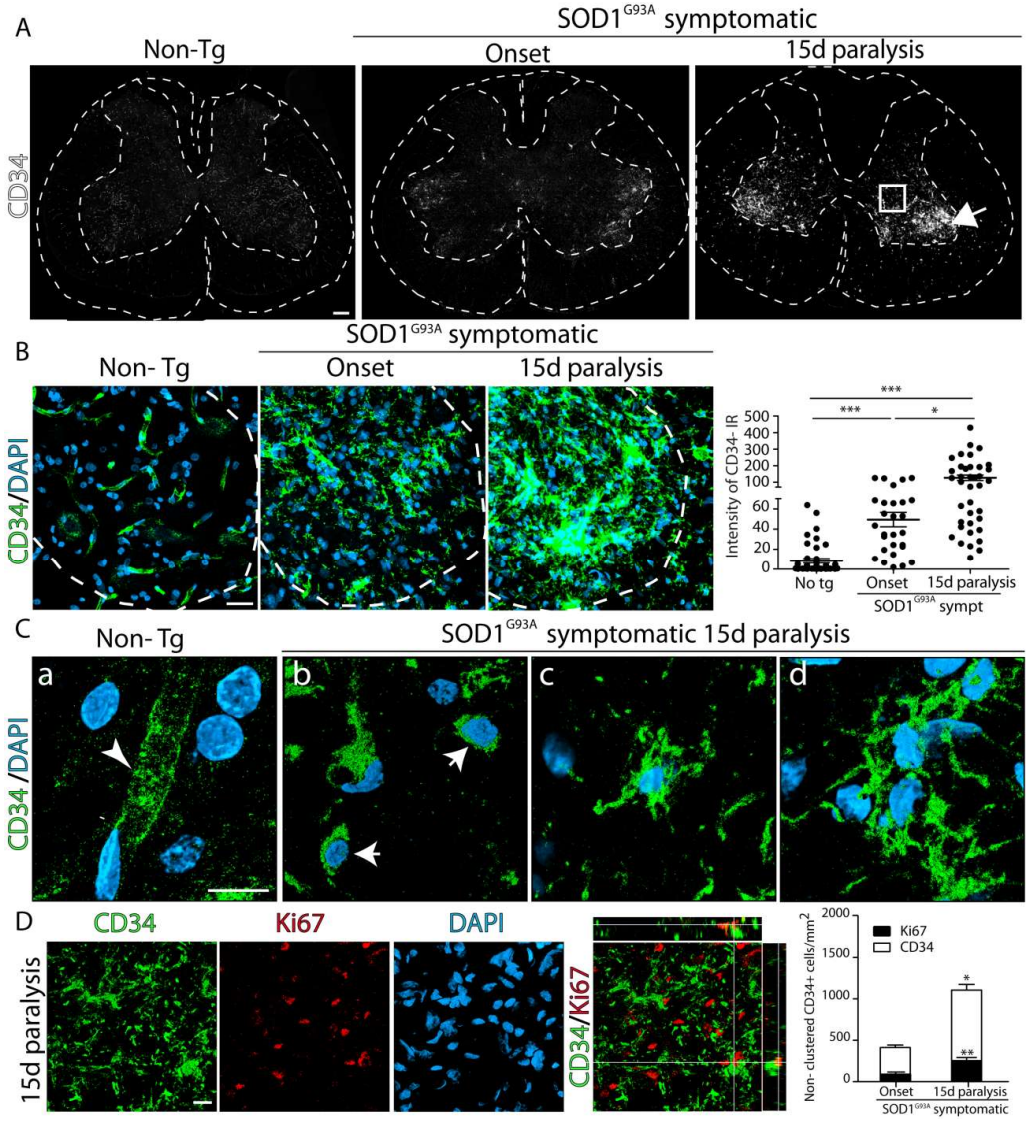

Figure 1. CD34$^+$ immunoreactivity in the degenerating spinal cord during the course of paralysis in SOD1^{G93A} rats. Representative confocal microscopy images showing the expression of CD34 in the spinal cord of Non-transgenic (Non-Tg), SOD1^{G93A}-onset, and SOD1^{G93A}-15d paralysis rats. (**A**) Confocal tile reconstruction of the spinal cord showing increasing CD34 expression (white) in the ventral horn. The arrow and square indicate CD34 distribution in clustered and non-clustered cells, respectively. (**B**) Representative confocal images of CD34 expression (green) showing the detailed distribution of CD34$^+$ cells in the ventral horn. Note CD34 staining in Non-Tg spinal cord was restricted to blood vessels while an increased immunoreactivity and different distribution was noted in SOD1^{G93A} rats. Dotted lines show the limit between grey and white matter in the lumbar cord. The graph to the right shows the quantitative analysis of CD34 immunoreactivity among groups. Quantitative data are expressed as mean ± SEM; data were analyzed by Kruskal–Wallis followed by Dunn's multiple comparison test, * $p < 0.05$, *** $p < 0.001$ was considered statistically significant (**C**) Representative confocal images showing the different CD34$^+$ cell phenotypes present in non-clustered regions. **a)** Blood vessels in Non-Tg animals. **b)** Two round cells. **c)** Ramified cell. **d)** Small cluster of three cells. (**D**) Confocal images showing proliferating CD34$^+$ cells in non-clustered regions stained with Ki67. Orthogonal view shows Ki67$^+$ nuclei on the CD34$^+$ cell. The graph to the right shows the quantitative analysis of non-vascular CD34$^+$ and CD34$^+$/Ki67$^+$ cells in non-clustered regions. Quantitative data are expressed as mean ± SEM; data were analyzed by Mann-Whitney test, * $p < 0.05$, ** $p < 0.01$ was considered statistically significant. $n = 4$ animals/condition. Scale bars: 100 µm (**A**), 25 µm (**B**), and 10 µm (**C**,**D**).

In control non-transgenic rats, CD34 immunoreactivity of the lumbar spinal cord was restricted to capillaries, as shown in Figure 1B,C. In symptomatic SOD1^{G93A} rats, CD34 immunoreactivity displayed two morphological patterns: (i) clusters of CD34$^+$ cells containing small, round cells packed together, as shown in Figure 1B, and (ii) non-clustered, isolated CD34$^+$ cells displaying rounded or ramified morphology, as shown in Figure 1C. Quantitative analysis of non-clustered CD34$^+$ cells in the ventral horn showed a significant number of cells at paralysis onset, increasing by 3-fold at advanced paralysis, as shown in Figure 1D. About 15% of non-clustered CD34$^+$ cells also displayed nuclear staining for the proliferation marker Ki67 at disease onset and advanced paralysis, suggesting a rapid expansion, as shown in Figure 1D.

2.2. CD34$^+$ Cells Co-Express Myeloid and Microglia Markers

Figure 2A shows that almost 80% of CD34$^+$ cells in the ventral horn expressed the myeloid marker CD11b, while only 60% and 15% of cells expressed the microglia markers Iba1 or CD68, respectively, as shown in Figure 2B,C. In comparison, cells organized in large clusters mostly displayed staining for CD34 in the center and co-expressed CD11b or Iba1 in the periphery, as shown in Figure 2D, suggesting a center–periphery differentiation process.

2.3. CD34$^+$ Cells Progressively Invade Damaged Motor Neurons Accumulating Misfolded SOD1

Figure 3 shows the early association between CD34$^+$ cells and ventral horn motor neurons identified by Nissl or βIII-tubulin staining in SOD1^{G93A} rats. In non-transgenic rats, CD34 staining is restricted to blood vessels, while already in SOD1^{G93A} symptomatic onset rats CD34$^+$ cells begin to surround motor neurons, as shown in Supplementary Figure S1. Typically, CD34$^+$ cells locate adjacent to damaged motor neuron cell bodies and proximal neurites, which could suggest a progressive pathogenic process for individual degenerating motor neurons.

As paralysis progressed, large motor neurons showed a tendency to lose Nissl staining and develop immunoreactivity for misfolded SOD1, indicative of dismantled endoplasmic reticulum and accumulation of misfolded proteins. Interestingly, motor neurons accumulating misfolded SOD1 were surrounded by a high number of proliferating CD34$^+$ cells, as shown in Figure 4A,B, suggesting specific chemoattraction. However, as shown in Figure 4Bc, some motor neuron accumulating misfolded SOD1 may have low numbers of CD34$^+$ surrounding cells. Also, these CD34$^+$ cells displayed nuclear staining for Ki67, as shown in Figure 4C, suggesting a site-specific expansion of CD34$^+$ cells in the surroundings of degenerating motor neurons.

2.4. Identification of CD34$^+$ Cells in the Spinal Cord from Amyotrophic Lateral Sclerosis (ALS) Autopsied Subjects

Next, we tested the hypothesis that CD34$^+$ cells also accumulate in autopsied spinal cord from ALS subjects. Supplementary Table S1 shows the characteristics of five ALS and three control donors analyzed as well as the time of postmortem tissue processing. At the time of ALS diagnosis, there was electrophysiological evidence of leg muscle denervation in each patient, supporting the involvement of the lumbar spinal cord.

The histological analysis of lumbar spinal cord sections showed a systematic increase in CD34$^+$ cells in ALS subjects, respect to controls, where CD34$^+$ immunostaining was restricted to capillaries close to motor neurons, as shown in Figure 5A,B. ALS specimens showed a decreased density of CD34$^+$ immunoreactivity in capillaries. Notably, a significant number of non-vascular CD34$^+$ cells with round morphology were also identified in the spinal cord of ALS subjects but not in controls, with frequent CD34$^+$ cells being localized in the proximity of apparent motor neuron cell bodies morphologically identified by typical shape, size, and localization in the ventral horn as described in other reports, and as shown in Figure 5C. CD34$^+$ cells in ALS subjects were not grouped in clusters and only a subpopulation of CD34$^+$ cells co-expressed Iba1, as shown in Figure 5D,E.

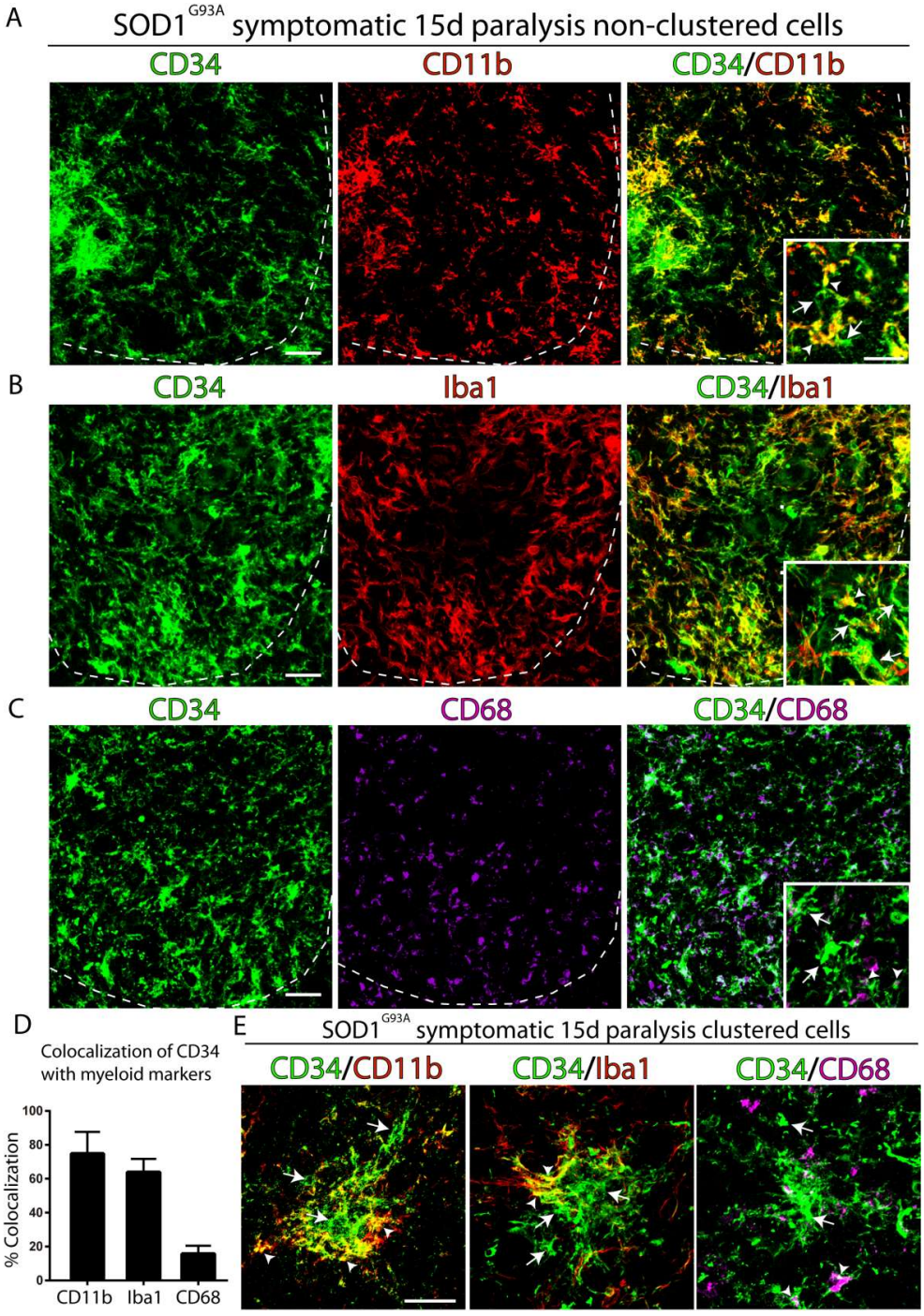

Figure 2. Co-expression of microglia markers and CD34. Representative confocal immunostaining of the ventral horn of symptomatic SOD1^{G93A} rat spinal cord showing the co-localization of myeloid/microglia markers CD11b (red, **A**), Iba1 (red, **B**), and CD68 (magenta, **C**). Insets show cell morphology and co-localization with CD34 at higher magnification. White arrows indicate CD34+ cells. White arrowheads indicate co-localization of CD34 with CD11b, Iba1, and CD68. Dotted lines show the limit between grey and white matter in the lumbar cord. (**D**) Confocal quantitative analysis of co-localization for CD34 and CD11b, Iba1, or CD68 in the ventral horn of symptomatic SOD1^{G93A} rat spinal cord. (**E**) Confocal analysis of the co-expression of CD34 and microglia markers in cell clusters observed in the degenerating spinal cord. Arrows indicate CD34^{+} cells in the cluster. Arrowheads indicate co-localization of CD34 with myeloid markers in the periphery of clusters. n = 4 animals/condition. Scale bars: 25 µm and 15 µm in insets.

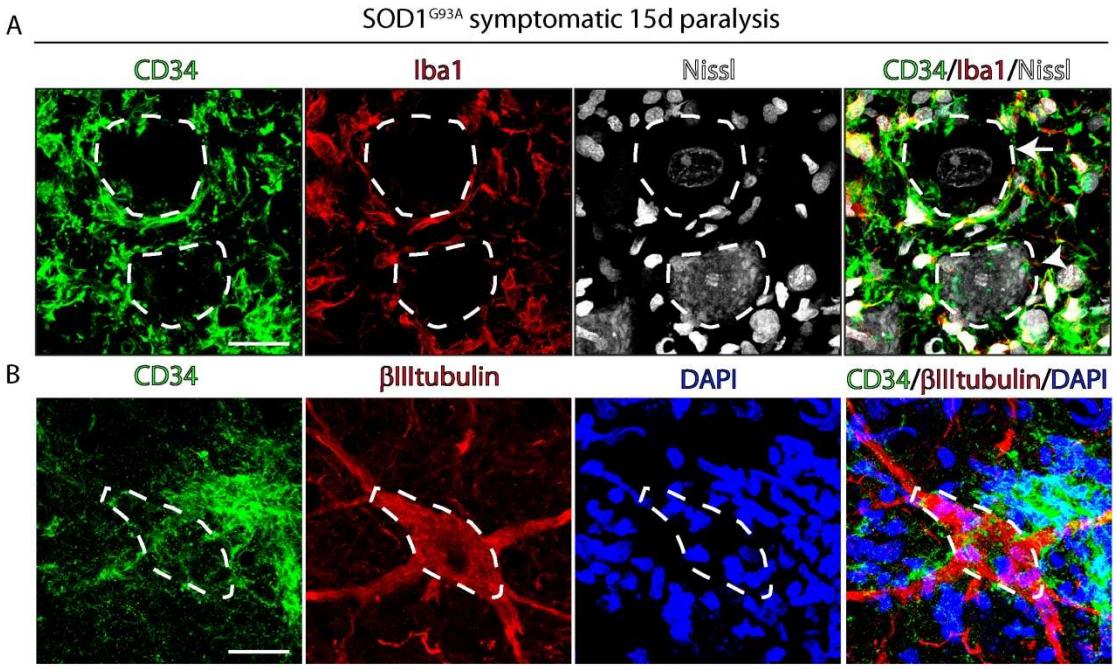

Figure 3. Spatial interaction of CD34$^+$ cells with spinal motor neurons in symptomatic SOD1^{G93A} rats. Confocal microphotograph analyzing the association of CD34$^+$ cells with motor neurons (dotted white lines) stained with Nissl (**A**) and βIII-tubulin (**B**). Note that CD34$^+$/Iba1$^+$ cells are adjacent to spinal motor neurons. Scale bars: 25 μm.

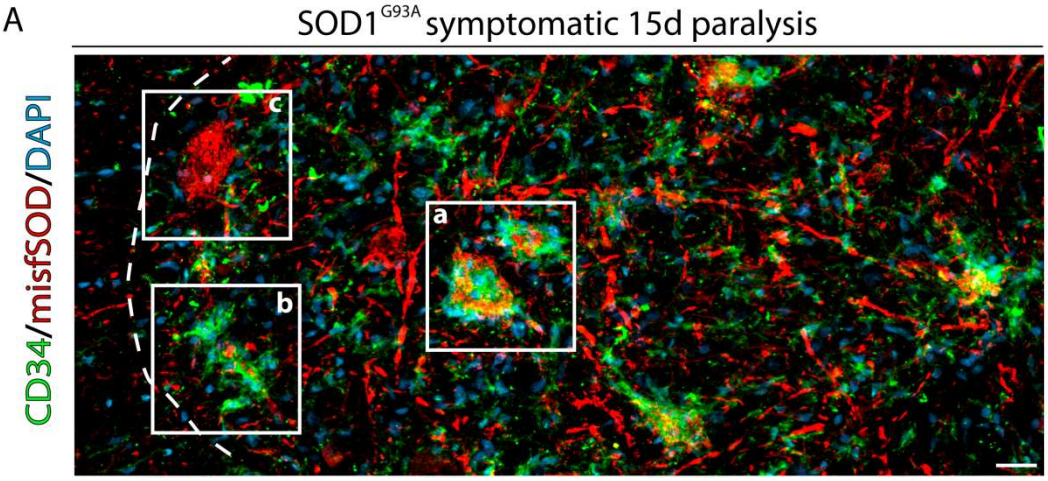

Figure 4. *Cont.*

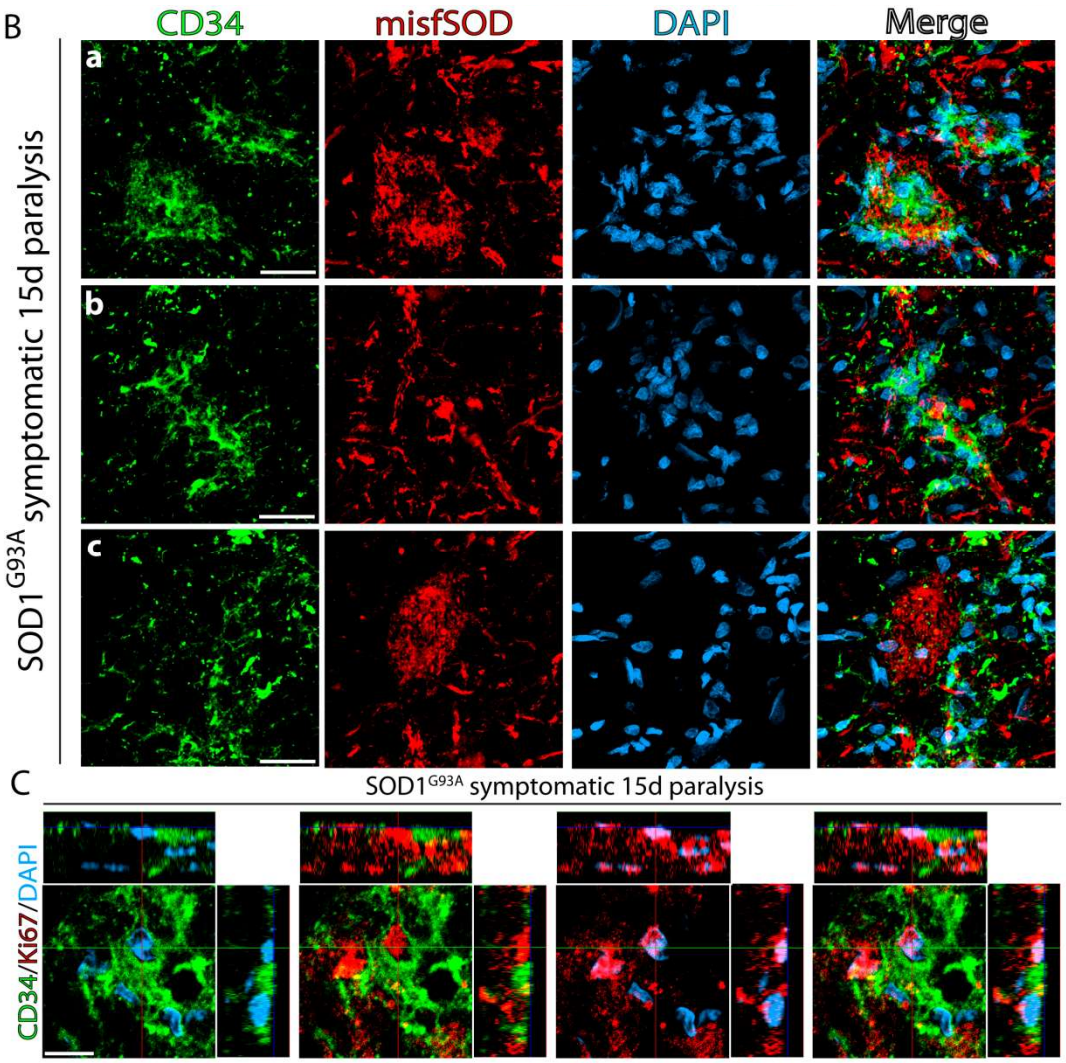

Figure 4. CD34$^+$ cells accumulate adjacent to motor neurons expressing misfolded SOD1. (**A**) Confocal tile reconstruction of the ventral horn showing CD34$^+$ cell clusters adjacent to motor neurons expressing misfolded SOD1. CD34$^+$ cells completely surround and attach to damaged motor neurons expressing misfolded forms of SOD1 and form compact clusters of cells, both around motor neuron somas (**a**) and processes (**b**). Other motor neurons accumulating misfolded SOD1 have less CD34$^+$ cells invading them (**c**). (**B**) Higher magnification analysis showing the clustering of CD34$^+$ cells around motor neuron somas and processes. (**C**) Orthogonal view of the staining of proliferating CD34$^+$ cell clusters expressing nuclear Ki67. Arrows indicate Ki67$^+$ nuclei in a CD34$^+$ cell cluster. Scale bars: 25 μm (**A**,**B**) and 10 μm (**C**).

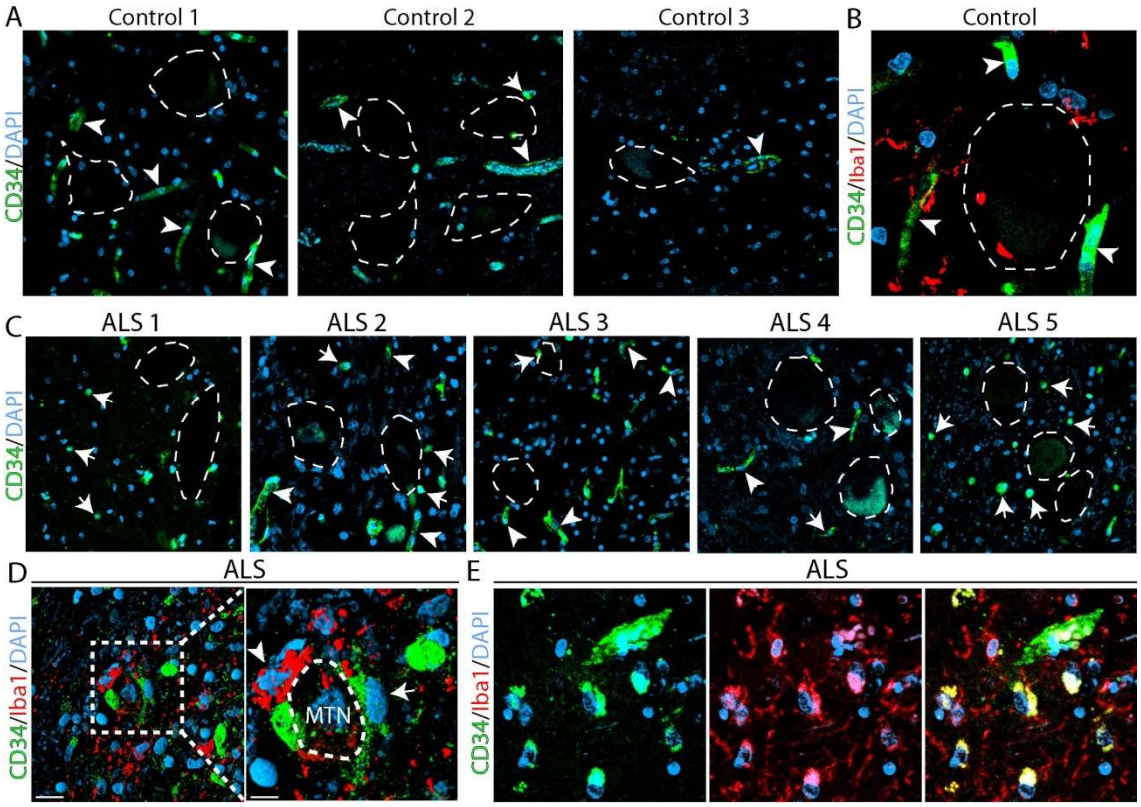

Figure 5. Identification of CD34$^+$ cells in autopsied spinal cords from subjects with sporadic amyotrophic lateral sclerosis (ALS). Representative confocal microphotograph showing the occurrence of non-vascular CD34$^+$ cells in sporadic ALS and control donors. (**A–C**) CD34$^+$ cells (green) in controls and ALS subjects, respectively. Dotted lines delimitate the soma of spinal motor neurons. Note that in control subjects CD34$^+$ cells were associated to blood vessels (arrowheads) with none or few rounded CD34$^+$ cells located adjacent to motor neurons. In comparison, in ALS donors numerous CD34$^+$ cells with round morphology were located in the proximity to apparent motor neuron cell bodies (arrows). (**D**) Confocal image showing the coexistence of Iba1$^+$ cells (red) that surround an apparent motor neuron cell body (dotted lines in right panel) with CD34$^+$ cells in ALS specimens. Note non-vascular CD34$^+$ cells adjacent to motor neurons in ALS specimens but not in controls. (**E**) Co-expression of CD34 with Iba1 in myeloid cells at the ventral horn of the spinal cord of ALS patients. Scale bars: 25 μm (**A**), 10 μm (**B**), 50 μm (**C**), 10 μm (**D**), 20 μm (**E**).

2.5. Non-Adherent CD34$^+$ Cells Isolated from SOD1^{G93A} Symptomatic Spinal Cord Give Rise to Microglia

To determine the behavior of CD34$^+$ cells, we isolated and cultured cells from symptomatic SOD1^{G93A} rat spinal cord. As previously reported [9], such cultures yield numerous adherent phagocytic microglia labeled with CD11b, CD68, and Iba1, as compared to only a few cells in non-transgenic controls. In the current study, CD34+ cells were not found in the adherent phase but accumulated in great number in the non-adherent phase, as shown in Figure 6A–D.

Cytological analysis of the non-adherent phase denoted that CD34$^+$ cells organized in clusters of 10–20 cells, with CD34$^+$ cores showing peripheral expression of CD11b, as shown in Figure 6B, suggesting a gradient of center-to-periphery differentiation. Approximately 35% of non-adherent cells displayed nuclear labeling with Ki67, indicative of active proliferation, as shown in Figure 6E.

When non-adherent cells from symptomatic SOD1^{G93A} rat spinal cords were subsequently passaged to another culture dish, numerous adherent and fully differentiated microglia were obtained in the adherent phase, as shown in Figure 6C,F,G, suggesting their ability to further differentiate as a conventional vacuolated microglia which firmly attach to the plate.

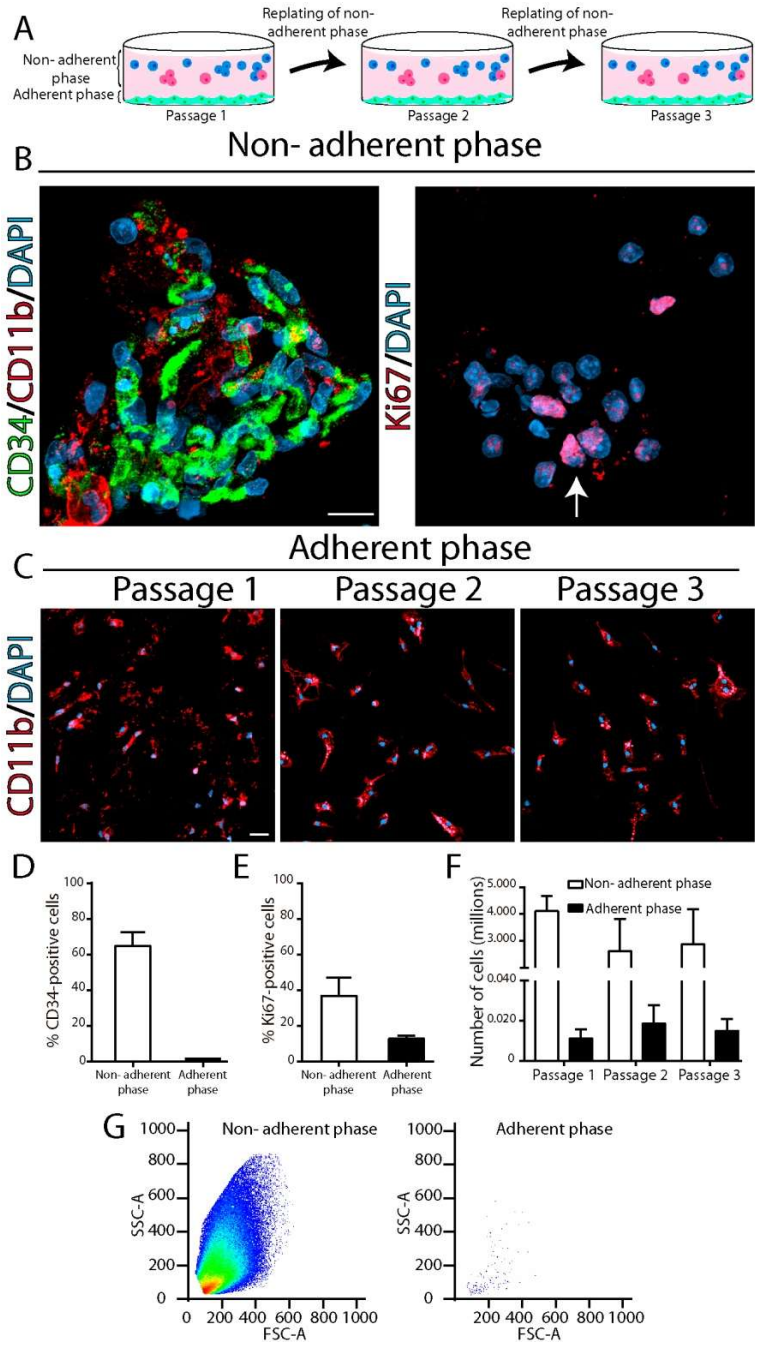

Figure 6. Characterization of CD34$^+$ cells in primary spinal cord cultures from symptomatic SOD1^{G93A} rats. Primary cultures were prepared from symptomatic rat's (n = 6) spinal cords and cells from the adherent and non-adherent phases were characterized. (**A**) Scheme showing the method used for analyzing the CD34$^+$ and microglia cells (green attached cells) found in non-adherent cells (blue and red cells represent the heterogeneity of cultured non-adherent cells) after successive passages. (**B**) Cytological analysis of cell clusters found in the non-adherent phase showing CD34$^+$ (green) and CD11$^+$ (red, in left panel) cells as well as active proliferation as denoted by Ki67 nuclei staining (red, in right panel). (**C**) Immunostaining of adherent cells in successive passages showing sustained number of CD11b$^+$ cells (red). (**D**) Quantitative analysis showing CD34$^+$ cells only in the non-adherent phase. (**E**) Quantitative analysis of Ki67$^+$ cells in the non-adherent and adherent phase. (**F**) Quantitative analysis showing that cells accumulate in great number in the non-adherent phase and generate adherent CD11b$^+$ microglia in successive passages. (**G**) Representative plots of flow cytometry analysis showing the density of cells in both non-adherent and adherent phases. Scale bars: 10 μm (**B**) and 25 μm (**C**).

3. Discussion

The present study characterizes a subpopulation of $CD34^+$ cells that accumulate in the ventral horn of the ALS spinal cord during the symptomatic phase of the disease. This cell type has not been previously reported in ALS. Intriguingly, these cells seem to be attracted to damaged motor neurons in the spinal cord of $SOD1^{G93A}$ rats and in autopsied spinal cords of ALS subjects. Evidence indicates that $CD34^+$ cells behave as not fully differentiated proliferating microglia, most cells expressing the broad myeloid marker CD11b. In primary cell cultures of $SOD1^{G93A}$ symptomatic spinal cord, $CD34^+$ cells are non-adherent and give rise to fully differentiated microglia, a behavior previously observed for microglia non-adherent precursor cells from the bone marrow [24]. Moreover, $CD34^+$ cells exhibit an enormous proliferative capacity in $SOD1^{G93A}$ rats forming clusters of many cells, suggesting a multi-clonal expansion process. Our findings in $SOD1^{G93A}$rats and sporadic ALS patients are in accordance with the analysis of a public database released by a spatial transcriptome study in $SOD1^{G93A}$ mice (https://als-st.nygenome.org/) [25], which shows a significant increase in CD34 transcripts in the lumbar spinal cord of mice over the course of the disease. Understanding the mechanism of controlling $CD34^+$ precursors in ALS may have translational relevance in motor neuron diseases.

While previous reports have described the pathological features of reactive microglia and neuroinflammation in the spinal cords of ALS patients [6,26,27], this is the first observation of the occurrence of $CD34^+$ cells in sporadic ALS. The finding of $CD34^+$ cells surrounding motor neurons was intriguing and clearly contrasted with control subjects, where CD34 was almost exclusively expressed in capillaries. However, the number of $CD34^+$ cells among sporadic ALS subjects was much lower than in the $SOD1^{G93A}$ rats and failed to form clusters, suggesting a lower rate of proliferation. Such differences might be related to the fact that the course of the disease in rat models develops in only few weeks as compared with months to years in subjects with ALS. Also, autopsied samples from terminally ill ALS patients might not be representative of active disease and motor neuron loss. Thus, $CD34^+$ cells appear to be a novel and relevant cell type involved in the ALS cellular microenvironment. It would be interesting to assess whether CD34 transcripts or CD34 protein leak into the cerebrospinal fluid of ALS patients as potential biomarkers.

The present study has not addressed the question of whether $CD34^+$ cells in the spinal cord of symptomatic $SOD1^{G93A}$ rats originate from resident microglia, perivascular macrophages, or circulating hematopoietic stem cells, a subject that would require a detailed immunophenotyping analysis. In the absence of a major blood–brain barrier breakdown, microglia expansion has been attributed to proliferation and/or migration of resident microglia [28–31], which can exhibit an impressive proliferative capacity. Here, we found that most of the $CD34^+$ cells co-expressed myeloid/microglial markers such as CD11b or Iba1, suggesting the vast majority of $CD34^+$ cells correspond to a subpopulation of microglia. It is possible that a subset of proliferative microglia downregulate canonical myeloid markers to levels that escaped the immunodetection. In accordance, CD34 transcripts have been detected in microglia and brain endothelial cells during development [32], while the expression of CD34 proteins is upregulated following tissue injury or blood–brain barrier disruption [22,23]. Alternatively, $CD34^+$ cells in ALS could originate from the influx and subsequent expansion of blood precursor cells. In support of this mechanism, previous studies have shown that bone marrow-derived myeloid progenitors are the source for microglia in different pathological conditions, such as ischemia [32,33], Experimental autoimmune encephalomyelitis [34], and CNS axonal damage [22,35]. In ALS models, blood myeloid cells can penetrate into the spinal cord and induce pathology [36] and $CD34^+$ human bone marrow cells or CD34+ blood cord cells can engraft into spinal cord capillaries and parenchyma [37–40]. Thus, it will be important to determine the origin of CD34+ microglia and the mechanism controlling their proliferation.

The remarkable cluster proliferation of $CD34^+$ cells adjacent to damaged motor neurons accumulating misfolded SOD1 is intriguing and has not been previously reported in ALS. Misfolded SOD1 is considered a pathological hallmark of ALS-affected motor neurons [41,42], not only in individuals carrying SOD1 mutations but also in sporadic ALS [43]. Here, we show evidence that

accumulation of misfolded SOD1 in motor neurons may stimulate the focal proliferation and clustering of $CD34^+$ cells. This effect may be partially explained by the ability of misfolded SOD1 to act as a damage-associated molecular pattern activating TLR receptors [44,45]. $SOD1^{G93A}$ mice exhibit an improved hematopoiesis compared to mice expressing wild type SOD1, suggesting a specific effect of mutant SOD1 on hematopoietic progenitors [46]. In addition, other factors produced by motor neurons upon damage may potentially induce myeloid and microglial cell attraction and proliferation, including CSF1, MCP1, and ATP, among others [47–51]. It remains unknown whether damaged motor neurons in ALS express stromal cell-derived factor-1α (SDF-1α), which is a potent chemokine and chemoattractant interacting with CD34 and CXCR4 in hematopoietic cells [19,52,53].

In cell culture, blood myeloid precursors are non-adherent, and adherence to substrate is characteristic of differentiation into macrophages [54,55]. Here, we provide direct evidence that, in contrast to differentiated microglia which attach to the dish, $CD34^+$ cells behave as immature myeloid cells remaining in the non-adherent phase, as previously described [24]. It remains to be elucidated whether adherent fully differentiated microglia originated from a subpopulation of non-adherent $CD11b^+$ cells. In addition, cultured $CD34^+$ cells proliferated, formed clusters, and displayed the potential to differentiate into microglia after successive passages, as described for progenitor cells [24]. Further studies are needed to determine the stemness potential of $CD34^+$ cells in the spinal cord.

In conclusion, the present study identifies $CD34^+$ cells abnormally emerging in sporadic human ALS and $SOD1^{G93A}$ rat spinal cords. Our findings broaden the myeloid/microglia phenotypic diversity in motor neuron disease. The accumulation of $CD34^+$ microglia precursors around degenerating motor neurons harboring misfolded SOD1 deserves deeper mechanistic studies. $CD34^+$ cells may represent a potential cell target for therapeutic development in ALS and other neurodegenerative diseases.

4. Materials and Methods

4.1. Animals

Male $SOD1^{G93A}$ progeny, purchased from Taconic bioscience (NTac:SD-Tg($SOD1^{G93A}$)L26H), were used for further breeding to maintain the line [11]. Rats were housed in a centralized animal facility with a 12 h light-dark cycle with ad libitum access to food and water. Perfusion with fixative was performed under 90% ketamine/10% xylazine anesthesia and all efforts were made to minimize animal suffering, discomfort, or stress. All procedures using laboratory animals were performed in accordance with the national and international guidelines and were approved by the Institutional Animal Committee for animal experimentation. This study was carried out in strict accordance with the Institut Pasteur de Montevideo ethical committee's requirements (CEUA Approved protocol: #005-17 to Dr. Luis Barbeito on 2nd June 2017) and the national law (N° 18.611) for animal experimentation that follows the Guide for the Care and Use of Laboratory Animals of the National Institutes of Health (USA).

4.2. Experimental Conditions

At least 4 male rats were analyzed for the experimental condition. Non-transgenic (Non-Tg) rats were 160–180 days old, transgenic $SOD1^{G93A}$ rats developing hind limb paralysis were differentiated at the stage of disease onset (180–190 days old), and advanced paralysis (195–210 days old) defined as 15 days after disease onset.

4.3. Determination of Disease Onset and End-Stage

As described previously [56], all rats were weighed and evaluated for motor activity daily. Disease onset was determined for each animal when pronounced muscle atrophy was accompanied by an abnormal gait, typically expressed as subtle limping or dragging of one hind limb. When necessary, end-stage was defined by a lack of righting reflexes or the inability to reach food and water.

4.4. Human Tissue Collection

The collection of post-mortem human ALS and control samples was approved by The University of Alabama at Birmingham (UAB) Institutional Review Board (Approved IRB Protocol: X091222037 to Dr. Peter H. King). All ALS patients were cared for at UAB and so detailed clinical records were available. Control samples were age-matched and were harvested from patients who expired from non-neurological causes. The average collection time after death was less than 10 h. All tissues were collected by Peter H. King and Uing Si.

4.5. Human Spinal Cord Immunohistochemistry

In this study, 10 µm spinal cord paraffin sections were sliced using a microtome. Following deparaffinization, slices were blocked and permeabilized in BSA 5%/Triton X-100 0.5% for 2 h at room temperature. Primary antibodies were incubated in BSA 1%/Triton X-100 0.5% at 4 °C overnight. After washing, secondary antibodies were incubated for 3 h at room temperature. After PBS washing, Mowiol medium (Sigma, St. Louis, MO, USA) was used for mounting. Only ventral lumbar spinal cord sections were analyzed. Motor neuron somas were identified in the ventral spinal cord by typical morphology and nuclei. Saturated DAPI staining was used to better differentiate motor neuron somas as shown in Supplementary Figure S2.

4.6. Immunohistochemistry of Spinal Cord

Four percent paraformaldehyde fixed spinal cords were cryopreserved in 30% sucrose (Sigma, St. Louis, MO, USA) at 4 °C. After 72 h, tissue was embedded in Tissue-Tek (Sakura), sectioned (longitudinal) using a cryostat, and collected on gelatin-coated slides. Then, 20 µm sections were blocked for 2 h at room temperature in 5% BSA, 0.3% Triton X-100 in PBS, incubated with primary antibodies overnight at 4 °C in BSA 1%/Triton X-100 0.3%. After washing, secondary antibodies were incubated during 2 h at room temperature in BSA 1%/Triton X-100 0.3%. To determine primary antibodies' specificity, immunohistochemistry was carried out in the absence of primary antibodies. Non-significant immunofluorescence was detected with secondary antibodies incubation. DPX mounting medium (Sigma, St. Louis, MO, USA) was used for mounting. ImageJ software was used for analysis. For CD34 expression, cell density analysis was measured in the ventral horn of spinal cord images in at least 20 sections per spinal cord per animal (n = 4), as shown in Figure 1.

4.7. Co-Expression Analysis of CD34 and Myeloid Markers

The co-expression of CD34 with microglia markers Iba1, CD68, and CD11b was carried out using the maximum-intensity projections of images acquired from the ventral horn of spinal cord in at least 20 sections per spinal cord per animal among conditions (n = 4). The overlapped areas between CD34 and microglia markers were measured as previously described [57]. The number of $Ki67^+$ cells co-expressing CD34 was determined by assessment on confocal 63× microphotographs of clearly identified $CD34^+$ single cells in non-clustered $CD34^+$ areas in at least 20 sections per spinal cord per animal among conditions (n = 4).

4.8. $CD34^+$ Cell Cultures from Symptomatic $SOD1^{G93A}$ Rats

$CD34^+$ cells were obtained from a primary culture adult spinal cord of symptomatic $SOD1^{G93A}$ rats according to the procedures described by Trias et al. (2013) [9] with minor modifications. Briefly, animals were euthanized by administering an overdose of ketamine/xylazine, and the spinal cord was dissected on ice. After the meninges were removed, the spinal cord was chopped finely and dissociated with 0.25% trypsin in a calcium-free buffer for 5 min at 37 °C. Trypsin treatment was stopped by adding DMEM/10% (vol/vol) FBS in the presence of 50 µg/mL DNaseI and mechanical disaggregation by repeated pipetting. The resulting extract was passed through an 80 µm mesh to eliminate tissue debris and was then spun. The pellet was resuspended in culture medium [DMEM/10% (vol/vol) FBS, HEPES

(3.6 g/L), penicillin (100 IU/mL), and streptomycin (100 µg/mL)] and was then plated in glass-bottom p35 culture dishes for confocal microscopy or 25 cm^2 tissue culture flasks for flow cytometry analysis. Culture medium was replaced every 48 h. As described in Figure 6, the non-adherent phase of the culture was re-plated in new p35 dishes every 48 h. Before plating every passage, adherent and non-adherent cells were quantified using a Neubauer hemocytometer. Non-adherent and adherent cells were characterized by immunocytochemistry as described below. To study the number of cells in the non-adherent and adherent phase of the primary cell culture from the adult spinal cord of symptomatic $SOD1^{G93A}$ rats, after 2 days in vitro (DIV), both phases were analyzed by flow cytometry. Trypsin-EDTA, 0.05% (Thermo Fisher Scientific, Waltham, MA, USA) was used to remove adherent cells from the culture surface. Cells were analyzed using FlowJo software on an Attune NxT Flow Cytometer (Thermo Fisher Scientific, Waltham, MA, USA).

4.9. Immunocytochemical Staining of Cultured Cells

Cultured cells were fixed with 4% PFA for 20 min at 4 °C and then were washed three times with 10 mM PBS (pH 7.4). Cells were permeabilized using 0.3% Triton X-100 for 20 min. Nonspecific binding was blocked by incubating fixed cells with 5% BSA in PBS for 1 h at room temperature. Corresponding primary antibodies (see below) were diluted in blocking solution and incubated 3 h at room temperature. After washing, cells were incubated with secondary antibodies in blocking solution for 1 h at room temperature. DAPI was used for nuclei staining. At least 10 fields per plate were acquired in a confocal microscope for quantitative analysis using ImageJ software.

4.10. Antibodies Used

Primary antibodies used were: 1:200 rabbit monoclonal anti-CD34 (abcam, Cambridge, UK), 1:200 mouse monoclonal anti-CD34 (Thermo Fisher Scientific, Waltham, MA, USA), 1:300 mouse monoclonal anti-Iba1 (Millipore, Burlington, MA, USA), 1:200 mouse monoclonal CD68 (abcam, Cambridge, UK), 1:250 rat polyclonal anti-CD11b (BD Biosciences, Franklin Lakes, NJ, USA), 1:200 rabbit polyclonal anti-Ki67 (abcam, Cambridge, UK), 1:400 mouse monoclonal anti-GFAP (Sigma, St. Louis, MO, USA), 1:300 mouse monoclonal anti-S100β (Sigma, St. Louis, MO, USA), 1:300 mouse monoclonal anti-misfoldedSOD1 (MediMabs, Montreal, Northern Province, Canada), 1:400 mouse monoclonal anti-βIII-Tubulin (Millipore, Burlington, MA, USA). Secondary antibodies used were: 1:500 goat anti-rabbit-AlexaFluor546 or AlexaFluor633 (Thermo Fisher Scientific, Waltham, MA, USA), 1:500 goat anti-mouse-AlexaFluor488, AlexaFluor546, or AlexaFluor633 (Thermo Fisher Scientific, Waltham, MA, USA), 1:500 AlexaFluor633 (Thermo Fisher Scientific, Waltham, MA, USA).

4.11. Fluorescence Imaging

Fluorescence imaging was performed with a laser scanning Zeiss LSM 800 or LSM 880 confocal microscope with either a 25× (1.2 numerical aperture) objective or 63× (1.3 numerical aperture) oil-immersion objective using Zeiss Zen Black/Blue software. Maximum intensity projections of optical sections were created with Zeiss Zen software (Carl Zeiss Microscopy GmbH, Jena, Germany).

4.12. Statistics Analysis

Quantitative data were expressed as mean ± SEM. Two-tailed Mann–Whitney test or Kruskal–Wallis followed by Dunn's multiple comparison test were used for statistical analysis, with $p < 0.05$ considered significant. GraphPad Prism 7.03 software (GraphPad Software, San Diego, CA, USA) was used for statistical analyses.

Supplementary Materials: Supplementary materials can be found at http://www.mdpi.com/1422-0067/20/16/3880/s1. Table S1, Clinical characteristics of ALS and control subjects included in the study; Figure S1, Representative confocal microphotographs showing the association between CD34 and $Nissl^+$ motor neurons. Note that in Non-Tg animals, CD34 was restricted to blood vessels, while in the SOD1G93A symptomatic onset, CD34 is

expressed in cells that start to surround motor neurons. Figure S2, Representative confocal microphotographs showing motor neuron identification in the ventral horn of the lumbar spinal cord in sections stained with DAPI.

Author Contributions: Formal analysis, M.K., E.T., and L.B.; Funding acquisition, E.T., J.S.B., and L.B.; Investigation, M.K., E.T., O.H., P.H.K., and L.B.; Methodology, M.K., E.T., V.V., S.I., P.H.K., Y.S., Y.K., and L.B; Validation, E.T. and L.B.; Writing—original draft, M.K., E.T., and L.B.; Writing—review and editing, M.K., E.T., J.S.B., I.C.M., O.H., P.H.K., and L.B.

Funding: This work was supported by Institut Pasteur de Montevideo—FOCEM Mercosur (COF 03/11), the Amyotrophic Lateral Sclerosis Association (00482), Agencia Nacional de Investigación e Innovación (ANII), Programa de Desarrollo de las Ciencias Básicas (PEDECIBA), Sistema Nacional de Investigadores (SNI), and the Comisión Sectorial de Investigación Científica (CSIC), Universidad de la República, Uruguay; Grupos I+D Program, #1104.

Acknowledgments: We want to thank Tabaré de los Campos from the Microscopy Unit at Institut Pasteur de Montevideo for his assistance in imaging analysis. We also want to thank the staff from the Transgenic and Experimental Animal Unit from Institut Pasteur de Montevideo. We are grateful to our ALS patients who donated their skeletal muscle tissues post-mortem to advance ALS research.

Conflicts of Interest: Olivier Hermine is a cofounder and shareholder of AB science. Others have no conflict of interest.

References

1. Boillee, S.; Vande Velde, C.; Cleveland, D.W. ALS: A disease of motor neurons and their nonneuronal neighbors. *Neuron* **2006**, *52*, 39–59. [CrossRef]
2. Cleveland, D.W.; Rothstein, J.D. From Charcot to Lou Gehrig: Deciphering selective motor neuron death in ALS. *Nat. Rev. Neurosci.* **2001**, *2*, 806–819. [CrossRef]
3. Trias, E.; Ibarburu, S.; Barreto-Nunez, R.; Barbeito, L. Significance of aberrant glial cell phenotypes in pathophysiology of amyotrophic lateral sclerosis. *Neurosci. Lett.* **2017**, *636*, 27–31. [CrossRef]
4. Ilieva, H.; Polymenidou, M.; Cleveland, D.W. Non-cell autonomous toxicity in neurodegenerative disorders: ALS and beyond. *J. Cell Biol.* **2009**, *187*, 761–772. [CrossRef]
5. Corcia, P.; Tauber, C.; Vercoullie, J.; Arlicot, N.; Prunier, C.; Praline, J.; Nicolas, G.; Venel, Y.; Hommet, C.; Baulieu, J.L.; et al. Molecular imaging of microglial activation in amyotrophic lateral sclerosis. *PLoS ONE* **2012**, *7*, e52941. [CrossRef]
6. Henkel, J.S.; Beers, D.R.; Zhao, W.; Appel, S.H. Microglia in ALS: The good, the bad, and the resting. *J. Neuroimmune Pharm.* **2009**, *4*, 389–398. [CrossRef]
7. Liao, B.; Zhao, W.; Beers, D.R.; Henkel, J.S.; Appel, S.H. Transformation from a neuroprotective to a neurotoxic microglial phenotype in a mouse model of ALS. *Exp. Neurol.* **2012**, *237*, 147–152. [CrossRef]
8. Frakes, A.E.; Ferraiuolo, L.; Haidet-Phillips, A.M.; Schmelzer, L.; Braun, L.; Miranda, C.J.; Ladner, K.J.; Bevan, A.K.; Foust, K.D.; Godbout, J.P.; et al. Microglia induce motor neuron death via the classical NF-kappaB pathway in amyotrophic lateral sclerosis. *Neuron* **2014**, *81*, 1009–1023. [CrossRef]
9. Trias, E.; Diaz-Amarilla, P.; Olivera-Bravo, S.; Isasi, E.; Drechsel, D.A.; Lopez, N.; Bradford, C.S.; Ireton, K.E.; Beckman, J.S.; Barbeito, L. Phenotypic transition of microglia into astrocyte-like cells associated with disease onset in a model of inherited ALS. *Front. Cell. Neurosci.* **2013**, *7*, 274. [CrossRef]
10. Fendrick, S.E.; Xue, Q.S.; Streit, W.J. Formation of multinucleated giant cells and microglial degeneration in rats expressing a mutant Cu/Zn superoxide dismutase gene. *J. Neuroinflamm.* **2007**, *4*, 9. [CrossRef]
11. Howland, D.S.; Liu, J.; She, Y.; Goad, B.; Maragakis, N.J.; Kim, B.; Erickson, J.; Kulik, J.; DeVito, L.; Psaltis, G.; et al. Focal loss of the glutamate transporter EAAT2 in a transgenic rat model of SOD1 mutant-mediated amyotrophic lateral sclerosis (ALS). *Proc. Natl. Acad. Sci. USA* **2002**, *99*, 1604–1609. [CrossRef]
12. Trias, E.; Beilby, P.R.; Kovacs, M.; Ibarburu, S.; Varela, V.; Barreto-Nunez, R.; Bradford, S.C.; Beckman, J.S.; Barbeito, L. Emergence of Microglia Bearing Senescence Markers During Paralysis Progression in a Rat Model of Inherited ALS. *Front. Aging Neurosci.* **2019**, *11*, 42. [CrossRef]
13. Boillee, S.; Yamanaka, K.; Lobsiger, C.S.; Copeland, N.G.; Jenkins, N.A.; Kassiotis, G.; Kollias, G.; Cleveland, D.W. Onset and progression in inherited ALS determined by motor neurons and microglia. *Science* **2006**, *312*, 1389–1392. [CrossRef]
14. Diaz-Amarilla, P.; Olivera-Bravo, S.; Trias, E.; Cragnolini, A.; Martinez-Palma, L.; Cassina, P.; Beckman, J.; Barbeito, L. Phenotypically aberrant astrocytes that promote motoneuron damage in a model of inherited amyotrophic lateral sclerosis. *Proc. Natl. Acad. Sci. USA* **2011**, *108*, 18126–18131. [CrossRef]

15. Martinez-Palma, L.; Miquel, E.; Lagos-Rodriguez, V.; Barbeito, L.; Cassina, A.; Cassina, P. Mitochondrial Modulation by Dichloroacetate Reduces Toxicity of Aberrant Glial Cells and Gliosis in the SOD1G93A Rat Model of Amyotrophic Lateral Sclerosis. *Neurotherapeutics* **2019**, *16*, 203–215. [CrossRef]
16. Trias, E.; Ibarburu, S.; Barreto-Nunez, R.; Babdor, J.; Maciel, T.T.; Guillo, M.; Gros, L.; Dubreuil, P.; Diaz-Amarilla, P.; Cassina, P.; et al. Post-paralysis tyrosine kinase inhibition with masitinib abrogates neuroinflammation and slows disease progression in inherited amyotrophic lateral sclerosis. *J. Neuroinflammation* **2016**, *13*, 177. [CrossRef]
17. Martinez-Muriana, A.; Mancuso, R.; Francos-Quijorna, I.; Olmos-Alonso, A.; Osta, R.; Perry, V.H.; Navarro, X.; Gomez-Nicola, D.; Lopez-Vales, R. CSF1R blockade slows the progression of amyotrophic lateral sclerosis by reducing microgliosis and invasion of macrophages into peripheral nerves. *Sci. Rep.* **2016**, *6*, 25663. [CrossRef]
18. Krause, D.S.; Ito, T.; Fackler, M.J.; Smith, O.M.; Collector, M.I.; Sharkis, S.J.; May, W.S. Characterization of murine CD34, a marker for hematopoietic progenitor and stem cells. *Blood* **1994**, *84*, 691–701.
19. Sidney, L.E.; Branch, M.J.; Dunphy, S.E.; Dua, H.S.; Hopkinson, A. Concise review: Evidence for CD34 as a common marker for diverse progenitors. *Stem Cells* **2014**, *32*, 1380–1389. [CrossRef]
20. AbuSamra, D.B.; Aleisa, F.A.; Al-Amoodi, A.S.; Jalal Ahmed, H.M.; Chin, C.J.; Abuelela, A.F.; Bergam, P.; Sougrat, R.; Merzaban, J.S. Not just a marker: CD34 on human hematopoietic stem/progenitor cells dominates vascular selectin binding along with CD44. *Blood Adv.* **2017**, *1*, 2799–2816. [CrossRef]
21. Asheuer, M.; Pflumio, F.; Benhamida, S.; Dubart-Kupperschmitt, A.; Fouquet, F.; Imai, Y.; Aubourg, P.; Cartier, N. Human CD34+ cells differentiate into microglia and express recombinant therapeutic protein. *Proc. Natl. Acad. Sci. USA* **2004**, *101*, 3557–3562. [CrossRef]
22. Ladeby, R.; Wirenfeldt, M.; Dalmau, I.; Gregersen, R.; Garcia-Ovejero, D.; Babcock, A.; Owens, T.; Finsen, B. Proliferating resident microglia express the stem cell antigen CD34 in response to acute neural injury. *Glia* **2005**, *50*, 121–131. [CrossRef]
23. Graumann, U.; Ritz, M.F.; Rivero, B.G.; Hausmann, O. CD133 expressing pericytes and relationship to SDF-1 and CXCR4 in spinal cord injury. *Curr. Neurovascular Res.* **2010**, *7*, 144–154. [CrossRef]
24. Hinze, A.; Stolzing, A. Microglia differentiation using a culture system for the expansion of mice non-adherent bone marrow stem cells. *J. Inflamm.* **2012**, *9*, 12. [CrossRef]
25. Maniatis, S.; Aijo, T.; Vickovic, S.; Braine, C.; Kang, K.; Mollbrink, A.; Fagegaltier, D.; Andrusivova, Z.; Saarenpaa, S.; Saiz-Castro, G.; et al. Spatiotemporal dynamics of molecular pathology in amyotrophic lateral sclerosis. *Science* **2019**, *364*, 89–93. [CrossRef]
26. McGeer, P.L.; McGeer, E.G. Inflammatory processes in amyotrophic lateral sclerosis. *Muscle Nerve* **2002**, *26*, 459–470. [CrossRef]
27. Brettschneider, J.; Toledo, J.B.; Van Deerlin, V.M.; Elman, L.; McCluskey, L.; Lee, V.M.; Trojanowski, J.Q. Microglial activation correlates with disease progression and upper motor neuron clinical symptoms in amyotrophic lateral sclerosis. *PLoS ONE* **2012**, *7*, e39216. [CrossRef]
28. Fagan, A.M.; Gage, F.H. Mechanisms of sprouting in the adult central nervous system: Cellular responses in areas of terminal degeneration and reinnervation in the rat hippocampus. *Neuroscience* **1994**, *58*, 705–725. [CrossRef]
29. Ladeby, R.; Wirenfeldt, M.; Garcia-Ovejero, D.; Fenger, C.; Dissing-Olesen, L.; Dalmau, I.; Finsen, B. Microglial cell population dynamics in the injured adult central nervous system. *Brain Res. Brain Res. Rev.* **2005**, *48*, 196–206. [CrossRef]
30. Zhan, L.; Krabbe, G.; Du, F.; Jones, I.; Reichert, M.C.; Telpoukhovskaia, M.; Kodama, L.; Wang, C.; Cho, S.H.; Sayed, F.; et al. Proximal recolonization by self-renewing microglia re-establishes microglial homeostasis in the adult mouse brain. *PLoS Biol.* **2019**, *17*, e3000134. [CrossRef]
31. Streit, W.J.; Walter, S.A.; Pennell, N.A. Reactive microgliosis. *Prog. Neurobiol.* **1999**, *57*, 563–581. [CrossRef]
32. Schilling, M.; Besselmann, M.; Leonhard, C.; Mueller, M.; Ringelstein, E.B.; Kiefer, R. Microglial activation precedes and predominates over macrophage infiltration in transient focal cerebral ischemia: A study in green fluorescent protein transgenic bone marrow chimeric mice. *Exp. Neurol.* **2003**, *183*, 25–33. [CrossRef]
33. Tanaka, R.; Komine-Kobayashi, M.; Mochizuki, H.; Yamada, M.; Furuya, T.; Migita, M.; Shimada, T.; Mizuno, Y.; Urabe, T. Migration of enhanced green fluorescent protein expressing bone marrow-derived microglia/macrophage into the mouse brain following permanent focal ischemia. *Neuroscience* **2003**, *117*, 531–539. [CrossRef]

34. Davoust, N.; Vuaillat, C.; Cavillon, G.; Domenget, C.; Hatterer, E.; Bernard, A.; Dumontel, C.; Jurdic, P.; Malcus, C.; Confavreux, C.; et al. Bone marrow CD34+/B220+ progenitors target the inflamed brain and display in vitro differentiation potential toward microglia. *Faseb J. Off. Publ. Fed. Am. Soc. Exp. Biol.* **2006**, *20*, 2081–2092. [CrossRef]
35. Dissing-Olesen, L.; Ladeby, R.; Nielsen, H.H.; Toft-Hansen, H.; Dalmau, I.; Finsen, B. Axonal lesion-induced microglial proliferation and microglial cluster formation in the mouse. *Neuroscience* **2007**, *149*, 112–122. [CrossRef]
36. Butovsky, O.; Siddiqui, S.; Gabriely, G.; Lanser, A.J.; Dake, B.; Murugaiyan, G.; Doykan, C.E.; Wu, P.M.; Gali, R.R.; Iyer, L.K.; et al. Modulating inflammatory monocytes with a unique microRNA gene signature ameliorates murine ALS. *J. Clin. Investig.* **2012**, *122*, 3063–3087. [CrossRef]
37. Garbuzova-Davis, S.; Haller, E.; Navarro, S.; Besong, T.E.; Boccio, K.J.; Hailu, S.; Khatib, M.; Sanberg, P.R.; Appel, S.H.; Borlongan, C.V. Transplantation of human bone marrow stem cells into symptomatic ALS mice enhances structural and functional blood-spinal cord barrier repair. *Exp. Neurol.* **2018**, *310*, 33–47. [CrossRef]
38. Garbuzova-Davis, S.; Willing, A.E.; Zigova, T.; Saporta, S.; Justen, E.B.; Lane, J.C.; Hudson, J.E.; Chen, N.; Davis, C.D.; Sanberg, P.R. Intravenous administration of human umbilical cord blood cells in a mouse model of amyotrophic lateral sclerosis: Distribution, migration, and differentiation. *J. Hematother Stem Cell Res.* **2003**, *12*, 255–270. [CrossRef]
39. Garbuzova-Davis, S.; Kurien, C.; Thomson, A.; Falco, D.; Ahmad, S.; Staffetti, J.; Steiner, G.; Abraham, S.; James, G.; Mahendrasah, A.; et al. Endothelial and Astrocytic Support by Human Bone Marrow Stem Cell Grafts into Symptomatic ALS Mice towards Blood-Spinal Cord Barrier Repair. *Sci. Rep.* **2017**, *7*, 884. [CrossRef]
40. Eve, D.J.; Steiner, G.; Mahendrasah, A.; Sanberg, P.R.; Kurien, C.; Thomson, A.; Borlongan, C.V.; Garbuzova-Davis, S. Reduction of microhemorrhages in the spinal cord of symptomatic ALS mice after intravenous human bone marrow stem cell transplantation accompanies repair of the blood-spinal cord barrier. *Oncotarget* **2018**, *9*, 10621–10634. [CrossRef]
41. Forsberg, K.; Graffmo, K.; Pakkenberg, B.; Weber, M.; Nielsen, M.; Marklund, S.; Brannstrom, T.; Andersen, P.M. Misfolded SOD1 inclusions in patients with mutations in C9orf72 and other ALS/FTD-associated genes. *J. Neurol. Neurosurg. Psychiatry* **2019**, *90*, 861–869. [CrossRef]
42. Forsberg, K.; Andersen, P.M.; Marklund, S.L.; Brannstrom, T. Glial nuclear aggregates of superoxide dismutase-1 are regularly present in patients with amyotrophic lateral sclerosis. *Acta Neuropathol.* **2011**, *121*, 623–634. [CrossRef]
43. Pare, B.; Lehmann, M.; Beaudin, M.; Nordstrom, U.; Saikali, S.; Julien, J.P.; Gilthorpe, J.D.; Marklund, S.L.; Cashman, N.R.; Andersen, P.M.; et al. Misfolded SOD1 pathology in sporadic Amyotrophic Lateral Sclerosis. *Sci. Rep.* **2018**, *8*, 14223. [CrossRef]
44. Gravel, M.; Beland, L.C.; Soucy, G.; Abdelhamid, E.; Rahimian, R.; Gravel, C.; Kriz, J. IL-10 Controls Early Microglial Phenotypes and Disease Onset in ALS Caused by Misfolded Superoxide Dismutase 1. *J. Neurosci.* **2016**, *36*, 1031–1048. [CrossRef]
45. Zhao, W.; Beers, D.R.; Henkel, J.S.; Zhang, W.; Urushitani, M.; Julien, J.P.; Appel, S.H. Extracellular mutant SOD1 induces microglial-mediated motoneuron injury. *Glia* **2010**, *58*, 231–243. [CrossRef]
46. Epperly, M.W.; Fisher, R.; Rigatti, L.; Watkins, S.; Zhang, X.; Hou, W.; Shields, D.; Franicola, D.; Bayir, H.; Wang, H.; et al. Amelioration of Amyotrophic Lateral Sclerosis in SOD1(G93A) Mice by M2 Microglia from Transplanted Marrow. *Vivo* **2019**, *33*, 675–688. [CrossRef]
47. Guan, Z.; Kuhn, J.A.; Wang, X.; Colquitt, B.; Solorzano, C.; Vaman, S.; Guan, A.K.; Evans-Reinsch, Z.; Braz, J.; Devor, M.; et al. Injured sensory neuron-derived CSF1 induces microglial proliferation and DAP12-dependent pain. *Nat. Neurosci.* **2016**, *19*, 94–101. [CrossRef]
48. White, F.A.; Sun, J.; Waters, S.M.; Ma, C.; Ren, D.; Ripsch, M.; Steflik, J.; Cortright, D.N.; Lamotte, R.H.; Miller, R.J. Excitatory monocyte chemoattractant protein-1 signaling is up-regulated in sensory neurons after chronic compression of the dorsal root ganglion. *Proc. Natl. Acad. Sci. USA* **2005**, *102*, 14092–14097. [CrossRef]
49. Kwon, M.J.; Shin, H.Y.; Cui, Y.; Kim, H.; Thi, A.H.; Choi, J.Y.; Kim, E.Y.; Hwang, D.H.; Kim, B.G. CCL2 Mediates Neuron-Macrophage Interactions to Drive Proregenerative Macrophage Activation Following Preconditioning Injury. *J. Neurosci.* **2015**, *35*, 15934–15947. [CrossRef]

50. Szepesi, Z.; Manouchehrian, O.; Bachiller, S.; Deierborg, T. Bidirectional Microglia-Neuron Communication in Health and Disease. *Front. Cell. Neurosci.* **2018**, *12*, 323. [CrossRef]
51. Posfai, B.; Cserep, C.; Orsolits, B.; Denes, A. New Insights into Microglia-Neuron Interactions: A Neuron's Perspective. *Neuroscience* **2019**, *405*, 103–117. [CrossRef]
52. Bleul, C.C.; Fuhlbrigge, R.C.; Casasnovas, J.M.; Aiuti, A.; Springer, T.A. A highly efficacious lymphocyte chemoattractant, stromal cell-derived factor 1 (SDF-1). *J. Exp. Med.* **1996**, *184*, 1101–1109. [CrossRef]
53. Kucia, M.; Jankowski, K.; Reca, R.; Wysoczynski, M.; Bandura, L.; Allendorf, D.J.; Zhang, J.; Ratajczak, J.; Ratajczak, M.Z. CXCR4-SDF-1 signalling, locomotion, chemotaxis and adhesion. *J. Mol. Histol.* **2004**, *35*, 233–245. [CrossRef]
54. Klinder, A.; Markhoff, J.; Jonitz-Heincke, A.; Sterna, P.; Salamon, A.; Bader, R. Comparison of different cell culture plates for the enrichment of non-adherent human mononuclear cells. *Exp. Med.* **2019**, *17*, 2004–2012. [CrossRef]
55. Jobe, O.; Kim, J.; Tycksen, E.; Onkar, S.; Michael, N.L.; Alving, C.R.; Rao, M. Human Primary Macrophages Derived In Vitro from Circulating Monocytes Comprise Adherent and Non-Adherent Subsets with Differential Expression of Siglec-1 and CD4 and Permissiveness to HIV-1 Infection. *Front. Immunol.* **2017**, *8*, 1352. [CrossRef]
56. Trias, E.; King, P.H.; Si, Y.; Kwon, Y.; Varela, V.; Ibarburu, S.; Kovacs, M.; Moura, I.C.; Beckman, J.S.; Hermine, O.; et al. Mast cells and neutrophils mediate peripheral motor pathway degeneration in ALS. *Jci Insight* **2018**, *3*.
57. Tian, F.; Yang, W.; Mordes, D.A.; Wang, J.Y.; Salameh, J.S.; Mok, J.; Chew, J.; Sharma, A.; Leno-Duran, E.; Suzuki-Uematsu, S.; et al. Monitoring peripheral nerve degeneration in ALS by label-free stimulated Raman scattering imaging. *Nat. Commun.* **2016**, *7*, 13283. [CrossRef]

International Journal of
Molecular Sciences

MDPI

Supplementary Table S1

Table S1. characteristics of ALS and control subjects included in the study.

Subject	Age (years)	Gender	Survival (Months)	Post-mortem Tissue Processing (hours)	EMG Denervation	Disease Onset
ALS #1	63	M	44	7.0	Active and chronic	Leg
ALS #2	69	F	50	3.0	Active	Leg
ALS #3	64	M	35	6.5	Chronic	Leg
ALS #4	59	F	26	13.0	Active	Arm
ALS #5	75	M	55	4.3	Active and chronic	Bulbar
Control #1	61	M		10.0		
Control #2	68	M		19		
Control #3	59	M		9.5		

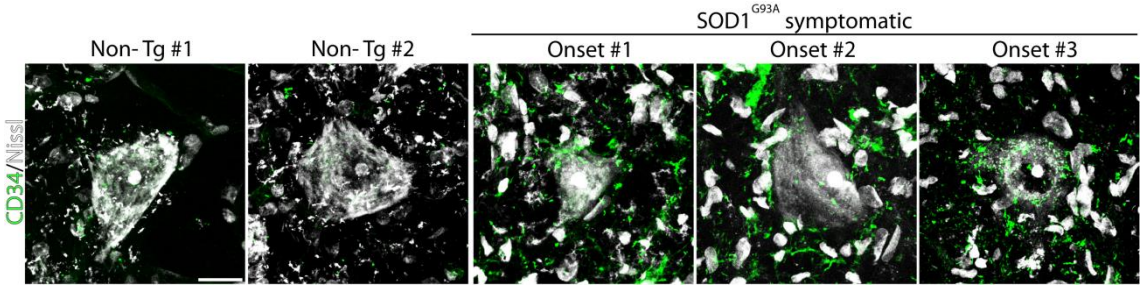

Figure S1. Representative confocal microphotographs showing the association between CD34 and Nissl+ motor neurons. Note that in Non-Tg animals, CD34 was restricted to blood vessels, while in the SOD1^{G93A} symptomatic onset, CD34 is expressed in cells that start to surround motor neurons.

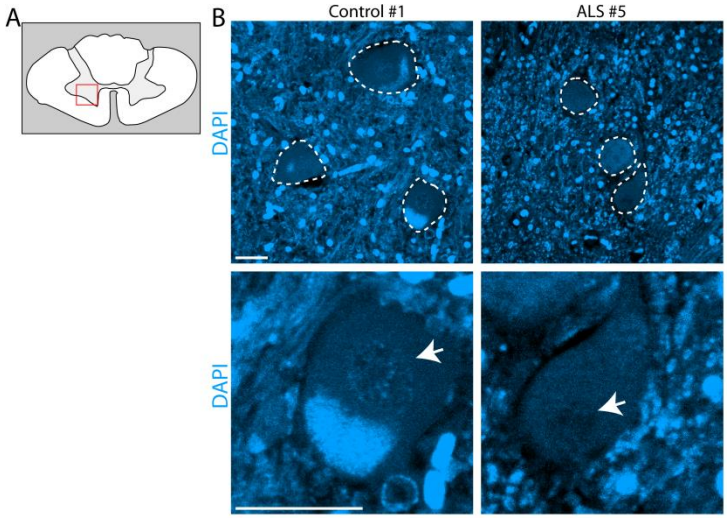

Figure S2. Representative confocal microphotographs showing motor neuron identification in the ventral horn of the lumbar spinal cord in sections stained with DAPI. (**A**) Scheme showing the human lumbar spinal cord region analyzed. (**B**) DAPI staining of one representative control and one ALS

case, showing motor neuron somas, with low and high magnification in upper and lower panels, respectively. Dotted lines indicate motor neuron cell bodies. Arrows indicate typical motor neuron nuclei. Scale bars: 50 μm.

Publicación 2

Schwann cells orchestrate peripheral nerve inflammation through the expression of CSF1, IL-34, and SCF in amyotrophic lateral sclerosis

(Las células de Schwann organizan la inflamación en nervios periféricos mediante la expresión de CSF1, IL-34, y SCF en la ELA)

Emiliano Trias, Mariángeles Kovacs, Peter H. King, Ying Si, Yuri Kwon, Valentina Varela, Sofia Ibarburu, Ivan C. Moura, Olivier Hermine, Joseph S. Beckman and Luis Barbeito.

Resumen

Las células precursoras hematopoyéticas expresan tanto el receptor CD34 como el receptor c-Kit. Luego de identificar precursores hematopoyéticos asociados a la microgliosis en la médula espinal en degeneración en la ELA, nos propusimos desafiar la hipótesis de que precursores $CD34^+$/c-Kit^+ podrían generar mastocitos, una célula mieloide efectora con reconocida actividad proinflamatoria, que participa de los procesos que llevan al establecimiento de la inflamación crónica.

Como primera aproximación, fuimos a estudiar el sistema nervioso periférico, en donde nuestro grupo había identificado previamente un número significativo de mastocitos infiltrando las raíces ventrales, el nervio ciático e incluso el músculo esquelético, en modelos murinos y pacientes con ELA.

En particular, nuestra investigación estuvo dirigida a estudiar las señales locales tróficas y quimiotácticas que actúan en la invasión y diferenciación local de mastocitos, a través del receptor c-Kit. Como el receptor CD34 no tiene un ligando bien reconocido y por tanto es muy difícil de analizar su papel funcional, nos centramos en el receptor c-Kit que identifica a precursores hematopoyéticos en la médula ósea, y a los mastocitos y sus precursores en la periferia.

El receptor c-Kit es un receptor de tirosina quinasa del grupo III y tiene como ligando a SCF, cuyo origen y su función como factor trófico de mastocitos no eran bien conocidos en la ELA. En este estudio se analizó la expresión de SCF por inmunohistoquímica e histoquímica, así como también por transcriptómica del nervio ciático y las raíces ventrales en la ELA. También se profundizó en la interacción espacial de mastocitos c-Kit^+ y células expresando SCF.

Por otro lado, pese a reconocerse a la ELA como una axonopatía distal, caracterizada por células de Schwann denervadas e infiltración de células inmunes, el rol patogénico de las células de Schwann en esta enfermedad no se conoce en profundidad, así como tampoco su interacción con células inmunes. Además de analizar la infiltración de mastocitos y sus precursores, durante este estudio analizamos los diferentes fenotipos que presentaban las células de Schwann, basados en la expresión de S100β, S100, GFAP, Isolectina y p75NTR. Además, analizamos la expresión de tres citoquinas claves en la

comunicación entre las células de Schwann y las células del sistema inmune, como son CSF-1, IL-34 y SCF.

Finalmente, es sabido que los fármacos inhibidores de tirosina quinasa han sido utilizados para modular la neuroinflamación (21,160). En particular, el masitinib, un inhibidor de la clase III de estos receptores, inhibe potentemente CSF-1R y c-Kit. Nuestro grupo ha mostrado efectos protectores de este fármaco a nivel central, mostrando un mecanismo directo sobre microglías que expresan CSF-1R. Por esta razón, durante este estudio estudiamos los efectos de masitinib para modular la neuroinflamación en el nervio ciático y raíces ventrales en ratas SOD1^{G93A}.

Resultados

- En cortes histológicos de nervio ciático de ratas SOD1^{G93A} sintomáticas (15 días post-parálisis), observamos que las células de Schwann presentan diferentes fenotipos caracterizados por la alta expresión de GFAP y S100β, en comparación con la baja expresión observada en ratas no transgénicas. La expresión de GFAP se observó principalmente en células de Schwann alargadas, con morfología que se asemeja a la observada en células de Schwann denervadas, que también se caracterizaban por la expresión de Isolectina. Por otro lado, las células de Schwann mielinizantes se caracterizaban por su típica expresión de S100β, además de S100 y p75NTR.
- La expresión de CSF-1 en tejido nervioso periférico dañado, se encuentra asociada al reclutamiento de macrófagos. En el nervio ciático de ratas SOD1^{G93A} observamos un aumento en la expresión tanto de CSF-1 como de IL-34 al inicio de la parálisis, con posterior aumento en la expresión a medida que avanza la enfermedad. Estos resultados observados por inmunohistoquímica, fueron confirmados por análisis de Western blot y RT-PCR. Mientras que CSF-1 se expresa en la subpoblación de células de Schwann mielinizantes, la expresión de IL-34 se observó en las células de Schwann denervadas. El aumento de CSF-1 e IL-34 también fue observado en el nervio ciático de pacientes con ELA, pero no así en sujetos control. A su vez, se demostró que las células de Schwann que expresan estas citoquinas, interactúan espacialmente con monocitos/macrófagos que expresan CSF-1R, el receptor de CSF-1 e IL-34.
- En el nervio ciático en degeneración, observamos precursores de mastocitos que expresan c-Kit, infiltrando el endoneuro de los nervios ciáticos en degeneración. También se observó una infiltración de mastocitos metacromáticos que expresan c-Kit, triptasa y quimasa, en el nervio ciático y en las raíces ventrales en tejido post-mortem de pacientes con ELA. Esta infiltración está acompañada de una desgranulación significativa en comparación con animales no transgénicos y tejido post-mortem de sujetos control.
- Acompañando esta infiltración de mastocitos c-Kit^{+} en el nervio ciático sintomático, también observamos, por primera vez, cambios en la expresión del ligando SCF. Se observó un aumento significativo en la inmunorreactividad de SCF en el nervio ciático de ratas SOD1^{G93A}. Además, también se observó un aumento en los niveles de ARNm de SCF en el nervio ciático sintomático de ratas SOD1^{G93A} en etapa de parálisis, comparado con animales no transgénicos.

- En particular, la expresión aumentada de SCF en el nervio ciático de ratas $SOD1^{G93A}$ sintomáticas, se observó en una subpoblación de células de Schwann $p75NTR^{+}$ con características fagocíticas, cargadas de ovoides de mielina degenerada. También se observó aumentada la expresión de SCF en monocitos y macrófagos caracterizados por la expresión de CD11b y CD68, respectivamente. En el nervio ciático de pacientes con ELA, se observó la expresión de SCF asociada a macrófagos $Iba1^{+}$ infiltrantes.
- El tratamiento con masitinib, un inhibidor específico de receptores de tirosina quinasa, como c-Kit y CSF-1R, comenzado luego del inicio clínico de los síntomas, previno de forma significativa la infiltración de mastocitos, así como de neutrófilos y macrófagos.

Conclusiones

Si bien el trabajo publicado abarca estudios más profundos que exceden al contenido de esta tesis, este estudio muestra evidencia de que la infiltración de mastocitos $c\text{-}Kit^{+}$, conjuntamente con otras células inmunes, contribuye a la constitución de una axonopatía periférica que acompaña a la degeneración de los axones motores en la ELA. Esta infiltración ocurre masivamente luego del comienzo de los síntomas y se correlaciona con la progresión de la enfermedad.

Un resultado novedoso y original de este estudio, fue que en el nervio ciático y en las raíces ventrales en la ELA, hay un aumento en la expresión de SCF tanto en las células de Schwann como en células inmunes, lo que sugiere una función quimiotáctica que explica la infiltración de mastocitos y sus precursores $c\text{-}Kit^{+}$. Este trabajo también evidenció que SCF actúa simultáneamente con otros factores tróficos como CSF-1 e IL-34, que estimulan la proliferación de monocitos/macrófagos, sugiriendo una respuesta celular inflamatoria compleja y orquestada principalmente por las células de Schwann. Sin embargo, no pudimos profundizar en el mecanismo de interacción de las células de Schwann con los mastocitos $c\text{-}Kit^{+}$, a través de SCF, utilizando modelos *in vitro*.

Finalmente, demostramos que la inhibición farmacológica de c-Kit y CSF-1R con masitinib, previno la infiltración inmune, lo que podría explicar, al menos en parte, los efectos terapéuticos de este fármaco inhibidor de receptores de tirosina quinasa observados en pacientes con ELA en varios ensayos clínicos.

Received: 4 July 2019 | Revised: 3 December 2019 | Accepted: 10 December 2019

DOI: 10.1002/glia.23768

GLIA

WILEY

RESEARCH ARTICLE

Schwann cells orchestrate peripheral nerve inflammation through the expression of CSF1, IL-34, and SCF in amyotrophic lateral sclerosis

Emiliano Trias[1] | Mariángeles Kovacs[1] | Peter H. King[2,3] | Ying Si[2,3] | Yuri Kwon[2] | Valentina Varela[1] | Sofía Ibarburu[1] | Ivan C. Moura[4,5,6,7,8,9] | Olivier Hermine[4,5,6,7,8,9,10,11,12] | Joseph S. Beckman[13] | Luis Barbeito[1]

[1]Institut Pasteur de Montevideo, Montevideo, Uruguay

[2]Department of Neurology, University of Alabama, Birmingham, Alabama

[3]Birmingham Veterans Affairs Medical Center, Birmingham, Alabama

[4]Imagine Institute, Hôpital Necker, Paris, France

[5]INSERM UMR 1163, Laboratory of Cellular and Molecular Mechanisms of Hematological Disorders and Therapeutic Implications, Paris, France

[6]Paris Descartes–Sorbonne Paris Cité University, Imagine Institute, Paris, France

[7]CNRS ERL 8254, Paris, France

[8]Laboratory of Excellence GR-Ex, Paris, France

[9]Equipe Labélisée par la Ligue Nationale contre le cancer, Paris, France

[10]AB Science, Paris, France

[11]Department of Hematology, Necker Hospital, Paris, France

[12]Centre national de référence des mastocytoses (CEREMAST), Paris, France

[13]Linus Pauling Institute, Department of Biochemistry and Biophysics, Environmental Health Sciences Center, Oregon State University, Corvallis, Oregon

Correspondence
Luis Barbeito, Institut Pasteur de Montevideo, Mataojo 2020, Montevideo 11.400, Uruguay.
Email: barbeito@pateur.edu.uy

Funding information
Grupos I+D Program, Grant/Award Number: #1104; Universidad de la República; Comisión Sectorial de Investigación Científica; Sistema Nacional de Investigadores; Programa de Desarrollo de las Ciencias Básicas (PEDECIBA); Agencia Nacional de Investigación e Innovación, Grant/Award Number: NINDS R01NS092651; Amyotrophic Lateral Sclerosis Association, Grant/Award Number: 00482; Institut Pasteur, Grant/Award Number: COF 03/11

Abstract

Distal axonopathy is a recognized pathological feature of amyotrophic lateral sclerosis (ALS). In the peripheral nerves of ALS patients, motor axon loss elicits a Wallerian-like degeneration characterized by denervated Schwann cells (SCs) together with immune cell infiltration. However, the pathogenic significance of denervated SCs accumulating following impaired axonal growth in ALS remains unclear. Here, we analyze SC phenotypes in sciatic nerves of ALS patients and paralytic SOD1^{G93A} rats, and identify remarkably similar and specific reactive SC phenotypes based on the pattern of S100β, GFAP, isolectin and/or p75^{NTR} immunoreactivity. Different subsets of reactive SCs expressed colony-stimulating factor-1 (CSF1) and Interleukin-34 (IL-34) and closely interacted with numerous endoneurial CSF-1R-expressing monocyte/macrophages, suggesting a paracrine mechanism of myeloid cell expansion and activation. SCs bearing phagocytic phenotypes as well as endoneurial macrophages expressed stem cell factor (SCF), a trophic factor that attracts and activates mast cells through the c-Kit receptor. Notably, a subpopulation of Ki67+ SCs expressed c-Kit in the sciatic nerves of SOD1^{G93A} rats, suggesting a signaling pathway that fuels SC

Ivan C. Moura author deceased on August 28, 2019.

proliferation in ALS. c-Kit+ mast cells were also abundant in the sciatic nerve from ALS donors but not in controls. Pharmacological inhibition of CSF-1R and c-Kit with masitinib in SOD1^{G93A} rats potently reduced SC reactivity and immune cell infiltration in the sciatic nerve and ventral roots, suggesting a mechanism by which the drug ameliorates peripheral nerve pathology. These findings provide strong evidence for a previously unknown inflammatory mechanism triggered by SCs in ALS peripheral nerves that has broad application in developing novel therapies.

KEYWORDS

inflammation, masitinib, peripheral nerve pathology, Schwann cells, tyrosine kinase receptors

1 | INTRODUCTION

Distal motor axonopathy is one pathological feature of amyotrophic lateral sclerosis (ALS) that underlies the progressive skeletal muscle weakness and paralysis characteristic of the disease (Fischer et al., 2004). Evidence in ALS patients and murine models expressing ALS-linked SOD1 mutations indicate that peripheral axons are lost before the death of cell bodies in the central nervous system (CNS; Fischer et al., 2004; Frey et al., 2000; Kennel, Finiels, Revah, & Mallet, 1996). Degeneration of motor axons in ALS has been associated with defective axonal transport, mitochondria function, and/or destabilization of neuromuscular junctions, among others (Arbour, Tremblay, Martineau, Julien, & Robitaille, 2015; Campanari, Garcia-Ayllon, Ciura, Saez-Valero, & Kabashi, 2016; Kong & Xu, 1998; Millecamps & Julien, 2013). The progressive loss of motor axons in ALS results in a Wallerian-like degeneration characterized by axon fragmentation, the disintegration of the axonal cytoskeleton, myelin degradation, and immune cell infiltration (Chiu et al., 2009; Fischer & Glass, 2007), representing a stereotyped response to promote axonal growth and nerve repair. Following axonal loss, Schwann cell (SCs) become denervated and adopt an undifferentiated cell phenotype with profound transcriptional reprogramming and the upregulation of cytokines, chemokines and trophic factors (Jessen & Mirsky, 2016). In nerve injury, SCs can proliferate (Chang & Winkelstein, 2011), extend long processes across the gap to guide axonal growth (Gomez-Sanchez et al., 2017) or adopt phagocytic features to remove myelin (Brosius Lutz et al., 2017; Lindborg, Mack, & Zigmond, 2017). Unlike Wallerian degeneration, peripheral nerve pathology in ALS is not solely a reparative condition because the inexorable failure in effective axonal growth leads to a chronic and progressive degenerative and inflammatory condition. In this context, there is scarce knowledge about the specific phenotypes of SCs in ALS-associated degenerating peripheral nerves, in animal models or humans.

During Wallerian degeneration, a first step in the removal of myelin debris involves phagocytic SCs. This is followed by a second wave of phagocytic macrophages that are recruited by cytokines released by denervated SCs, such as LIF and MCP1 (Bigbee, Yoshino, & DeVries, 1987; Hirata & Kawabuchi, 2002; Stoll, Griffin, Li, & Trapp, 1989; Tofaris, Patterson, Jessen, & Mirsky, 2002). In turn, recruited macrophages become a source of secreted cytokine and trophic factor release, inducing a complex inflammatory cascade (Stratton et al., 2018; Tomlinson, Zygelyte, Grenier, Edwards, & Cheetham, 2018). Mast cells are also recruited (Esposito, De Santis, Monteforte, & Baccari, 2002), orchestrating complex vascular and immune cell responses, including the chemoattraction of phagocytic neutrophils that further contribute to myelin clearance (Lindborg et al., 2017). In comparison, ALS nerve pathology similarly involves reactive changes in SCs (Keller, Gravel, & Kriz, 2009) as well as the recruitment of monocytes, macrophages, mast cells, and neutrophils (Chiu et al., 2009; Trias et al., 2018; Van Dyke et al., 2016).Such immune cell infiltration of the peripheral motor pathways in ALS has been linked to both protective and deleterious effects on motor neuron degeneration and disease progression (Nardo et al., 2016). However, the functional link between SCs and immune cell influx to degenerating peripheral nerves in ALS remains unknown.

Of therapeutic interest in ALS, it has been demonstrated that downregulation of inflammation by tyrosine kinase inhibitor drugs such as GW2580 or masitinib is associated with decreased spinal nerve pathology and NMJ denervation, and prolonged survival in rodent models of ALS (Martinez-Muriana et al., 2016; Trias et al., 2016; Trias et al., 2018). In particular, masitinib has successfully completed a randomized, controlled, phase 2/3 trial in ALS patients, showing a significant and clinically meaningful benefit for masitinib over placebo in relevant measures of disease progression (Mora et al., 2019). Thus, analysis of the cellular targets of masitinib in ALS peripheral nerve pathology may provide valuable information about disease mechanisms. Masitinib potently inhibits the ATPase subunit of CSF-1R and c-Kit receptors, both belonging to Class III receptor tyrosine kinases (Anastassiadis, Deacon, Devarajan, Ma, & Peterson, 2011; Dubreuil et al., 2009). CSF-1R and c-Kit are typically expressed in myeloid cells and mast cells, respectively (Galli, Tsai, & Wershil, 1993; Stanley & Chitu, 2014). In SOD1^{G93A} rats developing paralysis, masitinib downregulates mast cells and neutrophil infiltration in both the sciatic nerve and skeletal muscle motor nerve terminals (Trias et al., 2017; Trias et al., 2018). In addition, masitinib decreases CSF-1R-dependent microgliosis in the lumbar spinal cord, suggesting a multitarget and multifaceted effect involving various inflammatory pathways in the central and peripheral nervous systems (Trias et al., 2016). However,

there is little understanding of the specific cellular mechanisms that mediate the recruitment of CSF-1R- and c-Kit-expressing immune cells in the ALS peripheral nerve.

CSF1 and IL-34 are the two endogenous cognate ligands of CSF-1R, which upon activation stimulates monocyte/macrophage differentiation pattern and the acquisition of a phagocytic phenotype (Boulakirba et al., 2018). On the other hand, SCF is the ligand of c-Kit, which in peripheral tissues is mainly expressed in mast cells (Iemura, Tsai, Ando, Wershil, & Galli, 1994). SCF/c-Kit signaling drives chemoattraction of mast cell precursors, their differentiation into mature mast cells and ultimate degranulation, with the release of inflammatory and vasoactive molecules (Galli et al., 1993). Mast cells are key in orchestrating chronic inflammation and immune cell infiltration (Metz et al., 2007) and recently have been reported to extensively infiltrate the muscle and sciatic nerve of ALS patients and SOD1^{G93A} rats (Trias et al., 2017; Trias et al., 2018). The cellular sources of CSF1, IL-34, and SCF in ALS peripheral nerves remain largely unknown.

Here, we have analyzed the cellular localization of cytokines CSF1, IL-34, and SCF expressed in sciatic nerves of ALS patients and SOD1^{G93A} rats. We report for the first time, the upregulation of the three ligands in specific subsets of SCs, which are spatially associated with macrophages and mast cells expressing CSF-1R and c-Kit, respectively. Notably, a subset of proliferating SCs expressed c-Kit. Finally, systemic pharmacological inhibition of CSF-1R and c-Kit by masitinib sharply decreased SC reactivity, immune cell infiltration and proliferation along the peripheral motor pathways, providing evidence for an inflammatory mechanism triggered by SCs that can be therapeutically targeted in ALS.

2 | MATERIALS AND METHODS

2.1 | Animals

Male SOD1^{G93A} progeny were used for further breeding to maintain the line. Rats were housed in a centralized animal facility with a 12-hr light-dark cycle with ad libitum access to food and water. Perfusion with fixative was performed under 90% ketamine—10% xylazine anesthesia and all efforts were made to minimize animal suffering, discomfort or stress. All procedures using laboratory animals were performed in accordance with the national and international guidelines and were approved by the Institutional Animal Committee for animal experimentation (CEUA Approved protocol: #005-17 to Dr. Luis Barbeito). This study was carried out in strict accordance with the Institut Pasteur de Montevideo Committee's requirements and under the current ethical regulations of the Uruguayan Law N°18.611 for animal experimentation that follow the Guide for the Care and Use of Laboratory Animals of the National Institutes of Health (USA).

2.2 | Experimental conditions

At least five rats were analyzed for each experiment. Four different conditions were studied as follow: (a) nontransgenic (NonTg) rats of 160–180 days; (b) transgenic SOD1^{G93A} rats of 180–190 days (symptomatic, onset); (c) transgenic SOD1^{G93A} rats of 195–210 days treated with vehicle (paralysis, 15d-vehicle); and (d) transgenic SOD1^{G93A} rats of 195–210 days treated with 30 mg/kg/day of masitinib during 15 days (paralysis, 15 days-masitinib).

2.3 | Determination of disease onset

All rats were weighed and evaluated for motor activity daily as described (Trias et al., 2016, 2017). Disease onset was determined for each animal when pronounced muscle atrophy was accompanied by an abnormal gait, typically expressed as subtle limping or dragging of one hind limb.

2.4 | Masitinib administration

As described previously (Trias et al., 2017, 2018), only transgenic rats showing weakness and gait alterations in hind limbs as the first clinical sign were selected for masitinib treatment studies. Male rats were divided randomly into the masitinib or vehicle-treated groups. Masitinib mesylate (AB1010), freshly prepared in drinking sterilized water, was administrated daily at a dose of 30 mg/kg using a curved stainless steel gavage needle with 3-mm ball tip. Dosing was defined in accordance to previous studies in the same rat model of ALS that was shown to be safe for chronic treatments (Trias et al., 2016, 2017). Rats were treated from Day-1 post-paralysis for an additional 15 days, when they were then euthanized.

2.5 | Sciatic nerve and ventral roots cryopreserved sections

Paraformaldehyde (4%) fixed sciatic nerve and ventral roots were cryopreserved in 30% sucrose (Sigma) at 4°C. The 72 hr preserved sciatic nerve was embedded in TissueTek (Sakura), sectioned (longitudinal and transverse) at 10 μm using a cryostat, and collected on gelatin-coated slides.

2.6 | Immunohistochemistry of SOD1^{G93A} rat sciatic nerve and ventral root slices

Longitudinal sciatic nerve sections and cross sections of ventral roots were blocked for 2 hr at room temperature (5% BSA, 0.5% Triton X-100 in PBS), incubated with primary antibodies overnight at 4°C in 1% BSA, 0.3%Triton X-100 in PBS. Antibodies used were: 1:250 rat polyclonal anti-c-Kit-biotin (abcam, #ab25022), 1:200 mouse anti-Tryptase (abcam, #ab134932), 1:300 mouse-anti Chymase (abcam, #ab111239), 1:200 mouse monoclonal anti-CD11b (BD Bioscience, #BD550299), 1:200 rabbit polyclonal anti-CSF-1R (Santa Cruz Biotechnology, #sc-692), 1:200 mouse monoclonal anti-CSF-1R (Santa Cruz Biotechnology, #sc-46662), 1:250 mouse monoclonal anti-CD68

(abcam, #ab31630), 1:300 Isolectin-Biotin probe (Thermo Fisher Scientific, #I21414), 1:400 mouse monoclonal anti-GFAP (Sigma, #G3893), 1:400 rabbit polyclonal anti-GFAP (Sigma, #G9269), 1:300 mouse monoclonal anti-S100β (Sigma, #S2532), 1:300 mouse monoclonal anti-neurofilament200-AlexaFluor555 (Thermo Fisher Scientific, #MAB5256A5), 1:200 rabbit polyclonal anti-IL34 (Santa Cruz Biotechnology, #sc-135176), 1:250 rabbit polyclonal anti-CSF1 (Thermo Fisher Scientific, #PA5-42558), 1:300 Myelin-AlexaFluor488 or AlexaFluor546 probes (Thermo Fisher Scientific, #F34652), 1:250 rabbit polyclonal SCF (Thermo Fisher Scientific, #PA5-20746), 1:250 rabbit polyclonal anti-$p75^{NTR}$ (abcam #ab8874), 1:300 mouse monoclonal anti-S100 (Dako, Z0311), 1:200 rabbit polyclonal anti-Iba1 (Wako, #019-19741), 1:300 rabbit polyclonal anti-Ki67 (abcam, #ab16667). After incubation with primary antibodies, slices were washed with PBS 3 times for 10 min, incubated with secondary antibodies for 2 hr at room temperature, 1:500 goat anti-rabbit-AlexaFluor488 (Thermo Fisher Scientific, #A21052), 1:500 goat anti-mouse-AlexaFluor546 (Thermo Fisher Scientific, #A11035), 1:500 goat anti-mouse-AlexaFluor633 (Thermo Fisher Scientific, #A21052), 1:500 Streptavidin-AlexaFluor405 or AlexaFluor633 (Thermo Fisher Scientific, #S21375), washed with PBS three times for 5 min, and mounted in DPX mounting medium (Sigma). The specificity of CSF1, IL-34, and SCF antibodies was determined by performing antibody preincubation with CSF1, IL-34, and SCF proteins (ProsPec, #CYT-856, # CYT-863, and #CYT-323, respectively) at a 1:5 ratio antibody/ligand concentration (Figure S2).

2.7 | Histochemistry quantitative analysis

For cytokines density analysis, CSF1, IL-34, and SCF density analysis were measured using ImageJ as previously described (Trias et al., 2018). At least 20 sections per sciatic nerve per animal (n = 4) were analyzed. The number of CSF-1R, CD11b, CD68+, Iba1+, c-Kit+, and Ki67+ cells infiltrating the sciatic nerve and ventral roots of $SOD1^{G93A}$ rats were counted in ×25 and ×63 (for ventral roots) magnification confocal images using the ImageJ software. At least 20 confocal stacks ($320 \times 320 \times 10$ μm in Z) from four animals among conditions were analyzed. For SC density analysis in the ventral roots, GFAP/S100β density analysis was measured using ImageJ as previously described (Trias et al., 2018).

2.8 | Human tissue collection

The collection of postmortem human ALS and control samples was approved by the University of Alabama, Birmingham (UAB) Institutional Review Board. (Approved IRB Protocol: X091222037 to Dr. Peter H. King) All ALS patients were cared for at UAB and so detailed clinical records were available. Control samples were age-matched and were harvested from patients who expired from non-neurological causes. The average collection time after death was less than 10 hr. All tissues were harvested by PHK and YS at the time of autopsy and preserved within 30 min. Control sciatic nerve tissues were obtained from the National Disease Research Interchange (NDRI).

2.9 | Human sciatic nerve and ventral root immunohistochemistry

Sciatic nerve and ventral root paraffin sections were sliced (10 μm) using a microtome. Following deparaffinization, slices were blocked and permeabilized in 5% BSA/0.5% Triton X-100 for 2 hr at room temperature. Primary antibodies were incubated in 1% BSA/0.5% Triton X-100 at 4°C overnight. Primary antibodies used were described. After washing, secondary antibodies were incubated for 3 hr at room temperature. After PBS washing, Mowiol medium (Sigma-Aldrich) was used for mounting.

2.10 | Toluidine blue staining of the human sciatic nerve

For the mast cell analysis based in metachromasia observation, as previously described (Trias et al., 2018), 10 μm sections of paraffin-embed human sciatic nerves were microtome sliced and mounted in positive-charged slides. Slides were deparaffinized before starting staining. Sections were washed and hydrated two times in distilled water for 10 min and embedded in 1% toluidine blue solution for 20 min. Then, slides were washed in distilled water three times 5 min and dehydrated during 3 min in 70% ethanol, 3 min in 95% ethanol, and finally 2 min in 100% ethanol. Slides were cleared in xylene twice, 3 min each and finally mounted in DPX (Sigma). ×10, ×20, and ×100 images were acquired using an Olympus CX41 microscope connected to a EvolutionTMLC Color camera and using ImagePro Express software for acquisition.

2.11 | Real-time PCR analysis of the proximal sciatic nerve

At least 4 proximal sections of sciatic nerve were dissected from NonTg and $SOD1^{G93A}$ symptomatic rats. Tissue was processed for each mRNA extraction using Trizol Reagent (Thermo Fisher) and the aqueous phase was further purified using the RNeasy Mini kit (QIAGEN) according to the manufacturer's instructions. mRNA yields were measured on Nanodrop device (Thermo Scientific) and cDNA were obtained from 0.5 μg of RNA (−80°C), 4 μl of iScript reverse transcription Supermix for RT-qPCR (BIORAD, −20°C) in a final volume of 20 μl filled with nuclease free water. The Thermo cycler was set as follows: priming 5 min at 25°C followed by 20 min at 46°C for reverse transcription and 1 min at 95°C for RT inactivation. RT-qPCR was performed on reverse transcribed cDNA using SsoAdvanced™ Universal SYBR® Green Supermix (BIO-RAD) on a Step One Plus Real-Time PCR System. For each well, 2 μl of diluted DNA was added

to 8 μl of mix (containing 1 μl of each primer, 5 μl of SsoAdvanced™ Universal SYBR® Green Supermix, 1 μl of nuclease free water). Each sample was run in triplicate. The cycling parameters were as follows: 10 min at 95°C then 40 cycles at 95°C for 15 s and 1 min at 60°C. Cq values were obtained for every cycle. Primers were designed on NCBI Primer-BLAST following the best guidelines to exclude genomic DNA amplification. The analysis was done using the StepOne Software. Variations between samples were normalized using hypoxanthine-guanine phosphoribosyl transferase (HPRT) as a housekeeping gene. All primers were validated for specificity and efficiency. Primers used are:

CS1-Fw: 5′-AAAGTTTGCCTCGGTGCTCTC-3′
CSF1-Rv: 5′-TTCGTTCGCTTCCTTGCTCG-3′.
IL-34-Fw:5′-TCTTGCTGCAAACAAAGTCCC-3′
IL-34-Rv: 5′ACACGTTGGTAGCTGCACAT-3′.
SCF-Fw: 5′-TCCTCTCGTCAAAACTCAGGA-3′
SCF-Rv: 5′-CGGCGACATAGTTGAGGGTT-3′.
HPRT-Fw: 5′-GTCATGTCGACCCTCAGTCC-3′
HPRT-Rv: 5′-GCAAGTCTTTCAGTCCTGTCC-3′.

2.12 | Western blot analysis

For protein extraction, proximal sciatic nerves from four non-transgenic and four symptomatic animals were dissected and homogenized in lysis buffer (50 mM HEPES pH 7.5, 50 mM NaCl, 1% Triton X-100, and complete protease inhibitor mixture (Roche, #11873580001), and then sonicated three times for 3 s. Protein concentration was measured with a Bicinchoninic Acid (BCA) kit (Sigma, #QPBCA). Then, protein extracts were placed in loading buffer containing 15% SDS, 0.3 M Tris pH 6.8, 25% Glycerol, 1.5 M β-mercaptoethanol and 0.01% Bromphenol Blue. Protein samples (30 μg) were resolved on 12% SDS-polyacrylamide gel and transferred to PVDF membrane (Thermo, #88518). Membranes were blocked for 1 hr in Tris-buffered saline (TBS), 0.1% Tween-20, and 5% BSA, followed by overnight incubation at 4°C with the correspondent primary antibody diluted in the same buffer. Primary antibodies used in this study were rabbit anti-CSF1 (Thermo Fisher Scientific, #PA5-42558) and rabbit anti-IL34 (MBS, #2001373). After washing with 0.1% Tween in TBS, membranes were incubated with peroxidase-conjugated secondary antibody, goat anti-rabbit IgG to (Abcam, #ab6721) for 1 hr, washed and developed using the SuperSignal West Pico Chemiluminiescent Substrate (Thermo Fisher Scientific, #34080). αActin was used as housekeeping. For αActin membranes were stripped according to the Mild Stripping protocol from Abcam and then were incubated with mouse anti-αActin antibody (SIGMA #A5441). After washing with 0.1% Tween in TBS, the membranes were incubated with secondary antibody, goat anti-mouse IgG (Abcam, #ab6728), and developed. All antibodies were used at dilutions recommended by the manufacturers. The images were obtained with Syngene GBox-Chemi 16 Bio Imaging System and densitometry was analyzed using ImageJ.

2.13 | Fluorescence imaging

Fluorescence imaging was performed with a laser scanning Zeiss LSM 800 or LSM 880 confocal microscope with either a ×25 (1.2 numerical aperture) objective or ×63 (1.3 numerical aperture) oil-immersion objective using the Zeiss Zen Black software. Maximum intensity projections of optical sections were created with the Zeiss Zen software. Maximum intensity projections of optical sections, as well as 3D reconstructions, were created with the Zeiss Zen software.

2.14 | Statistics analysis

Quantitative data were expressed as mean ± *SEM*. Two-tailed Mann–Whitney test or Kruskal–Wallis followed by Dunn's multiple comparison test were used for statistical analysis, with $p < .05$ considered significant. The GraphPad Prism 7.03 software was used for statistical analyses.

3 | RESULTS

3.1 | Characterization of SCs in the ALS degenerating sciatic nerve

Previous studies on ALS postmortem peripheral nerve pathology have provided scarce information on SC phenotypes (Nardo et al., 2016; Riva et al., 2016). We examined SCs by immunohistochemical analysis of three nerve specimens from ALS subjects and three control donors, as well as one ALS ventral root specimen. Table 1 shows the characteristics of ALS patients and control subjects.

In longitudinal and transversal sections of the sciatic nerves from control donors, SCs were identified by S100β immunohistochemistry, with typical staining restricted to Schmidt–Lanterman clefts (Figure 1a-b). GFAP staining was low or absent in sections from control nerves. In contrast, all ALS specimens displayed a robust increase in both GFAP and S100β staining (Figure 1c,d), suggesting a significant SC reactivity. In longitudinal sections, GFAP staining labeled elongated SCs with a morphology resembling denervated or repair nonmyelinating SCs (Figure 1c). S100β labeled a different subset of SCs, the morphology of which resembled myelinating or remyelinating SCs (Figure 1c, lower panel). These SC phenotypes are similar to those observed in Wallerian degeneration (Gomez-Sanchez et al., 2017). A similar pattern of differential GFAP and S100β staining in SC subsets was observed in sciatic nerve sections from two other ALS patients and in one ventral root specimen (Figure 1d,e).

Understanding how specific SC phenotypes develop during active motor axon degeneration in $SOD1^{G93A}$ rats may allow a better understanding of nerve pathology in ALS. Sciatic nerves from nontransgenic control rats showed low GFAP expression in a few nonmyelinating SCs and the typical S100β staining of myelinating SCs restricted to

Subject	Age[a] (years)	Gender	Disease onset	Survival[b] (months)	Cause of death
ALS #1	69	F	Leg	52	-
ALS #2	40	M	Arm	63	-
ALS #3	76	M	Bulbar	32	-
ALS #4	75	M	Leg	58	-
Control #1	64	M	-	-	Cardiac
Control #2	79	M	-	-	Cardiac
Control #3	74	F	-	-	Stroke

[a]Age of death.
[b]From onset to death.

TABLE 1 Clinical characteristics of amyotrophic lateral sclerosis and control subjects included in the study

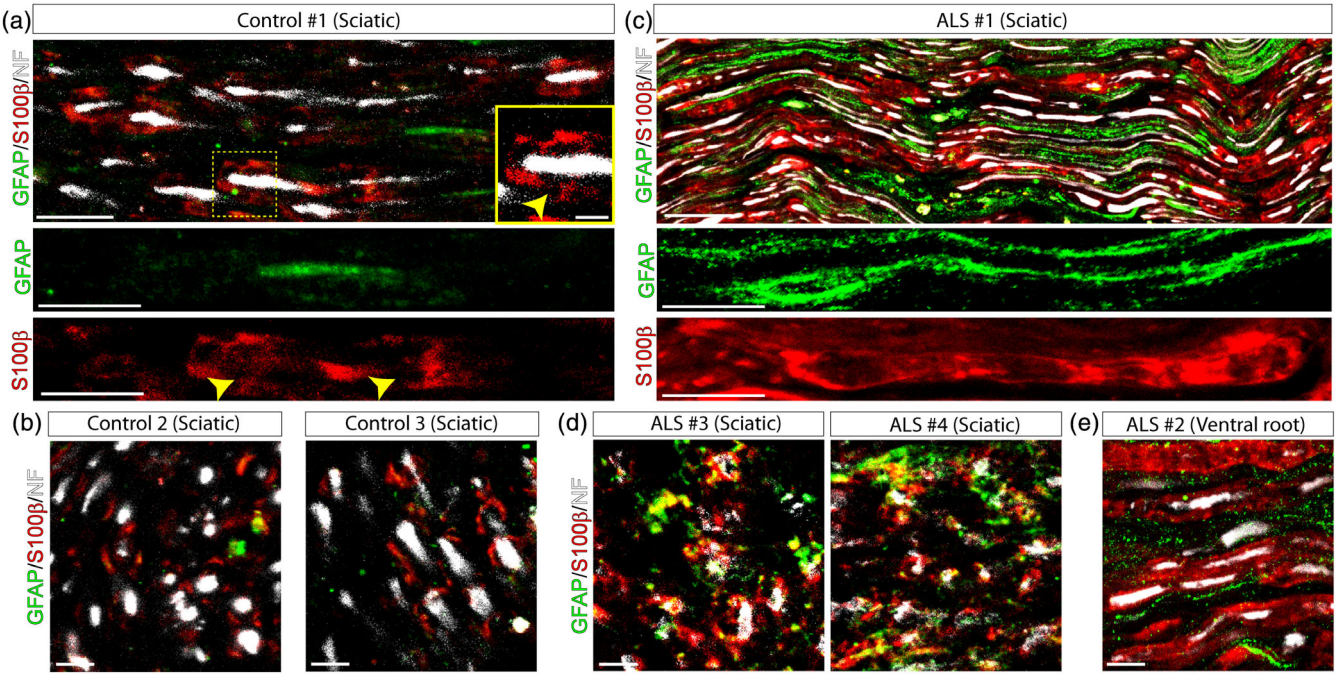

FIGURE 1 Schwann cell (SC) phenotypes in the sciatic nerve of amyotrophic lateral sclerosis (ALS) patients. GFAP and S100β immunofluorescence confocal characterization of SCs in 10 μm sections of the sciatic nerve and one ventral root of ALS patients as compared with control donors. (a,b) Three sciatic nerves from control donors were analyzed in longitudinal sections (upper panels) and cross-sections (lower panels). Note low GFAP expression, while S100β was restricted to Schmidt—Lanterman clefts (yellow arrowheads in inset). (c,d) Four sciatic nerves from ALS patients were analyzed in longitudinal and cross-sections. Note GFAP and S100β increase in denervated and myelinating SCs, respectively, labeling different subsets of cells. (e) In comparison, GFAP and S100β were also expressed in different subsets of SCs in the ventral root from one ALS patient. Scale bars: 100 μm in (a,c), 10 μm in (b–e) [Color figure can be viewed at wileyonlinelibrary.com]

Schmidt-Lanterman clefts (Figure 2a), the morphology being closely similar to human control cases. Also, the SOD1^{G93A} rat sciatic nerve analyzed either at hind limb paralysis onset or advanced paralysis, largely reproduced the SCs pathology observed in ALS subjects, with a robust upregulation of S100β and the appearance of a variety of SC phenotypes expressing GFAP (Figure 2a). As depicted in Figure 2b, SCs bearing S100β+ and GFAP+ represent two different cell populations corresponding to myelinating and denervated SCs, respectively. Denervated SCs were also identified by isolectin immunoreactivity, and myelin-laden SCs by S100 and p75^{NTR} immunoreactivity (Figure 2b).

3.2 | SCs express of CSF1 and IL-34 in the ALS sciatic nerve

Previous reports have shown the expression of CSF1 in damaged peripheral nerve tissue associated with local recruitment of macrophages (Groh et al., 2012). In ALS rodent models, drugs inhibiting CSF-1R therapeutically decreased monocyte/macrophage infiltration (Martinez-Muriana et al., 2016), suggesting that locally expressed CSF1 and IL-34 are cognate CSF-1R ligands. As shown in Figure 3a,e, CSF1 and IL-34 were barely expressed in nerves from nontransgenic rats. In comparison, SOD1^{G93A} rats showed

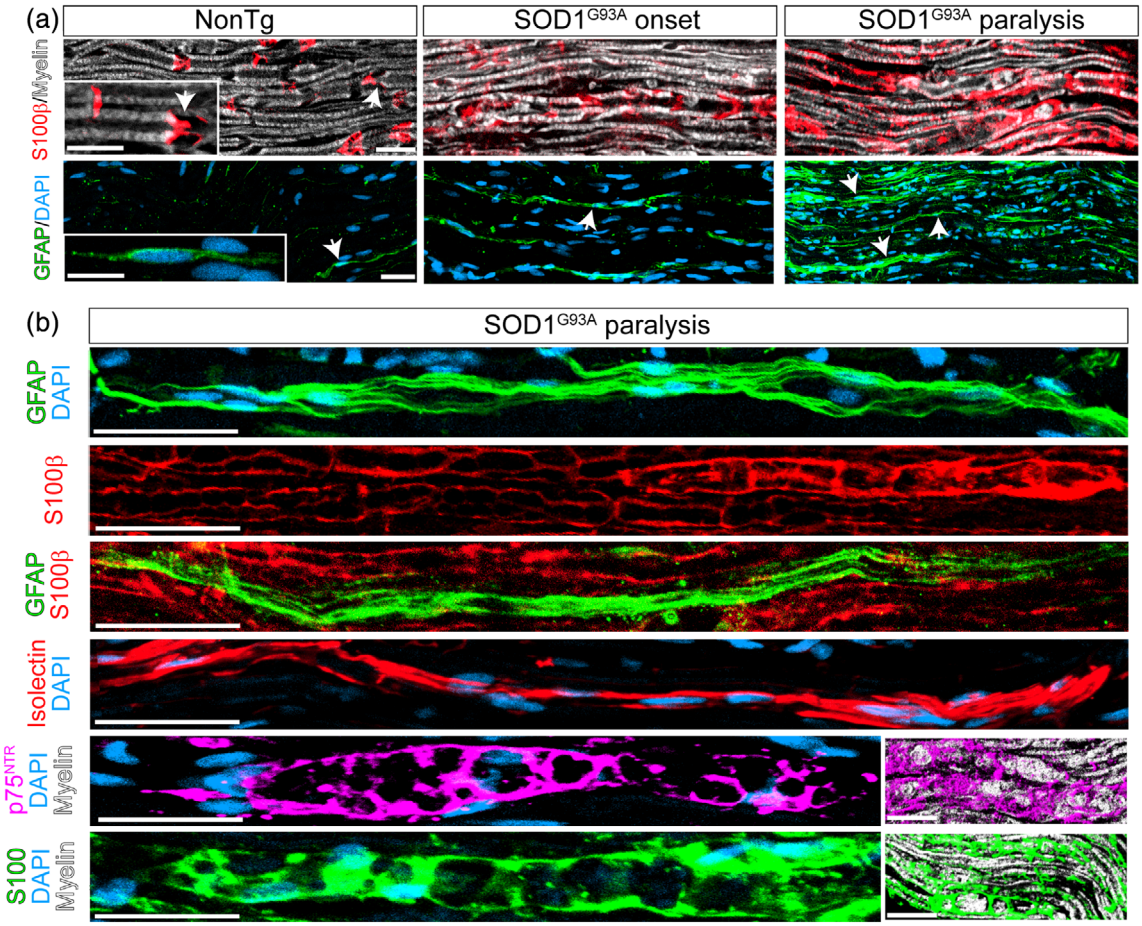

FIGURE 2 Schwann cell (SC) phenotypes in the sciatic nerve of SOD1^{G93A} rats during paralysis progression. Confocal immunostaining analysis of SC phenotypes in 10 μm sciatic nerve sections at onset and advanced paralysis as compared with nontransgenic littermates. (a) S100β and GFAP staining among conditions. Note S100β and GFAP expression restricted to Schmidt–Lanterman clefts (inset in the upper panel, white arrows) and Remak-like cells (arrow in the inset of lower panel), in NonTg rats, respectively, while both sharply increased during the course of the paralysis. (b) Confocal Immunophenotyping of SCs subpopulation in SOD1^{G93A} symptomatic rats. Note that GFAP and Isolectin label denervated SCs, while S100, S100β, and p75^{NTR} label phagocytic or myelin-laden SCs (insets). Scale bars: 20 μm in (a) and 50 μm in (b) [Color figure can be viewed at wileyonlinelibrary.com]

robust endoneurial expression of CSF1 and IL-34 at paralysis onset, which further increased by five to six-fold at advanced paralysis (Figure 3b,f). Upregulation of CSF1 and IL-34 in the degenerating SOD1^{G93A} rat sciatic nerves was further confirmed by RT-PCR and Western blot analysis (Figure 3c,d,g,h; Figure S1).

CSF1 was mainly expressed by a subset of phagocytic SCs typically engulfing myelin debris and stained with S100, S100β, or p75^{NTR} (Figure 3i, Figure S3). In comparison, IL-34 was mainly expressed in a subset of denervated SCs (GFAP+/Isolectin+) with the morphology of repair SCs (or Bungner cells), aligned on the apparent trajectory of degenerating axons (Figure 3j, Figure S3). In symptomatic SOD1^{G93A} rats, CSF1 and IL-34 were also localized in a subset of axons colocalizing with neurofilament staining (Figure S4).

In the sciatic nerves from ALS donors, CSF1 and IL-34 were upregulated in the endoneurium as compared with weak immunoreactivity in control subjects (Figure 3k). While, the exact cellular localization of CSF1 and IL-34 in postmortem tissues was not precise, in some ALS nerve specimens, CSF1 and IL-34 were localized in elongated SC-like cells.

3.3 | SCs spatially interact with CSF-1R+ monocytes/macrophages

In the degenerating sciatic nerves of SOD1^{G93A} rats, SCs were typically surrounded by clusters of CSF-1R+ macrophages (Figure 4a). CSF-1R immunoreactivity sharply increased by 10- and 20-fold at onset and advanced paralysis, respectively, when compared to nontransgenic rats (Figure 4a and Figure S5a). Most CSF-1R immunoreactivity was found in the surface of small myeloid cells expressing CD68 or CD11b (Figure 4b and Figure S5b) but not in myelin-laden phagocytic CD68+ macrophages (Figure 4c), suggesting CSF-1R expression in newly infiltrating monocyte/macrophages cells but not in fully differentiated macrophages.

Next, we addressed whether CSF-1R immune cells infiltrate the sciatic nerve of ALS patients. Figure 4d shows the immunostaining of CSF-1R and CD68 in one sciatic and one ventral root from ALS patients, compared with control donors. CSF-1R+ immune cells infiltrated the ALS tissue in both the sciatic nerve and the ventral root but not in control donors (Figure 4d).

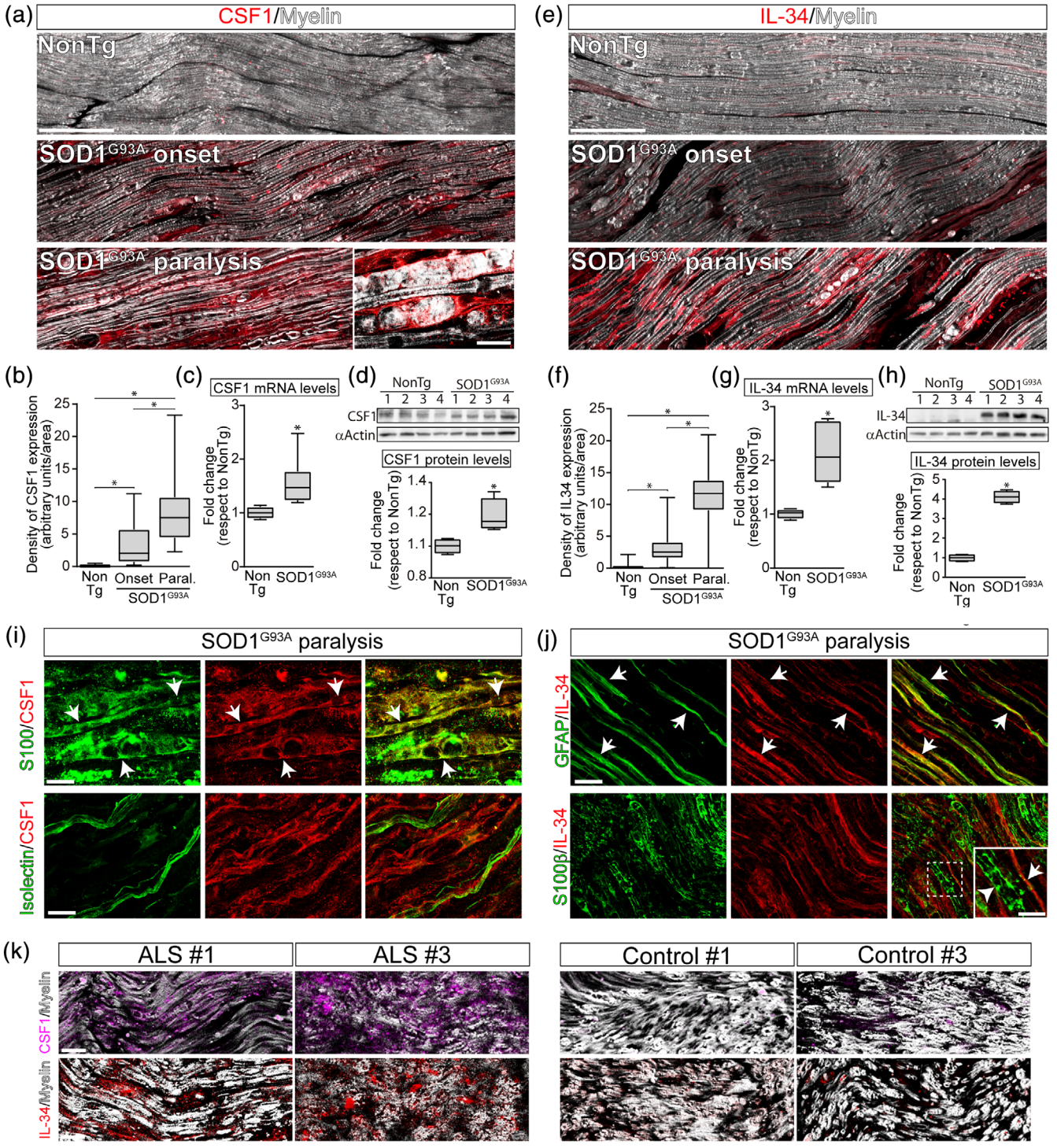

FIGURE 3 Schwann cells (SCs) upregulate CSF1 and IL-34 in SOD1^{G93A} sciatic nerve. (a) Immunohistochemical analysis of CSF1 expression in proximal sciatic nerve longitudinal sections during the course of the paralysis. Inset shows the characteristic phenotype of a phagocytic SCs expressing CSF1. (b) Quantitative analysis of the immunoreactivity for CSF1. (c,d) Analysis of mRNA and protein levels of CSF1 by RT-PCR and western blot in proximal sciatic nerves. The graph below shows western blot quantitative analysis. (e) Immunohistochemical analysis of Il-34 expression in proximal sciatic nerve longitudinal sections during the course of the paralysis. (f) Quantitative analysis of the immunoreactivity for IL-34. (g,h) Analysis of mRNA and protein levels of IL-34 by RT-PCR and western blot in proximal sciatic nerves. The graph below shows western blot quantitative analysis. (i,j) Identification of SCs expressing CSF1 (i) and IL-34 (j) in longitudinal sections of sciatic nerves during advanced paralysis in SOD1^{G93A} rats. Note that CSF1 is mainly expressed in phagocytic S100+ SCs (white arrows) but not in denervated Isolectin+ SCs (lower panels), while IL-34 was mainly expressed in denervated GFAP+ SCs (white arrows). (k) Longitudinal sections of sciatic nerve showing the immunostaining analysis of CSF1 (magenta, upper panels) and IL-34 (red, lower panels) expression in amyotrophic lateral sclerosis patients and controls. All data are expressed as mean ± *SEM*; data were analyzed by Kruskal-Wallis followed by Dunn's multiple comparison test (b,f) or Mann–Whitney test (c,d,g,h), $p < .05$ was considered statistically significant. $n = 4/6$ animals/condition. Scale bars: 100 μm in (a), 10 μm in (c,d). Scale bars: 100 μm in (a) and (e), 10 μm in (i) and (j), 25 μm in (k) [Color figure can be viewed at wileyonlinelibrary.com]

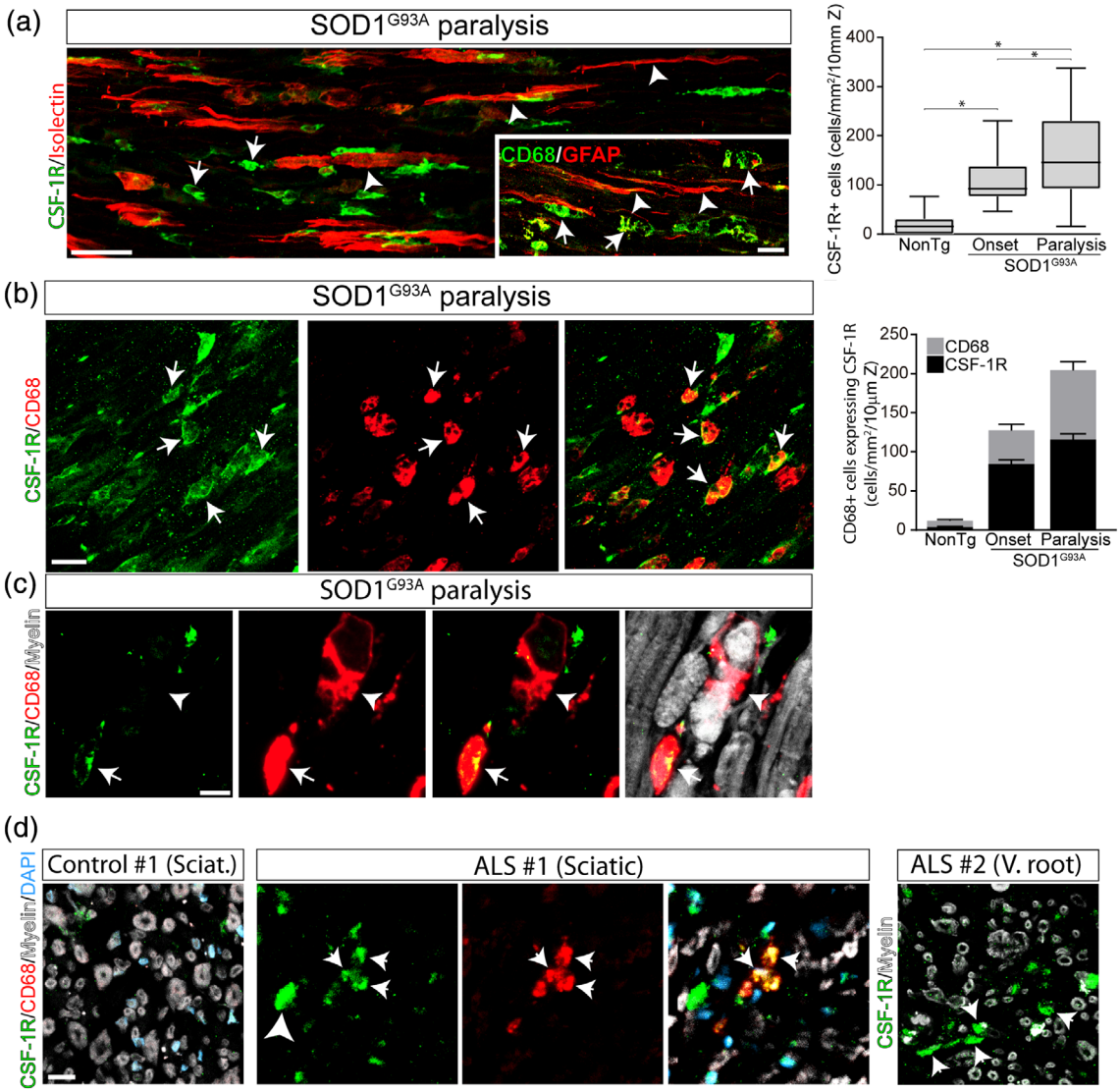

FIGURE 4 Schwann cells (SCs) interact with CSF-1R+ macrophages. (a) Spatial association of denervated SCs expressing Isolectin or GFAP (white arrowheads) with CSF-1R+ and CD68+ macrophages (white arrows) in SOD1^{G93A} rats and NonTg littermates. The graph to the right shows the quantitative analysis of CSF-1R+ cells into the sciatic nerve among conditions. (b) Identification of cells expressing CSF-1R. Note that CSF-1R+ cells mainly correspond to macrophages expressing CD68 (white arrows). The graph to the right shows the quantitative analysis of CD68+ macrophages expressing CSF-1R. (c) High magnification analysis showing a subset nonphagocytic CD68+ macrophages express CSF-1R (white arrow), while phagocytic macrophages lose CSF-1R staining (white arrowhead). (d) CSF-1R expression analysis in cross-sections of the sciatic nerve and ventral root from amyotrophic lateral sclerosis subjects. All quantitative data are expressed as mean ± *SEM*; Data were analyzed by Kruskal–Wallis followed by Dunn's multiple comparison test. * indicates $p < .05$. $n = 4$ animals/condition. Scale bars: 20 µm in (a,b,d) and 10 µm in (c) [Color figure can be viewed at wileyonlinelibrary.com]

3.4 | SCF is expressed in phagocytic SCs and endoneurial macrophages

We have previously reported that c-Kit+ mast cells significantly infiltrate the peripheral motor pathway in ALS rats (Trias et al., 2018), suggesting the presence of increased levels of the ligand SCF. As shown in Figure 5a, SCF was below the limit of detection in the sciatic nerves of nontransgenic rats. In contrast, SCF immunoreactivity was increased in the sciatic nerve of SOD1^{G93A} rats at disease onset and further increased by fourfold at advanced paralysis as compared with onset (Figure 5b). Similarly, mRNA levels for SCF were increased by ~twofold in the sciatic nerve of SOD1^{G93A} rats at paralysis stage respect to nontransgenic controls (Figure 5c).

SCF was localized in a minority subset of phagocytic SCs bearing myelin debris and displaying p75^{NTR} staining (Figure 5d) and also in monocytes and macrophages labeled with CD11b or CD68, respectively (Figure 5e).

Figure 5f shows that SCF was expressed in Iba1+ macrophages that infiltrate into the sciatic nerve of ALS patients but not in control donors.

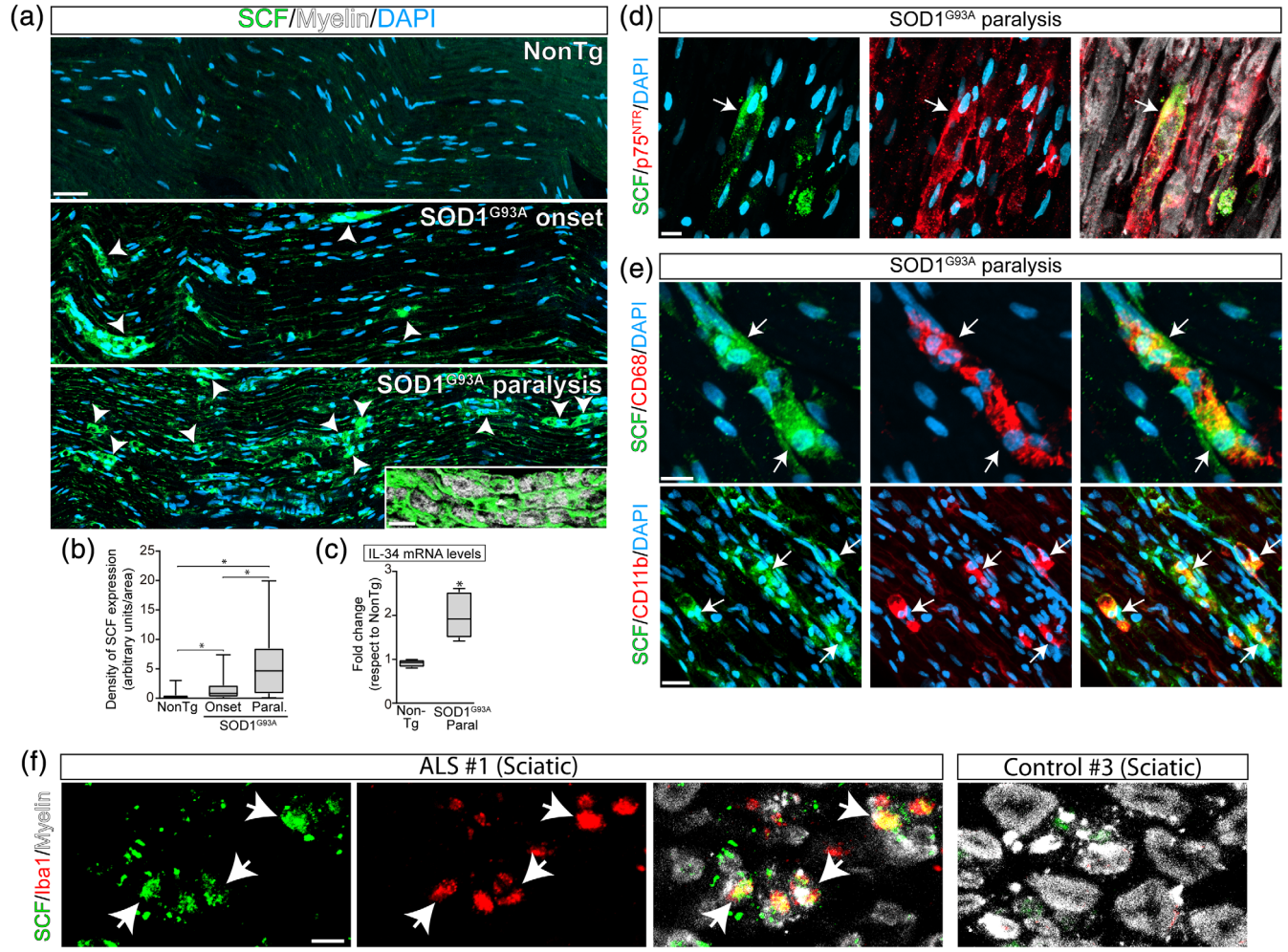

FIGURE 5 Schwann cells (SCs) and macrophages express SCF in amyotrophic lateral sclerosis (ALS) sciatic nerve. (a) Immunohistochemical analysis of SCF expression in longitudinal sections during the course of the paralysis in SOD1^{G93A} rats. Note the sharp increase of the cytokine in phagocytic SCs in symptomatic rats (white arrowheads and inset). (b) Quantitative analysis of SCF expression among groups. (c) Analysis of mRNA levels of SCF by RT-PCR. (d) Confocal images showing the expression of SCF in SCs. Note that, SCF is expressed by reactive p75^{NTR}+ SCs (white arrow). (e) Confocal images showing the SCF expression in macrophages. Note that, SCF is also expressed by CD68+/CD11b + cells (white arrows). (f) SCF expression analysis in cross sections sciatic nerves from ALS subjects. All data are expressed as mean ± *SEM*; Data were analyzed by Kruskal–Wallis followed by Dunn's multiple comparison test (b) or Mann–Whitney test (c), $p < .05$ was considered statistically significant. $n = 4/6$ animals/condition. Scale bars: 50 μm in (a), 20 μm in inset (a), 10 μm in (c,d), and 10 μm in (e) [Color figure can be viewed at wileyonlinelibrary.com]

3.5 | c-Kit is expressed in proliferating SCs and mast cells

Signaling through c-Kit supports the proliferation of undifferentiated SCs in neurofibromatosis Type-1 (Dang, Nelson, & DeVries, 2005), however, it is unknown whether non-neoplastic SCs can also express the receptor. Here, we explored whether SCF upregulation in ALS sciatic nerve was associated with SC proliferation. Remarkably, c-Kit was expressed in a subset of denervated SCs stained with GFAP or Isolectin (Figure 6a) but not in nontransgenic rats (Figure 6a, inset). Some c-Kit+ SCs also displayed immunoreactivity for the cell proliferation marker Ki67 (Figure 6b).

In accordance with our previous reports showing mast cell infiltration along the peripheral motor pathway of SOD1^{G93A} rats (Trias et al., 2017, 2018), the c-Kit receptor was mostly expressed in mast cells infiltrating the ALS sciatic nerves. Figure 6c shows the spatial interaction between denervated SCs and c-Kit+ mast cells. Comparatively, c-Kit+ mast cells were increased in all sciatic nerve and ventral root specimens from ALS subjects, as compared with controls (Figure 6d,e and Figure S6).

3.6 | Pharmacological inhibition of CSF1-R and c-kit prevents SC reactivity in degenerating ventral roots

We have previously shown that sciatic nerve pathology in symptomatic SOD1^{G93A} rats is reduced by postparalysis treatment with

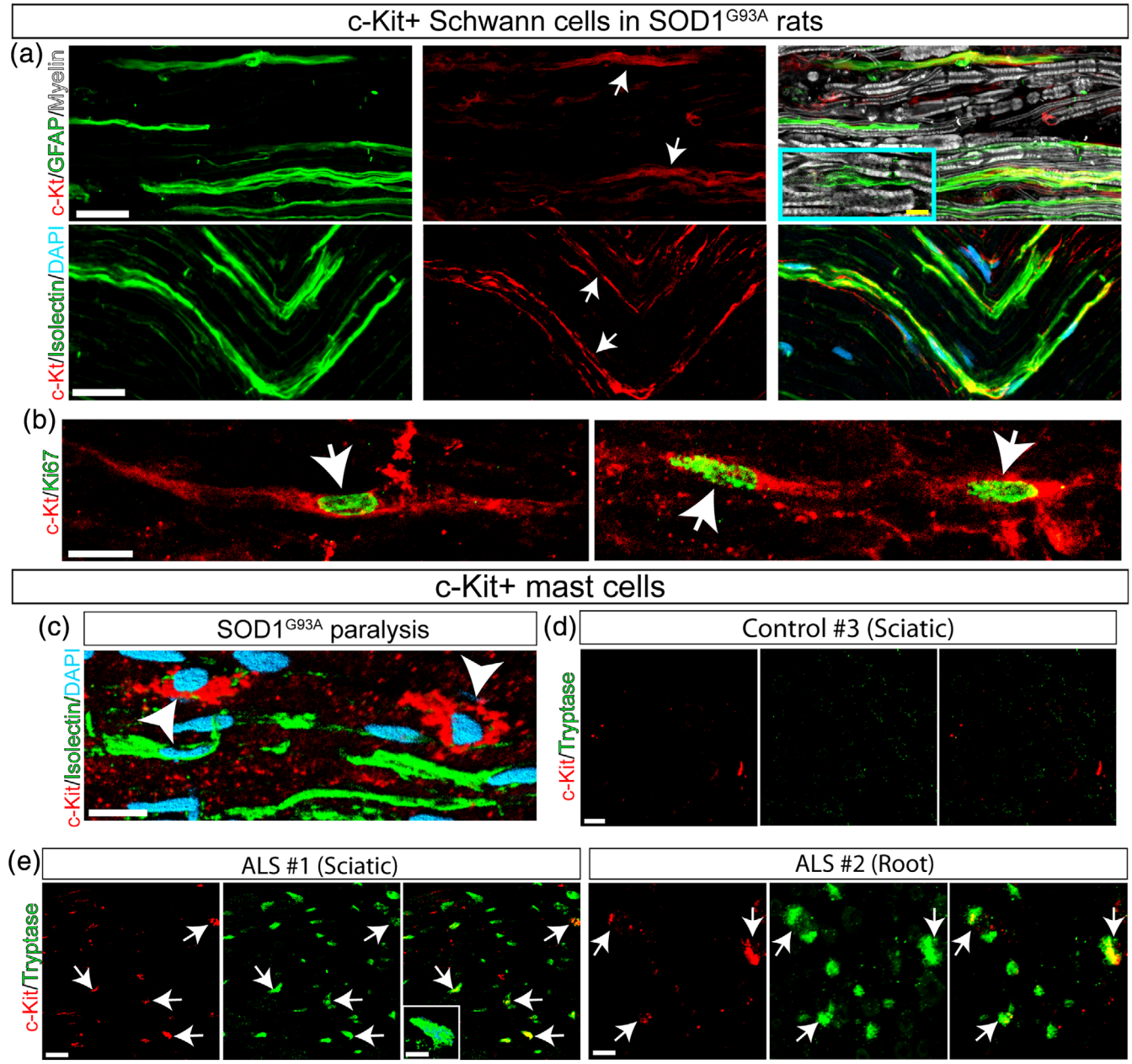

FIGURE 6 Proliferating SCs and mast cells express c-Kit in the amyotrophic lateral sclerosis (ALS) sciatic nerve. (a) Longitudinal sections of SOD1^{G93A} sciatic nerve during advanced paralysis showing c-Kit expression in denervated GFAP+/Isolectin+ SCs (white arrows). Inset shows GFAP+ SCs in NonTg rats. (b) A subpopulation of c-Kit+ SCs expresses the proliferation marker Ki67 (white arrows). (c) c-Kit is also expressed in endoneurial mast cells (white arrowhead). (d,e) Confocal images showing c-Kit+ mast cells infiltrating into the human ALS sciatic nerve. Note that c-Kit+ or Tryptase+ cells were not detected in sciatic nerve cross-sections from controls (d), while endoneurial c-Kit+/Tryptase+ mast cells accumulate in the sciatic nerve and ventral root from ALS cases (white arrows in e). Dotted lines represent the border of myelin sheaths. Scale bars: 10 μm in (a–c) and 5 μm in (e) [Color figure can be viewed at wileyonlinelibrary.com]

masitinib (Trias et al., 2018), a drug inhibiting CSF1-R and c-Kit receptors. Here, we have found that lumbar ventral roots at SOD1^{G93A} rat at advanced paralysis also displayed an increased number of reactive SCs expressing GFAP and S100β as compared with nontransgenic rats (Figure 7a). A 15-day treatment with masitinib (30 mg/Kg/day) starting overt paralysis onset resulted in a 57 and 44% decrease in GFAP and S100β immunoreactivity, respectively, as compared to vehicle (Figure 7b).

3.7 | Masitinib reduces immune cell infiltration and cell proliferation in the sciatic nerve

Next, we have explored whether masitinib also reduced the number of immune cells dependent of CSF-1R and c-Kit receptors as well as cell proliferation. As shown in Figure 8a,b the number of infiltrating CD68+/Iba1+ macrophages, and c-Kit+ mast cells sharply increased during the course of the disease, with respect to nontransgenic animals.

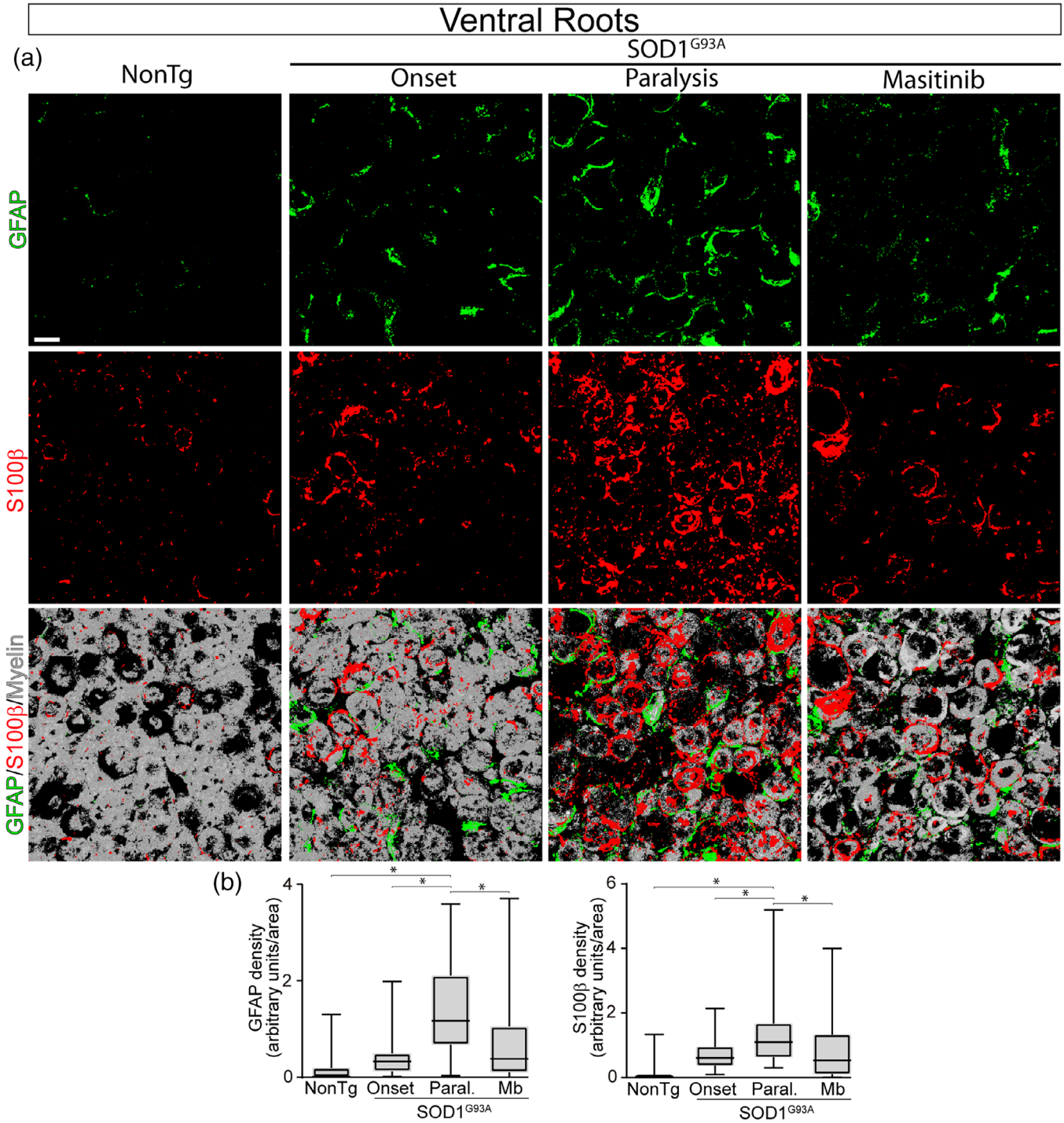

FIGURE 7 Masitinib prevents SC reactivity in degenerating ventral roots of SOD1^{G93A} rats. Masitinib (30 mg/kg/day) was orally administered for 15 days starting after paralysis onset. (a) Representative 3D confocal images of ventral root cross-sections showing SCs stained for GFAP (green) and S100β (red). Note that few SCs were observed in NonTg rats, but reactive SCs accumulated during disease progression. Masitinib treatment significantly prevented SC reactivity and improved ventral root pathology estimated by myelin staining (white). Scale bar: 10 μm. (b) Graphs show the quantitative analysis of the density of SCs per area. All quantitative data are expressed as mean ± *SEM*; Data were analyzed by Kruskal–Wallis followed by Dunn's multiple comparison test, $p < .05$ was considered statistically significant. $n = 4$ animals/condition [Color figure can be viewed at wileyonlinelibrary.com]

Postparalysis treatment with masitinib reduced the number of CD68+ and Iba1+ macrophages by 30 and 60%, respectively (Graph in Figure 7a) as well as c-Kit+ mast cells by 30% (Graph in Figure 7b). Moreover, the number of proliferating cells estimated by Ki67+ nuclei staining decreased by fivefold in masitinib-treated SOD1^{G93A} rats (graph in Figure 7c). More than 80% of Ki67+ nuclei in the degenerating sciatic nerve were localized in small S100+ SCs, while only a small percent were localized other cell types including macrophages (Figure S7).

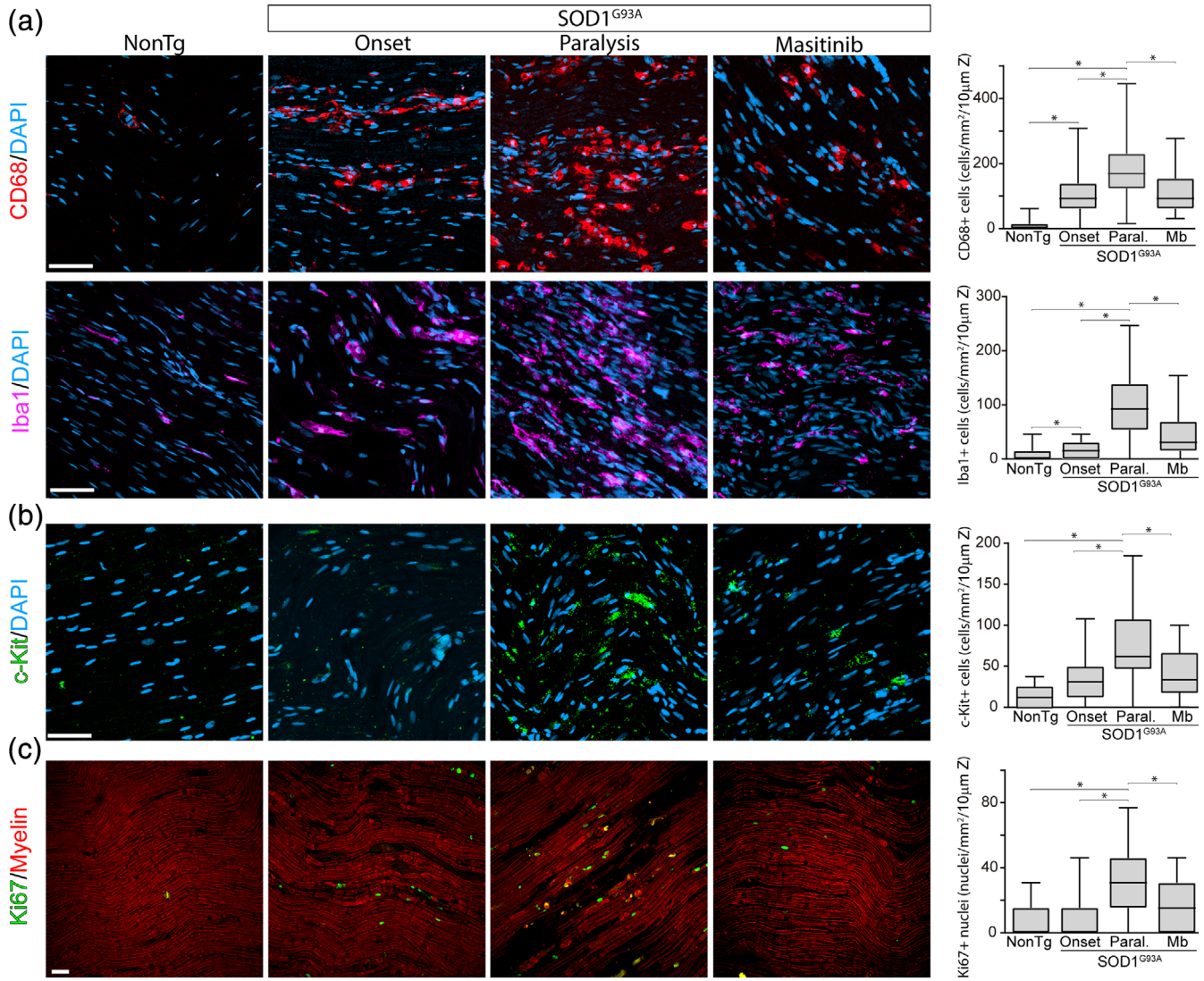

FIGURE 8 Masitinib reduces immune cell infiltration and proliferation. Immunohistochemical analysis of immune cell infiltration and cell proliferation in the sciatic nerve among conditions. Rats were treated as described in Figure 7a,b. Confocal images show the increasing accumulation of CD68+ and Iba1+ macrophages, and c-Kit+ mast cells during the course of the paralysis, as compared with nontransgenic littermates. In all cases, masitinib treatment significantly reduced immune cell infiltration. Graphs to the right show the quantitative analysis of the respective immune cell types among conditions. (c) Analysis of cell proliferation in the sciatic nerve assessed by Ki67 immunostaining. The graph to the right shows Ki67 quantitative analysis. All quantitative data are expressed as mean ± *SEM*; Data were analyzed by Kruskal–Wallis followed by Dunn's multiple comparison test, * indicates $p < .05$. $n = 4$ animals/condition. Scale bars: 20 µm in (a–c) [Color figure can be viewed at wileyonlinelibrary.com]

4 | DISCUSSION

We identified specific SC phenotypes in ALS degenerating peripheral nerves with the potential to trigger local inflammation through the expression of ligands for CSF-1R and c-Kit. SCs in human and SOD1^{G93A} rat ALS sciatic nerves displayed remarkably similar phenotypic features, suggesting a conserved and stereotyped glial response to motor axon degeneration. SCs are regarded as key players in repair following nerve injury through the upregulation of cytokines and trophic factors (Jessen & Arthur-Farraj, 2019; Jessen & Mirsky, 2016). SCs in ALS expressed significant levels of CSF1, IL-34, and SCF and spatially interacted with immune effector cells bearing CSF-1R and c-Kit, suggesting a complex cellular interplay leading to local inflammation. Previous studies have shown infiltrating macrophages, mast cells and neutrophils (Chiu et al., 2009; Nardo et al., 2016; Trias et al., 2018) as well as SC proliferation (Deng et al., 2018) in the sciatic nerve of rodent ALS models. Here, we identified that these immune effectors express CSF-1R and c-Kit in human ALS nerves. Therefore, SCs expressing CSF1, IL-34, and SCF become pathophysiologically and therapeutically relevant in ALS.

It is known that SCs follow a profound phenotypic remodeling after nerve injury allowing repair and axonal growth (Gomez-Sanchez et al., 2017; Jessen & Arthur-Farraj, 2019). In ALS-affected nerves from patients with advanced paralysis and several years of disease

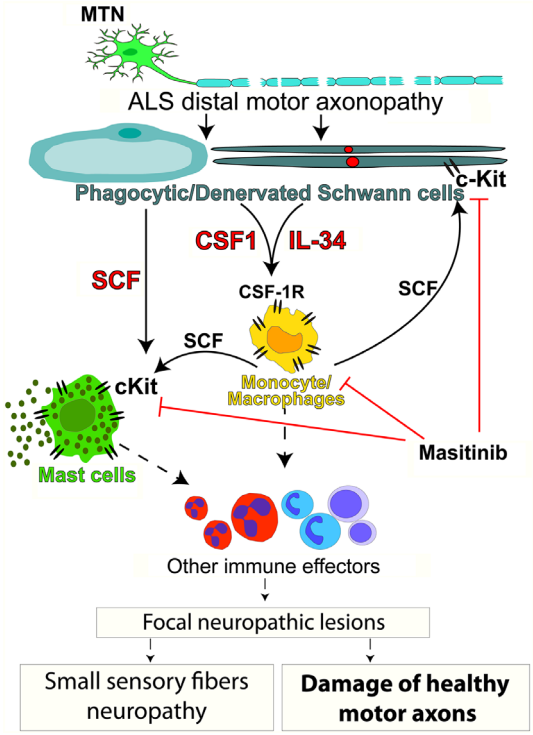

FIGURE 9 Schematic hypothesis about the pathogenic role of SCs in amyotrophic lateral sclerosis (ALS). Reactive SCs expressing CSF1, IL-34, and SCF accumulate in ALS peripheral nerves as a consequence of primary motor axon pathology. These cytokines trigger monocytes/macrophages and mast cell influx and activation through CSF-1R and c-Kit, which in turn, stimulate a complex inflammatory response involving other immune cell effectors, leading to focal neuropathic lesions with the potential to induce damage of adjacent healthy motor axons and sensory fibers. Pharmacological inhibition of CSF-1R and c-Kit may reduce the inflammatory load [Color figure can be viewed at wileyonlinelibrary.com]

progression, we found a comparable reactivity of SCs together with immune cell infiltration, suggesting SCs chronically retain pro-inflammatory features. Thus, the common perception of SCs as pathogenically passive cells in ALS peripheral nerves should be revised in view of their ability to orchestrate local inflammation in advanced stages of the disease. By comparing SCs in the sciatic nerve of sporadic ALS subjects and rats bearing the $SOD1^{G93A}$ mutation, we found similar SC phenotypes and inflammatory effectors, suggesting SC response to denervation is not greatly influenced by SOD1 mutations. Our study has not analyzed whether the expression of cytokines by SCs in ALS is influenced by the simultaneous expression of mutant SOD1. Of note, the reduction of mutant SOD1 levels within SCs in $SOD1^{G37R}$ mice significantly accelerates the paralysis progression (Lobsiger et al., 2009), suggesting mutant SOD1 could promote a protective activity in SCs.

Increased levels of CSF1 in peripheral nerves have been implicated in Charcot–Marie–Tooth disease Type 1 neuropathy, where CSF1 appears to be expressed in endoneurial fibroblasts (Groh et al., 2015). In the ALS degenerating sciatic nerve, we found that CSF1 was mainly expressed in S100+/S100β+/$p75^{NTR}$+ phagocytic SCs containing myelin debris, suggesting a mechanism inducing CSF1 expression in SCs and indirectly promoting monocyte/macrophage recruitment. However, because nonmyelinating reactive SCs display fibroblast-like features (Ma et al., 2018), it cannot be excluded that endoneurial fibroblasts also express CSF1 in ALS degenerating nerves. In comparison, IL-34 was strongly expressed in a different subset of GFAP+/Isolectin+, nonphagocytic reactive SCs, indicating that CSF1 and IL-34 expression is differently regulated in SCs phenotypes.

As far as we know, IL-34 expression in SCs has not been previously described. Because this cytokine does not solely activate CSF-1R but also exert local immunomodulatory function through the activation of PTPζ receptors, it remains to be determined whether IL-34 exerts local immunoregulation on macrophages (Nandi et al., 2013). Thus, while CSF1 and IL-34 are CSF-1R ligands, the production of these cytokines by different subsets of SCs may be a key pathway underlying endoneurial monocyte/macrophage accumulation and their subsequent local protective or pathogenic effects.

While accumulation of macrophages has been previously described in the degenerating nerves of ALS subjects and murine models (Chiu et al., 2009; Kano, Beers, Henkel, & Appel, 2012; Kerkhoff et al., 1993), there is conflicting evidence as to whether macrophage infiltration is deleterious or rather protective in ALS (Nardo et al., 2016). We found that the number of endoneurial myeloid cells closely correlates with axon loss and paralysis progression in $SOD1^{G93A}$ rats, suggesting a pathogenic role. This is in agreement with previous reports showing that pharmacological blockade of macrophages through CSF-1R inhibition is neuroprotective in the sciatic nerve of $SOD1^{G93A}$ mice (Martinez-Muriana et al., 2016; Trias et al., 2018) as well as in a mouse models of Charcot–Marie–Tooth Type 1 neuropathies (Klein et al., 2015). Thus, SCs could orchestrate focal nerve inflammation by expressing CSF1 and IL-34 in ALS, through the recruitment of a specific subset of "disease amplifier" macrophages (Klein & Martini, 2016).

The finding that CSF1 and IL-34 are also expressed in peripheral axons suggests that damaged neurons in ALS express and anterogradely transport the cytokines. Neurons are an important source of IL-34 and CSF1 (Greter et al., 2012; Wang et al., 2012) and CSF1 has a recognized trophic activity in several types of neurons (Chitu, Gokhan, Nandi, Mehler, & Stanley, 2016; Luo et al., 2013). In addition, CSF1 is induced in motor neurons following peripheral nerve lesions and mediates microglia expansion in the spinal cord (Guan et al., 2016; Okubo et al., 2016). Thus, the upregulation of CSF1 and IL-34 in the ALS sciatic nerve could have protective roles, stimulating axon growth or sprouting during nascent stages of the disease but deleterious effects during active nerve degeneration.

Previously, we have reported a significant infiltration of mast cells, macrophages and neutrophils along the degenerating motor axons in sciatic nerves and skeletal muscle (Trias et al., 2017; Trias et al., 2018). Here, we show that c-Kit-expressing mast cells also accumulate in the endoneurium of postmortem sciatic nerve from ALS donors. Because mast cells crosstalk with macrophages and neutrophils, amplifying the inflammatory and cytotoxic potential (De Filippo et al., 2013), our data further support a complex cellular mechanism leading to focal neuropathy in ALS. We also found that SCF was

progressively upregulated in the ALS degenerating sciatic nerve during paralysis progression, being mainly expressed by phagocytic SCs and infiltrating macrophages. Thus, SCF appears as a novel cytokine expressed by SCs in ALS, with the potential to promote mast cell differentiation, proliferation and degranulation (Ito et al., 2012). c-Kit+ mast cells are abundant in neurofibromatosis Type-1 where SCF is produced by tumorigenic SCs carrying the *Nf1*$^{-/-}$ mutation (Staser, Yang, & Clapp, 2010), suggesting a role for SCF in mediating tumor growth and nerve tissue remodeling. Remarkably, we also identified a subset of proliferating SCs expressing the c-Kit receptor in the SOD1^{G93A} rat sciatic nerve, suggesting SCF/c-Kit signaling also regulates SC expansion.

The therapeutic use of tyrosine kinase inhibitor drugs targeting CSF-1R and c-Kit in neurodegenerative diseases has gained increasing attention in the past years as an alternative mechanism to downregulate central and peripheral nervous system inflammation (Klein et al., 2015; Martinez-Muriana et al., 2016; Olmos-Alonso et al., 2016; Trias et al., 2016, 2017). Two drugs of this class have been shown to prevent sciatic nerve pathology and prolong survival in ALS rodent models (Martinez-Muriana et al., 2016; Trias et al., 2016, 2018). In particular, masitinib is in an advanced stage of clinical development and has demonstrated significant treatment-effect in a prospectively defined subpopulation of ALS patients (Mora et al., 2019). In this context, the present study shows evidence that masitinib protection along the degenerating ALS ventral roots and sciatic nerves is mediated, at least in part, by inhibition of CSF-1R- and c-Kit-mediated inflammation. In addition, masitinib ameliorated the increased cell proliferation observed in SOD1^{G93A} rats' sciatic nerves. Because S100+ cells bearing nonmyelinating SCs morphology appear to account for 80% of dividing cells in degenerating nerves, these cells appear to be significant targets for masitinib.

In conclusion, the present study shows further evidence for the role of SCs orchestrating inflammation along the peripheral motor pathway in sporadic ALS subjects and SOD1^{G93A} rats. Although CSF1, IL-34, and SCF are expressed by specific subsets of SCs, the coordinated upregulation of the three cytokines suggests that they act in concert to trigger a complex cellular response, as summarized in Figure 9. The resulting accumulation of CSF-1R+ and c-Kit+ immune cells into ALS-affected ventral roots and peripheral nerves may become deleterious, leading to the development of secondary neuropathic lesions. In turn, healthy motor and sensory axons as well as intact myelinating SCs could be damaged, further accelerating motor neuron peripheral axonopathy and disease progression. Pharmacological inhibition by masitinib of deleterious inflammatory nerve damage, may further explain the multifaceted therapeutic effects of masitinib in ALS patients and animal models.

ACKNOWLEDGMENTS

We want to thank Colin Mansfield for his critical comments and helpful suggestions revising the manuscript and the staff from the Transgenic and Experimental Animal Unit from Institut Pasteur de Montevideo. We are very grateful to our ALS patients who donated their tissues postmortem to advance ALS research. We also thank the National Disease Research Interchange (NDRI) who provide control tissue. This work was supported by Institut Pasteur de Montevideo—FOCEM Mercosur (COF 03/11), the Amyotrophic Lateral Sclerosis Association (00482), Agencia Nacional de Investigación e Innovación (ANII), NINDS R01NS092651 (to P.H.K.), Merit Review BX001148 from the Department of Veterans Affairs (to P.H.K.), Programa de Desarrollo de las Ciencias Básicas (PEDECIBA), Sistema Nacional de Investigadores (SNI), and the Comisión Sectorial de Investigación Científica (CSIC), Universidad de la República, Uruguay; Grupos I+D Program, #1104.

CONFLICT OF INTEREST

O.H. is a co-founder and shareholder of AB science. Others have no conflict of interest.

AUTHOR CONTRIBUTIONS

E.T. and L.B. designed the study. E.T., M.K., P.H.K., Y.S., Y.K., V.V., and S.I. performed experiments. E.T., P.H.K., Y.S., I.C.M., O.H., J.S.B., and L.B. analyzed data. E.T., P.H.K., I.C.M., J.S.B., O.H., and L.B. prepared the manuscript. All authors contributed to the discussion of the results, and edited and approved the final version of the manuscript.

DATA AVAILABILITY STATEMENT

The data that support the findings of this study are available from the corresponding author upon reasonable request.

ORCID

Emiliano Trias https://orcid.org/0000-0001-7187-511X
Peter H. King https://orcid.org/0000-0001-9391-7464
Luis Barbeito https://orcid.org/0000-0002-3047-232X

REFERENCES

Anastassiadis, T., Deacon, S. W., Devarajan, K., Ma, H., & Peterson, J. R. (2011). Comprehensive assay of kinase catalytic activity reveals features of kinase inhibitor selectivity. *Nature Biotechnology*, *29*(11), 1039–1045. https://doi.org/10.1038/nbt.2017

Arbour, D., Tremblay, E., Martineau, E., Julien, J. P., & Robitaille, R. (2015). Early and persistent abnormal decoding by glial cells at the neuromuscular junction in an ALS model. *The Journal of Neuroscience*, *35*(2), 688–706. https://doi.org/10.1523/JNEUROSCI.1379-14.2015

Bigbee, J. W., Yoshino, J. E., & DeVries, G. H. (1987). Morphological and proliferative responses of cultured Schwann cells following rapid phagocytosis of a myelin-enriched fraction. *Journal of Neurocytology*, *16*(4), 487–496.

Boulakirba, S., Pfeifer, A., Mhaidly, R., Obba, S., Goulard, M., Schmitt, T., … Jacquel, A. (2018). IL-34 and CSF-1 display an equivalent macrophage differentiation ability but a different polarization potential. *Scientific Reports*, *8*(1), 256. https://doi.org/10.1038/s41598-017-18433-4

Brosius Lutz, A., Chung, W. S., Sloan, S. A., Carson, G. A., Zhou, L., Lovelett, E., … Barres, B. A. (2017). Schwann cells use TAM receptor-mediated phagocytosis in addition to autophagy to clear myelin in a mouse model of nerve injury. *Proceedings of the National Academy of Sciences of the United States of America*, *114*(38), E8072–E8080. https://doi.org/10.1073/pnas.1710566114

Campanari, M. L., Garcia-Ayllon, M. S., Ciura, S., Saez-Valero, J., & Kabashi, E. (2016). Neuromuscular junction impairment in amyotrophic lateral Sclerosis: Reassessing the role of Acetylcholinesterase. *Frontiers in Molecular Neuroscience*, *9*, 160. https://doi.org/10.3389/fnmol.2016.00160

Chang, Y. W., & Winkelstein, B. A. (2011). Schwann cell proliferation and macrophage infiltration are evident at day 14 after painful cervical nerve root compression in the rat. *Journal of Neurotrauma*, *28*(12), 2429–2438. https://doi.org/10.1089/neu.2011.1918

Chitu, V., Gokhan, S., Nandi, S., Mehler, M. F., & Stanley, E. R. (2016). Emerging roles for CSF-1 receptor and its ligands in the nervous system. *Trends in Neurosciences*, *39*(6), 378–393. https://doi.org/10.1016/j.tins.2016.03.005

Chiu, I. M., Phatnani, H., Kuligowski, M., Tapia, J. C., Carrasco, M. A., Zhang, M., … Carroll, M. C. (2009). Activation of innate and humoral immunity in the peripheral nervous system of ALS transgenic mice. *Proceedings of the National Academy of Sciences of the United States of America*, *106*(49), 20960–20965. https://doi.org/10.1073/pnas.0911405106

Dang, I., Nelson, J. K., & DeVries, G. H. (2005). C-kit receptor expression in normal human Schwann cells and Schwann cell lines derived from neurofibromatosis type 1 tumors. *Journal of Neuroscience Research*, *82*(4), 465–471. https://doi.org/10.1002/jnr.20648

De Filippo, K., Dudeck, A., Hasenberg, M., Nye, E., van Rooijen, N., Hartmann, K., … Hogg, N. (2013). Mast cell and macrophage chemokines CXCL1/CXCL2 control the early stage of neutrophil recruitment during tissue inflammation. *Blood*, *121*(24), 4930–4937. https://doi.org/10.1182/blood-2013-02-486217

Deng, B., Lv, W., Duan, W., Liu, Y., Li, Z., Ma, Y., … Li, C. (2018). Progressive degeneration and inhibition of peripheral nerve regeneration in the SOD1-G93A mouse model of amyotrophic lateral Sclerosis. *Cellular Physiology and Biochemistry*, *46*(6), 2358–2372. https://doi.org/10.1159/000489627

Dubreuil, P., Letard, S., Ciufolini, M., Gros, L., Humbert, M., Casteran, N., … Hermine, O. (2009). Masitinib (AB1010), a potent and selective tyrosine kinase inhibitor targeting KIT. *PLoS One*, *4*(9), e7258. https://doi.org/10.1371/journal.pone.0007258

Esposito, B., De Santis, A., Monteforte, R., & Baccari, G. C. (2002). Mast cells in Wallerian degeneration: Morphologic and ultrastructural changes. *The Journal of Comparative Neurology*, *445*(3), 199–210.

Fischer, L. R., Culver, D. G., Tennant, P., Davis, A. A., Wang, M., Castellano-Sanchez, A., … Glass, J. D. (2004). Amyotrophic lateral sclerosis is a distal axonopathy: Evidence in mice and man. *Experimental Neurology*, *185*(2), 232–240.

Fischer, L. R., & Glass, J. D. (2007). Axonal degeneration in motor neuron disease. *Neurodegenerative Diseases*, *4*(6), 431–442. https://doi.org/10.1159/000107704

Frey, D., Schneider, C., Xu, L., Borg, J., Spooren, W., & Caroni, P. (2000). Early and selective loss of neuromuscular synapse subtypes with low sprouting competence in motoneuron diseases. *The Journal of Neuroscience*, *20*(7), 2534–2542.

Galli, S. J., Tsai, M., & Wershil, B. K. (1993). The c-kit receptor, stem cell factor, and mast cells. What each is teaching us about the others. *The American Journal of Pathology*, *142*(4), 965–974.

Gomez-Sanchez, J. A., Pilch, K. S., van der Lans, M., Fazal, S. V., Benito, C., Wagstaff, L. J., … Jessen, K. R. (2017). After nerve injury, lineage tracing shows that myelin and Remak Schwann cells elongate extensively and branch to form repair Schwann cells, which shorten radically on Remyelination. *The Journal of Neuroscience*, *37*(37), 9086–9099. https://doi.org/10.1523/JNEUROSCI.1453-17.2017

Greter, M., Lelios, I., Pelczar, P., Hoeffel, G., Price, J., Leboeuf, M., … Becher, B. (2012). Stroma-derived interleukin-34 controls the development and maintenance of langerhans cells and the maintenance of microglia. *Immunity*, *37*(6), 1050–1060. https://doi.org/10.1016/j.immuni.2012.11.001

Groh, J., Klein, I., Hollmann, C., Wettmarshausen, J., Klein, D., & Martini, R. (2015). CSF-1-activated macrophages are target-directed and essential mediators of Schwann cell dedifferentiation and dysfunction in Cx32-deficient mice. *Glia*, *63*(6), 977–986. https://doi.org/10.1002/glia.22796

Groh, J., Weis, J., Zieger, H., Stanley, E. R., Heuer, H., & Martini, R. (2012). Colony-stimulating factor-1 mediates macrophage-related neural damage in a model for Charcot-Marie-tooth disease type 1X. *Brain*, *135*(Pt 1), 88–104. https://doi.org/10.1093/brain/awr283

Guan, Z., Kuhn, J. A., Wang, X., Colquitt, B., Solorzano, C., Vaman, S., … Basbaum, A. I. (2016). Injured sensory neuron-derived CSF1 induces microglial proliferation and DAP12-dependent pain. *Nature Neuroscience*, *19*(1), 94–101. https://doi.org/10.1038/nn.4189

Hirata, K., & Kawabuchi, M. (2002). Myelin phagocytosis by macrophages and nonmacrophages during Wallerian degeneration. *Microscopy Research and Technique*, *57*(6), 541–547. https://doi.org/10.1002/jemt.10108

Iemura, A., Tsai, M., Ando, A., Wershil, B. K., & Galli, S. J. (1994). The c-kit ligand, stem cell factor, promotes mast cell survival by suppressing apoptosis. *The American Journal of Pathology*, *144*(2), 321–328.

Ito, T., Smrz, D., Jung, M. Y., Bandara, G., Desai, A., Smrzova, S., … Gilfillan, A. M. (2012). Stem cell factor programs the mast cell activation phenotype. *Journal of Immunology*, *188*(11), 5428–5437. https://doi.org/10.4049/jimmunol.1103366

Jessen, K. R., & Arthur-Farraj, P. (2019). Repair Schwann cell update: Adaptive reprogramming, EMT, and stemness in regenerating nerves. *Glia*, *67*(3), 421–437. https://doi.org/10.1002/glia.23532

Jessen, K. R., & Mirsky, R. (2016). The repair Schwann cell and its function in regenerating nerves. *The Journal of Physiology*, *594*(13), 3521–3531. https://doi.org/10.1113/JP270874

Kano, O., Beers, D. R., Henkel, J. S., & Appel, S. H. (2012). Peripheral nerve inflammation in ALS mice: Cause or consequence. *Neurology*, *78*(11), 833–835. https://doi.org/10.1212/WNL.0b013e318249f776

Keller, A. F., Gravel, M., & Kriz, J. (2009). Live imaging of amyotrophic lateral sclerosis pathogenesis: Disease onset is characterized by marked induction of GFAP in Schwann cells. *Glia*, *57*(10), 1130–1142. https://doi.org/10.1002/glia.20836

Kennel, P. F., Finiels, F., Revah, F., & Mallet, J. (1996). Neuromuscular function impairment is not caused by motor neurone loss in FALS mice: An electromyographic study. *Neuroreport*, *7*(8), 1427–1431.

Kerkhoff, H., Troost, D., Louwerse, E. S., van Dijk, M., Veldman, H., & Jennekens, F. G. (1993). Inflammatory cells in the peripheral nervous system in motor neuron disease. *Acta Neuropathologica*, *85*(5), 560–565.

Klein, D., & Martini, R. (2016). Myelin and macrophages in the PNS: An intimate relationship in trauma and disease. *Brain Research*, *1641* ((Pt A)), 130–138. https://doi.org/10.1016/j.brainres.2015.11.033

Klein, D., Patzko, A., Schreiber, D., van Hauwermeiren, A., Baier, M., Groh, J., … Martini, R. (2015). Targeting the colony stimulating factor 1 receptor alleviates two forms of Charcot-Marie-tooth disease in mice. *Brain*, *138*(Pt 11), 3193–3205. https://doi.org/10.1093/brain/awv240

Kong, J., & Xu, Z. (1998). Massive mitochondrial degeneration in motor neurons triggers the onset of amyotrophic lateral sclerosis in mice expressing a mutant SOD1. *The Journal of Neuroscience*, *18*(9), 3241–3250.

Lindborg, J. A., Mack, M., & Zigmond, R. E. (2017). Neutrophils are critical for myelin removal in a peripheral nerve injury model of Wallerian degeneration. *The Journal of Neuroscience*, *37*(43), 10258–10277. https://doi.org/10.1523/JNEUROSCI.2085-17.2017

Lobsiger, C. S., Boillee, S., McAlonis-Downes, M., Khan, A. M., Feltri, M. L., Yamanaka, K., & Cleveland, D. W. (2009). Schwann cells expressing dismutase active mutant SOD1 unexpectedly slow disease progression in ALS mice. *Proceedings of the National Academy of Sciences of the United States of America*, *106*(11), 4465–4470. https://doi.org/10.1073/pnas.0813339106

Luo, J., Elwood, F., Britschgi, M., Villeda, S., Zhang, H., Ding, Z., … Wyss-Coray, T. (2013). Colony-stimulating factor 1 receptor (CSF1R) signaling in injured neurons facilitates protection and survival. *The Journal of Experimental Medicine*, *210*(1), 157–172. https://doi.org/10.1084/jem.20120412

Ma, D., Wang, B., Zawadzka, M., Gonzalez, G., Wu, Z., Yu, B., … Zhao, C. (2018). A subpopulation of Foxj1-expressing, Nonmyelinating Schwann cells of the peripheral nervous system contribute to Schwann cell Remyelination in the central nervous system. *The Journal of Neuroscience*, *38*(43), 9228–9239. https://doi.org/10.1523/JNEUROSCI.0585-18.2018

Martinez-Muriana, A., Mancuso, R., Francos-Quijorna, I., Olmos-Alonso, A., Osta, R., Perry, V. H., … Lopez-Vales, R. (2016). CSF1R blockade slows the progression of amyotrophic lateral sclerosis by reducing microgliosis and invasion of macrophages into peripheral nerves. *Scientific Reports*, *6*, 25663. https://doi.org/10.1038/srep25663

Metz, M., Grimbaldeston, M. A., Nakae, S., Piliponsky, A. M., Tsai, M., & Galli, S. J. (2007). Mast cells in the promotion and limitation of chronic inflammation. *Immunological Reviews*, *217*, 304–328. https://doi.org/10.1111/j.1600-065X.2007.00520.x

Millecamps, S., & Julien, J. P. (2013). Axonal transport deficits and neurodegenerative diseases. *Nature Reviews. Neuroscience*, *14*(3), 161–176. https://doi.org/10.1038/nrn3380

Mora, J., Genge, A., Chio, A., Estol, C. J., Chaverri, D., Hernandez, M., … Group, A. S. (2019). Masitinib as an add-on therapy to riluzole in patients with amyotrophic lateral sclerosis: A randomised clinical trial. *Amyotrophic Lateral Sclerosis and Frontotemporal Degeneration*, 1–10. https://doi.org/10.1080/21678421.2019.1632346

Nandi, S., Cioce, M., Yeung, Y. G., Nieves, E., Tesfa, L., Lin, H., … Stanley, E. R. (2013). Receptor-type protein-tyrosine phosphatase zeta is a functional receptor for interleukin-34. *The Journal of Biological Chemistry*, *288*(30), 21972–21986. https://doi.org/10.1074/jbc.M112.442731

Nardo, G., Trolese, M. C., de Vito, G., Cecchi, R., Riva, N., Dina, G., … Bendotti, C. (2016). Immune response in peripheral axons delays disease progression in SOD1(G93A) mice. *Journal of Neuroinflammation*, *13*(1), 261. https://doi.org/10.1186/s12974-016-0732-2

Okubo, M., Yamanaka, H., Kobayashi, K., Dai, Y., Kanda, H., Yagi, H., & Noguchi, K. (2016). Macrophage-Colony stimulating factor derived from injured primary afferent induces proliferation of spinal microglia and neuropathic pain in rats. *PLoS One*, *11*(4), e0153375. https://doi.org/10.1371/journal.pone.0153375

Olmos-Alonso, A., Schetters, S. T., Sri, S., Askew, K., Mancuso, R., Vargas-Caballero, M., … Gomez-Nicola, D. (2016). Pharmacological targeting of CSF1R inhibits microglial proliferation and prevents the progression of Alzheimer's-like pathology. *Brain*, *139*(Pt 3), 891–907. https://doi.org/10.1093/brain/awv379

Riva, N., Clarelli, F., Domi, T., Cerri, F., Gallia, F., Trimarco, A., … Quattrini, A. (2016). Unraveling gene expression profiles in peripheral motor nerve from amyotrophic lateral sclerosis patients: Insights into pathogenesis. *Scientific Reports*, *6*, 39297. https://doi.org/10.1038/srep39297

Stanley, E. R., & Chitu, V. (2014). CSF-1 receptor signaling in myeloid cells. *Cold Spring Harbor Perspectives in Biology*, *6*(6). https://doi.org/10.1101/cshperspect.a021857

Staser, K., Yang, F. C., & Clapp, D. W. (2010). Mast cells and the neurofibroma microenvironment. *Blood*, *116*(2), 157–164. https://doi.org/10.1182/blood-2009-09-242875

Stoll, G., Griffin, J. W., Li, C. Y., & Trapp, B. D. (1989). Wallerian degeneration in the peripheral nervous system: Participation of both Schwann cells and macrophages in myelin degradation. *Journal of Neurocytology*, *18*(5), 671–683.

Stratton, J. A., Holmes, A., Rosin, N. L., Sinha, S., Vohra, M., Burma, N. E., … Biernaskie, J. (2018). Macrophages regulate Schwann cell maturation after nerve injury. *Cell Reports*, *24*(10), 2561–2572 e2566. https://doi.org/10.1016/j.celrep.2018.08.004

Tofaris, G. K., Patterson, P. H., Jessen, K. R., & Mirsky, R. (2002). Denervated Schwann cells attract macrophages by secretion of leukemia inhibitory factor (LIF) and monocyte chemoattractant protein-1 in a process regulated by interleukin-6 and LIF. *The Journal of Neuroscience*, *22*(15), 6696, 20026699–6703.

Tomlinson, J. E., Zygelyte, E., Grenier, J. K., Edwards, M. G., & Cheetham, J. (2018). Temporal changes in macrophage phenotype after peripheral nerve injury. *Journal of Neuroinflammation*, *15*(1), 185. https://doi.org/10.1186/s12974-018-1219-0

Trias, E., Ibarburu, S., Barreto-Nunez, R., Babdor, J., Maciel, T. T., Guillo, M., … Barbeito, L. (2016). Post-paralysis tyrosine kinase inhibition with masitinib abrogates neuroinflammation and slows disease progression in inherited amyotrophic lateral sclerosis. *Journal of Neuroinflammation*, *13*(1), 177. https://doi.org/10.1186/s12974-016-0620-9

Trias, E., Ibarburu, S., Barreto-Nunez, R., Varela, V., Moura, I. C., Dubreuil, P., … Barbeito, L. (2017). Evidence for mast cells contributing to neuromuscular pathology in an inherited model of ALS. *JCI Insight*, *2*(20). https://doi.org/10.1172/jci.insight.95934

Trias, E., King, P. H., Si, Y., Kwon, Y., Varela, V., Ibarburu, S., … Barbeito, L. (2018). Mast cells and neutrophils mediate peripheral motor pathway degeneration in ALS. *JCI Insight*, *3*(19). https://doi.org/10.1172/jci.insight.123249

Van Dyke, J. M., Smit-Oistad, I. M., Macrander, C., Krakora, D., Meyer, M. G., & Suzuki, M. (2016). Macrophage-mediated inflammation and glial response in the skeletal muscle of a rat model of familial amyotrophic lateral sclerosis (ALS). *Experimental Neurology*, *277*, 275–282. https://doi.org/10.1016/j.expneurol.2016.01.008

Wang, Y., Szretter, K. J., Vermi, W., Gilfillan, S., Rossini, C., Cella, M., … Colonna, M. (2012). IL-34 is a tissue-restricted ligand of CSF1R required for the development of Langerhans cells and microglia. *Nature Immunology*, *13*(8), 753–760. https://doi.org/10.1038/ni.2360

SUPPORTING INFORMATION

Additional supporting information may be found online in the Supporting Information section at the end of this article.

How to cite this article: Trias E, Kovacs M, King PH, et al. Schwann cells orchestrate peripheral nerve inflammation through the expression of CSF1, IL-34, and SCF in amyotrophic lateral sclerosis. *Glia*. 2019;1–17. https://doi.org/10.1002/glia.23768

Supplementary Figures

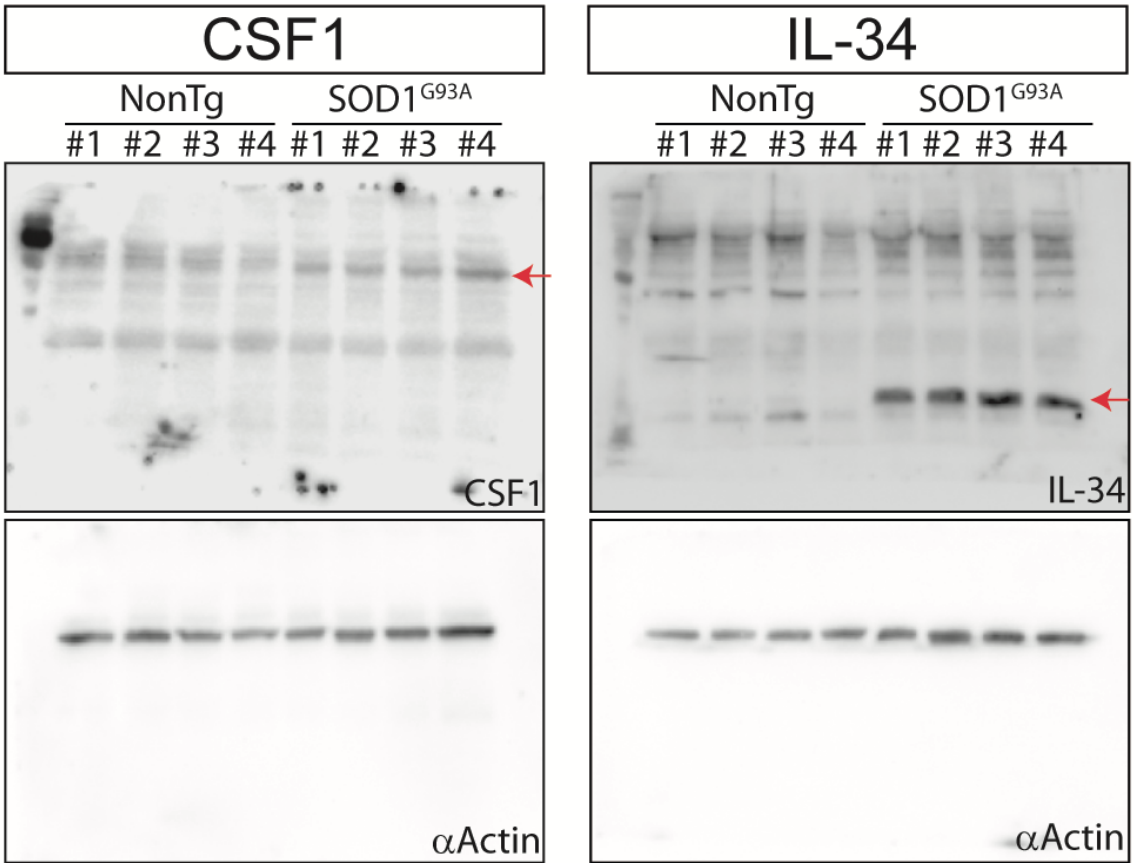

Supplementary Figure 1. Western blot analysis of CSF1 and IL-34 levels in the proximal sciatic nerve of non-transgenic and symptomatic SOD1^{G93A} rats. Upper panels show original western blot membranes where CSF1 and IL-34 were analyzed using specific antibodies (CSF 1:500 dilution; IL-34 1:500 dilution). Red arrows indicate the bands that were used for quantitive analysis, according to manufacturer instructions. In lower panels, primary antibodies were stripped and membranes were reincubated with anti-αActin antibody (1:4000) as housekeeping protein for loading control. n= 4 animals/group.

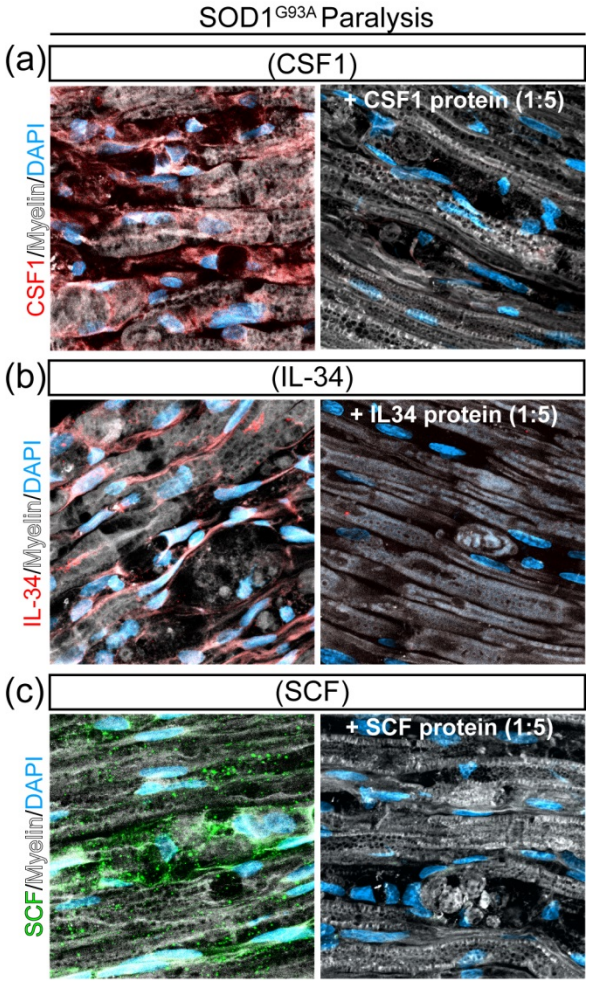

Supplementary Figure 2. Analysis of antibodies (CSF1, IL-34 and SCF) sepecificity using blocking peptides. Images show confocal immunohistochemistry using CSF1, IL-34 and SCF antibodies in longitudinal sections of proximal sciatic nerves from symptomatic SOD1G^{93A} rats **(a-c)** Representative confocal images showing immunohistochemistry analysis of the indicated antibodies before (left panels) and after (right panels) primary antibody preincubation with the respective proteins. Competition of each primary antibodies with their respective ligand (ratio= 1:5) completely abrogated the immunohistological staining. Scale bars: 10 μm in all panels.

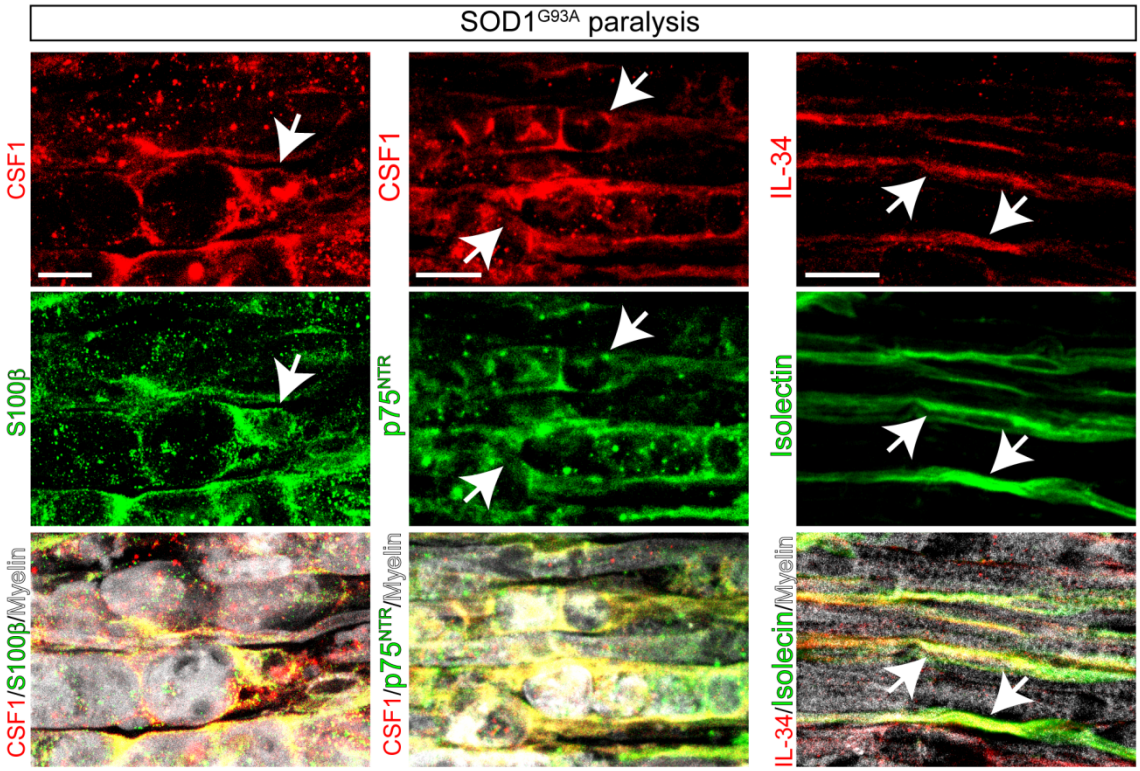

Supplementary Figure 3. Phenotypic characterization of SCs expressing CSF1 in SOD1^{G93A} proximal sciatic nerve. Immunohistochemical analysis of CSF1 (red, left and midle panel) and IL-34 (red, right panel) expression in proximal sciatic nerve longitudinal sections co-stained with SCs markers S100β (green), p75^{NTR} (green) and Isolectin (green). Note that CSF1 was clearly expressed in a subset of S100β+ (lef panels) and p75^{NTR}+ (right panels) SCs bearing phagocytic morphology (white arrows), while IL-34 was expressed by denervated SCs stained with Isolectin (right panel, white arrows). Scale bars: 20 μm.

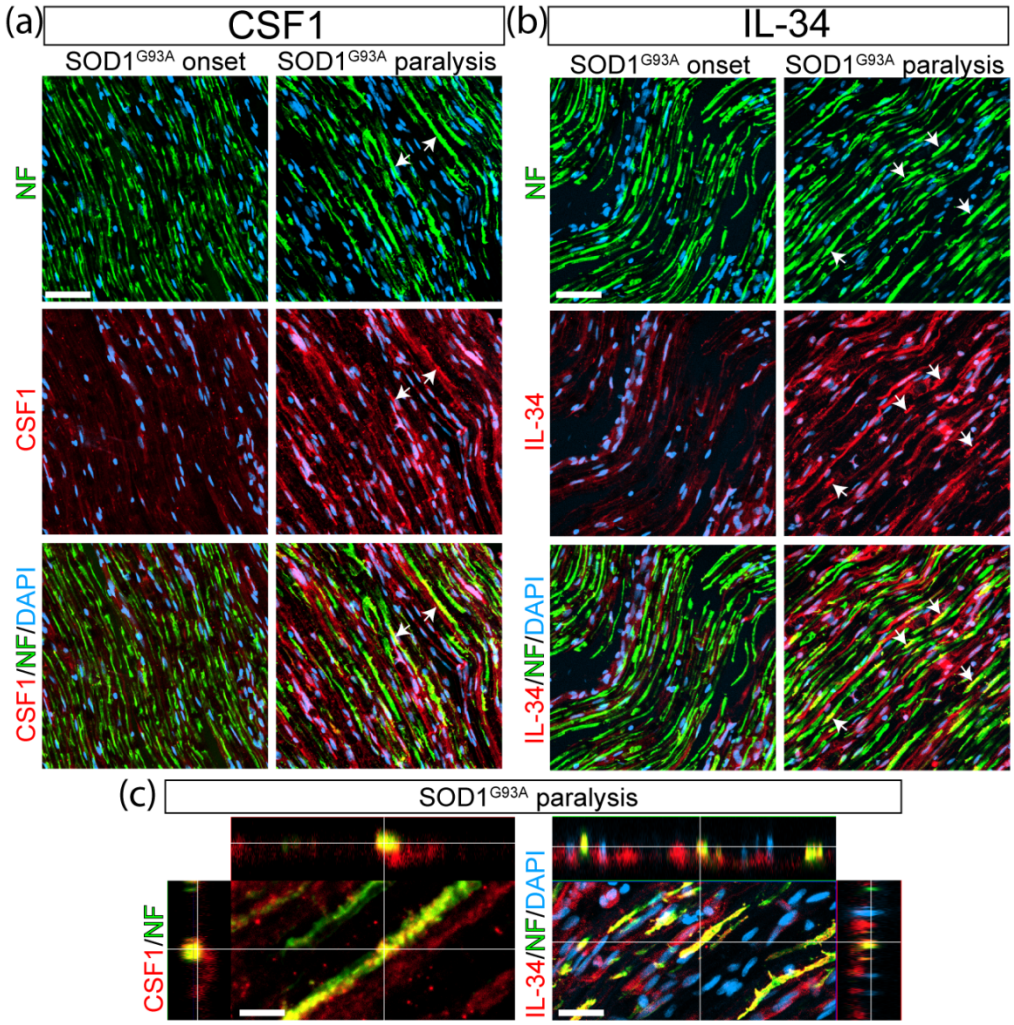

Supplementary Figure 4. A subset of axons express CSF1 and IL-34 in the sciatic nerve of symptomatic SOD11^{G93A} rats. **(a, b)** Longitudinal section of sciatic nerve showing the colocalization analysis between neurofilament (NF-200 heavy chain) with CSF1 or IL-34. Note CSF1 (left panels) and IL-34 (right panels) colocalize with a subset of NF-200+ axons (green) (white arrows). **(c)** Higher magnification images showing the orthogonal view of the colocalization. Scale bars: 50 μm in (a); 20 μm in (c).

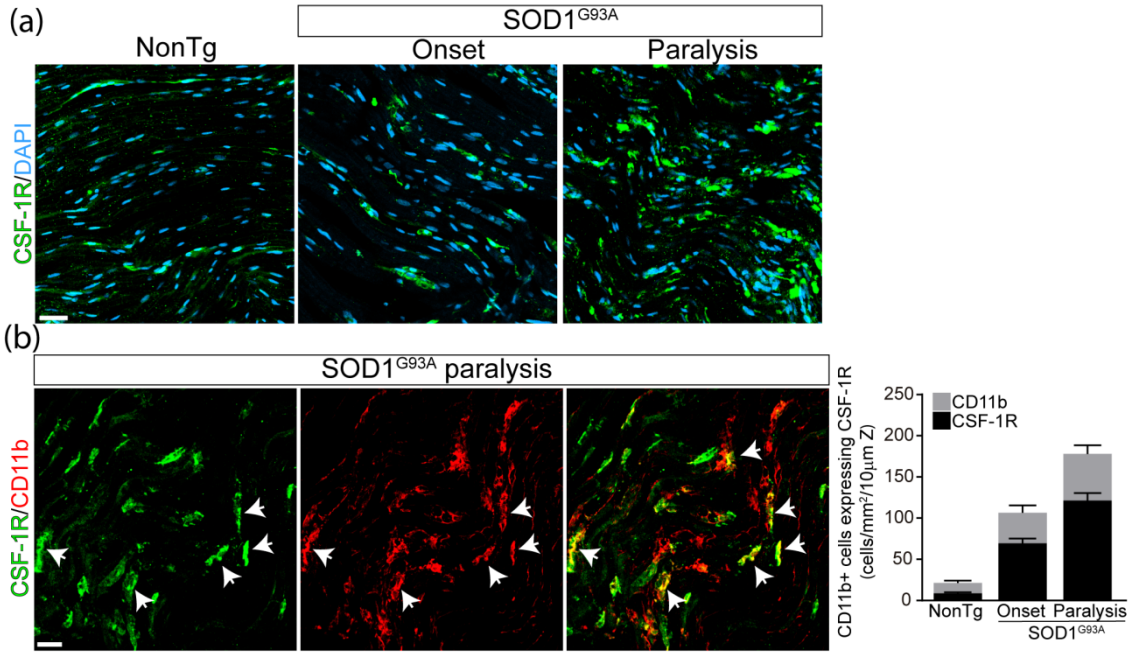

Supplementary Figure 5. Accumulation of CSF-1R+ myeloid cells into the sciatic nerve of SOD1^{G93A} rats. (a) Representative confocal images showing the comparative infiltration of CSF-1R+ cells into the degenerating sciatic nerve among conditions. Note the significant increase of CSF-1R+ cells in rats developing overt paralysis. **(b)** Note that CSF-1R+ cells mostly correspond to myeloid cells expressing CD11b (white arrows). The graph to the right shows the quantitative analysis of CD11b+ myeloid cells expressing CSF-1R. Scale bars: 20 μm in (a) and (b).

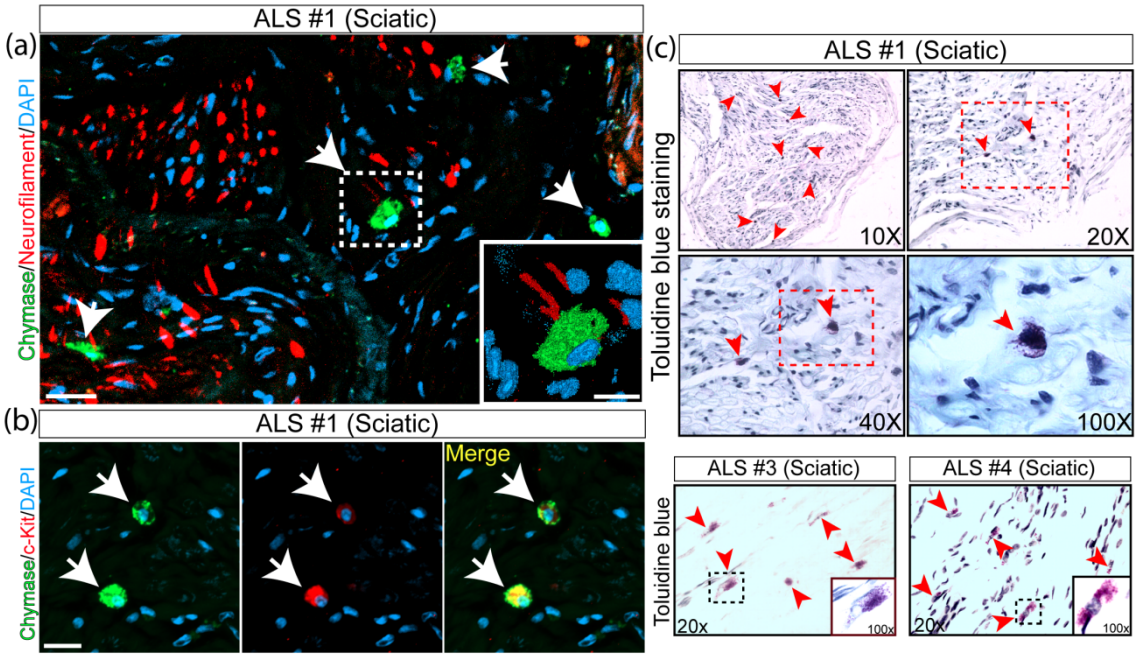

Supplementary Figure 6. Accumulation of c-Kit+ mast cells into the sciatic nerve of ALS patients. (a) Representative confocal images showing Chymase+ mast cells infiltrating the degenerating sciatic nerve of an ALS patient (white arrows). The inset shows the interaction of mast cells (green for Chymase) with neurofilaments (red, NF-200). **(b)** High magnification images showing that Chymase+ mast cells (green) express c-Kit (red, white arrows). **(c)** Sections of three ALS sciatic nerves stained for toluidine blue, showing accumulation of mast cells displaying metachromasia (red arrows). Scale bars: 20 μm in (a) and (b).

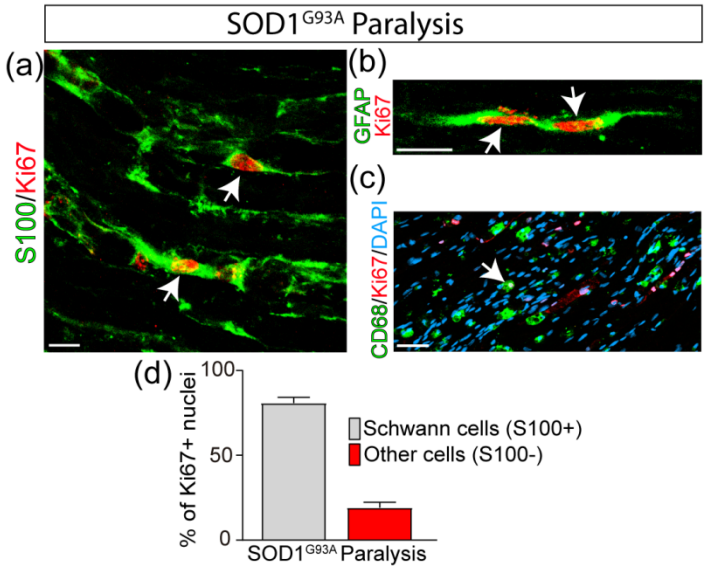

Supplementary Figure 7. Analysis of cell proliferation in the degenerating sciatic nerve of symptomatic SOD1^{G93A} rats. Images show confocal immunohistochemical analysis of Ki67, SCs and infiltrating macrophages in longitudinal sections of proximal sciatic nerve during the symptomatic phase of SOD1^{G93A} rats. (a) Representantive confocal image showing S100+ SCs (green, white arrows) expressing Ki67 nuclei (red). (b) Representative image of GFAP+ small SCs expressing Ki67 (red, white arrows). (c) Confocal tile reconstruction showing CD68+ macrophages (green) and Ki67 expression (red). Note that most Ki67+ nuclei are not localized in infiltrating CD68+ cells. White arrow denote one small monocyte/macrophage expressing Ki67. (d) Quantitative analysis shows that most Ki67+ nuclei belongs to S100+ SCs (80%, grey bar), while 20% of the Ki67+ nuclei were localized in cells devoid of S100 staining (red bar).

Publicación 3

The pathogenic role of c-Kit$^+$ mast cells in the spinal motor neuron-vascular niche in ALS

(El rol patogénico de mastocitos c-Kit$^+$ en el nicho motoneurona espinal- vascular de la ELA)

Mariángeles Kovacs, Catalina Alamón, Cecilia Maciel, Valentina Varela, Sofia Ibarburu, Lucas Tarragó, Peter H. King, Ying Si, Yuri Kwon, Olivier Hermine, Luis Barbeito and Emiliano Trias.

Resumen

Luego de identificar mastocitos y sus precursores c-Kit$^+$ en las vías motoras periféricas de animales y pacientes con ELA, quisimos desafiar la hipótesis de que mastocitos derivados de precursores c-Kit$^+$ podían infiltrar la médula espinal en degeneración, contribuyendo a la constitución de la neuroinflamación crónica observada en la ELA en el SNC.

En el análisis histopatológico de la médula espinal de modelos murinos en su fase sintomática, así como en el tejido post-mortem de pacientes con ELA, pudimos demostrar por primera vez la acumulación de precursores de mastocitos c-Kit$^+$, asociados espacialmente a motoneuronas y elementos microvasculares vecinos, sugiriendo la asociación con aumento local de la permeabilidad de la BHE. También pudimos observar que estos precursores se encuentran en estrecha relación espacial con células gliales del microambiente celular neurodegenerativo, en particular astrocitos reactivos.

Un hallazgo significativo de este estudio fue el aislamiento, por primera vez en la literatura, de precursores de mastocitos c-Kit$^+$ a partir de la médula espinal de animales SOD1^{G93A} sintomáticos y su posterior diferenciación *ex vivo* en mastocitos totalmente diferenciados.
Por otro lado, demostramos mecanismos quimiotácticos asociados a la expresión de SCF en astrocitos reactivos, sugiriendo una dependencia de la vía c-Kit/SCF en la infiltración y diferenciación a partir de precursores de mastocitos en la ELA.

Por último, mostramos evidencia de que los mastocitos c-Kit$^+$ de la médula espinal también pueden ser blanco terapéutico de masitinib, inhibidor del receptor mencionado, lo que disminuye la infiltración y acumulación de estos en las cercanías de las motoneuronas, a la vez que mejora el estado de la BHE. En conjunto, este estudio sostiene el concepto de que los mastocitos son células inmunes que contribuyen a la neuroinflamación crónica y a la constitución del microambiente celular neurodegenerativo en la ELA.

Resultados

- En la médula espinal post-mortem de pacientes con ELA observamos una

acumulación sistemática de mastocitos formando "*clusters*" rodeando los somas de las motoneuronas en degeneración. Estos mastocitos presentan dos fenotipos característicos: por un lado, una morfología típica, hipertrofiada y granular, caracterizada por explosiva desgranulación con fuerte expresión de c-Kit, Cox-2, triptasa y quimasa, dos proteasas características; por otro lado, encontramos una subpoblación de células c-Kit^{+} pequeñas y redondeadas, que se caracterizan por la falta de gránulos. Ambos fenotipos se encuentran aumentados de manera significativa en la médula espinal de pacientes con ELA, en comparación con lo que se observa en los controles.

- En cortes histológicos de la médula espinal de modelos murinos SOD1^{G93A} (ratones y ratas) también observamos una acumulación de células que expresan c-Kit, quimasa y Cox-2, que se acumulan rodeando los cuerpos de las motoneuronas en degeneración en el asta ventral lumbar, comparado con pocas células con estas características en los animales no-transgénicos. En los modelos murinos, el fenotipo predominante correspondió a células pequeñas con pocos gránulos, encontrando pocas células con desgranulación activa. En las tinciones realizadas no se pudo identificar células positivas para el ensayo de azul de Toluidina, que típicamente caracteriza mastocitos en el tejido conectivo. También pudimos observar por técnicas de citometría de flujo un aumento en una subpoblación de mastocitos CD45^{+}/c-Kit^{+} en la médula espinal sintomática.
- Por primera vez, pudimos obtener mastocitos diferenciados *ex vivo*, a partir de precursores c-Kit^{+} aislados de la médula espinal de ratas sintomáticas. Al igual que los precursores CD34^{+} aislados en nuestro primer artículo, los precursores c-Kit^{+} de mastocitos se ubicaron en la fase no-adherente del cultivo celular y fueron diferenciados al fenotipo maduro con SCF en presencia de IL-3. El análisis citológico comprobó la presencia de mastocitos diferenciados caracterizados por la expresión de c-Kit, CD45, quimasa y Cox-2, además de la positividad para azul de toluidina.
- Se observó que los precursores de mastocitos c-Kit^{+} derivados de médula ósea y marcados exógenamente con un marcador fluorescente, CFSE, eran capaces de infiltrar y acumularse en el parénquima en la médula espinal luego de ser inyectados por vía intravenosa en ratones sintomáticos. Los precursores c-Kit^{+}/CSFE^{+}, se localizaban en la médula espinal sintomática luego de 48h de ser inyectados en ratones SOD1^{G93A}, pero no en animales no transgénicos. La invasión de mastocitos tuvo una localización peri-vascular, sugiriendo su pasaje a través de la barrera hemato-espinal defectuosa.
- Se observó una asociación espacial entre mastocitos y elementos microvasculares con anormalidades morfológicas (interrupciones en la marcación de colágeno, "*sprouts*" y "*strings*"), tanto en tejido post-mortem de pacientes con ELA como en animales sintomáticos, sugiriendo un efecto de los mastocitos remodelando la microvasculatura a través de la liberación de proteasas. En comparación, el nicho vascular que rodea a las motoneuronas en sujetos control y animales no-transgénicos, no presentaba las anormalidades observadas en pacientes o modelos murinos de ELA.
- Debido a lo observado en la publicación previa, acerca de la vía quimiotáctica c-Kit/SCF, decidimos analizar la expresión del ligando SCF en el microambiente celular neurodegenerativo de la médula espinal en ratones SOD1^{G93A}

sintomáticos. Allí observamos una expresión aumentada de SCF en astrocitos reactivos y una interacción espacial entre estos astrocitos SCF^+ y mastocitos c-Kit^+, sugiriendo un mecanismo quimiotáctico.

- Finalmente, observamos que el tratamiento sistémico con masitinib en ratones $SOD1^{G93A}$ sintomáticos, pudo prevenir el tráfico y acumulación de mastocitos en la médula espinal de ratones con ELA, con consecuentes efectos en los defectos de la BHE.

Conclusiones

Este estudio muestra evidencia experimental apoyando la presencia de mastocitos y sus precursores c-Kit^+ en el microambiente que rodea a las motoneuronas en degeneración en la ELA, tanto en pacientes como en modelos murinos de la enfermedad. Los mastocitos parecen infiltrar en el parénquima de la médula espinal desde la periferia a través de elementos microvasculares defectuosos de la BHE, guiados quimiotácticamente por astrocitos reactivos que expresan SCF, el ligando de c-Kit. Además, estos mastocitos y sus precursores aparecen como importantes mediadores de la neuroinflamación crónica y pueden ser blancos de inhibidores de tirosina quinasa.

Sin embargo, durante este estudio no pudimos profundizar en los mecanismos por los cuales ocurre la interacción entre los astrocitos reactivos expresando SCF y los precursores de mastocitos c-Kit^+, tanto a nivel de la quimioatracción como promoviendo su posterior diferenciación. Por otro lado, pese a observar un aumento en la expresión de SCF por técnicas de inmunohistoquímica, al observarse en una subpoblación de astrocitos reactivos, no profundizamos en su expresión, tanto a nivel proteico como a nivel de ARNm, utilizando técnicas de biología molecular.

Acta Neuropathologica Communications

RESEARCH

Open Access

The pathogenic role of c-Kit+ mast cells in the spinal motor neuron-vascular niche in ALS

Mariángeles Kovacs[1], Catalina Alamón[1], Cecilia Maciel[1], Valentina Varela[1], Sofía Ibarburu[1], Lucas Tarragó[1], Peter H. King[2,3], Ying Si[2,3], Yuri Kwon[2], Olivier Hermine[4,5,6,7,8,9,10], Luis Barbeito[1] and Emiliano Trias[1*]

Abstract

Degeneration of motor neurons, glial cell reactivity, and vascular alterations in the CNS are important neuropathological features of amyotrophic lateral sclerosis (ALS). Immune cells trafficking from the blood also infiltrate the affected CNS parenchyma and contribute to neuroinflammation. Mast cells (MCs) are hematopoietic-derived immune cells whose precursors differentiate upon migration into tissues. Upon activation, MCs undergo degranulation with the ability to increase vascular permeability, orchestrate neuroinflammation and modulate the neuroimmune response. However, the prevalence, pathological significance, and pharmacology of MCs in the CNS of ALS patients remain largely unknown. In autopsy ALS spinal cords, we identified for the first time that MCs express c-Kit together with chymase, tryptase, and Cox-2 and display granular or degranulating morphology, as compared with scarce MCs in control cords. In ALS, MCs were mainly found in the niche between spinal motor neuron somas and nearby microvascular elements, and they displayed remarkable pathological abnormalities. Similarly, MCs accumulated in the motor neuron-vascular niche of ALS murine models, in the vicinity of astrocytes and motor neurons expressing the c-Kit ligand stem cell factor (SCF), suggesting an SCF/c-Kit-dependent mechanism of MC differentiation from precursors. Mechanistically, we provide evidence that fully differentiated MCs in cell cultures can be generated from the murine ALS spinal cord tissue, further supporting the presence of c-Kit+ MC precursors. Moreover, intravenous administration of bone marrow-derived c-Kit+ MC precursors infiltrated the spinal cord in ALS mice but not in controls, consistent with aberrant trafficking through a defective microvasculature. Pharmacological inhibition of c-Kit with masitinib in ALS mice reduced the MC number and the influx of MC precursors from the periphery. Our results suggest a previously unknown pathogenic mechanism triggered by MCs in the ALS motor neuron-vascular niche that might be targeted pharmacologically.

Keywords: Mast cells, Motor neuron-vascular niche, ALS, Masitinib, Spinal cord

Introduction

The pathogenesis of amyotrophic lateral sclerosis (ALS) is multifactorial and remains partially understood. However, recent evidence suggests that peripheral immune cells such as lymphocytes, monocytes/macrophages, and mast cells (MCs), significantly contribute to deleterious inflammation and disease progression [3, 5, 6, 49]. Evidence indicate that peripheral MCs play a pathogenic role in ALS, through close contact with motor axons and NMJs (neuromuscular junctions) undergoing active peripheral motor pathway degeneration in ALS [48, 49]. While MCs have been described in the CNS of ALS subjects [19], little is known, however, about the mechanisms controlling the MC influx to the Central Nervous

*Correspondence: etrias@pasteur.edu.uy
[1] Institut Pasteur de Montevideo, 2020 Montevideo, Uruguay
Full list of author information is available at the end of the article

System (CNS) and their interaction with motor neurons and perineuronal microvasculature in the spinal cord.

MCs are effectors cells of the innate immune system derived from hematopoietic myeloid precursors that can be found in low numbers in all vascularized tissues including specific brain regions [14, 26, 52]. MC precursors expressing the tyrosine kinase receptor c-Kit, leave the bone marrow to enter the circulation and are recruited to tissues through a trans-endothelial passage, and are often found close to blood vessels [26]. Immature MCs achieve maturation within the local tissue microenvironment, a process that involves changes in phenotype and accumulation of granules containing neuroactive and vasoactive molecules, proteases, and proteoglycans [10, 31, 56]. Functionally, MCs play a key role in inflammatory processes via controlled degranulation (secretion) of several cytokines, trophic factors, proteases, lipid metabolites, and nitric oxides [42]. MC accumulation and activation in the CNS pathologies such as multiple sclerosis are known to mediate chronic neuroinflammation, microglial activation, and disruption of the blood–brain barrier (BBB) and brain-spinal cord barrier (BSCB) [12, 40, 43]. Although a growing body of evidence supports the pathogenic role of MCs in neurodegenerative conditions, little is known about the potential role of MCs inducing motor neuron damage and/or vascular dysfunction in ALS.

The tyrosine kinase receptor c-Kit (KIT or CD117) belongs to a family of transmembrane growth factor receptors [39]. The c-Kit specific ligand is Stem Cell Factor (SCF), also known as mast cell growth factor [13]. While c-Kit is expressed extensively in hematopoietic cells, it is generally lost during the differentiation process, except for MCs that retain c-Kit through their lifespan [27]. Thus, the SCF/c-Kit pathway is required for the survival, differentiation, and degranulation of MCs [27]. Pharmacological inhibition of c-Kit in ALS murine models with masitinib results in significant amelioration of paralysis progression and a sharp decrease in MC infiltration into the degenerating peripheral motor pathways and NMJs [47–50]. Masitinib is a tyrosine kinase inhibitor drug that also targets type III kinases [11], including CSF-1R in microglia, monocytes, and macrophages, resulting in decreased microgliosis in the spinal cord [47–49]. Evidence from clinical trials indicate that masitinib exerts therapeutic effects in ALS [24, 32], as well as in progressive forms of multiple sclerosis [53] and Alzheimer's disease [38], indicating therefore that it can target neuroinflammatory and neurodegeneration processes through multifaceted mechanisms, including MCs downregulation.

Because MCs are mainly localized nearby blood vessels [4] and cluster around degenerating motor nerve terminals in ALS [49], we analyzed whether MCs also infiltrated around the motor neuron cell bodies and surrounding microvasculature elements in the spinal cord of both ALS subjects and murine models. We report for the first time that MCs accumulate in significant numbers within the motor neuron-vascular niche in ALS and provide evidence for undifferentiated MCs trafficking from the periphery through microvasculature that shows remarkable morphological abnormalities. Moreover, we show in ALS mice that MCs number and trafficking into the spinal cord were downregulated by masitinib, a drug that modulates MCs activity via inhibition of c-Kit, LYN, and FYN kinases, with subsequent anti-inflammatory and neuroprotective effects in ALS [32, 47].

Material and methods

Human tissue collection

The collection of post-mortem human ALS and control samples was approved by The University of Alabama at Birmingham (UAB) Institutional Review Board (Approved IRB Protocol: X091222037 to Dr. Peter H. King). All ALS patients were cared for at UAB and detailed clinical records were available. Control samples were age-matched and were harvested from patients who expired from non-neurological causes. None of the ALS cases correspond to familiar cases associated with SOD1 mutations. The average collection time after death was less than 10 h (Additional file 1: Table 1). All tissues were collected by Peter H. King and Ying Si.

Human spinal cord immunohistochemistry

In this study, 10 µm spinal cord paraffin sections were sliced using a microtome. Following deparaffinization, antigen retrieval was performed in 10 mM citrate buffer pH 6 using a steamer cooker, reaching 95 °C for 30 min. Then, slices were cooled down in the same citrate buffer at room temperature for 30 min and washed with PBS for 2 h. After washing, slices were blocked and permeabilized in BSA 5%/Triton X-100 0.5% for 2 h at room temperature. Primary antibodies were incubated in BSA 1%/Triton X-100 0.5% at 4 °C overnight. After washing, fluorophore-conjugated secondary antibodies were incubated for 3 h at room temperature. After PBS washing, Mowiol medium (Sigma, St. Louis, MO, USA) was used for mounting. Only ventral lumbar spinal cord sections were analyzed. Motor neuron somas were identified in the ventral spinal cord by typical morphology and nuclei. Saturated DAPI staining was used to better differentiate motor neuron somas as previously described [28]. For diaminobenzidine (DAB) staining, biotinylated anti-rabbit and anti-mouse secondary antibodies were used after primary incubation. The protocol described in the VECTASTAIN Elite ABC-HRP Kit (Vector Laboratories,

#PK-6101) was followed together with the ImmPACT DAB substrate (SK-4105). After washing, the hematoxylin staining protocol was performed for 3 min to stain nuclei.

Animals

Mice used in this study were obtained from The Jackson Laboratory, Bar Harbor, MA, USA. Animals were housed in a centralized animal facility with a 12-h light–dark cycle with ad libitum access to food and water. Male mice B6SJL-Tg(SOD1*G93A)1Gur/J mice, over-expressing human SOD1 mutation (G93A SOD1) were used for further breeding to maintain the line. Perfusion with fixative was performed under 90% ketamine/10% xylazine anesthesia and all efforts were made to minimize animal suffering, discomfort, or stress. All mice were weighed and evaluated for motor activity daily. Disease onset was determined for each animal when pronounced muscle atrophy was accompanied by an abnormal gait, typically expressed as subtle limping or dragging of one hind limb (~120 days old). Also, male $SOD1^{G93A}$ rat progeny, purchased from Taconic bioscience (NTac:SD-Tg (SOD1G93A)L26H), were used for further breeding to maintain the line [11]. Rats were housed in a centralized animal facility with a 12-h light–dark cycle with ad libitum access to food and water. Perfusion with fixative was performed under 90% ketamine/10% xylazine anesthesia and all efforts were made to minimize animal suffering, discomfort, or stress. All procedures using laboratory animals were performed following the national and international ARRIVE guidelines and were approved by the Institutional Animal Committee for animal experimentation. This study was carried out in strict accordance with the Institut Pasteur de Montevideo ethical committee's requirements (CEUA Approved protocols: #005-17, #016-19, #005-20, #007-20, to Dr. Luis Barbeito) and the national law (Number 18.611) for animal experimentation that follows the Guide for the Care and Use of Laboratory Animals of the National Institutes of Health (USA).

Immunohistochemistry of mice spinal cord

At least four animals of each condition were used for the immunohistochemistry experiment. Non-transgenic (Non-Tg) mice of 150–160 days and transgenic $SOD1^{G93A}$ symptomatic mice of 120–130 days ($SOD1^{G93A}$ Onset) and 150–160 days ($SOD1^{G93A}$ Symp) were used to perform experiments. Animals were deeply anesthetized and transcardial perfusion was performed with paraformaldehyde 4% (v/v) in PBS pH = 7.4. Fixed spinal cords were cryopreserved in 30% sucrose (Sigma, St. Louis, MO, USA) at 4 °C. After 72 h, tissue was embedded in Tissue-Tek (Sakura), sectioned (transversal) using a cryostat, and collected on gelatin-coated slides. Then, 25 µm sections were blocked for 2 h at room temperature in 5% BSA, 0.3% Triton X-100/2% Goat Serum in PBS, incubated with primary antibodies overnight at 4 °C in 1% BSA/0.3% Triton X-100/0.4% Goat Serum. After washing, fluorophore-conjugated secondary antibodies were incubated for 2 h at room temperature in 1% BSA/0.3% Triton X-100/0.4% Goat Serum. To determine primary antibodies' specificity, immunohistochemistry was carried out in the absence of primary antibodies. Non-significant immunofluorescence was detected with secondary antibodies incubation. DPX mounting medium (Sigma, St. Louis, MO, USA) was used for mounting. DAB staining was performed as described above.

Histochemistry quantitative analysis

MCs in the ventral horn of the lumbar spinal cord sections were identified by the typical granular morphology and tryptase+/chymase+, c-kit+/chymase+, c-Kit+/Cox-2+, chymase+/Cox-2+or c-Kit+/CD45+ immunohistochemical staining as well as c-Kit+/CFSE+, c-Kit+ or CFSE+ infiltrating MC precursors, using a stereological approach. The counting was performed only in the area surrounding motor neuron cell bodies within a radius of 150 µm of the soma. The counting was carried out using maximum-intensity projection confocal microphotographs with a magnification of 63x. At least fifteen sections per spinal cord were analyzed ($n = 4$ for mice spinal cord analysis, $n = 5$ for human spinal cord analysis). Image J software was used for analysis.

For co-expression of SCF with the astrocyte marker, GFAP was carried out using Image J software as previously described [28]. At least fifteen sections per spinal cord per animal per condition ($n = 4$) were used. The number of c-Kit+ cells surrounding SCF+ astrocytes and SCF+ motor neurons was assessed using ImageJ software, counting the positive cells in maximum-intensity projection confocal microphotographs with a magnification of 63x. At least fifteen sections per spinal cord per condition were analyzed ($n = 4$ for mice spinal cord analysis).

Toluidine blue staining of mast cells.

For the MC analysis based on metachromasia observation, as previously described [48], 10 µm sections of human (paraffin sections) and mice (fixed frozen sections) spinal cord were microtome and cryostat sliced and mounted in gelatin-coated slides respectively. Also, cultured cells obtained from the $SOD1^{G93A}$ rat spinal cord and mounted in slides were used. Slides were washed and hydrated 2 times in distilled water for 10 min and embedded in 1% toluidine blue solution for 10–20 min for human and mice tissue and 5 min in case of cultured

cells. Then, slides were washed in distilled water for 5 min and dehydrated for 3 min in 70% ethanol, 3 min in 95% ethanol, and finally 2 min in 100% ethanol. Slides were cleared in xylene twice, 3 min each, and finally mounted in DPX (Sigma-Aldrich). Images (at × 100 magnification) were acquired using an Olympus CX41 microscope connected to an Evolution LC Color camera and using ImagePro Express software for acquisition.

Flow cytometry analysis of the mice spinal cord

Spinal cords from both, Non-Tg or $SOD1^{G93A}$ symptomatic mice were dissected, and the meninges were carefully removed in animals deeply anesthetized as described above. Spinal cords were mechanically chopped and enzymatically dissociated using 0.25% trypsin for 5 min at 37 °C. Fetal Bovine Serum (FBS) 10% (vol/vol) in PBS was then added to halt trypsin digestion. Repetitive pipetting thoroughly disaggregated the tissue, which was then collected on an 80 µm mesh strainer and spun down. The resulting filtered cell suspensions were re-suspended in PBS-FBS 2%-1 mM EDTA.

Flow cytometry analysis was performed as previously described [18]. Briefly, single-cell suspensions from the spinal cord were incubated with fluorochrome-conjugated antibodies against the following antigens: CD45-PerCP (BioLegend, #103130) as an infiltrating hematopoietic cell marker, and c-Kit conjugated to biotin (Abcam, #ab25022) in PBS-FBS 2%-1 mM EDTA for 20 min at 4 °C. After incubation and washing, single-cell suspensions were incubated with 1:500 Streptavidin-Alexa Fluor 405 (Thermo Fisher Scientific, #S21375). Analysis was performed on an Attune NxT Flow Cytometer (Thermo Fisher Scientific, Waltham, MA, USA). Post-acquisition analysis was assessed using FlowJo software.

Cultures of mast cell precursors from the symptomatic $SOD1^{G93A}$ rats' spinal cord

Primary cell cultures were obtained from the spinal cord of symptomatic $SOD1^{G93A}$ rats according to the procedures described by Trias et al., 2013 with modifications [46]. Briefly, animals were euthanized by overdosing with ketamine/xylazine, and the spinal cords were carefully dissected on ice with meninges removal. Then, spinal cords were chopped finely and dissociated with 0.25% trypsin in a calcium-free buffer for 5 min at 37 °C. Trypsin treatment was stopped by adding RPMI 1640/15% (vol/vol) FBS. The resulting extract was passed through an 80-µm mesh to eliminate tissue debris and then was spun. The pellet was resuspended in a mast cell culture medium [RPMI 1640/15% (vol/vol) FBS, sodium pyruvate (1 mM), β-mercaptoethanol (50 µM)] and then placed in 75-cm^2 tissue culture flasks in presence of SCF and IL-3 (20 ng/mL) freshly added every 48 h. Non-adherent cells were resuspended with the culture medium subsequently replaced and detached cells were discarded every 48 h. Cells were analyzed by flow cytometry at 2 and 7 days and characterized by immunocytochemistry at 14 days, as described below.

Flow cytometry analysis of cultured c-Kit+ mast cells precursors from $SOD1^{G93A}$ spinal cord

After 2 and 7 days in vitro (DIV), the c-Kit+ population was analyzed by flow cytometry. Removal of cell debris was performed using the Debris Removal Solution (Miltenyi Biotec, #130-109-398) according to the manufacturer´s instructions. Briefly, the cell suspension was resuspended in cold PBS 1X, and 900 µL of Debris Removal Solution were added and overlaid gently with 4 mL of cold PBS. The cell suspension was centrifuged at 4 °C and 3000xg for 10 min. Two top phases were completely aspirated and discarded. Cold PBS was added to a final volume of 15 mL, and the cell suspension was centrifuged at 4 °C and 1000xg for 10 min. Finally, the supernatant was completely aspirated, and cells were resuspended carefully in PBS-FBS 2%-1 mM EDTA. Then, single-cell suspensions were incubated with c-Kit conjugated to biotin in PBS-FBS 2%-1 mM EDTA for 20 min at 4 °C. After incubation and washing, single-cell suspensions were incubated with 1:500 Streptavidin- Alexa Fluor 405. Analysis was performed on an Attune NxT Flow Cytometer (Thermo Fisher Scientific, Waltham, MA, USA). Post-acquisition analysis was assessed using FlowJo software.

Immunocytochemical staining of cultured cells

Cultured cells were mounted in slides and fixed with 4% PFA for 20 min at 4 °C and then were washed three times with 10 mM PBS (pH 7.4). Cells were permeabilized using 0.3% Triton X-100 for 20 min. Non-specific binding was blocked by incubating fixed cells with 5% BSA in PBS for 1 h at room temperature. Corresponding primary antibodies were diluted in BSA 1% and incubated overnight at room temperature. After washing, cells were incubated with secondary antibodies in BSA 1% for 1 h at room temperature. DAPI was used for nuclei staining.

Intravenous injection of bone marrow mast cells into ALS mice

Bone marrow-derived mast cells (BMMC) cultures were obtained from $SOD1^{G93A}$ symptomatic mice following the protocol previously described by Heig et al. 1994 [20]. Briefly, animals were euthanized by overdosing with ketamine/xylazine, and long bones were exposed. The bone marrow was flushed from the tibia and femur and collected in a 15 mL tube. After centrifugation for 10 min at 1000xg, pellet was resuspended in mast cell culture

medium [RPMI 1640 medium/15% (vol/vol) FBS, sodium pyruvate (1 mM), β-mercaptoethanol (50 μM)] in presence of IL-3 (20 ng/mL) and SCF (20 ng/mL) freshly added every 48 h. The attached cells were discarded, non-adherent cells were resuspended and the culture medium was replaced every 48 h. After 2, 7, and 14 DIV, cells were collected and purity of BMMC culture was analyzed using flow cytometry and immunocytochemistry by staining with c-Kit antibody. Cell viability was assessed using the 0.4% trypan blue dye exclusion method before transplantation. Cells were stained with Cell Trace CFSE according to the manufacturer´s instructions (Thermo Fisher Scientific, #C34554) allowing the cell tracking after transplantation. Transplant cell concentration was adjusted to a final concentration of 5000 cells/μL (1×10^6 cells/200 μL c-Kit+ BMMC) and were delivered intravenously by injection through the tail vein. Also, four Non-Tg mice were transplanted with c-Kit+ BMMC at a final concentration of 5000 cells/μL as control. The media-injected group received 200 μL of PBS, the same volume administered to the cell-transplanted mice. 48 h after injection, animals were euthanized by overdosing with ketamine/xylazine and spinal cords were processed for immunohistochemical analysis.

To determine whether masitinib could influence MCs trafficking and accumulation in the spinal cord, eight transgenic mice at 140 days old were randomly divided into the masitinib or vehicle-treated groups. Masitinib mesylate (AB1010) freshly prepared in drinking sterilized water was administrated daily at a dosage of 50 mg/kg/d using a curved stainless steel gavage needle with a 2-mm ball tip. Mice ($n=4$ per group) were treated for 10 days. On day 8, MC precursors were intravenously injected as previously described. On day 10, Evans Blue (EB) extravasation protocol was performed. Briefly, animals were intracardially perfused with 4% PFA/1% EB under 90% ketamine/10% xylazine anesthesia and euthanized. Spinal cords were processed for immunohistochemistry analysis. Far-red fluorescence EB emission was detected by confocal microscopy.

Analysis of microvasculature

To analyze vascular abnormalities in $SOD1^{G93A}$ symptomatic mice, using a stereological approach, the number of string vessels and vessel sprouts stained with collagen type I antibody [55] were assessed as previously described [15, 22]. The counting was performed only in the area that surrounds motor neurons within a radius of 150 μm of the soma in the ventral horn of the lumbar spinal cord. The counting was carried out using maximum-intensity projection confocal microphotographs with a magnification of 63x. At least fifteen sections per spinal cord were analyzed ($n=4$). Image J software was used for analysis.

EB extravasation analysis was performed as previously described [23]. Animals were intracardially perfused with 4% PFA/1% EB under 90% ketamine/10% xylazine anesthesia. Then, the spinal cords were dissected, maintained overnight in 4% PFA, and cryopreserved in 30% sucrose (Sigma, St. Louis, MO, USA) at 4 °C. After 72 h, tissue was embedded in Tissue-Tek (Sakura), and 25 μm thick slices were sectioned using a Leica cryostat and collected on gelatin-coated slides. Then, far-red fluorescence EB emission was detected by confocal microscopy. EB analysis was performed either alone or after immunostaining with other markers. Quantitative analysis of perivascular EB extravasation was measured as the intensity in a 5 μm radius surrounding blood vessels using Image J software.

Antibodies used

Primary antibodies: 1:250 mouse monoclonal anti-chymase (Abcam, #ab2377) 1:200 mouse monoclonal anti- tryptase (Abcam, #ab2378), 1:200 goat polyclonal anti-chymase (Abcam, #ab111239), 1:100 rat monoclonal anti-c-Kit (biotin) (Abcam, #ab25022), 1:300 rabbit polyclonal anti-collagen I (Abcam, #ab34710), 1:200 rabbit polyclonal anti- COX2 (Abcam, #ab15191), 1:200 mouse monoclonal anti-βIII-Tubulin (Millipore, #MAB1637), 1:100 rabbit polyclonal anti-SCF (Fisher Scientific, #PA520746), 1:400 mouse monoclonal anti-GFAP (Sigma, #G3893) and 1:100 rabbit polyclonal anti-CD45-PerCP (BioLegend, #103130). Secondary antibodies: 1:500 goat anti-rabbit- AlexaFluor488 or AlexaFluor546 (Thermo Fisher Scientific, #A11035 or #A11034), 1:500 goat anti-mouse-AlexaFluor488, AlexaFluor546 or AlexaFluor633 (Thermo Fisher Scientific, #A11029, #A11030, or #A21052), 1:500 donkey anti-goat- AlexaFluor488 (Thermo Fisher Scientific, #A11055) and 1:500 Streptavidin- AlexaFluor633 (Thermo Fisher Scientific, #S21375). NeuroTrace 530/615 red fluorescent Nissl stain (Thermo Fisher Scientific, #B34650) was also used for neuronal visualization.

Fluorescence imaging

Fluorescence imaging was performed with a laser scanning Zeiss LSM 800 confocal microscope with either a 25 × (1.2 numerical aperture) objective or 63 × (1.3 numerical aperture) oil- immersion objective using Zeiss Zen Black software. Maximum intensity projections of optical sections were created with Zeiss Zen software.

Bright-field imaging

DAB immunohistochemical imaging was acquired using a Zeiss LSM 800 microscope connected to an Evolution LC Color camera using 63 × (1.3 numerical aperture) oil-immersion objective using Zeiss Zen Black software.

Statistical analysis

Quantitative data were expressed as mean ± s.e.m. For statistical analysis two-tailed Mann–Whitney test, Kruskal–Wallis followed by Dunn's multiple-comparisons test, one-way ANOVA, or two-tailed unpaired t-test were used, with $p < 0.05$ considered significant. GraphPad Prism 7.03 software was used for statistical analysis.

Results

Mast cells accumulate nearby spinal motor neurons in ALS

Previous studies on ALS have provided scarce information on MC phenotypes and precise localization in the postmortem patients' spinal cords [19]. Thus, we examined five postmortem lumbar spinal cords from ALS subjects and four control donors by immunofluorescence confocal microscopy (Additional file 1: Table 1). In control donors, a scarce number of small cells expressing MC markers such as c-Kit, chymase, tryptase, or Cox-2 and bearing a granular cytoplasm, were identified in the grey matter surrounding motor neuron cell bodies (Fig. 1D and Additional file 1: Fig. 1). In comparison, all ALS specimens systematically displayed an increased density of cells bearing a MC phenotype (2.4 ± 1.6 vs. 0.6 ± 0.7 cells per analyzed field in ALS and controls, respectively), which preferentially accumulated in clusters nearby motor neuron somas (Fig. 1A and Additional file 1: Fig. 1). In ALS subjects, MCs displayed hypertrophy, granular morphology and frequent images of explosive degranulation, and strong staining with c-Kit, chymase, tryptase, and Cox-2 (Fig. 1B and Additional file 1: Fig. 1). In addition, a sub-set of c-Kit+ cells of small size and bearing few or no granules were also found in ALS specimens (Fig. 1D and Additional file 1: Fig. 1B). There was a fourfold increase in density of peri-neuronal c-Kit+ and chymase+/tryptase+ cells in the ALS spinal cord as compared with control donors (Fig. 1E and Additional file 1: Fig. 1).

c-Kit+ mast cells accumulate in the degenerating spinal cord of ALS mice and rats

Next, we examined MC accumulation in the spinal cord of ALS murine models as this is still unknown. As shown in Fig. 2 and Additional file 1: Fig. 2 and 3, cells expressing c-Kit, chymase, and/or Cox-2 accumulated nearby degenerating motor neurons in symptomatic SOD1^{G93A} mouse and rat lumbar spinal cords, as compared with significantly fewer cells observed in SOD1^{G93A} mice and rats at the onset of the disease as well as in Non-Tg littermates (Fig. 2 and Additional file 1: Fig. 2 and 3). The predominant MC phenotype in the symptomatic SOD1^{G93A} mouse spinal cord corresponded to small cells bearing few granules and scarce images of explosive degranulation. Metachromasia following staining with toluidine blue that typically identifies MCs in epithelial or connective tissues [41] was not observed in MCs from the murine or human spinal cord (Additional file 1: Fig. 4). Quantitative analysis showed that the number of c-Kit+/chymase+ and c-Kit+/Cox-2+ MCs outnumbered by 2- and fourfold, respectively, the number of MCs in non-transgenic animals (Fig. 2A and Additional file 1: Fig. 2). To quantitatively analyze the c-Kit+ MC population, we performed flow cytometry analysis of the spinal cord. As shown in Fig. 2B, there was a twofold increase in the number of c-Kit+ cells in the symptomatic spinal cord of SOD1^{G93A} mice relative to Non-Tg littermates.

Next, we performed flow cytometry analysis to further characterize the population of c-Kit+ cells expressing CD45 from the spinal cord of symptomatic SOD1^{G93A} mice. CD45 is a well-recognized surface receptor marker of hematopoietic cells[51] and tumoral MCs [45]. As shown in Fig. 2C, c-Kit+ cells co-expressing CD45 and bearing MC morphology were abundant near motor neurons in ALS mice. The quantitative analysis of CD45+ and CD45+/c-Kit+ populations in the spinal cord by flow cytometry showed that hematopoietic-derived cells were significantly increased by sixfold in the symptomatic SOD1^{G93A} spinal cord relative to Non-Tg, further suggesting the accumulation of blood-born c-Kit+ MC putative precursors into the degenerating spinal cord of ALS mice.

Ex vivo generation of mast cells from the spinal cord of SOD1^{G93A} rats

In peripheral tissues, MCs are originated from circulating blood MC-committed c-Kit+ progenitors in a process regulated by local factors that regulate trafficking, proliferation, and differentiation of MCs [7, 36]. We hypothesized that in ALS, similar c-Kit+ MC precursors infiltrate and accumulate into the spinal cord, preserving the ability to differentiate into mature MCs. To test this mechanism, we have used the already validated primary cell cultures from the spinal cord of symptomatic SOD1^{G93A} rats and non-transgenic littermates, in which a large number of precursor cells remain in a non-adherent phase [28]. Such non-adherent spinal cord cells were maintained for 7 days in the presence of SCF and interleukin-3 (IL-3) (Fig. 3A), cytokines that promote MC differentiation from bone marrow progenitors [20] as shown in Additional file 1: Fig. 7 in SOD1^{G93A} rats. During the SCF/IL3 differentiation protocol, the number of c-Kit+ cells in the spinal cord cultures increased from 8% after 2 days in culture to 13% at day 7 (Fig. 3B). Cytological analysis showed numerous images of fully differentiated, granular, metachromatic MCs expressing c-Kit, CD45, chymase, and Cox-2 (Fig. 3C), further indicating the

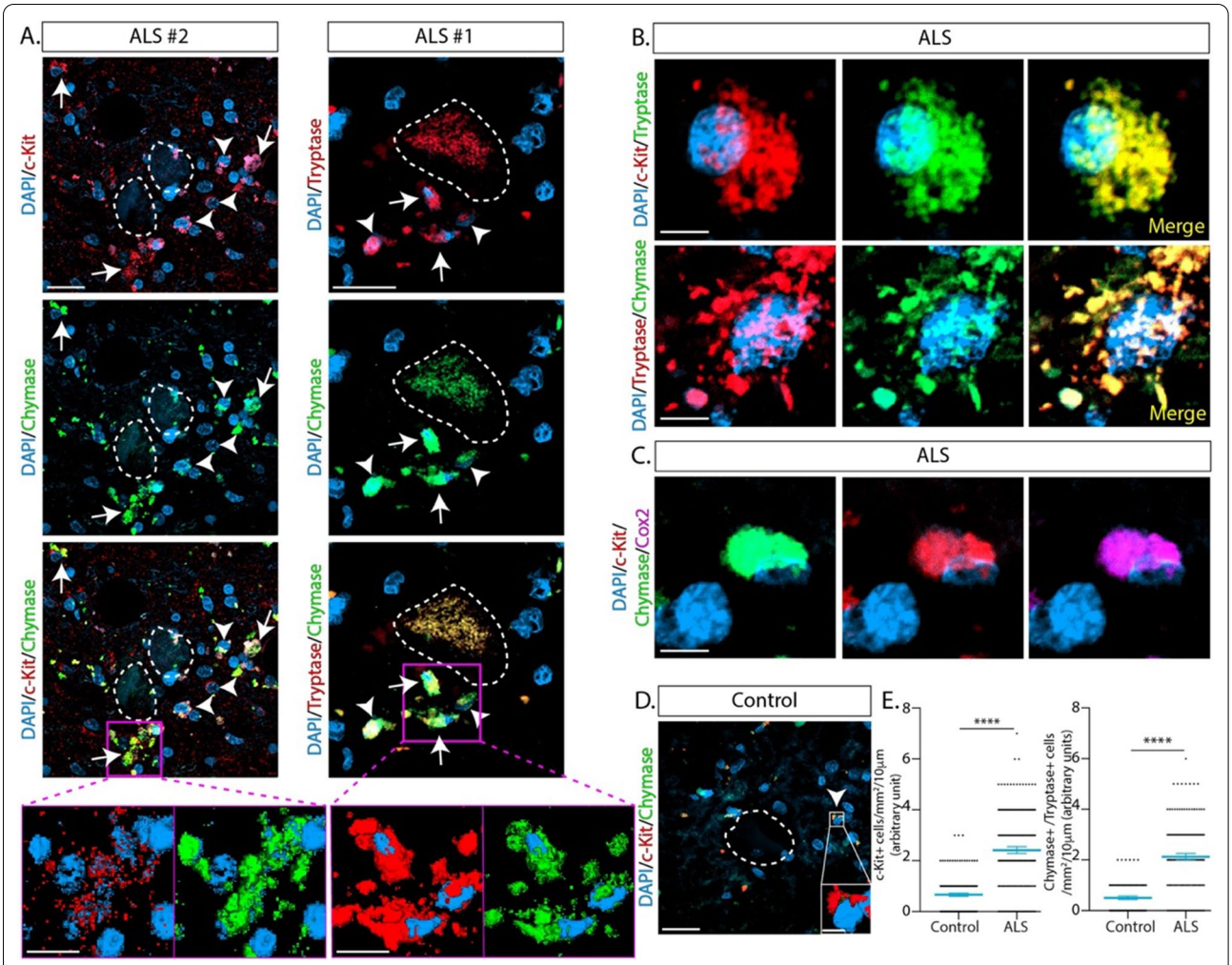

Fig. 1 Mast cells accumulate in the surrounding of degenerating motor neurons in the spinal cord of ALS patients. **A** Representative immunohistochemical confocal images of mast cells infiltrating into the ventral horn of lumbar spinal cord of autopsy ALS subjects. Left panels show the expression of c-Kit+ (red) and chymase+ (green) mast cells displaying typical granular (white arrows) and non-granular (white arrowheads) morphology in the surroundings of degenerating motor neurons (white lines). The right panels show the co-expression of chymase (green) and tryptase (red) in mast cells. Magenta squares show high magnification 3D reconstructions of both, small non-granular and degranulating cells. **B** Representative high magnification confocal phenotyping of mast cells in the spinal cord of ALS subjects. Upper panels show a granular mast cell co-expressing c-Kit (red) and tryptase (green). Lower panels show a typical degranulating mast cell that co-express tryptase (red) and chymase (green). **C** Representative microphotograph of non-granular small mast cells with none or few granules that typically express c-Kit (red), chymase (green), and Cox-2 (magenta). **D** Representative confocal image of the immunohistochemical analysis performed in autopsy control donors, showing only a few small non-granular cells expressing c-Kit (white arrowhead) in the surroundings of motor neurons (white lines). The white square shows a high magnification 3D reconstruction of typical non-granular cells expressing c-Kit (red). **E** The graphs show the quantitative analysis of c-Kit+ (left) and tryptase+/chymase+ (right) cells in the area that surrounds motor neurons in the ventral horn of the lumbar spinal cord of ALS subjects compared to control donors. Quantitative data are expressed as mean ± s.e.m. Data were analyzed by a two-tailed Mann–Whitney test, with ***$p < 0.0001$. Scale bars: 20 µm and 10 µm in (**A**, **D**) and 5 µ in (**B**, **C**)

accumulation of MC precursors in the ALS spinal cord. In comparison, spinal cord cultures from non-transgenic littermate rats maintained with SCF/IL-3 yielded a low number of c-Kit+ cells (Fig. 3 and Additional file 1: Fig. 8).

Circulating c-Kit+ mast cell precursors engraft into the motor neuron-vascular niche

Next, we explored whether peripheral c-Kit+ MC precursors isolated from the bone marrow of non-transgenic

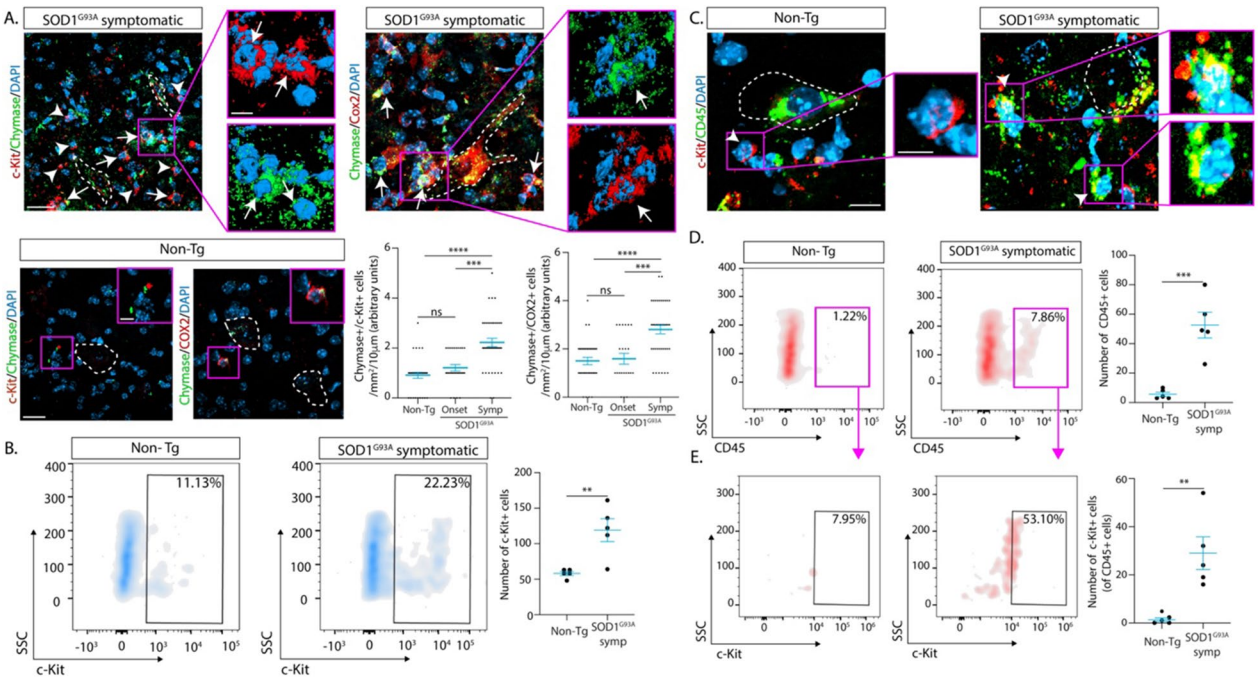

Fig. 2 Mast cells accumulate in the surrounding of motor neurons in the spinal cord of SOD1^{G93A} mice. **A** Representative confocal immunohistochemical images showing the co-expression of c-Kit+/chymase+ (left upper panels), and chymase+/Cox-2+ (right upper panels) mast cells in the surroundings of degenerating motor neurons (white dotted lines) in the ventral horn of the symptomatic SOD1^{G93A} lumbar spinal cord. Mast cells display two phenotypes, typically bearing granular morphology with images of explosive degranulation (white arrows) and small rounded cells with few or no granules (white arrowheads). Magenta squares show high magnification 3D reconstructions of both, small non-granular cells, and mast cells showing an irregular shape corresponding to an explosive degranulating state (white arrows). Lower panels to the left show representative confocal images of mast cell markers staining in non-transgenic littermates, where only small cells with non-apparent granules or degranulation were observed (magenta squares). The graphs to the right show the quantitative analysis of chymase+/c-Kit+ and chymase+/Cox-2+ mast cells in the ventral horn of the lumbar spinal cord of SOD1^{G93A} symptomatic mice compared to Non-Tg littermates. **B** Flow cytometry analysis of the c-Kit+ cell populations of the spinal cord of Non-Tg and SOD1^{G93A} symptomatic mice (150d). The images to the left show the representative density plots of c-Kit expression. The graph to the right shows the quantitative analysis between conditions. Note that a statistically significant increase of c-kit expression is observed in symptomatic ALS mice when compared with controls. **C** Representative confocal images analyzing cells that co-express c-Kit (red) and CD45 (green) in the surroundings of motor neurons (white dotted lines) in both Non-Tg (left panel) and symptomatic SOD1^{G93A} littermates (right panel). The magenta squares show a high magnification analysis of c-Kit+/CD45+ cells in both conditions. Note the presence of few granules in small cells in the symptomatic condition, while significantly fewer smaller cells with no granules are observed in Non-Tg mice. **D** Flow cytometry analysis of c-Kit+/CD45+ cell population in the spinal cord of Non-Tg and symptomatic SOD1^{G93A} mice. Upper panels show representative density plots of CD45 expression, where a significant increase is observed in the ALS condition. The lower panels show representative density plots of c-Kit expression within the CD45 population previously analyzed. Graphs to the right show the quantitative analysis for CD45 and CD45/c-Kit respectively. Quantitative data are expressed as mean ± s.e.m. Data were analyzed by Kruskal–Wallis followed by Dunn´s multiple comparison test (**A**) and two-tailed unpaired t-test (**B**, **D**, **E**), with $^{**}p < 0{,}01$, $^{***}p < 0.001$ and $^{****}p < 0.0001$ considered significant. $n = 4$ animals/condition. Scale bars: 20 µm and 5 µm in (**A**) in low and high magnification respectively, 10 µm and 5 µm in (**C**), in low and high magnification respectively

(See figure on next page.)

Fig. 3 Ex vivo generation of c-Kit+ mast cells from the spinal cord of ALS rats. **A** The scheme shows the procedure followed to obtain primary cultures of mast cells from the adult spinal cord of symptomatic SOD1^{G93A} rats and Non-Tg littermates. Spinal cords were maintained in the presence of IL-3 (20 ng/mL) and SCF (20 ng/mL) for 2, 7, and 14 days in vitro (DIV), and then mast cell markers, c-Kit, chymase, Cox-2, and CD45 were analyzed by flow cytometry and immunocytochemistry. **B** Flow cytometry analysis of c-Kit+ cultured mast cells after 2 and 7 DIV. Representative density plots show the expression of c-Kit at 2 and 7 days. The graph to the right shows the quantitative analysis of c-Kit expression in cells cultured from Non-Tg and SOD1^{G93A} rats. **C** Representative cytological and confocal immunohistochemical images of mast cells isolated from symptomatic SOD1^{G93A} spinal cord. Left panels show representative bright-field images of non-adherent cells with showing typical granular mast cells (upper panel) and metachromatic granular mast cells stained with toluidine blue (lower panel). Panels to the right show immunohistochemical phenotyping by confocal microscopy of cultured mast cells expressing typical markers such as c-Kit, CD45, chymase, and Cox-2 after 14 days in culture. Quantitative data are expressed as mean ± s.e.m. Data were analyzed by the Mann–Whitney test with $^{*}p < 0{,}05$ considered significant. $n = 4$ animals/condition. Scale bars: 5 µm

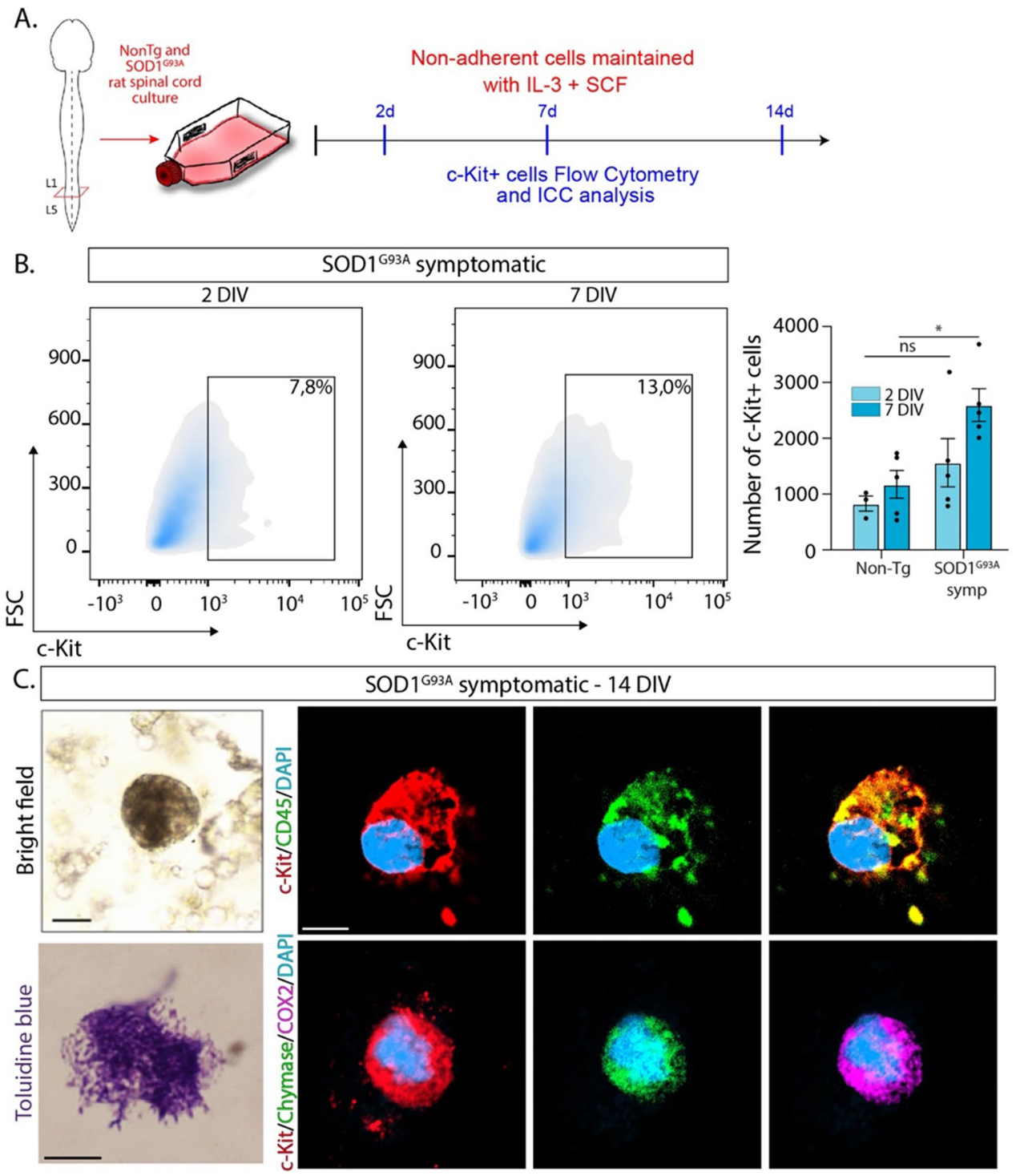

Fig. 3 (See legend on previous page.)

mouse donors and labeled with the cell tracer CFSE could infiltrate and engraft the spinal cord parenchyma following i.v. injection. Before transplantation, over 85% of MC precursors were c-Kit+ and CFSE+ (Fig. 4B). By 48 h following i.v. injection of 1×10^6 million MC precursors into symptomatic $SOD1^{G93A}$ recipient mice (150 days old), numerous CFSE+/c-Kit+ MC precursors were identified in the ventral horn in close association with microvascular elements (Fig. 4C). In comparison, no apparent or few CFSE+ cells were observed in the spinal cord of recipient non-transgenic mice, suggesting active trafficking of c-Kit+ MC precursors through the disrupted microvasculature in ALS mice.

Mast cells associate with abnormal perineuronal microvascular elements

To test whether increased vascular permeability to c-Kit+ MC precursors was due to disruption of microvascular elements previously described in ALS [16, 17, 23], we analyzed microvascular pathology in the discreet compartment surrounding spinal motor neuron cell bodies. Figure 5A shows that in the spinal cord of ALS patients, tryptase+/chymase+ and c-Kit+ MCs were localized close to microvascular elements stained with type-I collagen (Fig. 5A and Additional file 1: Fig. 9). Moreover, microvasculature associated with MCs showed frequent morphological abnormalities as observed by collagen-I interruptions, strings, and sprouts (Fig. 5C and Additional file 1: Fig. 9), which resemble abnormal microvasculature in other neurodegenerative conditions such as Alzheimer disease [15, 22]. In comparison, the motor neuron-vascular niche in control donor sections displayed a closer contact between the neuronal cell bodies and capillaries, absence of vascular abnormalities, and none or a scarce number of associated MCs (Fig. 5A, C, Additional file 1: Fig. 9). In addition, peri-neuronal vascular elements in ALS mice displayed morphological abnormalities like those described in ALS subjects (Fig. 5D).

c-Kit+ mast cells interact with astrocytes and motor neurons expressing stem cell factor

Because c-Kit receptor is activated by the cytokine SCF which mediates MC chemoattraction and differentiation [36], we explored whether c-Kit+ MCs were associated with increased expression of SCF in the ALS motor neuron-vascular niche. As shown in Fig. 6A, SCF was strongly upregulated in reactive astrocytes in the ventral horn of symptomatic $SOD1^{G93A}$ mice but not in controls. The number of reactive astrocytes co-expressing GFAP and SCF showed a 5 to sixfold increase relative to non-transgenic mice (Fig. 6A). SCF+ astrocytes spatially interacted with c-Kit+ MCs, suggesting astrocytic SCF may facilitate MC precursors infiltration and differentiation (Fig. 6B). In addition, spinal motor neurons from both non-transgenic and $SOD1^{G93A}$ mice appeared to express intense staining for SCF (Fig. 6C, Additional file 1: Fig. 10), indicating an alternative cellular source of the cytokine.

Post-paralysis c-Kit inhibition with masitinib prevents MCs trafficking and accumulation in the motor neuron-vascular niche

Because masitinib potently inhibits the SCF/c-Kit pathway in MCs [11], we hypothesized that systemic administration of masitinib (50 mg/kg/d) in $SOD1^{G93A}$ mice could prevent the trafficking and accumulation of MCs in the spinal motor neuron-vascular following i.v. injection. As shown in Fig. 7A, treatment with masitinib for 10 days significantly reduced by twofold the number of c-Kit+ and chymase+ MCs (Fig. 7B) in the lumbar motor neuron-vascular niche, respect to the vehicle-treated mice. Also, masitinib-treated animals showed a 30–40% reduction in microvascular abnormalities relative to vehicle-treated mice (Fig. 7C) and a 50% reduction in the number of CFSE-labeled c-Kit+ MC precursors infiltrating the spinal cord parenchyma (Fig. 7D). These results are consistent with a masitinib protective effect via c-Kit inhibition, preventing the trafficking of MC precursors and MC local differentiation in the motor neuron-vascular niche.

Discussion

Here we report that the cellular niche comprised between motor neuron somas and nearby microvascular elements in the spinal cord of ALS subjects and murine models is the recipient of yet unrecognized clusters of MCs that are not observed in controls. Within this niche, we identified an array of c-Kit+ MC phenotypes, including typical degranulating MCs bearing specific markers such as chymase, tryptase, and Cox-2, but distinctively lacking the toluidine blue metachromasia characteristic of MCs in the periphery. MC degranulation denotes active secretion of inflammatory and vasoactive compounds with the potential to locally affect the neurovascular crosstalk [44]. In accordance, microvascular elements associated with MCs were severely altered in ALS subjects and murine models as compared with controls, suggesting a bidirectional causality underlying MC infiltration and defective BSCB permeability. Furthermore, we provide evidence that overexpression of the c-Kit ligand SCF in reactive astrocytes may drive the local chemoattraction and subsequent differentiation of MCs. In accordance, treatment of ALS mice with the c-Kit inhibitor masitinib, which has recognized anti-inflammatory and neuroprotective effects in ALS, significantly reduced

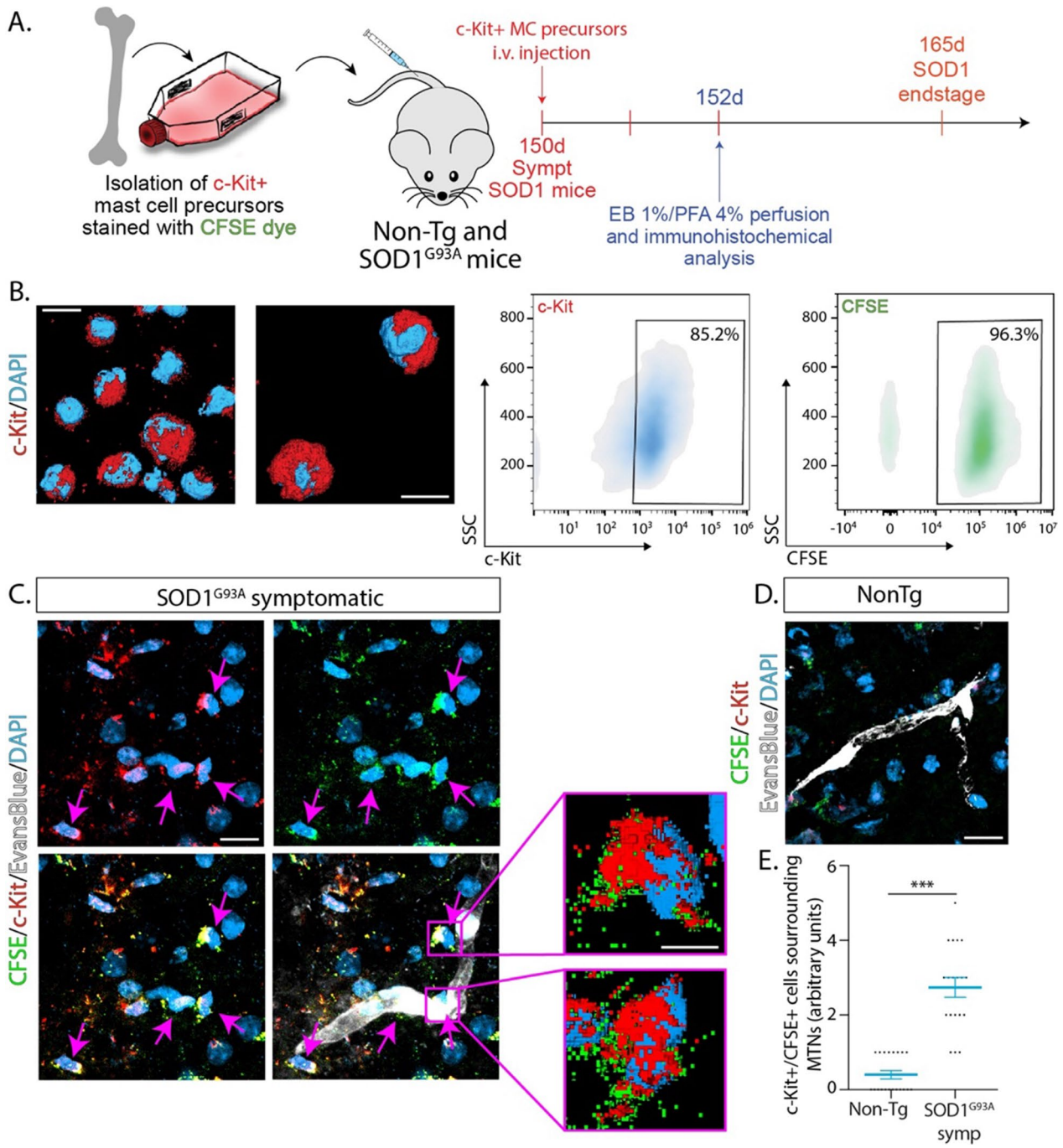

Fig. 4 c-Kit+ mast cell precursors engraft into the degenerating spinal cord of SOD1^{G93A} mice following i.v. administration. **A** The scheme shows the isolation and culture of mast cells precursors from the bone marrow of Non-Tg mice and the protocol followed for the i.v. injection c-Kit+ mast cell precursors stained with the CFSE cell tracer in Non-Tg and symptomatic SOD1^{G93A} littermates at 150 days. **B** Left panels show representative 3D confocal images of c-Kit immunostaining of mast cells precursors. Right panels show the flow cytometry density plot analysis c-Kit+ (red—left panel) precursors stained with CFSE+ (green—right panel). **C** Representative confocal images showing infiltration of c-Kit+/CFSE+ mast cells precursors (magenta arrows) into the symptomatic SOD1^{G93A} spinal cord parenchyma following 48 h after i.v. administration. c-Kit+/CFSE+ cells engrafted the parenchyma in the surroundings of blood vessels assessed by EB systemically perfused after euthanasia (white). Magenta squares show high magnifications 3D reconstructions of typical c-Kit+/CFSE+ precursor cells. **D** Representative confocal image of the co-expression of c-Kit and CFSE in the spinal cord of i.v. injected Non-Tg mice. None of few cells were observed in the spinal cord parenchyma of controls. **E** The graph shows the quantitative analysis of c-Kit+/CFSE+cells in Non-Tg and SOD1^{G93A} mice. Quantitative data are expressed as mean ± s.e.m. Data were analyzed by two-tailed Mann–Whitney test, with***$p < 0.001$ considered significant. Scale bars: 10 µm (**A**and **B**) and 5 µm in (**A**)

MC number and trafficking as well as the microvascular pathology in ALS mice. Together, these findings provide the first description of disease-associated MC phenotypes in the ALS spinal cord and reveal novel potential interactions between MCs and the cellular components of the motor neuron-vascular niche.

It is well-established that MCs infiltrate the CNS-affected regions in neurodegenerative diseases, including ALS [19], contributing to neuroinflammation [43]. However, the interplay between MCs, motor neurons, and microvascular elements has remained unknown. In the periphery, MCs accumulate in increased number and MC degranulation correlates with paralysis progression in the ALS peripheral motor nerves and denervated NMJs [48, 49]. Similarly, here we found that MCs spatially interact with ALS-affected spinal cord motor neurons. All patients analyzed displayed remarkable differences with respect to the controls regarding the pattern of MC infiltrating the motor neuron-vascular niche, including (i) significantly increased MC density, (ii) frequent images of MC degranulation, and iii) increased number of perineuronal small non-granular c-Kit+ cells, which could correspond to MC precursors. The interaction between motor neurons and degranulating MCs anticipates complex and relevant functional crosstalk mediated by MCs secreted proteases, cytokines, trophic factors, and vasoactive mediators [34]. MCs also release nerve growth factor (NGF) species [29], potentially leading to pro-apoptotic signaling through 75-kD neurotrophin receptors ($p75^{NTR}$) that are abnormally expressed in ALS-damaged motor neurons [37]. Thus, degranulating MCs in the subtle motor neuron-vascular compartment have the potential to trigger neuronal pathology and neuroinflammation, directly and indirectly.

The finding of MC clustering around defective perineuronal microvascular elements was associated with significant vascular abnormalities such as endothelial sprouts and string vessels, suggests a MC-mediated vascular pathology in ALS. Previous studies have shown impairment of microvascular endothelial cells and pericytes in the brain and spinal cord of rodent models of disease and ALS patients [16, 54], associated with compromised integrity of the blood–brain and blood-spinal cord barriers [17]. Similar microvascular aberrations have been described in Alzheimer's disease [15], however, the mechanisms of microvascular pathology remain elusive. MCs play important roles in increasing microvascular permeability, in part through the release of chymase and tryptase that are known to degrade adhesion proteins complexes between endothelial cells [8] as well as the extracellular matrix proteins vitronectin, procollagen, type IV collagen [9, 30]. The release of histamine and Cox-2-synthesized prostaglandins by MCs may further increase microvascular increased permeability [1], facilitating the influx of peripheral inflammatory cells. In parallel, degranulating MCs may also promote angiogenesis via the secretion of several proteins including VEGF [35], a recognized neuroprotective trophic factor in ALS [2]. The absence of toluidine blue staining could indicate that mast cells have already degranulated, but does not necessarily mean they are unable to continue to secrete compounds that affect the disease. Thus, MC activation and degranulation in the motor neuron-vascular niche may have protective and regenerative effects in the early stages of ALS, then switching to deleterious pro-inflammatory

(See figure on next page.)

Fig. 5 Mast cells are associated with altered microvascular elements in ALS patients and mice. **A** Representative confocal microphotographs of c-Kit+ (red)/chymase+ (green) mast cells (magenta arrows) associated with microvascular elements stained with Collagen-I (white) in the surroundings of degenerating motor neurons (white dotted lines) in the lumbar spinal cord of autopsy ALS subjects and control donors. Both small non-granular and degranulating mast cells are observed in the ALS spinal cords (left and middle panel), as compared with few small rounded cells present in the spinal cord of control donors (right panel). **B** High magnification confocal analysis of c-Kit+/chymase+ mast cells associated with pathological blood vessels. Note that granular mast cells seem to emerge from a blood vessel stained with collagen-I into the parenchyma of the spinal cord. High magnification analysis (magenta square) is shown in the right upper panel where the boundaries of the blood vessel were depicted only as a white solid line. The close contact between damaged blood vessels and mast cells is indicated by the magenta arrow. The three panels below show orthogonal views of the z stack, to illustrate the damage observed in the blood vessels in contact with mast cells (magenta arrows). **C** Representative confocal analysis of pathological features of microvasculature in the ALS lumbar spinal cord. Frequent morphological abnormalities as observed by collagen-I interruptions (yellow arrow ALS #1), strings (yellow asterisks ALS #2), and sprouts (yellow arrowheads ALS #4). Alterations in the microvasculature are not observed in control donors (control #2). **D** Representative confocal characterization of abnormal microvascular elements stained with collagen-I (white) in the spinal cord of symptomatic $SOD1^{G93A}$ mice but not in Non-Tg littermates (upper panels). Lower panels show the association of c-Kit+ mast cells with the motor neuron-vascular niche. βIII-Tubulin antibody was used to stain motor neurons (orange) and collagen-I to stain blood vessels (white). The magenta squares show a 3D high magnification analysis of the niche and c-Kit+ mast cells (red—magenta arrows) respectively. The graph to the right shows the quantitative analysis of the number of string vessels and vessel sprouts in $SOD1^{G93A}$ symptomatic compared to Non-Tg littermates. Data are expressed as mean ± s.e.m. For statistical analysis two-tailed Mann–Whitney test was used, with ***$p < 0.0001$ considered significant. $n = 4$ animals/condition. Scale bars: 20 µm in (**A**and **C**), 10 µm in (**D**), and 5 µm in (**B**)

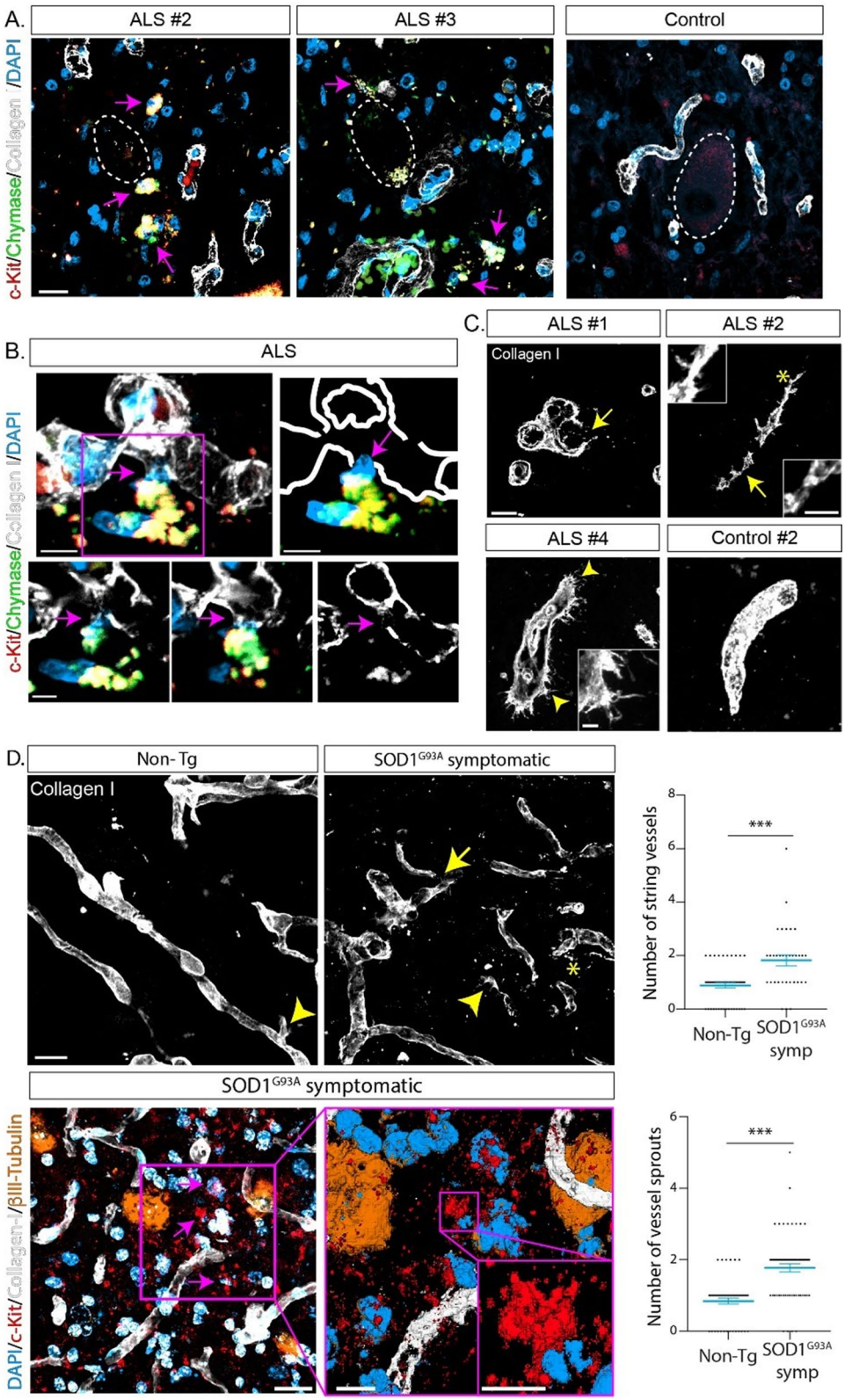

Fig. 5 (See legend on previous page.)

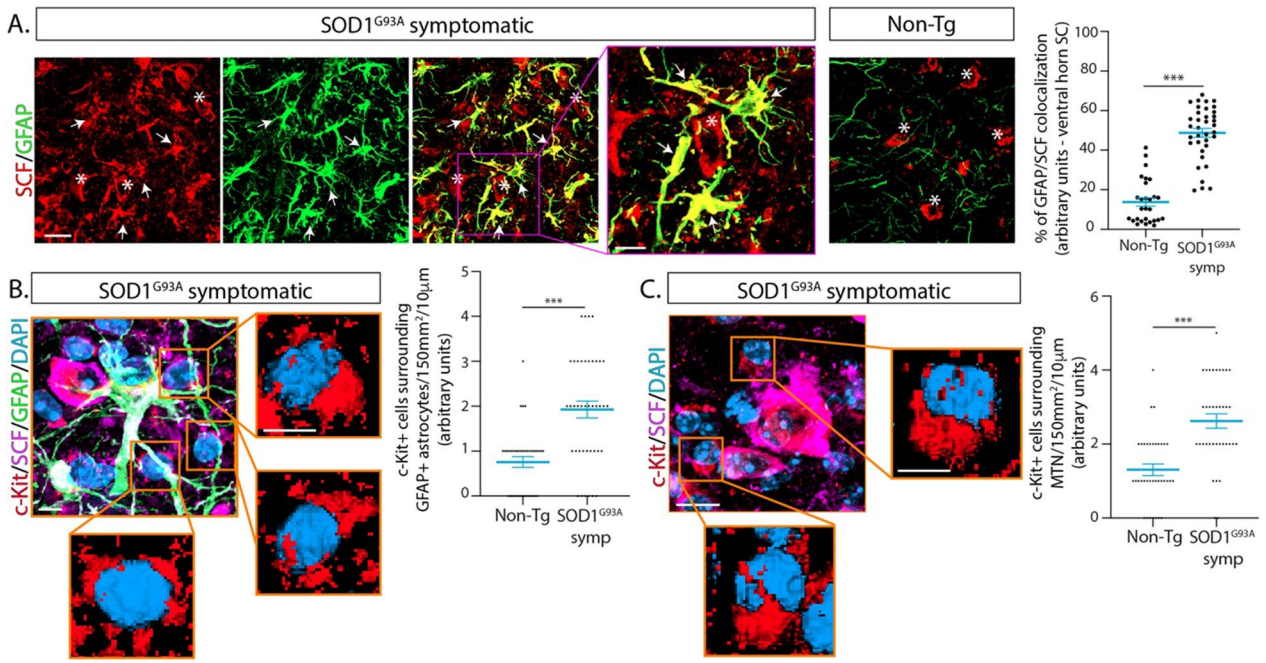

Fig. 6 Mast cells interact with astrocytes and motor neurons expressing Stem Cell Factor in ALS mice. **A** Representative immunohistochemical confocal images showing the characterization of the c-Kit ligand expression, SCF, in the lumbar spinal cord of Non-Tg and symptomatic SOD1^{G93A} mice. Note the significant upregulation of SCF in reactive GFAP+ astrocytes (white arrows) in symptomatic ALS mice as compared with Non-Tg littermates. Motor neurons (white asterisks) express similar levels of SCF in both Non-Tg and SOD1^{G93A} mice. The magenta square shows a high magnification analysis of a SCF+ motor neuron surrounded by reactive astrocytes co-expressing high levels of GFAP and SCF (colocalization in yellow). The graph to the right shows the quantitative analysis of the co-localization of SCF and GFAP in spinal cord sections of SOD1^{G93A} as compared with Non-Tg mice. **B** High magnification confocal analysis of c-Kit+cells lacking granules that spatially associate with SFC + /GFAP+ reactive astrocytes. Squares show higher magnification 3D images of c-Kit+ cells (red) that surround reactive astrocytes. The graph shows the quantitative analysis of c-Kit+ cells surrounding SCF+ astrocytes. **C** High magnification confocal analysis of c-Kit + cells that closely interact with SFC+ motor neurons. Squares show higher magnification 3D images of c-Kit+ cells (red). The graph shows the quantitative analysis of c-Kit+ cells surrounding SCF+ motor neurons. Data are expressed as mean ± s.e.m. For statistical analysis two-tailed Mann–Whitney test was used, with ***$p < 0.0001$ considered significant. $n = 4$ animals/condition. Scale bars: 20 µm (A) and 10 µm and 5 µm (**B**, **C**)

and neurotoxic effects in more advanced stages of the disease.

The degenerating spinal cord in ALS murine models is characterized by an increased number of NG2 [25] and CD34 glial precursors [28], which contribute to extensive gliosis. However, the presence of MC precursors in the CNS affected regions in ALS remained unexplored. Here, we show evidence that fully differentiated MCs can be generated *ex-vivo* from the spinal cord of symptomatic ALS rats when non-adherent cells obtained in primary culture are maintained in the presence of IL-3 and SCF, conditions known to generate MCs from bone marrow [20]. We speculate MC precursors in the ALS spinal cord could correspond to the population of small non-granular c-Kit+ cells that are found in significant numbers in the motor neuron-vascular niche of both ALS subjects and murine models, suggesting that only a portion of c-Kit+ MC precursors trafficking from blood to the spinal cord readily differentiate into typical MCs containing granules. Moreover, we also show evidence that c-Kit+ MC precursors can traffic from the blood to the spinal cord following i.v. administration into symptomatic ALS mice. This trafficking was only observed in symptomatic ALS mice, indicating a prerequisite of permeable microvasculature. Thus, MCs precursors infiltration and subsequent differentiation into the spinal cord seem to be a complex process controlled by the integrity of BSCB and the overexpression of SCF in reactive astrocytes and neurons. In turn, MCs can also damage the BSCB suggesting a bidirectional pathogenic process that could be relevant for the integrity of the motor neuron-vascular niche.

We found that tyrosine kinase inhibition with masitinib downregulated the accumulation of MCs and trafficking of MC precursors into the motor neuron-vascular niche, which in turn resulted in a significant improvement of aberrant microvasculature. Because masitinib not only inhibits c-Kit but also kinases CSF-1R, PDGF-R, Lyn, and Fyn, the mechanism for this restorative effect could involve multiple pathways [11]. Neuroprotection by masitinib in ALS was originally

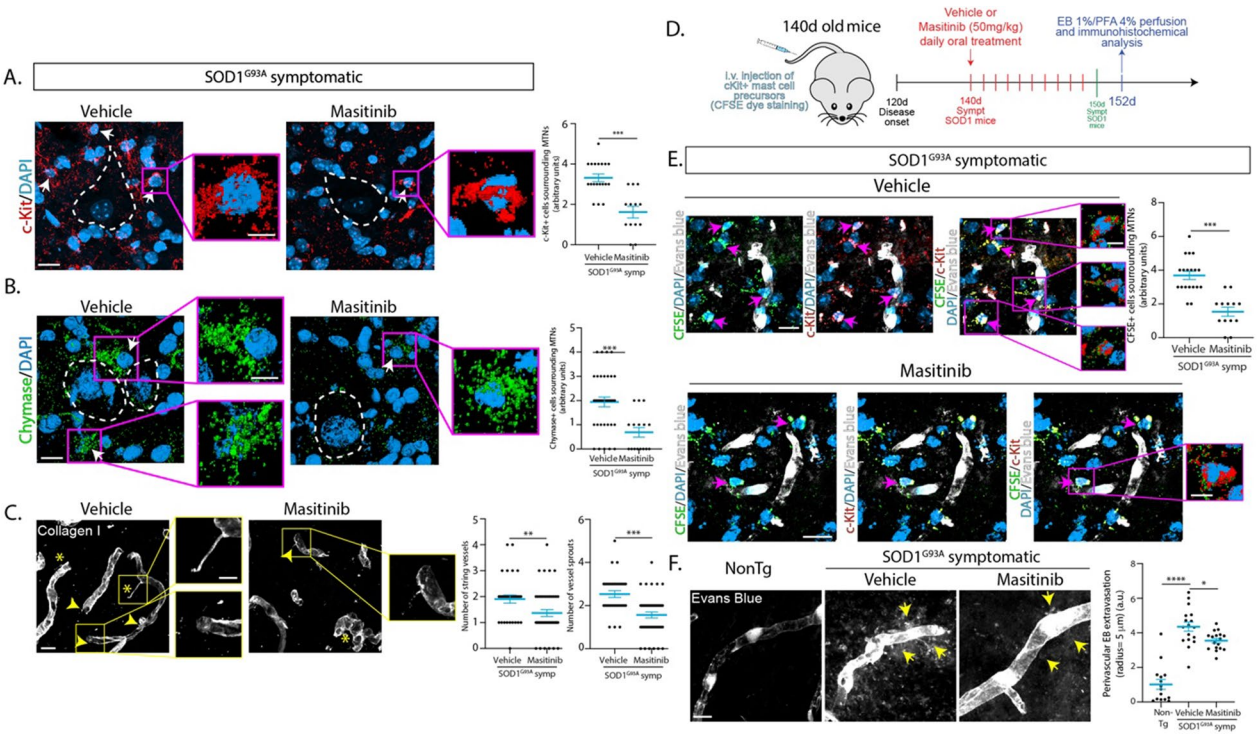

Fig. 7 Post-paralysis masitinib treatment prevents mast cell accumulation and trafficking into the spinal cord of ALS mice. SOD1^{G93A} 140d old symptomatic mice were orally (gavage) daily treated with 50 mg/Kg of masitinib (or vehicle) for 10 days and immunohistochemical analysis was performed to characterize the presence of mast cells in the lumbar spinal cord. **A** Representative confocal images show the analysis of c-Kit+ cells (red – white arrows) accumulated in the surroundings of motor neurons (white dotted lines) in the lumbar spinal cord of SOD1^{G93A} mice after vehicle or masitinib treatment. Magenta squares show high magnification 3D images of typical c-Kit+ mast cells in both conditions. The graph shows that masitinib treatment significantly prevents the accumulation of c-Kit+ cells in the parenchyma of the spinal cord when compared with vehicle-treated mice. **B** Representative confocal images that show the analysis of chymase+ mast cells (green—white arrows) associated with motor neurons (white dotted lines) in the spinal cord of vehicle- and masitinib-treated SOD1^{G93A} mice. Magenta squares show high magnification 3D images of typically degranulating mast cells in proximity to motor neurons. Quantitative analysis in the graph shows that masitinib treatment significantly prevents the accumulation of degranulating chymase+ cells in the spinal cord. **C** Confocal microscopy analysis of the microvasculature pathology in SOD1^{G93A} treated with vehicle or masitinib. The number of vessels strings and vessels sprouts were quantified between groups in Collagen-I stained spinal cords. The graph shows that after 10 days of treatment with masitinib, there is a significant reduction of microvasculature alterations. **D** The scheme shows the experimental protocol for the i.v. delivery of c-Kit+/CFSE+ cells, after 10 days of the vehicle or masitinib treatment. **E** After 10 days of vehicle (upper panels) or masitinib (lower panels) treatment, c-Kit+ mast cells precursors (red) stained with CFSE dye (green) were i.v. injected in symptomatic 150d old SOD1^{G93A} mice. c-Kit+/CFSE+ precursors (magenta arrows) were analyzed in the periphery of blood vessels stained with EB dye systemically perfused after euthanasia (white). Magenta squares show high magnification 3D images of typical c-Kit+/CFSE+ cells infiltrating the spinal cord. Masitinib treatment significantly reduced the number of c-Kit+ cells infiltrating the spinal cord parenchyma of SOD1^{G93A} mice. The graph shows the quantitative analysis of c-Kit+ /CFSE+ cells in the surroundings of motor neurons. **F** Non-Tg, and vehicle- and masitinib-treated SOD1^{G93A} mice were systemically perfused after euthanasia with EB to measure the perivascular dye extravasation in the parenchyma of the spinal cord. Note the significant perivascular EB extravasation in SOD1^{G93A} vehicle-treated mice when compared to Non-Tg littermates. Masitinib significantly reduced perivascular extravasation after 10 days of treatment. The graph shows the quantitative analysis of perivascular EB extravasation among groups. Quantitative data are expressed as mean ± s.e.m.; data were analyzed by a two-tailed Mann–Whitney test (**A**–**C**, **E**) and one-way ANOVA (**F**) with *$p < 0,05$, ***$p < 0.001$ and ****$p < 0.0001$ considered significant. $n = 4$ animals/condition. Scale bars: 10 µm (low magnification panels) and 5 µm (insets)

linked to inhibition of tyrosine kinase receptor CSF-1R in microglia and aberrant glial cells that typically proliferate after paralysis onset [46, 47]. Subsequent studies have shown the drug also downregulates MCs, neutrophils, and macrophages in the ALS peripheral motor pathways [21, 48–50]. The present data show evidence that masitinib downregulates MCs infiltration and differentiation and prevents microvascular pathology by inhibiting SCF/c-Kit signaling, which could be fueled by the strong upregulation of SCF in reactive astrocytes in ALS mice [36].

This study has two main limitations. The first one is the small number of ALS subjects analyzed which prevents any correlation of mast cell infiltration with

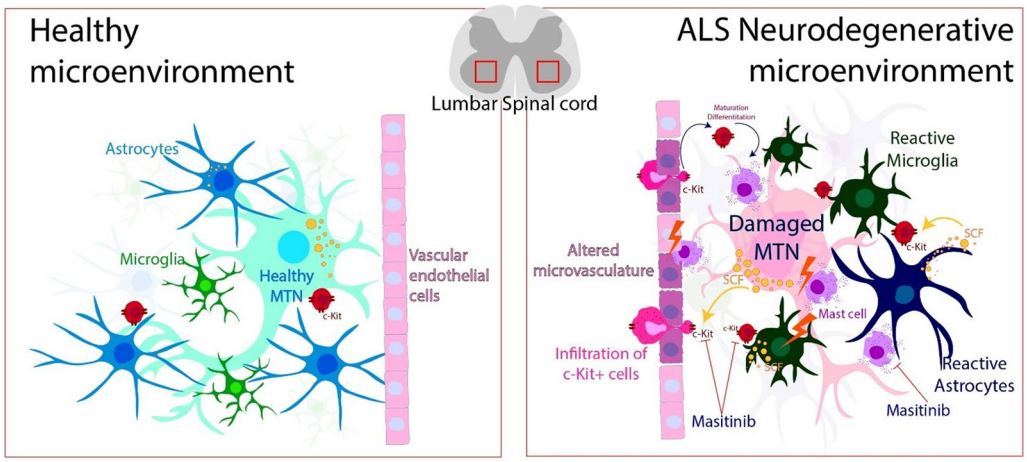

Fig. 8 Schematic hypothesis about the pathogenic role of mast cells in ALS. c-Kit+ MC precursors infiltrate from the blood through altered microvascular elements that surround the degenerating/damaged motor neurons (MTN) and accumulate in the ALS spinal cord. The c-Kit ligand SCF expressed in reactive astrocytes and motor neurons promotes chemoattraction of c-Kit+ precursors that differentiate into MC bearing granular morphology and expressing typical MC markers exerting a potentially toxic effect on the microvasculature, glial cells, and motor neurons. Pharmacological inhibition of c-Kit reduces the MC number and the microvasculature pathology

common genetic or ALS pathological features such as TDP-43 aggregates. The second limitation is the use of murine models based on overexpression of mutant human SOD1, which represent only a minor cause of familial ALS. However, the fact that mast cells and their precursors in the motor neuron-vascular niche are systemically found in all ALS subjects analyzed as well in the paralytic phase of animal models, suggest mast cells are an integral part of the neuroinflammatory response to motor neuron damage, as astrocytosis, microgliosis, and immune cell infiltration [6, 18, 33].

Collectively, the present study shows for the first time that MCs and their c-Kit+ precursors are abundant in the motor neuron-vascular niche, representing a potential pathogenic cell type underlying ALS pathology. As summarized in Fig. 8, MCs appear to infiltrate the spinal cord through a mechanism wherein MC precursors traffic from the periphery across defective microvascular elements with subsequent local differentiation that is possibly driven by reactive astrocytes and motor neurons expressing high levels of the c-Kit ligand SCF. Thus, MCs appear to be relevant pro-inflammatory and microvascular effectors in ALS with the potential to be pharmacologically targeted by tyrosine kinase inhibitor drugs such as masitinib.

Abbreviations

ALS: Amyotrophic lateral sclerosis; BBB: Blood brain barrier; BSCB: Blood spinal cord barrier; BMMC: Bone marrow mast cells; Cox-2: Cyclooxigenase 2; CSF-1R: Colony stimulating factor 1 receptor; EB: Evans Blue; IL-3: Interleukin-3; MCs: Mast cells; NMJ: Neuromuscular junction; PDGF-R: Platelet-derived growth factor receptor; SCF: Stem cell factor.

Supplementary Information

The online version contains supplementary material available at https://doi.org/10.1186/s40478-021-01241-3.

Additional file 1: Supplementary Results with Figures 1–10 and Table 1.

Acknowledgements

We want to thank Colin Mansfield for his critical comments and helpful suggestions for revising the manuscript. The authors also gratefully acknowledge the Advance Bioimaging Unit and the staff from the Transgenic and Experimental Animal Unit at the Institut Pasteur de Montevideo for their support and assistance in the present work. Finally, we are very grateful to our ALS patients who donated their tissues post-mortem to advance ALS research.

Funding

This work was supported by Institut Pasteur de Montevideo – FOCEM Mercosur (COF 03/11), the Amyotrophic Lateral Sclerosis Association (00482), Agencia Nacional de Investigación e Innovación (ANII), NINDS R01NS092651 (to PHK), Merit Review BX001148 from the Department of Veterans Affairs (to PHK), Programa de Desarrollo de las Ciencias Básicas (PEDECIBA) and the Sistema Nacional de Investigadores (SNI).

Availability of data and materials

The authors confirm that the data supporting the findings of this study are available within the article and its Supplementary Material.

Declarations

Competing interests

OH is a co-founder and shareholder of AB science. Others have no conflict of interest.

Author details

[1]Institut Pasteur de Montevideo, 2020 Montevideo, Uruguay. [2]Department of Neurology, University of Alabama, Birmingham, AL 35294, USA. [3]Birmingham Veterans Affairs Medical Center, Birmingham, AL 35295, USA. [4]Imagine

Institute, Hôpital Necker, Paris, France. [5]INSERM UMR 1163, Laboratory of Cellular and Molecular Mechanisms of Hematological Disorders and Therapeutic Implications, Paris, France. [6]Imagine Institute, Paris Descartes–Sorbonne Paris Cité University, Paris, France. [7]CNRS ERL 8254, Paris, France. [8]Laboratory of Excellence GR-Ex, Paris, France. [9]Equipe Labélisée par la Ligue Nationale contre le cancer; AB Science; Department of Hematology, Necker Hospital, Paris, France. [10]Centre national de référence des mastocytoses (CEREMAST), Paris, France.

Received: 3 August 2021 Accepted: 4 August 2021
Published online: 13 August 2021

References

1. Ashina K, Tsubosaka Y, Nakamura T, Omori K, Kobayashi K, Hori M, Ozaki H, Murata T (2015) Histamine induces vascular hyperpermeability by increasing blood flow and endothelial barrier disruption in vivo. PLoS ONE 10:e0132367. https://doi.org/10.1371/journal.pone.0132367
2. Barbeito AG, Martinez-Palma L, Vargas MR, Pehar M, Manay N, Beckman JS, Barbeito L, Cassina P (2010) Lead exposure stimulates VEGF expression in the spinal cord and extends survival in a mouse model of ALS. Neurobiol Dis 37:574–580. https://doi.org/10.1016/j.nbd.2009.11.007
3. Butovsky O, Siddiqui S, Gabriely G, Lanser AJ, Dake B, Murugaiyan G, Doykan CE, Wu PM, Gali RR, Iyer LK et al (2012) Modulating inflammatory monocytes with a unique microRNA gene signature ameliorates murine ALS. J Clin Invest 122:3063–3087. https://doi.org/10.1172/JCI62636
4. Cheng LE, Hartmann K, Roers A, Krummel MF, Locksley RM (2013) Perivascular mast cells dynamically probe cutaneous blood vessels to capture immunoglobulin E. Immunity 38:166–175. https://doi.org/10.1016/j.immuni.2012.09.022
5. Chiot A, Zaidi S, Iltis C, Ribon M, Berriat F, Schiaffino L, Jolly A, de la Grange P, Mallat M, Bohl D et al (2020) Modifying macrophages at the periphery has the capacity to change microglial reactivity and to extend ALS survival. Nat Neurosci 23:1339–1351. https://doi.org/10.1038/s41593-020-00718-z
6. Coque E, Salsac C, Espinosa-Carrasco G, Varga B, Degauque N, Cadoux M, Crabe R, Virenque A, Soulard C, Fierle JK et al (2019) Cytotoxic CD8(+) T lymphocytes expressing ALS-causing SOD1 mutant selectively trigger death of spinal motoneurons. Proc Natl Acad Sci U S A 116:2312–2317. https://doi.org/10.1073/pnas.1815961116
7. Dahlin JS, Hallgren J (2015) Mast cell progenitors: origin, development and migration to tissues. Mol Immunol 63:9–17. https://doi.org/10.1016/j.molimm.2014.01.018
8. Dai H, Korthuis RJ (2011) Mast Cell Proteases and Inflammation. Drug Discov Today Dis Models 8:47–55. https://doi.org/10.1016/j.ddmod.2011.06.004
9. Dell'Italia LJ, Collawn JF, Ferrario CM (2018) Multifunctional role of chymase in acute and chronic tissue injury and remodeling. Circ Res 122:319–336. https://doi.org/10.1161/CIRCRESAHA.117.310978
10. Dimitriadou V, Rouleau A, Tuong MD, Ligneau X, Newlands GF, Miller HR, Schwartz JC, Garbarg M (1996) Rat cerebral mast cells undergo phenotypic changes during development. Brain Res Dev Brain Res 97:29–41. https://doi.org/10.1016/s0165-3806(96)00127-7
11. Dubreuil P, Letard S, Ciufolini M, Gros L, Humbert M, Casteran N, Borge L, Hajem B, Lermet A, Sippl W et al (2009) Masitinib (AB1010), a potent and selective tyrosine kinase inhibitor targeting KIT. PLoS ONE 4:e7258. https://doi.org/10.1371/journal.pone.0007258
12. Elieh-Ali-Komi D, Cao Y (2017) Role of mast cells in the pathogenesis of multiple sclerosis and experimental autoimmune encephalomyelitis. Clin Rev Allergy Immunol 52:436–445. https://doi.org/10.1007/s12016-016-8595-y
13. Flanagan JG, Leder P (1990) The kit ligand: a cell surface molecule altered in steel mutant fibroblasts. Cell 63:185–194. https://doi.org/10.1016/0092-8674(90)90299-t
14. Florenzano F, Bentivoglio M (2000) Degranulation, density, and distribution of mast cells in the rat thalamus: a light and electron microscopic study in basal conditions and after intracerebroventricular administration of nerve growth factor. J Comp Neurol 424:651–669
15. Gama Sosa MA, Gasperi RD, Rocher AB, Wang AC, Janssen WG, Flores T, Perez GM, Schmeidler J, Dickstein DL, Hof PR et al (2010) Age-related vascular pathology in transgenic mice expressing presenilin 1-associated familial Alzheimer's disease mutations. Am J Pathol 176:353–368. https://doi.org/10.2353/ajpath.2010.090482
16. Garbuzova-Davis S, Hernandez-Ontiveros DG, Rodrigues MC, Haller E, Frisina-Deyo A, Mirtyl S, Sallot S, Saporta S, Borlongan CV, Sanberg PR (2012) Impaired blood-brain/spinal cord barrier in ALS patients. Brain Res 1469:114–128. https://doi.org/10.1016/j.brainres.2012.05.056
17. Garbuzova-Davis S, Sanberg PR (2014) Blood-CNS barrier impairment in ALS patients versus an animal model. Front Cell Neurosci 8:21. https://doi.org/10.3389/fncel.2014.00021
18. Garofalo S, Cocozza G, Porzia A, Inghilleri M, Raspa M, Scavizzi F, Aronica E, Bernardini G, Peng L, Ransohoff RM et al (2020) Natural killer cells modulate motor neuron-immune cell cross talk in models of Amyotrophic Lateral Sclerosis. Nat Commun 11:1773. https://doi.org/10.1038/s41467-020-15644-8
19. Graves MC, Fiala M, Dinglasan LA, Liu NQ, Sayre J, Chiappelli F, van Kooten C, Vinters HV (2004) Inflammation in amyotrophic lateral sclerosis spinal cord and brain is mediated by activated macrophages, mast cells and T cells. Amyotroph Lateral Scler Other Motor Neuron Disord 5:213–219. https://doi.org/10.1080/14660820410020286
20. Haig DM, Huntley JF, MacKellar A, Newlands GF, Inglis L, Sangha R, Cohen D, Hapel A, Galli SJ, Miller HR (1994) Effects of stem cell factor (kit-ligand) and interleukin-3 on the growth and serine proteinase expression of rat bone-marrow-derived or serosal mast cells. Blood 83:72–83
21. Harrison JM, Rafuse VF (2020) Muscle fiber-type specific terminal Schwann cell pathology leads to sprouting deficits following partial denervation in SOD1(G93A) mice. Neurobiol Dis 145:105052. https://doi.org/10.1016/j.nbd.2020.105052
22. Hunter JM, Kwan J, Malek-Ahmadi M, Maarouf CL, Kokjohn TA, Belden C, Sabbagh MN, Beach TG, Roher AE (2012) Morphological and pathological evolution of the brain microcirculation in aging and Alzheimer's disease. PLoS ONE 7:e36893. https://doi.org/10.1371/journal.pone.0036893
23. Isasi E, Barbeito L, Olivera-Bravo S (2014) Increased blood-brain barrier permeability and alterations in perivascular astrocytes and pericytes induced by intracisternal glutaric acid. Fluids Barriers CNS 11:15. https://doi.org/10.1186/2045-8118-11-15
24. Mora JS, Bradley WG, Chaverri D et al (2021) Long-term survival analysis of masitinib in amyotrophic lateral sclerosis. Ther Adv Neurol Disord. https://doi.org/10.1177/17562864211030365
25. Kang SH, Fukaya M, Yang JK, Rothstein JD, Bergles DE (2010) NG2+ CNS glial progenitors remain committed to the oligodendrocyte lineage in postnatal life and following neurodegeneration. Neuron 68:668–681. https://doi.org/10.1016/j.neuron.2010.09.009
26. Khalil M, Ronda J, Weintraub M, Jain K, Silver R, Silverman AJ (2007) Brain mast cell relationship to neurovasculature during development. Brain Res 1171:18–29. https://doi.org/10.1016/j.brainres.2007.07.034
27. Kitamura Y, Oboki K, Ito A (2006) Molecular mechanisms of mast cell development. Immunol Allergy Clin North Am 26(387–405):v. https://doi.org/10.1016/j.iac.2006.05.004
28. Kovacs M, Trias E, Varela V, Ibarburu S, Beckman JS, Moura IC, Hermine O, King PH, Si Y, Kwon Y et al (2019) CD34 identifies a subset of proliferating microglial cells associated with degenerating motor neurons in ALS. Int J Mol Sci. https://doi.org/10.3390/ijms20163880
29. Kritas SK, Caraffa A, Antinolfi P, Saggini A, Pantalone A, Rosati M, Tei M, Speziali A, Saggini R, Pandolfi F et al (2014) Nerve growth factor interactions with mast cells. Int J Immunopathol Pharmacol 27:15–19. https://doi.org/10.1177/039463201402700103
30. Kunder CA, St John AL, Abraham SN (2011) Mast cell modulation of the vascular and lymphatic endothelium. Blood 118:5383–5393. https://doi.org/10.1182/blood-2011-07-358432
31. Lambracht-Hall M, Dimitriadou V, Theoharides TC (1990) Migration of mast cells in the developing rat brain. Brain Res Dev Brain Res 56:151–159. https://doi.org/10.1016/0165-3806(90)90077-c
32. Mora JS, Genge A, Chio A, Estol CJ, Chaverri D, Hernandez M, Marin S, Mascias J, Rodriguez GE, Povedano M et al (2020) Masitinib as an add-on therapy to riluzole in patients with amyotrophic lateral sclerosis: a randomized clinical trial. Amyotroph Lateral Scler Frontotemporal Degener 21:5–14. https://doi.org/10.1080/21678421.2019.1632346
33. Murdock BJ, Famie JP, Piecuch CE, Raue KD, Mendelson FE, Pieroni CH, Iniguez SD, Zhao L, Goutman SA, Feldman EL (2021) NK cells associate

with ALS in a sex- and age-dependent manner. JCI Insight. https://doi.org/10.1172/jci.insight.147129
34. Nelissen S, Lemmens E, Geurts N, Kramer P, Maurer M, Hendriks J, Hendrix S (2013) The role of mast cells in neuroinflammation. Acta Neuropathol 125:637–650. https://doi.org/10.1007/s00401-013-1092-y
35. Norrby K (2002) Mast cells and angiogenesis. APMIS 110:355–371. https://doi.org/10.1034/j.1600-0463.2002.100501.x
36. Okayama Y, Kawakami T (2006) Development, migration, and survival of mast cells. Immunol Res 34:97–115. https://doi.org/10.1385/IR:34:2:97
37. Pehar M, Vargas MR, Cassina P, Barbeito AG, Beckman JS, Barbeito L (2005) Complexity of astrocyte-motor neuron interactions in amyotrophic lateral sclerosis. Neurodegener Dis 2:139–146. https://doi.org/10.1159/000089619
38. Piette F, Belmin J, Vincent H, Schmidt N, Pariel S, Verny M, Marquis C, Mely J, Hugonot-Diener L, Kinet JP et al (2011) Masitinib as an adjunct therapy for mild-to-moderate Alzheimer's disease: a randomised, placebo-controlled phase 2 trial. Alzheimers Res Ther 3:16. https://doi.org/10.1186/alzrt75
39. Qiu FH, Ray P, Brown K, Barker PE, Jhanwar S, Ruddle FH, Besmer P (1988) Primary structure of c-kit: relationship with the CSF-1/PDGF receptor kinase family–oncogenic activation of v-kit involves deletion of extracellular domain and C terminus. EMBO J 7:1003–1011
40. Ribatti D (2015) The crucial role of mast cells in blood-brain barrier alterations. Exp Cell Res 338:119–125. https://doi.org/10.1016/j.yexcr.2015.05.013
41. Ribatti D (2018) The Staining of Mast Cells: A Historical Overview. Int Arch Allergy Immunol 176:55–60. https://doi.org/10.1159/000487538
42. Skaper SD, Facci L, Giusti P (2013) Glia and mast cells as targets for palmitoylethanolamide, an anti-inflammatory and neuroprotective lipid mediator. Mol Neurobiol 48:340–352. https://doi.org/10.1007/s12035-013-8487-6
43. Skaper SD, Facci L, Giusti P (2014) Mast cells, glia and neuroinflammation: partners in crime? Immunology 141:314–327. https://doi.org/10.1111/imm.12170
44. Skaper SD, Facci L, Zusso M, Giusti P (2017) Neuroinflammation, Mast Cells, and Glia: Dangerous Liaisons. Neuroscientist 23:478–498. https://doi.org/10.1177/1073858416687249
45. Teodosio C, Garcia-Montero AC, Jara-Acevedo M, Sanchez-Munoz L, Alvarez-Twose I, Nunez R, Schwartz LB, Walls AF, Escribano L, Orfao A (2010) Mast cells from different molecular and prognostic subtypes of systemic mastocytosis display distinct immunophenotypes. J Allergy Clin Immunol 125: 719–726, 726 e711–726 e714. https://doi.org/10.1016/j.jaci.2009.10.020
46. Trias E, Diaz-Amarilla P, Olivera-Bravo S, Isasi E, Drechsel DA, Lopez N, Bradford CS, Ireton KE, Beckman JS, Barbeito L (2013) Phenotypic transition of microglia into astrocyte-like cells associated with disease onset in a model of inherited ALS. Front Cell Neurosci 7:274. https://doi.org/10.3389/fncel.2013.00274
47. Trias E, Ibarburu S, Barreto-Nunez R, Babdor J, Maciel TT, Guillo M, Gros L, Dubreuil P, Diaz-Amarilla P, Cassina P et al (2016) Post-paralysis tyrosine kinase inhibition with masitinib abrogates neuroinflammation and slows disease progression in inherited amyotrophic lateral sclerosis. J Neuroinflammation 13:177. https://doi.org/10.1186/s12974-016-0620-9
48. Trias E, Ibarburu S, Barreto-Nunez R, Varela V, Moura IC, Dubreuil P, Hermine O, Beckman JS, Barbeito L (2017) Evidence for mast cells contributing to neuromuscular pathology in an inherited model of ALS. JCI Insight. https://doi.org/10.1172/jci.insight.95934
49. Trias E, King PH, Si Y, Kwon Y, Varela V, Ibarburu S, Kovacs M, Moura IC, Beckman JS, Hermine O et al (2018) Mast cells and neutrophils mediate peripheral motor pathway degeneration in ALS. JCI Insight. https://doi.org/10.1172/jci.insight.123249
50. Trias E, Kovacs M, King PH, Si Y, Kwon Y, Varela V, Ibarburu S, Moura IC, Hermine O, Beckman JS et al (2020) Schwann cells orchestrate peripheral nerve inflammation through the expression of CSF1, IL-34, and SCF in amyotrophic lateral sclerosis. Glia 68:1165–1181. https://doi.org/10.1002/glia.23768
51. Trowbridge IS, Thomas ML (1994) CD45: an emerging role as a protein tyrosine phosphatase required for lymphocyte activation and development. Annu Rev Immunol 12:85–116. https://doi.org/10.1146/annurev.iy.12.040194.000505
52. Valent P, Akin C, Hartmann K, Nilsson G, Reiter A, Hermine O, Sotlar K, Sperr WR, Escribano L, George TI et al (2020) Mast cells as a unique hematopoietic lineage and cell system: from Paul Ehrlich's visions to precision medicine concepts. Theranostics 10:10743–10768. https://doi.org/10.7150/thno.46719
53. Vermersch P, Benrabah R, Schmidt N, Zephir H, Clavelou P, Vongsouthi C, Dubreuil P, Moussy A, Hermine O (2012) Masitinib treatment in patients with progressive multiple sclerosis: a randomized pilot study. BMC Neurol 12:36. https://doi.org/10.1186/1471-2377-12-36
54. Yamadera M, Fujimura H, Inoue K, Toyooka K, Mori C, Hirano H, Sakoda S (2015) Microvascular disturbance with decreased pericyte coverage is prominent in the ventral horn of patients with amyotrophic lateral sclerosis. Amyotroph Lateral Scler Frontotemporal Degener 16:393–401. https://doi.org/10.3109/21678421.2015.1011663
55. Zhou T, Zheng Y, Sun L, Badea SR, Jin Y, Liu Y, Rolfe AJ, Sun H, Wang X, Cheng Z et al (2019) Microvascular endothelial cells engulf myelin debris and promote macrophage recruitment and fibrosis after neural injury. Nat Neurosci 22:421–435. https://doi.org/10.1038/s41593-018-0324-9
56. Zhuang X, Silverman AJ, Silver R (1999) Distribution and local differentiation of mast cells in the parenchyma of the forebrain. J Comp Neurol 408:477–488. https://doi.org/10.1002/(sici)1096-9861(19990614)408:4%3c477::aid-cne3%3e3.0.co;2-o

Publisher's Note

Additional File 1

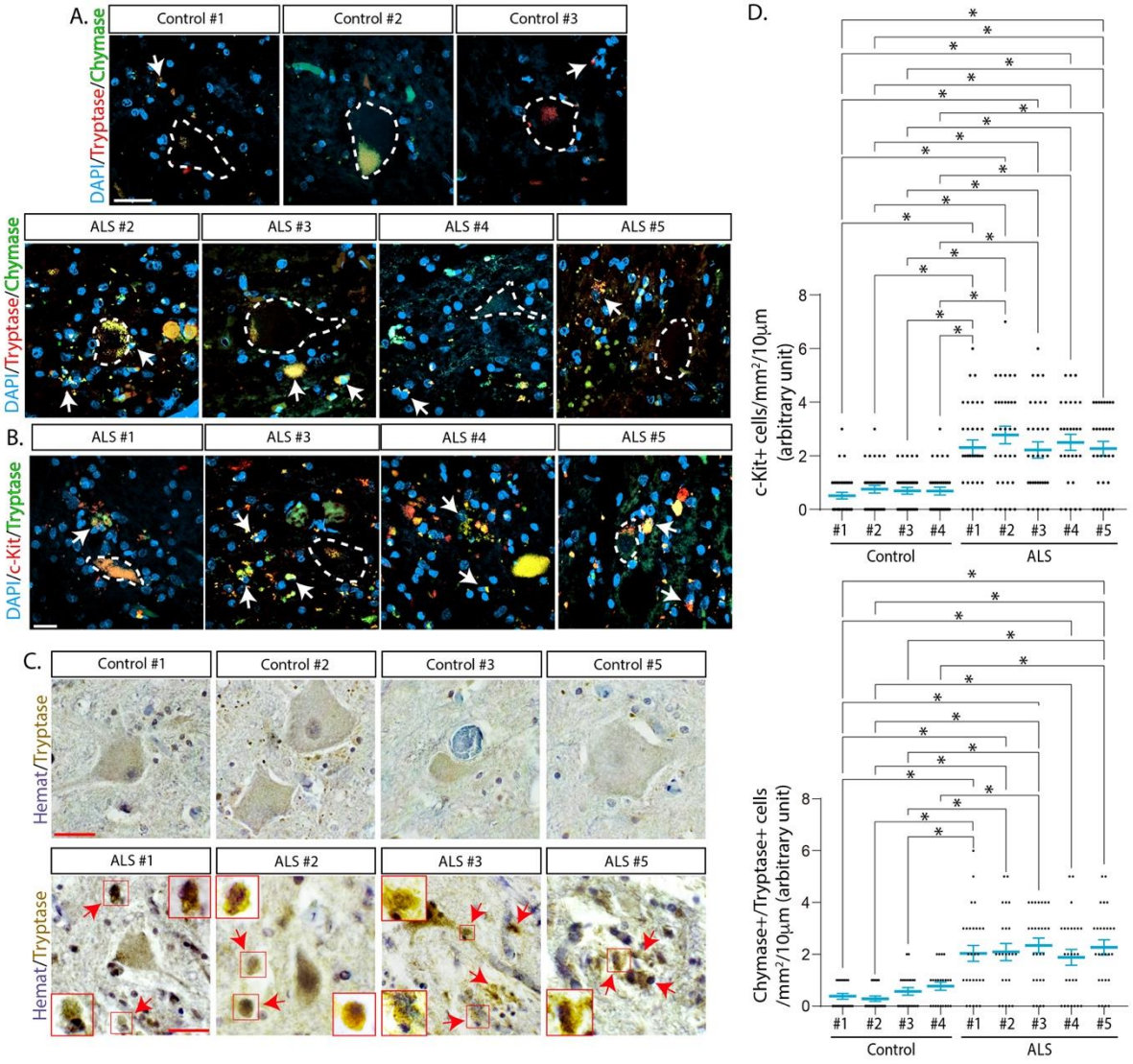

Figure 1. Mast cells accumulate in the surrounding of motor neurons in the spinal cord of ALS patients. **(A-B)** Representative confocal images of tryptase+/chymase+ **(A)** and c-Kit+/ tryptase+ **(B)** MCs infiltrating into the ventral horn of lumbar spinal cords of autopsy control and ALS patients. Arrows indicate cells stained with both markers (yellow). Motor neuron cell bodies are depicted in dotted lines. **(C)** Representative bright field microscopy images of tryptase (DAB)/Hematoxylin (Hemat) staining in autopsy ALS and control tissue. None or few tryptase+ mast cells were observed in control donors. Red arrows in lower panels show numerous MCs in the surroundings of motor neurons and microvasculature structures. Red squares show high magnification images of tryptase+mast cells. **(D)** Quantitative analysis of c-Kit+ (upper graph) and chymase+/tryptase+ (lower graph) cells in the area that surrounds motor neurons in the ventral horn of the lumbar spinal cord of ALS patients compared to control donors, individually. Only statistically significant comparisons are shown between control donors and ALS

subjects. Quantitative data are expressed as mean ± s.e.m. Data were analyzed by Kruskal-Wallis followed by Dunn's multiple-comparisons test. Scale bars: 20 μm.

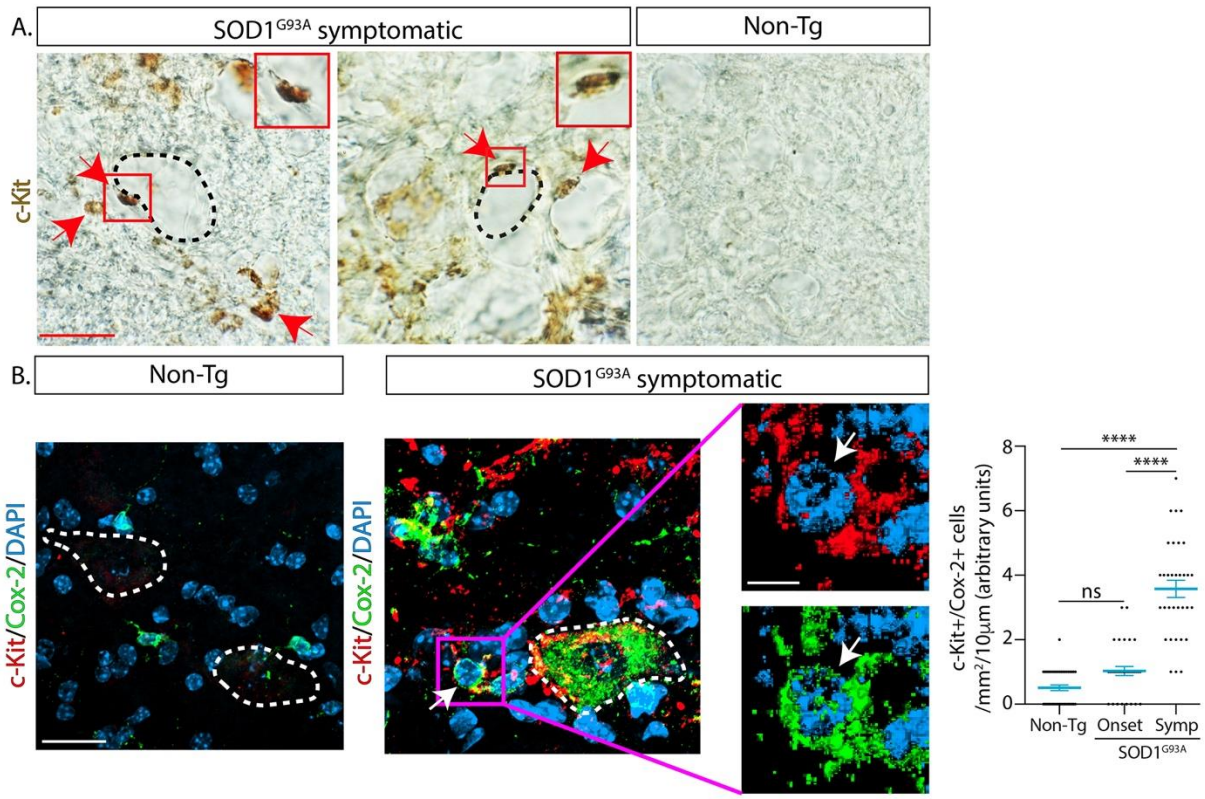

Fig. 2. c-Kit+/Cox-2+ mast cells in the spinal cord of ALS mice. **(A)** Representative bright-field microscopy images showing c-Kit (DAB) staining in the ventral horn of the spinal cord of symptomatic SOD1^{G93A} mice but not in Non-Tg mice. Red arrows show MCs in the surrounding of motor neurons (black dotted lines). Red squares show high magnification panels of c-Kit+ MCs. **(B)** Representative confocal images showing c-Kit+/Cox-2+ MCs in the surrounding of motor neurons (white dotted lines) in the ventral horn of the lumbar spinal cord of symptomatic SOD1^{G93A} mice and Non-Tg mice. Magenta square shows the area taken for 3D reconstructions of MCs. The graph to the right shows the quantitative analysis of c-Kit+/Cox-2+ MCs among conditions. Quantitative data are expressed as mean ± s.e.m. Data were analyzed by Kruskal-Wallis followed by Dunn´s multiple comparison test with ****p<0,0001 considered significant. n=4 animals/condition. Scale bars: 20 µm (low magnification panels) and 5 µm (insets).

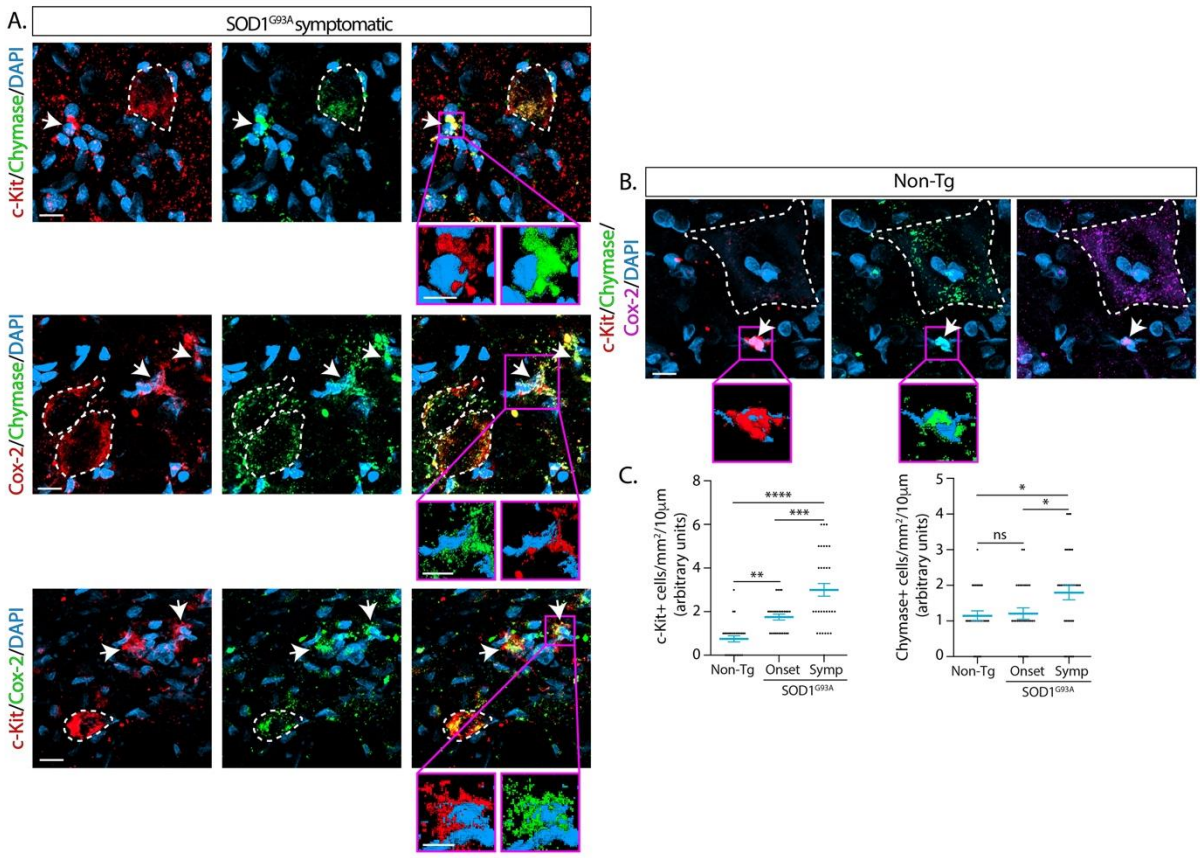

Fig. 3. Mast cells in the SOD1^{G93A} rat ventral horn. (A) Representative confocal images showing c-Kit+/chymase+ (left upper panels), Cox-2+/chymase+ (left middle panels) and c-Kit+/Cox-2+ (left bottom panels) MCs associated with motor neurons (white dotted lines) in the ventral horn of symptomatic SOD1^{G93A} lumbar spinal cord. Arrows indicate typical mast cells bearing granular morphology. Magenta squares indicate the area taken for 3D reconstructions of mast cells. (**B)** Representative confocal images of c-Kit+, chymase + and Cox-2 + MCs in Non-Tg rats. Arrows indicate small MCs. (**C)** Quantitative analysis of c-Kit+ (left) and chymase+ (right) MCs in the ventral horn of the lumbar spinal cord among conditions. Quantitative data are expressed as mean ± s.e.m. Data were analyzed by Kruskal-Wallis followed by Dunn´s multiple comparison test with *p<0,05, **p<0,01, ***p<0,001 and ****p>0,0001 considered significant. n = 4 animals/condition. Scale bars: 10 µm.

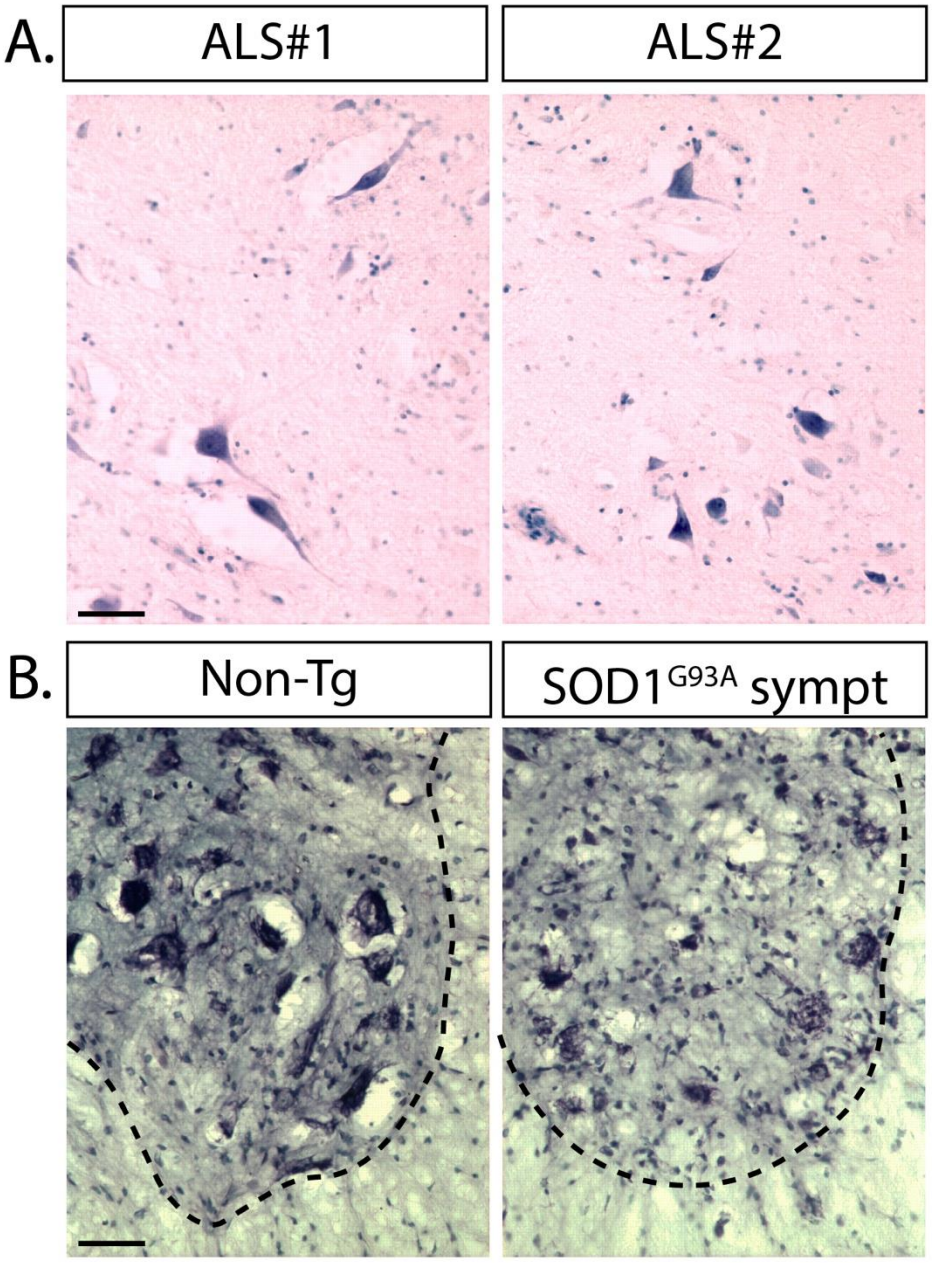

Fig. 4. Lack of metachromasia following toluidine blue staining in the spinal cord of ALS patients and mice. Representative histological images showing the lack of metachromatic MCs in sections stained with toluidine blue from **(A)** ALS patients and control donors, and **(B)** Non-tg and SOD1^{G93A} symptomatic mice. Scale bars: 50 μm in (A) and 40 μm in (B).

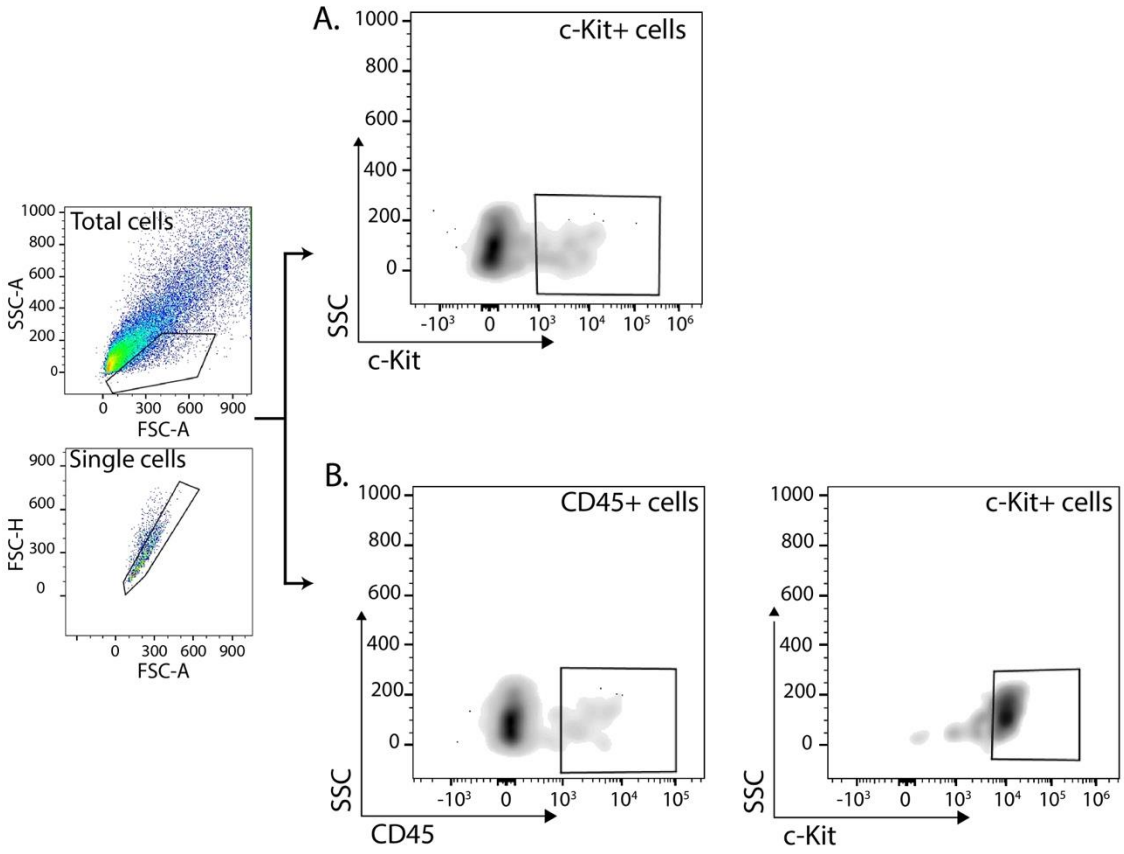

Fig. 5. Gating strategy in flow cytometry analysis of c-kit+ and CD45+ population in the spinal cord of ALS mice. Hematopoietic cells were labeled with primary antibodies against CD45 and c-Kit in a cell suspension obtained from the spinal of Non-Tg and SOD1^{G93A} symptomatic mice (150d). Mast cell population was analyzed following two different strategies. **(A)** c-Kit+ cell population was directly analyzed from total hematopoietic cell population, and **(B)** c-Kit+ cell population was selected among CD45+ cell population.

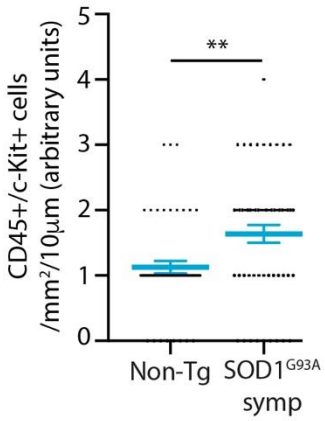

Fig. 6. Quantitative analysis of CD45+/c-Kit+ mast cells. The graph shows the quantitative analysis of CD45+/c-Kit+ in the surrounding of motor neurons in the ventral horn of the spinal cord of SOD1^{G93A} mice compared to Non-Tg littermates. Quantitative data are expressed as mean ± s.e.m. Data were analyzed by Mann- Whitney test with ** p<0,001 considered significant. n=4 animals/condition.

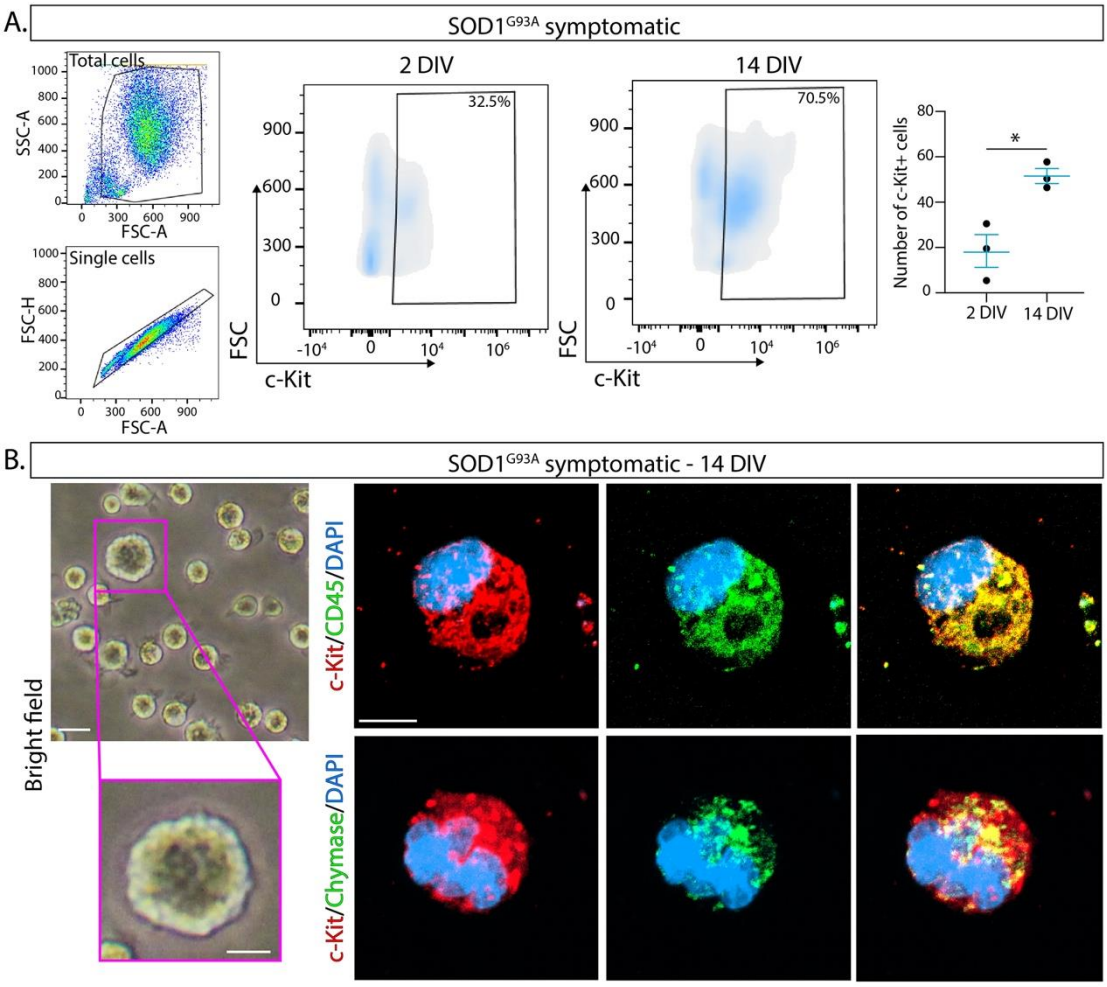

Fig. 7. Generation of c-Kit+ mast cells from the bone marrow of symptomatic SOD1^{G93A} rat. Bone marrows were cultured with IL-3 and SCF to induce MC differentiation, and c-Kit+ cell population was analyzed after 2 and 14 days by flow cytometry. (**A)** Representative plots showing gating strategy followed (left panels) and the c-Kit+ cell population analyzed at 2 and 14 days (right panels). The graph to the right shows the increase of c-Kit+ cell population from 2 to 14 days *in vitro*. (**B)** Representative cytological analysis of MCs isolated from SOD1^{G93A} bone marrow. Left panels show representative bright-field images of MCs. Magenta square shows the area taken for high magnification analysis. Right panels show immunocytochemical phenotyping of MCs after 14 days in culture assessed by confocal microscopy using staining for c-Kit (red), CD45 (green) and chymase (green). Quantitative data are expressed as mean ± s.e.m. Data were analyzed by Mann- Whitney test with *p<0,05 considered significant. n=3 animals/condition. Scale bars: 20 μm in (B) lower magnification, 10 μm in high magnification, and 5 μm in immunocytochemical analysis.

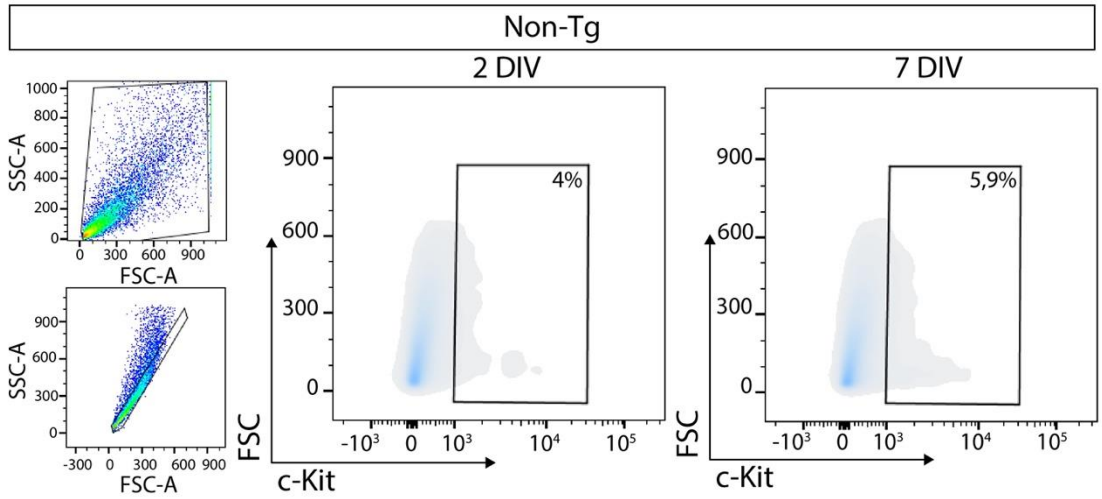

Fig. 8. Flow cytometry analysis of c-Kit+ mast cells isolated from the spinal cord of Non-Tg mice. Primary cultures of spinal cord of Non-Tg animals were maintained in presence IL-3 (20 ng/mL) and SCF (20 ng/mL) and c-Kit+ cell population was analyzed after 2 and 7 days *in vitro* by flow cytometry. Representative flow cytometry dot plots (left panels) showing the gating strategy followed and density plots (right panels) showing the expression of c-Kit at 2 and 7 days.

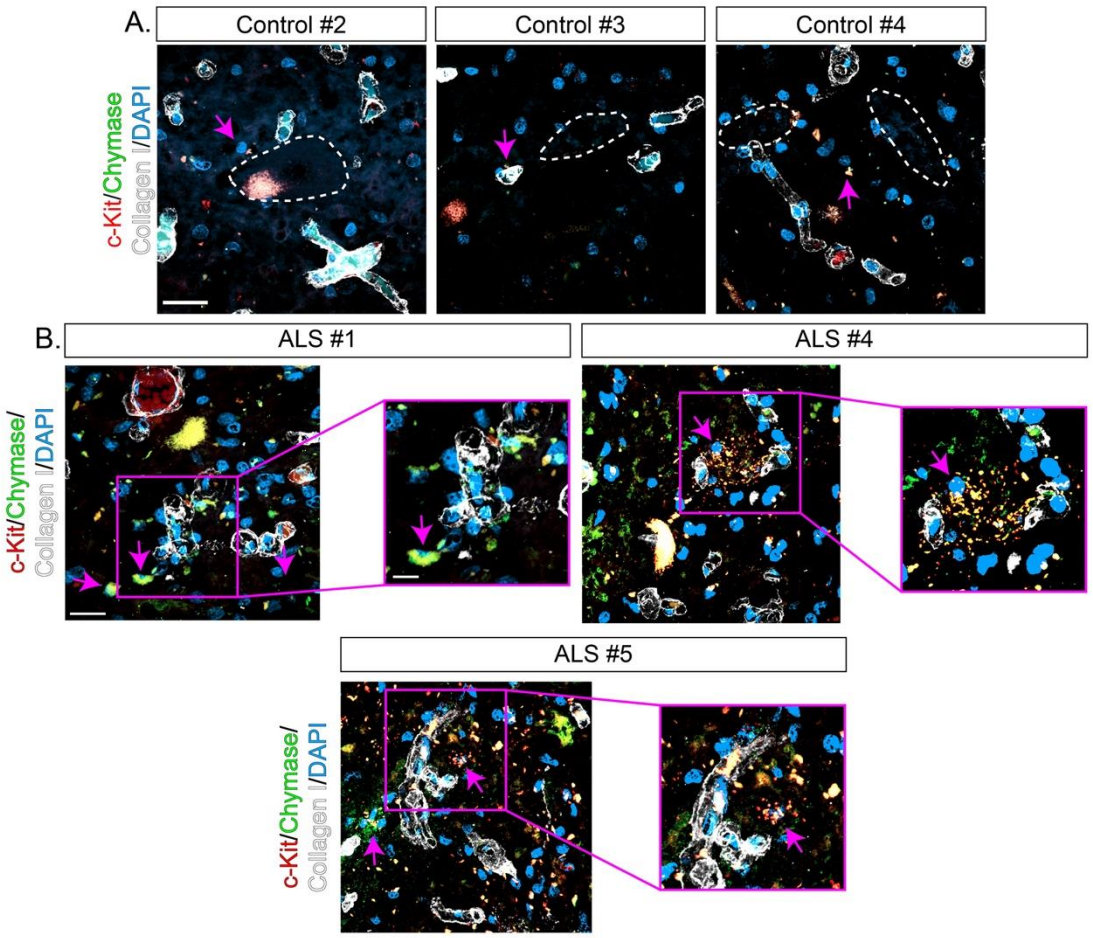

Fig. 9. Mast cells are associated with altered microvascular elements in ALS subjects but not in control donors. (A) Representative confocal microphotographs showing scarce number of c-Kit+/chymase+ MCs associated with microvascular elements stained with Collagen-I (white) in the ventral horn of the spinal cord of control donors. Magenta arrows indicate small MCs stained with both markers. **(B)** Representative confocal images of c-Kit+/chymase+ MCs (magenta arrows) associated with altered microvascular elements stained with Collagen-I (white) in the ventral horn of ALS subjects. Magenta squares show the area taken for high magnification analysis. Scale bars: 20 μm (low magnification panels) and 10 μm (insets).

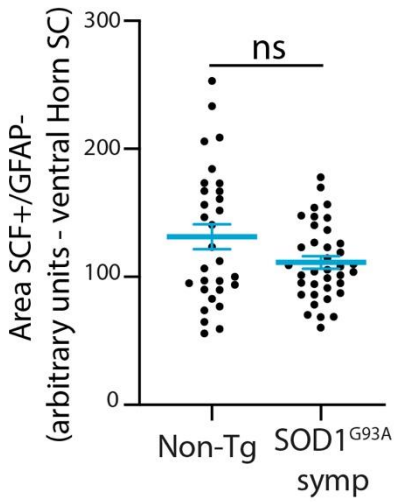

Fig. 10. Quantitative analysis of SCF immunoreactivity in motor neurons in the spinal cord of Non-Tg and symptomatic SOD1^{G93A} mice. Quantitative data are expressed as mean ± s.e.m. Data were analyzed by Mann- Whitney test. There was no significant difference among conditions. n=4 animals/condition.

Subjet	Tissue	MRC grade[a]	EMGb denervation	Age (years)	Gender	Disease onset	Survival (Months)	Post-mortem tissue processing (hours)	Sporadic/ familial
ALS #1	Lumbar Spinal Cord	3	Active and chronic	63	M	Leg	44	7.0	Sporadic
ALS #2	Lumbar Spinal Cord	1	Active	69	F	Leg	50	3.0	Sporadic
ALS #3	Lumbar Spinal Cord	3	Chronic	64	M	Leg	35	6.5	Sporadic
ALS #4	Lumbar Spinal Cord	3[c]	Active	59	F	Arm	26	13.0	Sporadic
ALS #5	Lumbar Spinal Cord	3	Active and chronic	75	M	Bulbar	55	4.3	Sporadic
Control #1	Lumbar Spinal Cord	-	-	68	M	-	-	19	-
Control #2	Lumbar Spinal Cord	-	-	59	M	-	-	9.5	-
Control #3	Lumbar Spinal Cord	-	-	90	M	-	-	4.5	-
Control #4	Lumbar Spinal Cord	-	-	62	M	-	-	3.0	-

Table 1. Clinical characteristics of ALS and control subjects included in the study. [a]Medical Research Council (MRC), muscle power grade at clinic visit prior to death. [b]EMG performed at time of ALS diagnosis. [c]Muscle showed predominant spasticity.

Discusión

Durante este trabajo de doctorado, hemos realizado algunos aportes significativos que contribuyen a entender los mecanismos patogénicos que intervienen en la neuroinflamación y degeneración de motoneuronas en la ELA. Considerando el concepto de microambiente celular degenerativo que se constituye alrededor de las motoneuronas y sus axones periféricos en degeneración, nuestros resultados han contribuido a identificar formalmente, por histopatología, citometría de flujo y cultivo celular, dos nuevos tipos de precursores para microglías y mastocitos, expresando los receptores de membrana CD34 y c-Kit, respectivamente, que forman parte de dicho microambiente. Además, mostramos evidencias de que ambos tipos celulares cumplen un papel patogénico en la ELA, acelerando la degeneración neuronal, promoviendo la neuroinflamación y afectando en algunos casos a la microvasculatura y la barrera hemato-espinal. Los precursores hematopoyéticos $CD34^+$ de microglías y los c-Kit^+ de mastocitos no habían sido reconocidos anteriormente en el contexto de la ELA y representan potencialmente importantes blancos terapéuticos para las enfermedades neurodegenerativas.

Precursores $CD34^+$ y microglías

Diversos estudios previos han mostrado que varios tipos de células del linaje mieloide, incluyendo monocitos, células dendríticas y "macrófagos cerebrales", aparecen en el parénquima nervioso en situaciones patológicas, como en modelos de enfermedad de Alzheimer, encefalitis autoinmune experimental o lesiones traumáticas (308–310). Esto implica que, a diferencia del SNC normal o sano, el cerebro enfermo o precondicionado se hace receptivo a la entrada de células mieloides en el parénquima nervioso. El ingreso de células mieloides al SNC da lugar a "macrófagos cerebrales" que tienen un fenotipo similar pero no idéntico a las microglías (311,312), y que desaparecen tras el final de la situación patológica (313). Sin embargo, la identidad de los precursores de los "macrófagos cerebrales" que invaden el SNC lesionado no está del todo aclarado (314), con la posibilidad de que provengan de monocitos circulantes Ly-$6C^{hi}$ (315) o incluso de precursores hematopoyéticos inmaduros que se movilizan desde la médula ósea al torrente sanguíneo frente a estímulos inflamatorios (316), lo que podría incluir células $CD34^+$.

Nuestro resultado de que la microgliosis en la médula espinal de animales o pacientes con ELA se acompaña de "*clusters*" de células expresando el marcador CD34 y localizadas alrededor de las motoneuronas, sugiere que estas células tienen un origen hemático. Sin embargo, también es reconocido que CD34 se expresa en otros tipos de células progenitoras, caracterizadas por un fenotipo indiferenciado (151). Además, las células $CD34^+$ que en la médula espinal en la ELA expresan el marcador mieloide CD11b, muestran una enorme capacidad proliferativa y forman "*clusters*" de células, sugiriendo un mecanismo de expansión poliiclonal que denota un comportamiento agresivo y patogénico de las células $CD34^+$ en el contexto de esta enfermedad. Nuestro descubrimiento de células

$CD34^+$ en la ELA está apoyado por un estudio reciente de transcriptómica espacial, que muestra un aumento significativo de transcriptos de CD34 en la médula espinal de ratones $SOD1^{G93A}$ (124).

Un requisito fundamental para la entrada de células mieloides en el parénquima nervioso es el aumento de la permeabilidad de la BHE (317,318). Por ejemplo, en ratones con daño de la BHE por irradiación aparecen células mieloides de origen donante en el lado lesionado y no así en el no lesionado (319). De la misma forma, varias citoquinas/quimioquinas producidas en el cerebro lesionado alteran la permeabilidad de la BHE (317). Uno de los principales factores. quimioatrayentes de las células mieloides es el MCP-1 liberado por astrocitos, células microgliales y neuronas (320). Además, otros factores como el CSF-1 y ATP son sobre-expresados o liberados en condiciones de daño de las motoneuronas y podrían contribuir a la atracción y proliferación de precursores mieloides o microglía (321,322).

Complementariamente, la entrada de precursores mieloides al SNC es regulada negativamente por las células microgliales residentes, a través de mecanismos complejos (308). En el caso de las células $CD34^+$ descubiertas en nuestro estudio, no es claro si responden a un mecanismo quimiotáctico que sea señalizado por CD34, ya que si bien CD34 se comporta a veces como un receptor o co-receptor de membrana, el ligando de este receptor no ha sido identificado cabalmente (31). Por ejemplo, existe la posibilidad de que las motoneuronas dañadas en la ELA produzcan el factor trófico CXCL12 en su entorno, el cual interacciona con CD34 y CXCR4 para atraer y estimular a células hematopoyéticas (323).

Una característica principal de los precursores mieloides sanguíneos es que son células que en cultivo se comportan como no-adherentes, comparado con los macrófagos ya diferenciados que muestran adherencia al sustrato (324,325). En este sentido, en este trabajo demostramos que, a diferencia de las microglías, las células $CD34^+$ se comportan como células mieloides indiferenciadas (326) y se mantienen en la fase no-adherente del cultivo. Asimismo, las células $CD34^+$ en cultivo proliferan, forman "*clusters*" y presentan el potencial de diferenciarse en microglía luego de sucesivos pasajes, características que describen a células progenitoras (327).

Células c-Kit^+ e invasión de mastocitos.

Las investigaciones realizadas durante la primera parte del doctorado nos llevaron a profundizar en la hipótesis de que células precursoras hematopoyéticas podrían dar origen a otros tipos de células inmunes proinflamatorias alrededor de las motoneuronas y sus axones periféricos en degeneración en la ELA. Si bien CD34 es un marcador de células precursoras de origen mieloide presentes en la médula ósea, las mismas también suelen co-expresar c-Kit (34,328). A su vez, c-Kit es un proto-oncogen que codifica para un receptor con actividad tirosina quinasa específica (329). Varios reportes coinciden en que c-Kit identifica a precursores hematopoyéticos del linaje mieloide en la médula ósea, con

potencial de dar lugar finalmente a granulocitos/monocitos (33,330,331). En la médula ósea de ratón, aproximadamente el 8% de las células presentes expresan c-Kit y, cuando se aíslan, son capaces de responder a factores como SCF, IL-3, GM-CSF y M-CSF, dando lugar a células diferenciadas de origen mieloide (331). Fuera de la médula ósea, el receptor c-Kit se expresa además en precursores de mastocitos y mastocitos maduros situados en tejidos epiteliales y conectivos (34,332), regulando su desarrollo, migración y activación (333,334). Por otra parte, la identificación de células que expresan el receptor c-Kit y, particularmente, de mastocitos c-Kit$^+$ en el SNC de animales adultos, ha sido pobremente caracterizada, especialmente en el contexto de la neurodegeneración. Conociendo el potencial proinflamatorio de los mastocitos, nos propusimos desafiar la hipótesis de que precursores CD34$^+$/c-Kit$^+$ de la médula ósea podrían migran a las diferentes regiones de las vías motoras centrales y periféricas, donde completan su maduración y diferenciación gracias a factores quimiotácticos locales. De esta manera, la invasión de mastocitos en los tejidos comprometidos en la ELA podría explicar un componente significativo de la neuroinflamación crónica.

Los mastocitos activados liberan numerosas sustancias vasoactivas, nociceptivas, sustancias quimioatrayentes y mediadores proinflamatorios en respuesta a una gran variedad de estímulos (35,190,196). La desgranulación y exocitosis en mastocitos es un proceso regulado que lleva a patrones de secreción específicos dependientes del sitio y el estímulo (196,335). En particular, los mastocitos regulan la permeabilidad vascular facilitando la extravasación de células sanguíneas (336), y secretan proteasas, como triptasa y quimasa, metaloproteasas como MMP-9 y factores tróficos (337). De esta manera, estas células efectoras podrían mediar potentes mecanismos regenerativos en respuestas a lesiones reversibles de las vías motoras periféricas, secretando en forma regulada, por ejemplo, factores neurotróficos y angiogénicos (338,339). Sin embargo, en condiciones de inflamación como en la ELA, la invasión exagerada de mastocitos podría conducir a la neuroinflamación crónica, remodelación vascular y neurotoxicidad.

En acuerdo con estudios previos de nuestro laboratorio que identificaron una infiltración significativa de mastocitos a lo largo de la vía motora periférica (26,27), nuestros resultados mostraron detalles sobre posibles mecanismos de reclutamiento de los mastocitos y su contribución a la axonopatía distal en la ELA. En particular, observamos que la infiltración de mastocitos c-Kit$^+$ está asociada temporal y espacialmente a la expresión de SCF por parte de las células de Schwann y macrófagos. SCF constituye el ligando endógeno de c-Kit, conocido por estimular la proliferación y diferenciación de los precursores de mastocitos (232). Estas observaciones sugieren que los mastocitos se insertan en complejas interacciones celulares del microambiente que involucra a macrófagos o neutrófilos que rodean a los axones motores en degeneración, tanto en las raíces ventrales como en los nervios periféricos (340). Observamos que SCF surge como una citoquina relevante en la ELA que se expresa en células de Schwann y que potencialmente actúa promoviendo la infiltración, diferenciación, proliferación y desgranulación de mastocitos (276). Los mastocitos c-Kit$^+$ son abundantes en la fibromatosis de tipo 1, donde SCF es producido por células de Schwann tumorales que portan la mutación Nf1$^{-/-}$ (341). Además, en nuestros

estudios se observó un aumento en la expresión de SCF en macrófagos, lo que sugiere una compleja interacción celular entre mastocitos, células de Schwann y macrófagos que contribuye al establecimiento de la neuroinflamación crónica y la axonopatía distal característica en la ELA.

En la última parte del trabajo de doctorado, nos propusimos evaluar la infiltración y rol de los mastocitos en la constitución del microambiente celular neurodegenerativo en la médula espinal en degeneración en la ELA. Estudios previos mostraron la presencia de mastocitos infiltrando regiones afectadas del SNC en enfermedades neurodegenerativas como la EA y la ELA (37,219), contribuyendo a la neuroinflamación característica de estas (36). Sin embargo, poco se conocía acerca de su interacción con las motoneuronas espinales en degeneración, células gliales activadas y la microvasculatura peri-neuronal.

En el microambiente celular que rodea los somas de las motoneuronas espinales de animales y pacientes con ELA, pudimos describir, por primera vez, la formación de "*clusters*" de precursores de mastocitos c-Kit^{+} y mastocitos que no se observan en los tejidos controles. Se pudieron destacar dos fenotipos claros de mastocitos c-Kit^{+} en la médula espinal de animales y pacientes con ELA: primero, mastocitos diferenciados con gránulos y desgranulación activa que expresan marcadores típicos como quimasa, triptasa y Cox-2, pero que no presentan la metacromasia a la tinción con azul de toluidina característica de los mastocitos del tejido conectivo; segundo, mastocitos pobremente diferenciados, que podrían corresponder a precursores, caracterizados por su pequeño tamaño, falta de gránulos y tinción positiva para c-Kit.

Estos resultados sugieren un mecanismo de quimiotaxis por el cual los mastocitos son atraídos anormalmente hacia el parénquima nervioso afectado en la ELA. A su vez, los mastocitos podrían incidir sobre los mecanismos de sobrevida de la motoneurona, por ejemplo, a través de la liberación de NGF, llevando potencialmente a generar una señal apoptótica mediante la interacción con su receptor p75NTR, que se expresa de manera anormal en motoneuronas dañadas en la ELA (342). Además, los mastocitos pueden responder a NGF de manera autocrina/paracrina, generando un circuito o "*loop*" proinflamatorio (339,343). Los mastocitos también tienen interacciones bidireccionales con microglías y astrocitos (36), por las cuales pueden contribuir a mantener un estado de neuroinflamación, particularmente al estado crónico de la misma. También observamos que en la médula espinal la expresión de SCF está aumentada y asociada a astrocitos reactivos en los ratones SOD1^{G93A}, siendo potencialmente un mecanismo quimiotáctico que podría explicar la infiltración y posterior diferenciación de los precursores c-Kit^{+}. Por lo tanto, los mastocitos desgranulantes en el microambiente que rodea a las motoneuronas tienen el potencial de promover la patología neuronal y neuroinflamación por varios mecanismos y de manera directa e indirecta, como ha sido sugerido en otros estudios (36,344,345).

Adicionalmente, observamos que los mastocitos infiltrantes se asociaban espacialmente con elementos microvasculares, sugiriendo su pasaje al parénquima nervioso y posterior

diferenciación a través de una permeabilidad vascular alterada. Actualmente, existe evidencia que demuestra la disfunción de las células endoteliales y pericitos en el cerebro y médula espinal de modelos murinos de ELA (268,346), asociado a la integridad y permeabilidad comprometida de las BHE (221). Las aberraciones microvasculares encontradas en este estudio (interrupciones en la marcación de colágeno, vasos - *strings y sprouts* -), han sido previamente descritas en otra enfermedad neurodegenerativa, como la EA (347), pero, sin embargo, los mecanismos que llevan al establecimiento y progresión de la patología vascular asociada a los mastocitos permanecen desconocidos. Los mastocitos participan en aumentar la permeabilidad microvascular, en parte por la secreción de proteasas típicas, como quimasa y triptasa, que son conocidas por degradar las proteínas de adhesión que unen las células endoteliales en las BHE (348), así como también a las proteínas clave de la matriz extracelular como vitronectina, procolágeno y colágeno de tipo IV (226,349). Por otro lado, la liberación de histamina y prostaglandinas dependientes de Cox-2, también podrían promover el aumento en la permeabilidad microvascular (350), facilitando así la entrada de células inflamatorias de la periferia.

En apoyo a esta hipótesis, pudimos demostrar que los precursores de mastocitos c-Kit$^+$ pueden acceder al parénquima de la médula espinal luego de su inyección vía intravenosa. Este tráfico fue solamente observado en ratones sintomáticos, no así en animales no transgénicos, donde la integridad y permeabilidad de las BHE permanece intacta. De este modo, contribuimos a conocer el mecanismo patológico que lleva a la infiltración de precursores c-Kit$^+$ al SNC y que involucra potencialmente un aumento de permeabilidad de la BHE, así como también la expresión aumentada del ligando SCF en astrocitos reactivos y neuronas. De esta manera, los precursores de mastocitos c-Kit$^+$ pueden ingresar al parénquima y al mismo tiempo permanecer y diferenciarse en mastocitos maduros.

Al igual que las células CD34$^+$, pudimos mostrar formalmente la existencia de precursores c-Kit$^+$ de mastocitos en la médula espinal de ratas SOD1^{G93A}, utilizando cultivos celulares. Estas células son aisladas en la fase no-adherente del cultivo y luego pudieron ser diferenciadas *ex vivo* en mastocitos maduros, utilizando los factores tróficos IL-3 y SCF, que son reconocidos por tener la misma función de madurar y diferenciar mastocitos a partir de precursores c-Kit$^+$ de la médula ósea (351). Estos resultados sugieren fuertemente que precursores hematopoyéticos CD34$^+$ y c-Kit$^+$ invaden el parénquima nervioso en la ELA a través de vasos sanguíneos permeables, y que pueden diferenciarse en una variedad de células inmunes, incluyendo células similares a la microglía o mastocitos.

Implicancias terapéuticas de los progenitores c-Kit$^+$

Los fármacos inhibidores de tirosina quinasa, incluyendo inhibidores de CSF-1R y c-Kit, han ido concentrando especial atención en los últimos años, como un mecanismo alternativo para poder modular la neuroinflamación (21,26,27,160,352,353). En particular, masitinib, que es un inhibidor de la clase III de receptores de tirosina quinasa, específicamente de c-Kit, CSF-1R y PDGF-R (21,277). Este fármaco fue originalmente descrito como neuroprotector y anti-inflamatorio en la ELA por nuestro grupo, mostrando un mecanismo

directo sobre microglías que expresan el receptor CSF1-R (21). Masitinib se encuentra actualmente en etapas avanzadas en estudios clínicos y demostró efectos significativos para el tratamiento de una subpoblación de pacientes con ELA a mediano y largo plazo (354,355).

En este contexto, en nuestros trabajos más recientes hemos utilizado el masitinib para estimar el potencial patogénico de los precursores c-Kit^{+} de mastocitos. Los animales SOD1^{G93A} tratados con el fármaco luego de la aparición de los síntomas motores, mostraron una disminución en el número de mastocitos c-Kit^{+} infiltrantes en las raíces ventrales, nervio ciático y médula espinal, confirmando que estas poblaciones celulares son dependientes de las señales tróficas mediadas por SCF/c-Kit. Aún más interesante, los animales tratados mostraron una respuesta terapéutica significativa al masitinib, estimada por parámetros histopatológicos que miden preservación de neuronas/axones y de disminución de la neuroinflamación (21). De la misma manera, el tratamiento con masitinib también previno el tráfico y acumulación de mastocitos en el SNC, mejorando la patología microvascular. Por lo tanto, nuestros estudios aportan evidencia adicional sobre los efectos neuroprotectores del masitinib, actuando en forma paralela sobre microglías y mastocitos para reducir la neuroinflamación y la neurotoxicidad.

Conclusiones

La Figura 2 ofrece una visión integrada sobre la significación patológica de los precursores $CD34^+$ y c-Kit^+ en la ELA. Los precursores hematopoyéticos $CD34^+$ y c-Kit^+ parecen infiltrar significativamente el SNC y SNP en las áreas de neurodegeneración en el contexto de esta enfermedad. Mientras que las células $CD34^+$ parecen diferenciarse preferentemente a células similares a microglías, las células c-Kit^+ parecen quedar indiferenciadas en las áreas peri-vasculares o bien diferenciarse a mastocitos maduros. No se pueden excluir que estos precursores den origen también a otros tipos de células mieloides previamente descritas en la ELA, como monocitos y células dendríticas (151).

En virtud de que la emergencia de estos progenitores se observa en las fases avanzadas de la neurodegeneración, postulamos que la aparición de precursores $CD34^+$ y c-Kit^+ está asociada a un aumento de la permeabilidad vascular, incluyendo la barrera hemato-espinal.

El destino de estos progenitores extravasados del torrente sanguíneo seguramente sea determinado por las influencias moleculares del microambiente celular neurodegenerativo. Por ejemplo, la sobreexpresión local de factores quimiotácticos y tróficos para microglías y mastocitos incluyendo CSF-1/IL34 y SCF, respectivamente, podría ser un factor clave para que los precursores puedan sobrevivir y diferenciarse en su entorno.

Los precursores $CD34^+$ y c-Kit^+ parecen invadir preferentemente el nicho celular que rodea los somas de motoneuronas espinales en la ELA, en estrecha relación con los elementos microvasculares y células gliales. En la vía motora periférica, también se constata que la invasión de mastocitos c-Kit^+ se asocia a defectos vasculares y a la infiltración paralela de otras células inmunes, notablemente macrófagos y neutrófilos.

Ambos precursores, $CD34^+$ y c-Kit^+, pueden ser aislados en cultivo de la médula espinal de animales con ELA en la fase sintomática. Estos precursores se encuentran en la fase no-adherente del cultivo y luego pueden dar origen a microglías o mastocitos diferenciados, dependiendo de las condiciones de cultivo.

Planteamos que la invasión de microglías $CD34^+$ y de mastocitos c-Kit^+ constituye un mecanismo potenciador de la neuroinflamación crónica en la ELA y representa la culminación de cambios patológicos y de remodelación en el microambiente peri-neuronal o axonal. Esta infiltración no parece ocurrir en etapas tempranas de la enfermedad, sino en etapas avanzadas donde la neuroinflamación progresa rápidamente en paralelo a la progresión del déficit neurológico.

Es reconocido que la neuroinflamación forma parte de la fisiopatología de la ELA y que las células inmunitarias participan de manera compleja en la progresión de la enfermedad. En conclusión, nuestro trabajo de tesis ha permitido avanzar significativamente en la comprensión de la neuroinflamación que acompaña a las enfermedades neurodegenerativas, permitiendo identificar nuevos tipos celulares de origen

hematopoyético con escasa diferenciación y que tienen un claro potencial patogénico en la ELA, además de ser blancos terapéuticos de fármacos inhibidores de tirosinas-quinasas.

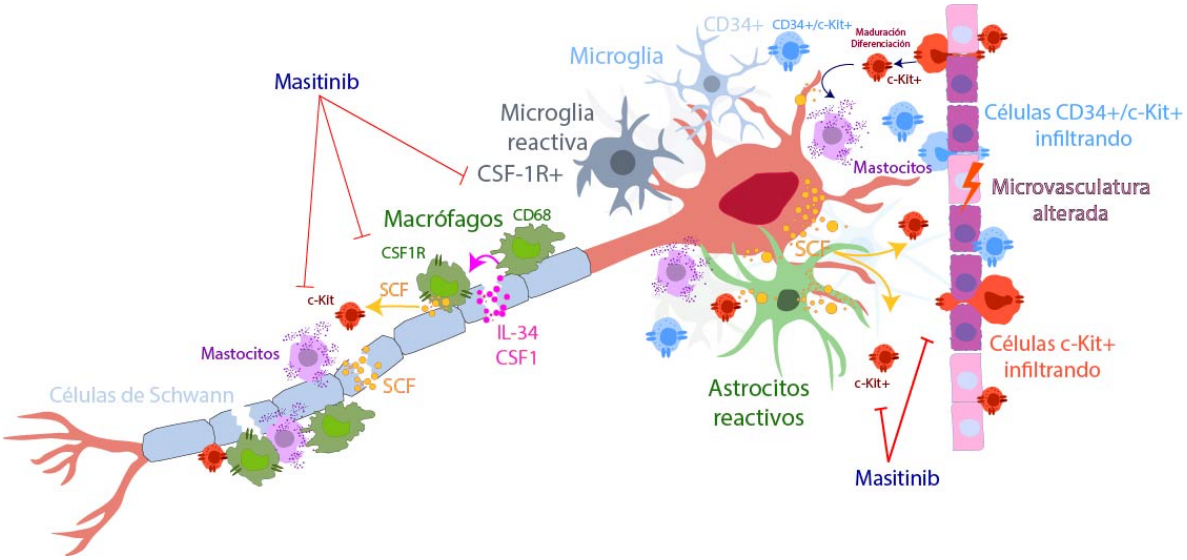

Figura 2. Microambiente celular neurodegenerativo en el SNC y SNP en la ELA. En la figura se resume la contribución de precursores hematopoyéticos $CD34^+$ y $c\text{-}Kit^+$, su interacción con células gliales y con elementos microvasculares y su modulación farmacológica por masitinib.

Limitaciones

Si bien este trabajo de tesis generó resultados consistentes, relevantes y potencialmente trasladables a la terapéutica de la ELA, también nos enfrentamos con varias limitaciones que deben ser mencionadas. Primero, para lograr una correcta caracterización de los fenotipos gliales aberrantes observados, hubiese sido necesario realizar un estudio transcriptómico por RNAseq en profundidad de las células $CD34^{+}$ aisladas de la médula espinal, así como también, un estudio inmunofenotípico detallado de las células $CD34^{+}$, con el fin de determinar o confirmar su origen. Esto debería incluir marcadores típicos de microglía ($Iba1^{high}$, CD206-, $CD45^{low}$, CD163-, $CD11b^{+}$, MHC-II^{+}, $F480^{+}$, $CX3CR1^{high}$, Ly6C-), de macrófagos perivasculares ($CD206^{+}$, $CD163^{+}$, $CD45^{high}$, $CD11b^{+}$, MHC-II^{high}, $Ly6C^{low}$, $F480^{+}$, $CX3CR1^{low}$, $Iba1^{low}$, $LYVE1^{+}$) (314,356), y diferenciarlas así de células provenientes de la periferia.

Para poder determinar si estas células poseen capacidad precursora o de “células madre”, el estudio debería haber incluido además de los marcadores CD34 y c-Kit, otros antígenos que sirven para su identificación, como el antígeno de células madre Sca1. También se debería confirmar que las células sean negativas para los llamados “marcadores de linaje”, que incluye marcadores de todas las células maduras del linaje hematopoyético (eritrocitos, linfocitos T, linfocitos B, células T Natural killer, monocitos y granulocitos). Por otro lado, para poder determinar el potencial progenitor, deberíamos haber profundizado en su diferenciación en otras células del linaje, además de macrófagos/microglía y mastocitos. Para eso, hubiese sido necesario aislar estas células y cultivarlas en presencia de distintos factores tróficos, necesarios para obtener los diferentes tipos celulares diferenciados del linaje mieloide y también linfoide (357–359).

Finalmente, también hubiese sido importante caracterizar la inhibición farmacológica de estos precursores hematopoyéticos c-Kit^{+} utilizando además de masitinib, otros inhibidores de tirosina quinasa como ibrutinib. Este fármaco es conocido por inhibir específicamente al receptor de tirosina quinasa BTK (360). Es sabido que su inhibición afecta la expresión de CXCR4, proteína que se expresa en mastocitos y media su quimioatracción a los tejidos periféricos vía la interacción con su ligando, CXCL12 (256). CXCL12 se encuentra aumentado en el LCR de pacientes con ELA esporádica y la inhibición específica de esta vía tiene efectos neuroprotectores en la ELA (257,361).

Perspectivas

Si bien nuestros trabajos generan nuevos conocimientos sobre los mecanismos de la neurodegeneración y neuroinflamación en la ELA, principalmente generan nuevas preguntas y perspectivas.

Por ejemplo, en el caso de los precursores $CD34^{+}$ descubiertos en la médula espinal de ratas $SOD1^{G93A}$ sintomáticas, no pudimos determinar si estas células se originaban a partir de microglía residente, macrófagos perivasculares o de células madre hematopoyéticas de la periferia. La realización de esta investigación supone, entre otras aproximaciones, técnicas de trasplante de precursores de células mieloides de médula ósea marcados, como un estudio fenotípico detallado de las células CD34 aisladas de la médula espinal, por ejemplo, por "*fate mapping*".

De la misma manera, si bien nuestro trabajo permite predecir un potencial precursor hematopoyético de las células $CD34^{+}$ y c-Kit^{+} presentes en la médula espinal, nuestros estudios no han analizado formalmente si estos precursores actúan como células madre hematopoyéticas dando origen los diferentes linajes.

Para determinar que los mastocitos que infiltran el SNC en la ELA cumplen un rol patogénico a través de la activación y desgranulación, se podrían validar biomarcadores específicos de desgranulación de mastocitos en el LCR de animales o pacientes con ELA. Por ejemplo, existen kits para medir la actividad triptasa y quimasa en la clínica, que podrían utilizarse para explorar la potencialidad de estos como biomarcadores y su utilidad en la clínica o terapéutica.

Bibliografía

1. Kovacs M, Trias E, Varela V, Ibarburu S, Beckman JS, Moura IC, et al. CD34 identifies a subset of proliferating microglial cells associated with degenerating motor neurons in ALS. Int J Mol Sci. 2019;20(16).
2. Kovacs M, Alamón C, Maciel C, Varela V, Ibarburu S, Tarragó L, et al. The pathogenic role of c-Kit+ mast cells in the spinal motor neuron-vascular niche in ALS. Acta Neuropathol Commun. 2021;9(1).
3. Zahra W, Rai SN, Birla H, Singh S sen, Dilnashin H, Rathore AS, et al. The global economic impact of neurodegenerative diseases: Opportunities and challenges. Bioeconomy for sustainable development. 2020;333–45.
4. Przedborski S, Vila M, Jackson-Lewis V. Neurodegeneration: what is it and where are we? J Clin Invest. 2003 Jan;111(1):3–10.
5. Dugger BN, Dickson DW. Pathology of neurodegenerative diseases. Vol. 9, Cold Spring Harbor Perspectives in Biology. 2017.
6. Trapp BD, Nave KA. Multiple sclerosis: An immune or neurodegenerative disorder? Vol. 31, Annual Review of Neuroscience. 2008.
7. Seeley WW. Mapping neurodegenerative disease onset and progression. Cold Spring Harb Perspect Biol. 2017;9(8).
8. Mason AR, Ziemann A, Finkbeiner S. Targeting the low-hanging fruit of neurodegeneration. Vol. 83, Neurology. 2014.
9. Kwon HS, Koh SH. Neuroinflammation in neurodegenerative disorders: the roles of microglia and astrocytes. Vol. 9, Translational Neurodegeneration. 2020.
10. Chen WW, Zhang X, Huang WJ. Role of neuroinflammation in neurodegenerative diseases (Review). Mol Med Rep. 2016;13(4).
11. DiSabato DJ, Quan N, Godbout JP. Neuroinflammation: the devil is in the details. J Neurochem. 2016;139.
12. Ransohoff RM. How neuroinflammation contributes to neurodegeneration. Vol. 353, Science. 2016.
13. Kölliker-Frers R, Udovin L, Otero-Losada M, Kobiec T, Herrera MI, Palacios J, et al. Neuroinflammation: An Integrating Overview of Reactive-Neuroimmune Cell Interactions in Health and Disease. Vol. 2021, Mediators of Inflammation. 2021.
14. Streit WJ, Mrak RE, Griffin WST. Microglia and neuroinflammation: A pathological perspective. J Neuroinflammation. 2004;1.
15. Trias E, Ibarburu S, Barreto-Núñez R, Barbeito L. Significance of aberrant glial cell phenotypes in pathophysiology of amyotrophic lateral sclerosis. Neurosci Lett. 2017;636:27–31.
16. Ellwardt E, Zipp F. Molecular mechanisms linking neuroinflammation and neurodegeneration in MS. Vol. 262, Experimental Neurology. 2014.
17. Evans MC, Couch Y, Sibson N, Turner MR. Inflammation and neurovascular changes in amyotrophic lateral sclerosis. Molecular and Cellular Neuroscience. 2013 Mar;53:34–41.
18. Miquel E, Cassina A, Martínez-Palma L, Souza JM, Bolatto C, Rodríguez-Bottero S, et al. Neuroprotective effects of the mitochondria-targeted antioxidant MitoQ in a model of

inherited amyotrophic lateral sclerosis. Free Radic Biol Med. 2014;70.
19. Martínez-Palma L, Miquel E, Lagos-Rodríguez V, Barbeito L, Cassina A, Cassina P. Mitochondrial Modulation by Dichloroacetate Reduces Toxicity of Aberrant Glial Cells and Gliosis in the SOD1G93A Rat Model of Amyotrophic Lateral Sclerosis. Neurotherapeutics. 2019;16(1).
20. Diaz-Amarilla P, Miquel E, Trostchansky A, Trias E, Ferreira AM, Freeman BA, et al. Electrophilic nitro-fatty acids prevent astrocyte-mediated toxicity to motor neurons in a cell model of familial amyotrophic lateral sclerosis via nuclear factor erythroid 2-related factor activation. Free Radic Biol Med. 2016;95.
21. Trias E, Ibarburu S, Barreto-Núñez R, Babdor J, Maciel TT, Guillo M, et al. Post-paralysis tyrosine kinase inhibition with masitinib abrogates neuroinflammation and slows disease progression in inherited amyotrophic lateral sclerosis. J Neuroinflammation [Internet]. 2016;13(1):177. Available from: http://www.ncbi.nlm.nih.gov/pubmed/27400786\nhttp://www.pubmedcentral.nih.gov/articlerender.fcgi?artid=PMC4940876
22. Wijesekera LC, Nigel Leigh P. Amyotrophic lateral sclerosis. Orphanet J Rare Dis. 2009 Dec 3;4(1):3.
23. Brown RH, Al-Chalabi A. Amyotrophic Lateral Sclerosis. New England Journal of Medicine. 2017 Jul 13;377(2):162–72.
24. Diaz-Amarilla P, Olivera-Bravo S, Trias E, Cragnolini a., Martinez-Palma L, Cassina P, et al. From the Cover: Phenotypically aberrant astrocytes that promote motoneuron damage in a model of inherited amyotrophic lateral sclerosis. Proceedings of the National Academy of Sciences. 2011;108(44):18126–31.
25. Trias E, Díaz-Amarilla P, Olivera-Bravo S, Isasi E, Drechsel DA, Lopez N, et al. Phenotypic transition of microglia into astrocyte-like cells associated with disease onset in a model of inherited ALS. Front Cell Neurosci [Internet]. 2013;7(December):274. Available from: http://www.pubmedcentral.nih.gov/articlerender.fcgi?artid=3871969&tool=pmcentrez&rendertype=abstract
26. Trias E, Ibarburu S, Barreto-Núñez R, Varela V, Moura IC, Dubreuil P, et al. Evidence for mast cells contributing to neuromuscular pathology in an inherited model of ALS. JCI Insight. 2017;2(20).
27. Trias E, King PH, Si Y, Kwon Y, Varela V, Ibarburu S, et al. Mast cells and neutrophils mediate peripheral motor pathway degeneration in ALS. JCI Insight. 2018;3(19).
28. Trias E, Kovacs M, King PH, Si Y, Kwon Y, Varela V, et al. Schwann cells orchestrate peripheral nerve inflammation through the expression of CSF1, IL-34, and SCF in amyotrophic lateral sclerosis. Glia. 2020;68(6):1165–81.
29. Trias E, Barbeito L, Yamanaka K. Phenotypic heterogeneity of astrocytes in motor neuron disease. Clin Exp Neuroimmunol. 2018;9(4):225–34.
30. Liu J, Wang F. Role of neuroinflammation in amyotrophic lateral sclerosis: Cellular mechanisms and therapeutic implications. Vol. 8, Frontiers in Immunology. 2017.
31. AbuSamra DB, Aleisa FA, Al-Amoodi AS, Ahmed HMJ, Chin CJ, Abuelela AF, et al. Not just a marker: CD34 on human hematopoietic stem/progenitor cells dominates vascular selectin binding along with CD44. Blood Adv. 2017;1(27).
32. Asheuer M, Pflumio F, Benhamida S, Dubart-Kupperschmitt A, Fouquet F, Imai Y, et al.

Human CD34+ cells differentiate into microglia and express recombinant therapeutic protein. Proc Natl Acad Sci U S A. 2004;101(10).
33. Akashi K, Traver D, Miyamoto T, Weissman IL. A clonogenic common myeloid progenitor that gives rise to all myeloid lineages. Nature. 2000;404(6774).
34. Grootens J, Ungerstedt JS, Nilsson G, Dahlin JS. Deciphering the differentiation trajectory from hematopoietic stem cells to mast cells. Vol. 2, Blood Advances. 2018.
35. Frenzel L, Hermine O. Mast cells and inflammation. Vol. 80, Joint Bone Spine. 2013.
36. Skaper SD, Facci L, Giusti P. Mast cells, glia and neuroinflammation: Partners in crime? Vol. 141, Immunology. 2014.
37. Graves MC, Fiala M, Dinglasan LA v., Liu NQ, Sayre J, Chiappelli F, et al. Inflammation in amyotrophic lateral sclerosis spinal cord and brain is mediated by activated macrophages, mast cells and t cells. Amyotrophic Lateral Sclerosis and Other Motor Neuron Disorders. 2004;5(4).
38. Logroscino G, Traynor BJ, Hardiman O, Chió A, Couratier P, Mitchell JD, et al. Descriptive epidemiology of amyotrophic lateral sclerosis: New evidence and unsolved issues. Vol. 79, Journal of Neurology, Neurosurgery and Psychiatry. 2008.
39. Masrori P, van Damme P. Amyotrophic lateral sclerosis: a clinical review. Vol. 27, European Journal of Neurology. 2020.
40. Al-Chalabi A, Hardiman O, Kiernan MC, Chiò A, Rix-Brooks B, van den Berg LH. Amyotrophic lateral sclerosis: moving towards a new classification system. Vol. 15, The Lancet Neurology. 2016.
41. Xu L, Liu T, Liu L, Yao X, Chen L, Fan D, et al. Global variation in prevalence and incidence of amyotrophic lateral sclerosis: a systematic review and meta-analysis. J Neurol. 2020;267(4).
42. Vázquez MC, Ketzoián C, Legnani C, Rega I, Sánchez N, Perna A, et al. Incidence and prevalence of amyotrophic lateral sclerosis in Uruguay: A population-based study. Neuroepidemiology. 2008;30(2).
43. Marin B, Boumé diene F, Logroscino G, Couratier P, Babron MC, Leutenegger AL, et al. Variation in world wide incidence of amyotrophic lateral sclerosis: A meta-analysis. Int J Epidemiol. 2017;46(1).
44. Longinetti E, Fang F. Epidemiology of amyotrophic lateral sclerosis: An update of recent literature. Vol. 32, Current Opinion in Neurology. 2019.
45. Nowicka N, Juranek J, Juranek JK, Wojtkiewicz J. Risk factors and emerging therapies in amyotrophic lateral sclerosis. Vol. 20, International Journal of Molecular Sciences. 2019.
46. Ingre C, Roos PM, Piehl F, Kamel F, Fang F. Risk factors for amyotrophic lateral sclerosis. Vol. 7, Clinical Epidemiology. 2015.
47. Sun J, Huang T, Debelius JW, Fang F. Gut microbiome and amyotrophic lateral sclerosis: A systematic review of current evidence. Vol. 290, Journal of Internal Medicine. 2021.
48. Zoccolella S, Beghi E, Palagano G, Fraddosio A, Guerra V, Samarelli V, et al. Riluzole and amyotrophic lateral sclerosis survival: A population-based study in southern Italy. Eur J Neurol. 2007;14(3).
49. Abe K, Aoki M, Tsuji S, Itoyama Y, Sobue G, Togo M, et al. Safety and efficacy of edaravone in well defined patients with amyotrophic lateral sclerosis: a randomised, double-blind, placebo-controlled trial. Lancet Neurol. 2017;16(7).

50. Hogden A, Foley G, Henderson RD, James N, Aoun SM. Amyotrophic lateral sclerosis: Improving care with a multidisciplinary approach. Vol. 10, Journal of Multidisciplinary Healthcare. 2017.
51. Taylor JP, Brown RH, Cleveland DW. Decoding ALS: From genes to mechanism. Vol. 539, Nature. 2016.
52. Chia R, Chiò A, Traynor BJ. Novel genes associated with amyotrophic lateral sclerosis: diagnostic and clinical implications. Vol. 17, The Lancet Neurology. 2018.
53. Neumann M, Sampathu DM, Kwong LK, Truax AC, Micsenyi MC, Chou TT, et al. Ubiquitinated TDP-43 in frontotemporal lobar degeneration and amyotrophic lateral sclerosis. Science (1979). 2006;314(5796).
54. Arai T, Hasegawa M, Akiyama H, Ikeda K, Nonaka T, Mori H, et al. TDP-43 is a component of ubiquitin-positive tau-negative inclusions in frontotemporal lobar degeneration and amyotrophic lateral sclerosis. Biochem Biophys Res Commun. 2006;351(3).
55. Lattante S, Rouleau GA, Kabashi E. TARDBP and FUS Mutations Associated with Amyotrophic Lateral Sclerosis: Summary and Update. Hum Mutat. 2013;34(6).
56. Lai SL, Abramzon Y, Schymick JC, Stephan DA, Dunckley T, Dillman A, et al. FUS mutations in sporadic amyotrophic lateral sclerosis. Neurobiol Aging. 2011;32(3).
57. Kwiatkowski TJ, Bosco DA, LeClerc AL, Tamrazian E, Vanderburg CR, Russ C, et al. Mutations in the FUS/TLS gene on chromosome 16 cause familial amyotrophic lateral sclerosis. Science (1979). 2009;323(5918).
58. Balendra R, Isaacs AM. C9orf72-mediated ALS and FTD: multiple pathways to disease. Vol. 14, Nature Reviews Neurology. 2018.
59. Rosen DR, Siddique T, Patterson D, Figlewicz DA, Sapp P, Hentati A, et al. Mutations in Cu/Zn superoxide dismutase gene are associated with familial amyotrophic lateral sclerosis. Nature. 1993;362(6415).
60. Andersen PM. Amyotrophic lateral sclerosis associated with mutations in the CuZn superoxide dismutase gene. Vol. 6, Current Neurology and Neuroscience Reports. 2006.
61. Valentine JS, Doucette PA, Potter SZ. Copper-zinc superoxide dismutase and amyotrophic lateral sclerosis. Vol. 74, Annual Review of Biochemistry. 2005.
62. Boillée S, vande Velde C, Cleveland DWW. ALS: A Disease of Motor Neurons and Their Nonneuronal Neighbors. Vol. 52, Neuron. 2006.
63. Howland DS, Liu J, She Y, Goad B, Maragakis NJ, Kim B, et al. Focal loss of the glutamate transporter EAAT2 in a transgenic rat model of SOD1 mutant-mediated amyotrophic lateral sclerosis (ALS). Proc Natl Acad Sci U S A. 2002;99(3).
64. Gurney ME, Pu H, Chiu AY, Dal Canto MC, Polchow CY, Alexander DD, et al. Motor neuron degeneration in mice that express a human Cu,Zn superoxide dismutase mutation. Science (1979). 1994;264(5166).
65. McGoldrick P, Joyce PI, Fisher EMC, Greensmith L. Rodent models of amyotrophic lateral sclerosis. Vol. 1832, Biochimica et Biophysica Acta - Molecular Basis of Disease. 2013.
66. Philips T, Rothstein JD. Rodent models of amyotrophic lateral sclerosis. Curr Protoc Pharmacol. 2015;2015.
67. van den Bosch L. Genetic rodent models of amyotrophic lateral sclerosis. Vol. 2011, Journal of Biomedicine and Biotechnology. 2011.
68. Bonifacino T, Zerbo RA, Balbi M, Torazza C, Frumento G, Fedele E, et al. Nearly 30 years of

animal models to study amyotrophic lateral sclerosis: A historical overview and future perspectives. Vol. 22, International Journal of Molecular Sciences. 2021.
69. Tian L, Ma L, Kaarela T, Li Z. Neuroimmune crosstalk in the central nervous system and its significance for neurological diseases. Vol. 9, Journal of Neuroinflammation. 2012.
70. Ransohoff RM, Brown MA. Innate immunity in the central nervous system. Vol. 122, Journal of Clinical Investigation. 2012.
71. Sweeney MD, Sagare AP, Zlokovic B v. Blood-brain barrier breakdown in Alzheimer disease and other neurodegenerative disorders. Vol. 14, Nature Reviews Neurology. 2018.
72. Cheng CF, Liao HJ, Wu CS. Tissue microenvironment dictates inflammation and disease activity in rheumatoid arthritis. Vol. 121, Journal of the Formosan Medical Association. 2022.
73. Kawai T, Autieri M v., Scalia R. Adipose tissue inflammation and metabolic dysfunction in obesity. Am J Physiol Cell Physiol. 2021;320(3).
74. Quail DF, Joyce JA. Microenvironmental regulation of tumor progression and metastasis. Vol. 19, Nature Medicine. 2013.
75. Ilieva H, Polymenidou M, Cleveland DW. Non-cell autonomous toxicity in neurodegenerative disorders: ALS and beyond. Vol. 187, Journal of Cell Biology. 2009.
76. Fritz E, Izaurieta P, Weiss A, Mir FR, Rojas P, Gonzalez D, et al. Mutant SOD1-expressing astrocytes release toxic factors that trigger motoneuron death by inducing hyperexcitability. J Neurophysiol. 2013;109(11).
77. Lee S, Kim S, Kang HY, Lim HR, Kwon Y, Jo M, et al. The overexpression of TDP-43 in astrocytes causes neurodegeneration via a PTP1B-mediated inflammatory response. J Neuroinflammation. 2020;17(1).
78. Papadeas ST, Kraig SE, O'Banion C, Lepore AC, Maragakis NJ. Astrocytes carrying the superoxide dismutase 1 (SOD1 G93A) mutation induce wild-type motor neuron degeneration in vivo. Proc Natl Acad Sci U S A. 2011;108(43).
79. Cassina P, Cassina A, Pehar M, Castellanos R, Gandelman M, de León A, et al. Mitochondrial dysfunction in SOD1G93A-bearing astrocytes promotes motor neuron degeneration: Prevention by mitochondrial-targeted antioxidants. Journal of Neuroscience. 2008;28(16).
80. Nagai M, Re DB, Nagata T, Chalazonitis A, Jessell TM, Wichterle H, et al. Astrocytes expressing ALS-linked mutated SOD1 release factors selectively toxic to motor neurons. Nat Neurosci. 2007;10(5).
81. Ferraiuolo L, Meyer K, Sherwood TW, Vick J, Likhite S, Frakes A, et al. Oligodendrocytes contribute to motor neuron death in ALS via SOD1-dependent mechanism. Proc Natl Acad Sci U S A. 2016;113(42).
82. Lobsiger CS, Boillee S, McAlonis-Downes M, Khan AM, Feltri ML, Yamanaka K, et al. Schwann cells expressing dismutase active mutant SOD1 unexpectedly slow disease progression in ALS mice. Proc Natl Acad Sci U S A. 2009;106(11).
83. Sofroniew M v., Vinters H v. Astrocytes: Biology and pathology. Vol. 119, Acta Neuropathologica. 2010.
84. Bezzi P, Volterra A. A neuron-glia signalling network in the active brain. Vol. 11, Current Opinion in Neurobiology. 2001.
85. Mogensen FLH, Delle C, Nedergaard M. The glymphatic system (En)during inflammation.

Vol. 22, International Journal of Molecular Sciences. 2021.
86. Macvicar BA, Newman EA. Astrocyte regulation of blood flow in the brain. Cold Spring Harb Perspect Biol. 2015;7(5).
87. Peluffo H, Estevez A, Barbeito L, Stutzmann JM. Riluzole promotes survival of rat motoneurons in vitro by stimulating trophic activity produced by spinal astrocyte monolayers. Neurosci Lett. 1997;228(3).
88. Ang LC, Bhaumick B, Juurlink BHJ. Neurite promoting activity of insulin, insulin-like growth factor I and nerve growth factor on spinal motoneurons is astrocyte dependent. Developmental Brain Research. 1993;74(1).
89. Cassina P, Peluffo H, Pehar M, Martinez-Palma L, Ressia A, Beckman JS, et al. Peroxynitrite triggers a phenotypic transformation in spinal cord astrocytes that induces motor neuron apoptosis. J Neurosci Res. 2002;67(1).
90. Sofroniew M v. Astrogliosis. Cold Spring Harb Perspect Biol. 2015;7(2).
91. Pekny M, Pekna M. Astrocyte reactivity and reactive astrogliosis: Costs and benefits. Physiol Rev. 2014;94(4).
92. Falsig J, Pörzgen P, Lund S, Schrattenholz A, Leist M. The inflammatory transcriptome of reactive murine astrocytes and implications for their innate immune function. J Neurochem. 2006;96(3).
93. Dong Y, Benveniste EN. Immune function of astrocytes. Glia. 2001;36(2).
94. Ridet JL, Malhotra SK, Privat A, Gage FH. Reactive astrocytes: Cellular and molecular cues to biological function. Vol. 20, Trends in Neurosciences. 1997.
95. Vargas MR, Pehar M, Díaz-Amarilla PJ, Beckman JS, Barbeito L. Transcriptional profile of primary astrocytes expressing ALS-linked mutant SOD1. J Neurosci Res. 2008;86(16).
96. Pehar M, Vargas MR, Robinson KM, Cassina P, England P, Beckman JS, et al. Peroxynitrite transforms nerve growth factor into an apoptotic factor for motor neurons. Free Radic Biol Med. 2006;41(11).
97. Cassina P, Pehar M, Vargas MR, Castellanos R, Barbeito AG, Estévez AG, et al. Astrocyte activation by fibroblast growth factor-1 and motor neuron apoptosis: Implications for amyotrophic lateral sclerosis. J Neurochem. 2005;93(1).
98. Barbeito LH, Pehar M, Cassina P, Vargas MR, Peluffo H, Viera L, et al. A role for astrocytes in motor neuron loss in amyotrophic lateral sclerosis. Brain Res Rev. 2004;47(1–3):263–74.
99. Pehar M, Martinez-Palma L, Peluffo H, Kamaid A, Cassina P, Barbeito L. Peroxynitrite-induced cytotoxicity in cultured astrocytes is associated with morphological changes and increased nitrotyrosine immunoreactivity. Neurotox Res. 2002;4(2).
100. Estévez AG, Spear N, Manuel SM, Radi R, Henderson CE, Barbeito L, et al. Nitric oxide and superoxide contribute to motor neuron apoptosis induced by trophic factor deprivation. Journal of Neuroscience. 1998;18(3).
101. Dawson VL, Brahmbhatt HP, Mong JA, Dawson TM. Expression of inducible nitric oxide synthase causes delayed neurotoxicity in primary mixed neuronal-glial cortical cultures. Neuropharmacology. 1994;33(11).
102. Vargas MR, Johnson DA, Sirkis DW, Messing A, Johnson JA. Nrf2 activation in astrocytes protects against neurodegeneration in mouse models of familial amyotrophic lateral sclerosis. Journal of Neuroscience. 2008;28(50).
103. Vargas MR, Pehar M, Cassina P, Beckman JS, Barbeito L. Increased glutathione

biosynthesis by Nrf2 activation in astrocytes prevents p75NTR-dependent motor neuron apoptosis. J Neurochem. 2006;97(3).
104. Sasabe J, Miyoshi Y, Suzuki M, Mita M, Konno R, Matsuoka M, et al. D-Amino acid oxidase controls motoneuron degeneration through D-serine. Proc Natl Acad Sci U S A. 2012;109(2).
105. Aloisi F. Immune function of microglia. Glia. 2001;36(2).
106. Cuadros MA, Navascués J. The origin and differentiation of microglial cells during development. Prog Neurobiol. 1998;56(2).
107. Perry VH, Hume DA, Gordon S. Immunohistochemical localization of macrophages and microglia in the adult and developing mouse brain. Neuroscience. 1985;15(2).
108. Colton CA, Wilcock DM. Assessing Activation States in Microglia. CNS Neurol Disord Drug Targets. 2012;9(2).
109. Hanisch UK, Kettenmann H. Microglia: Active sensor and versatile effector cells in the normal and pathologic brain. Vol. 10, Nature Neuroscience. 2007.
110. McGeer PL, McGeer EG. Inflammatory processes in amyotrophic lateral sclerosis. Vol. 26, Muscle and Nerve. 2002.
111. Doens D, Fernández PL. Microglia receptors and their implications in the response to amyloid β for Alzheimer's disease pathogenesis. Vol. 11, Journal of Neuroinflammation. 2014.
112. Onyango IG, Jauregui G v., Čarná M, Bennett JP, Stokin GB. Neuroinflammation in Alzheimer's disease. Vol. 9, Biomedicines. 2021.
113. Solé-Domènech S, Cruz DL, Capetillo-Zarate E, Maxfield FR. The endocytic pathway in microglia during health, aging and Alzheimer's disease. Vol. 32, Ageing Research Reviews. 2016.
114. Bajetto A, Bonavia R, Barbero S, Schettini G. Characterization of chemokines and their receptors in the central nervous system: Physiopathological implications. Vol. 82, Journal of Neurochemistry. 2002.
115. Vilhardt F. Microglia: Phagocyte and glia cell. Vol. 37, International Journal of Biochemistry and Cell Biology. 2005.
116. Streit WJ. Microglia as neuroprotective, immunocompetent cells of the CNS. Vol. 40, GLIA. 2002.
117. Perry VH, Nicoll JAR, Holmes C. Microglia in neurodegenerative disease. Vol. 6, Nature Reviews Neurology. 2010.
118. Leng F, Edison P. Neuroinflammation and microglial activation in Alzheimer disease: where do we go from here? Vol. 17, Nature Reviews Neurology. 2021.
119. Deczkowska A, Keren-Shaul H, Weiner A, Colonna M, Schwartz M, Amit I. Disease-Associated Microglia: A Universal Immune Sensor of Neurodegeneration. Vol. 173, Cell. 2018.
120. Graber DJ, Hickey WF, Harris BT. Progressive changes in microglia and macrophages in spinal cord and peripheral nerve in the transgenic rat model of amyotrophic lateral sclerosis. J Neuroinflammation. 2010;7.
121. McGeer PL, McGeer EG. The inflammatory response system of brain: implications for therapy of Alzheimer and other neurodegenerative diseases. Vol. 21, Brain Research Reviews. 1995.

122. Keren-Shaul H, Spinrad A, Weiner A, Matcovitch-Natan O, Dvir-Szternfeld R, Ulland TK, et al. A Unique Microglia Type Associated with Restricting Development of Alzheimer's Disease. Cell. 2017;169(7).
123. Krasemann S, Madore C, Cialic R, Baufeld C, Calcagno N, el Fatimy R, et al. The TREM2-APOE Pathway Drives the Transcriptional Phenotype of Dysfunctional Microglia in Neurodegenerative Diseases. Immunity. 2017;47(3).
124. Maniatis S, Äijö T, Vickovic S, Braine C, Kang K, Mollbrink A, et al. Spatiotemporal dynamics of molecular pathology in amyotrophic lateral sclerosis. Science (1979). 2019;364(6435).
125. Frakes AE, Ferraiuolo L, Haidet-Phillips AM, Schmelzer L, Braun L, Miranda CJ, et al. Microglia induce motor neuron death via the classical NF-κB pathway in amyotrophic lateral sclerosis. Neuron. 2014;81(5).
126. Ibarburu S, Kovacs M, Varela V, Rodríguez-Duarte J, Ingold M, Invernizzi P, et al. A Nitroalkene Benzoic Acid Derivative Targets Reactive Microglia and Prolongs Survival in an Inherited Model of ALS via NF-κB Inhibition. Neurotherapeutics. 2021;18(1).
127. Hall ED, Oostveen JA, Gurney ME. Relationship of microglial and astrocytic activation to disease onset and progression in a transgenic model of familial ALS. Glia. 1998;23(3).
128. Alexianu ME, Kozovska M, Appel SH. Immune reactivity in a mouse model of familial ALS correlates with disease progression. Neurology. 2001;57(7).
129. Elliott JL. Cytokine upregulation in a murine model of familial amyotrophic lateral sclerosis. Molecular Brain Research. 2001;95(1–2).
130. Olsen MK, Roberds SL, Ellerbrock BR, Fleck TJ, McKinley DK, Gurney ME. Disease mechanisms revealed by transcription profiling in SOD1-G93A transgenic mouse spinal cord. Ann Neurol. 2001;50(6).
131. Fendrick SE, Xue QS, Streit WJ. Formation of multinucleated giant cells and microglial degeneration in rats expressing a mutant Cu/Zn superoxide dismutase gene. J Neuroinflammation. 2007;4.
132. Lobsiger CS, Cleveland DW. Glial cells as intrinsic components of non-cell-autonomous neurodegenerative disease. Vol. 10, Nature Neuroscience. 2007.
133. Gowing G, Philips T, van Wijmeersch B, Audet JN, Dewil M, van den Bosch L, et al. Ablation of proliferating microglia does not affect motor neuron degeneration in amyotrophic lateral sclerosis caused by mutant superoxide dismutase. Journal of Neuroscience. 2008;28(41).
134. Sanagi T, Yuasa S, Nakamura Y, Suzuki E, Aoki M, Warita H, et al. Appearance of phagocytic microglia adjacent to motoneurons in spinal cord tissue from a presymptomatic transgenic rat model of amyotrophic lateral sclerosis. J Neurosci Res. 2010;88(12).
135. Boillée S, Yamanaka K, Lobsiger CS, Copeland NG, Jenkins NA, Kassiotis G, et al. Onset and Progression in Inherited ALS Determined by Motor Neurons and Microglia. Science (1979). 2006 Jun 2;312(5778):1389–92.
136. Kriz J, Nguyen MD, Julien JP. Minocycline slows disease progression in a mouse model of amyotrophic lateral sclerosis. Neurobiol Dis. 2002;10(3).
137. Beers DR, Henkel JS, Xiao Q, Zhao W, Wang J, Yen AA, et al. Wild-type microglia extend survival in PU.1 knockout mice with familial amyotrophic lateral sclerosis. Proc Natl Acad Sci U S A. 2006;103(43).
138. Xiao Q, Zhao W, Beers DR, Yen AA, Xie W, Henkel JS, et al. Mutant SOD1G93A microglia

are more neurotoxic relative to wild-type microglia. J Neurochem. 2007;102(6).
139. Zhao W, Xie W, Le W, Beers DR, He Y, Henkel JS, et al. Activated microglia initiate motor neuron injury by a nitric oxide and glutamate-mediated mechanism. J Neuropathol Exp Neurol. 2004;63(9).
140. Sofía Ibarburu, Emiliano Trias, Natalia Lago, Hugo Peluffo, Romina Barreto-Núñez, Valentina Varela, Joseph S. Beckman LB. Focal transplantation of aberrant glial cells carrying the SOD1G93A mutation into rat spinal cord induces extensive gliosis. Neuroimmunomodulation. 2017;
141. Ajami B, Bennett JL, Krieger C, Tetzlaff W, Rossi FMV. Local self-renewal can sustain CNS microglia maintenance and function throughout adult life. Nat Neurosci. 2007;10(12).
142. Shechter R, London A, Varol C, Raposo C, Cusimano M, Yovel G, et al. Infiltrating blood-derived macrophages are vital cells playing an anti-inflammatory role in recovery from spinal cord injury in mice. PLoS Med. 2009;6(7).
143. Mildner A, MacK M, Schmidt H, Brück W, Djukic M, Zabel MD, et al. CCR2+Ly-6Chi monocytes are crucial for the effector phase of autoimmunity in the central nervous system. Brain. 2009;132(9).
144. Zondler L, Müller K, Khalaji S, Bliederhäuser C, Ruf WP, Grozdanov V, et al. Peripheral monocytes are functionally altered and invade the CNS in ALS patients. Acta Neuropathol. 2016;132(3).
145. Butovsky O, Siddiqui S, Gabriely G, Lanser AJ, Dake B, Murugaiyan G, et al. Modulating inflammatory monocytes with a unique microRNA gene signature ameliorates murine ALS. Journal of Clinical Investigation. 2012;122(9).
146. Solomon JN, Lewis CAB, Ajami B, Corbel SY, Rossi FMV, Krieger C. Origin and distribution of bone marrow-derived cells in the central nervous system in a mouse model of amyotrophic lateral sclerosis. Glia. 2006;53(7).
147. Kunis G, Baruch K, Miller O, Schwartz M. Immunization with a myelin-derived antigen activates the brain's choroid plexus for recruitment of immunoregulatory cells to the CNS and attenuates disease progression in a mouse model of ALS. Journal of Neuroscience. 2015;35(16).
148. Henkel JS, Engelhardt JI, Siklós L, Simpson EP, Kim SH, Pan T, et al. Presence of Dendritic Cells, MCP-1, and Activated Microglia/Macrophages in Amyotrophic Lateral Sclerosis Spinal Cord Tissue. Ann Neurol. 2004;55(2).
149. Henkel JS, Beers DR, Siklós L, Appel SH. The chemokine MCP-1 and the dendritic and myeloid cells it attracts are increased in the mSOD1 mouse model of ALS. Molecular and Cellular Neuroscience. 2006;31(3).
150. Krause DS, Ito T, Fackler MJ, Smith OM, Collector MI, Sharkis SJ, et al. Characterization of murine CD34, a marker for hematopoietic progenitor and stem cells. Blood. 1994;84(3).
151. Sidney LE, Branch MJ, Dunphy SE, Dua HS, Hopkinson A. Concise review: Evidence for CD34 as a common marker for diverse progenitors. Vol. 32, Stem Cells. 2014.
152. Sutherland DR, Keating A. The CD34 Antigen: Structure, Biology, and Potential Clinical Applications. J Hematother Stem Cell Res. 1992;1(2).
153. Ladeby R, Wirenfeldt M, Dalmau I, Gregersen R, García-Ovejero D, Babcock A, et al. Proliferating resident microglia express the stem cell antigen CD34 in response to acute neural injury. Glia. 2005;50(2).

154. Kuhle J, Lindberg RLP, Regeniter A, Mehling M, Steck AJ, Kappos L, et al. Increased levels of inflammatory chemokines in amyotrophic lateral sclerosis. Eur J Neurol. 2009;16(6).
155. Nguyen MD, Julien JP, Rivest S. Induction of proinflammatory molecules in mice with amyotrophic lateral sclerosis: No requirement for proapoptotic interleukin-1β in neurodegeneration. Ann Neurol. 2001;50(5).
156. Wei S, Nandi S, Chitu V, Yeung YG, Yu W, Huang M, et al. Functional overlap but differential expression of CSF-1 and IL-34 in their CSF-1 receptor-mediated regulation of myeloid cells. J Leukoc Biol. 2010;88(3).
157. Wang Y, Szretter KJ, Vermi W, Gilfillan S, Rossini C, Cella M, et al. IL-34 is a tissue-restricted ligand of CSF1R required for the development of Langerhans cells and microglia. Nat Immunol. 2012;13(8).
158. Easley-Neal C, Foreman O, Sharma N, Zarrin AA, Weimer RM. CSF1R Ligands IL-34 and CSF1 Are Differentially Required for Microglia Development and Maintenance in White and Gray Matter Brain Regions. Front Immunol. 2019;10.
159. Verstraete K, Savvides SN. Extracellular assembly and activation principles of oncogenic class III receptor tyrosine kinases. Vol. 12, Nature Reviews Cancer. 2012.
160. Martínez-Muriana A, Mancuso R, Francos-Quijorna I, Olmos-Alonso A, Osta R, Perry VH, et al. CSF1R blockade slows the progression of amyotrophic lateral sclerosis by reducing microgliosis and invasion of macrophages into peripheral nerves. Sci Rep. 2016;6.
161. Lampson LA, Kushner PD, Sobel RA. Major histocompatibility complex antigen expression in the affected tissues in amyotrophic lateral sclerosis. Ann Neurol. 1990;28(3).
162. TROOST D, van den OORD JJ, JONG JMBV de. Immunohistochemical characterization of the inflammatory infiltrate in amyotrophic lateral sclerosis. Neuropathol Appl Neurobiol. 1990;16(5).
163. Kawamata T, Akiyama H, Yamada T, McGeer PL. Immunologic reactions in amyotrophic lateral sclerosis brain and spinal cord tissue. American Journal of Pathology. 1992;140(3).
164. Beers DR, Zhao W, Wang J, Zhang X, Wen S, Neal D, et al. ALS patients' regulatory T lymphocytes are dysfunctional, and correlate with disease progression rate and severity. JCI Insight. 2017;2(5).
165. Chiu IM, Phatnani H, Kuligowski M, Tapia JC, Carrasco MA, Zhang M, et al. Activation of innate and humoral immunity in the peripheral nervous system of ALS transgenic mice. Proc Natl Acad Sci U S A. 2009;106(49).
166. Coque E, Salsac C, Espinosa-Carrasco G, Varga B, Degauque N, Cadoux M, et al. Cytotoxic CD8 + T lymphocytes expressing ALS-causing SOD1 mutant selectively trigger death of spinal motoneurons. Proc Natl Acad Sci U S A. 2019;116(6).
167. Beers DR, Henkel JS, Zhao W, Wang J, Appel SH. CD4+ T cells support glial neuroprotection, slow disease progression, and modify glial morphology in an animal model of inherited ALS. Proc Natl Acad Sci U S A. 2008;105(40).
168. Beers DR, Henkel JS, Zhao W, Wang J, Huang A, Wen S, et al. Endogenous regulatory T lymphocytes ameliorate amyotrophic lateral sclerosis in mice and correlate with disease progression in patients with amyotrophic lateral sclerosis. Brain. 2011;134(5).
169. Zhong Z, Deane R, Ali Z, Parisi M, Shapovalov Y, O'Banion MK, et al. ALS-causing SOD1 mutants generate vascular changes prior to motor neuron degeneration. Nat Neurosci. 2008;11(4).

170. McCombe PA, Lee JD, Woodruff TM, Henderson RD. The Peripheral Immune System and Amyotrophic Lateral Sclerosis. Vol. 11, Frontiers in Neurology. 2020.
171. Murdock BJ, Zhou T, Kashlan SR, Little RJ, Goutman SA, Feldman EL. Correlation of Peripheral Immunity With Rapid Amyotrophic Lateral Sclerosis Progression. JAMA Neurol. 2017 Dec 1;74(12):1446.
172. Murdock BJ, Bender DE, Kashlan SR, Figueroa-Romero C, Backus C, Callaghan BC, et al. Increased ratio of circulating neutrophils to monocytes in amyotrophic lateral sclerosis. Neurol Neuroimmunol Neuroinflamm. 2016;3(4).
173. Swindell WR, Kruse CPS, List EO, Berryman DE, Kopchick JJ. ALS blood expression profiling identifies new biomarkers, patient subgroups, and evidence for neutrophilia and hypoxia. J Transl Med. 2019;17(1).
174. Gustafson MP, Staff NP, Bornschlegl S, Butler GW, Maas ML, Kazamel M, et al. Comprehensive immune profiling reveals substantial immune system alterations in a subset of patients with amyotrophic lateral sclerosis. PLoS One. 2017;12(7).
175. Mantovani S, Garbelli S, Pasini A, Alimonti D, Perotti C, Melazzini M, et al. Immune system alterations in sporadic amyotrophic lateral sclerosis patients suggest an ongoing neuroinflammatory process. J Neuroimmunol. 2009;210(1–2).
176. Zhang R, Gascon R, Miller RG, Gelinas DF, Mass J, Hadlock K, et al. Evidence for systemic immune system alterations in sporadic amyotrophic lateral sclerosis (sALS). J Neuroimmunol. 2005;159(1–2).
177. Chen X, Feng W, Huang R, Guo X, Chen Y, Zheng Z, et al. Evidence for peripheral immune activation in amyotrophic lateral sclerosis. J Neurol Sci. 2014;347(1–2).
178. Chiu IM, Chen A, Zheng Y, Kosaras B, Tsiftsoglou SA, Vartanian TK, et al. T lymphocytes potentiate endogenous neuroprotective inflammation in a mouse model of ALS. Proc Natl Acad Sci U S A. 2008;105(46).
179. Rentzos M, Evangelopoulos E, Sereti E, Zouvelou V, Marmara S, Alexakis T, et al. Alterations of T cell subsets in ALS: A systemic immune activation? Acta Neurol Scand. 2012;125(4).
180. Campisi L, Chizari S, Ho JSY, Gromova A, Arnold FJ, Mosca L, et al. Clonally expanded CD8 T cells characterize amyotrophic lateral sclerosis-4. Nature. 2022 Jun 30;606(7916):945–52.
181. Garofalo S, Cocozza G, Porzia A, Inghilleri M, Raspa M, Scavizzi F, et al. Natural killer cells modulate motor neuron-immune cell cross talk in models of Amyotrophic Lateral Sclerosis. Nat Commun. 2020;11(1).
182. Finkelstein A, Kunis G, Seksenyan A, Ronen A, Berkutzki T, Azoulay D, et al. Abnormal changes in NKT cells, the IGF-1 axis, and liver pathology in an animal model of ALS. PLoS One. 2011;6(8).
183. Henkel JS, Beers DR, Wen S, Rivera AL, Toennis KM, Appel JE, et al. Regulatory T-lymphocytes mediate amyotrophic lateral sclerosis progression and survival. EMBO Mol Med. 2013;5(1).
184. Sheean RK, McKay FC, Cretney E, Bye CR, Perera ND, Tomas D, et al. Association of regulatory T-Cell Expansion with progression of amyotrophic lateral sclerosis a study of humans and a transgenic mouse model. JAMA Neurol. 2018;75(6).
185. Murdock BJ, Zhou T, Kashlan SR, Little RJ, Goutman SA, Feldman EL. Correlation of peripheral immunity with rapid Amyotrophic lateral sclerosis progression. JAMA Neurol.

2017;74(12).
186. Mcgill RB, Steyn FJ, Ngo ST, Thorpe KA, Heggie S, Ruitenberg MJ, et al. Monocytes and neutrophils are associated with clinical features in amyotrophic lateral sclerosis. Brain Commun. 2020;2(1).
187. Zhao W, Beers DR, Hooten KG, Sieglaff DH, Zhang A, Kalyana-Sundaram S, et al. Characterization of gene expression phenotype in amyotrophic lateral sclerosis monocytes. JAMA Neurol. 2017;74(6).
188. Okayama Y, Kawakami T. Development, migration, and survival of mast cells. Vol. 34, Immunologic Research. 2006.
189. Zsebo KM, Williams DA, Geissler EN, Broudy VC, Martin FH, Atkins HL, et al. Stem cell factor is encoded at the SI locus of the mouse and is the ligand for the c-kit tyrosine kinase receptor. Cell. 1990;63(1).
190. Krystel-Whittemore M, Dileepan KN, Wood JG. Mast cell: A multi-functional master cell. Vol. 6, Frontiers in Immunology. 2016.
191. Saha SS, Samanas NB, Miralda I, Shubin NJ, Niino K, Bhise G, et al. Mast cell surfaceome characterization reveals CD98 heavy chain is critical for optimal cell function. Journal of Allergy and Clinical Immunology. 2022;149(2).
192. Wernersson S, Pejler G. Mast cell secretory granules: Armed for battle. Vol. 14, Nature Reviews Immunology. 2014.
193. Abonia JP, Friend DS, Austen WG, Moore FD, Carroll MC, Chan R, et al. Mast Cell Protease 5 Mediates Ischemia-Reperfusion Injury of Mouse Skeletal Muscle. The Journal of Immunology. 2005;174(11).
194. Zhang D, Spielmann A, Wang L, Ding G, Huang F, Gu Q, et al. Mast-cell degranulation induced by physical stimuli involves the activation of transient-receptor-potential channel TRPV2. Physiol Res. 2012;61(1).
195. Plum T, Wang X, Rettel M, Krijgsveld J, Feyerabend TB, Rodewald HR. Human Mast Cell Proteome Reveals Unique Lineage, Putative Functions, and Structural Basis for Cell Ablation. Immunity. 2020;52(2).
196. Vukman K v., Försönits A, Oszvald Á, Tóth E, Buzás EI. Mast cell secretome: Soluble and vesicular components. Vol. 67, Seminars in Cell and Developmental Biology. 2017.
197. Skaper SD, Facci L, Zusso M, Giusti P. An inflammation-centric view of neurological disease: Beyond the neuron. Vol. 12, Frontiers in Cellular Neuroscience. 2018.
198. Hendriksen E, van Bergeijk D, Oosting RS, Redegeld FA. Mast cells in neuroinflammation and brain disorders. Vol. 79, Neuroscience and Biobehavioral Reviews. 2017.
199. Forsythe P. Mast Cells in Neuroimmune Interactions. Vol. 42, Trends in Neurosciences. 2019.
200. Gupta K, Harvima IT. Mast cell-neural interactions contribute to pain and itch. Vol. 282, Immunological Reviews. 2018.
201. Dropp JJ. Mast cells in mammalian brain. Cells Tissues Organs. 1976;94(1).
202. Harcha PA, Garcés P, Arredondo C, Fernández G, Sáez JC, van Zundert B. Mast cell and astrocyte hemichannels and their role in alzheimer's disease, als, and harmful stress conditions. Int J Mol Sci. 2021;22(4):1–19.
203. Nakamura Y, Kambe N, Saito M, Nishikomori R, Kim YG, Murakami M, et al. Mast cells mediate neutrophil recruitment and vascular leakage through the NLRP3 inflammasome in

histamine-independent urticaria. Journal of Experimental Medicine. 2009;206(5).
204. Ribatti D. The crucial role of mast cells in blood-brain barrier alterations. Exp Cell Res [Internet]. 2015;338(1):119–25. Available from: http://dx.doi.org/10.1016/j.yexcr.2015.05.013
205. McKittrick CM, Lawrence CE, Carswell HVO. Mast cells promote blood brain barrier breakdown and neutrophil infiltration in a mouse model of focal cerebral ischemia. Journal of Cerebral Blood Flow and Metabolism [Internet]. 2015;35(4):638–47. Available from: http://dx.doi.org/10.1038/jcbfm.2014.239
206. Pertiwi KR, de Boer OJ, Mackaaij C, Pabittei DR, de Winter RJ, Li X, et al. Extracellular traps derived from macrophages, mast cells, eosinophils and neutrophils are generated in a time-dependent manner during atherothrombosis. Journal of Pathology. 2019;247(4).
207. Weng Z, Zhang B, Tsilioni I, Theoharides TC. Nanotube Formation: A Rapid Form of “alarm Signaling”? Clin Ther. 2016;38(5).
208. Stelekati E, Bahri R, D’Orlando O, Orinska Z, Mittrücker HW, Langenhaun R, et al. Mast Cell-Mediated Antigen Presentation Regulates CD8+ T Cell Effector Functions. Immunity. 2009;31(4).
209. Orinska Z, Bulanova E, Budagian V, Metz M, Maurer M, Bulfone-Paus S. TLR3-induced activation of mast cells modulates CD8+ T-cell recruitment. Blood. 2005;106(3).
210. Jones MK, Nair A, Gupta M. Mast cells in neurodegenerative disease. Vol. 13, Frontiers in Cellular Neuroscience. 2019.
211. Conti P, Kempuraj D. Important role of mast cells in multiple sclerosis. Vol. 5, Multiple Sclerosis and Related Disorders. 2016.
212. Georgin-Lavialle S, Moura DS, Salvador A, Chauvet-Gelinier JC, Launay JM, Damaj G, et al. Mast cells’ involvement in inflammation pathways linked to depression: Evidence in mastocytosis. Mol Psychiatry. 2016;21(11).
213. Conti P, Gallenga CE, Caraffa A, Ronconi G, Kritas SK. Impact of mast cells in fibromyalgia and low-grade chronic inflammation: Can IL-37 play a role? Vol. 33, Dermatologic Therapy. 2020.
214. Fang Q, Hu WW, Wang XF, Yang Y, Lou GD, Jin MM, et al. Histamine up-regulates astrocytic glutamate transporter 1 and protects neurons against ischemic injury. Neuropharmacology. 2014;77.
215. Skaper SD, Facci L, Kee WJ, Strijbos PJLM. Potentiation by histamine of synaptically mediated excitotoxicity in cultured hippocampal neurones: A possible role for mast cells. J Neurochem. 2001;76(1).
216. Maslinska D, Laure-Kamionowska M, Maslinski KT, Gujski M, Maslinski S. Distribution of tryptase-containing mast cells and metallothionein reactive astrocytes in human brains with amyloid deposits. In: Inflammation Research. 2007.
217. Harcha PA, Vargas A, Yi C, Koulakoff AA, Giaume C, Sáez JC. Hemichannels are required for amyloid β-Peptide-induced degranulation and are activated in brain mast cells of APPswe/PS1dE9 Mice. Journal of Neuroscience. 2015;35(25).
218. Shaik-Dasthagirisaheb YB, Conti P. The role of mast cells in Alzheimer’s disease. Vol. 25, Advances in Clinical and Experimental Medicine. 2016.
219. Fiala M, Chattopadhay M, la Cava A, Tse E, Liu G, Lourenco E, et al. IL-17A is increased in the serum and in spinal cord CD8 and mast cells of ALS patients. J Neuroinflammation.

2010;7.
220. Rentzos M, Rombos A, Nikolaou C, Zoga M, Zouvelou V, Dimitrakopoulos A, et al. Interleukin-15 and Interleukin-12 are elevated in serum and cerebrospinal fluid of patients with amyotrophic lateral sclerosis. Eur Neurol. 2010;63(5).
221. Garbuzova-Davis S, Sanberg PR. Blood-CNS barrier impairment in ALS patients versus an animal model. Vol. 8, Frontiers in Cellular Neuroscience. 2014.
222. Winkler EA, Sengillo JD, Sullivan JS, Henkel JS, Appel SH, Zlokovic B v. Blood-spinal cord barrier breakdown and pericyte reductions in amyotrophic lateral sclerosis. Acta Neuropathol. 2013;125(1).
223. Nicaise C, Mitrecic D, Demetter P, de Decker R, Authelet M, Boom A, et al. Impaired blood-brain and blood-spinal cord barriers in mutant SOD1-linked ALS rat. Brain Res [Internet]. 2009;1301:152–62. Available from: http://dx.doi.org/10.1016/j.brainres.2009.09.018
224. Heikkilä HM, Lätti S, Leskinen MJ, Hakala JK, Kovanen PT, Lindstedt KA. Activated mast cells induce endothelial cell apoptosis by a combined action of chymase and tumor necrosis factor-α. Arterioscler Thromb Vasc Biol. 2008;28(2).
225. Compton SJ, Cairns JA, Holgate ST, Walls AF. Interaction of human mast cell tryptase with endothelial cells to stimulate inflammatory cell recruitment. In: International Archives of Allergy and Immunology. 1999.
226. Kunder CA, St John AL, Abraham SN. Mast cell modulation of the vascular and lymphatic endothelium. Vol. 118, Blood. 2011.
227. Barbierato M, Borri M, Facci L, Zusso M, Skaper SD, Giusti P. Expression and Differential Responsiveness of Central Nervous System Glial Cell Populations to the Acute Phase Protein Serum Amyloid A. Sci Rep. 2017;7(1).
228. Piette F, Belmin J, Vincent H, Schmidt N, Pariel S, Verny M, et al. Masitinib as an adjunct therapy for mild-to-moderate Alzheimer's disease: A randomised, placebo-controlled phase 2 trial. Alzheimers Res Ther. 2011;3(2).
229. Kempuraj D, Selvakumar GP, Zaheer S, Thangavel R, Ahmed ME, Raikwar S, et al. Cross-Talk between Glia, Neurons and Mast Cells in Neuroinflammation Associated with Parkinson's Disease. Journal of Neuroimmune Pharmacology. 2018;13(1).
230. Kempuraj D, Thangavel R, Fattal R, Pattani S, Yang E, Zaheer S, et al. Mast Cells Release Chemokine CCL2 in Response to Parkinsonian Toxin 1-Methyl-4-Phenyl-Pyridinium (MPP+). Neurochem Res. 2016;41(5).
231. Hong GU, Cho JW, Kim SY, Shin JH, Ro JY. Inflammatory mediators resulting from transglutaminase 2 expressed in mast cells contribute to the development of Parkinson's disease in a mouse model. Toxicol Appl Pharmacol. 2018;358.
232. Galli SJ, Tsai M, Wershil BK. The c-kit receptor, stem cell factor, and mast cells: What each is teaching us about the others. Vol. 142, American Journal of Pathology. 1993.
233. Iemura A, Tsai M, Ando A, Wershil BK, Galli SJ. The c-kit ligand, stem cell factor, promotes mast cell survival by suppressing apoptosis. American Journal of Pathology. 1994;144(2).
234. Zhang SC, Fedoroff S. Cellular localization of stem cell factor and c-kit receptor in the mouse nervous system. J Neurosci Res. 1997;47(1).
235. Erlandsson A, Larsson J, Forsberg-Nilsson K. Stem cell factor is a chemoattractant and a survival factor for CNS stem cells. Exp Cell Res. 2004;301(2).
236. Xu Q, Wang S, Jiang X, Zhao Y, Gao M, Zhang Y, et al. Hypoxia-induced astrocytes promote

the migration of neural progenitor cells via vascular endothelial factor, stem cell factor, stromal-derived factor-1α and monocyte chemoattractant protein-1 upregulation in vitro. Clin Exp Pharmacol Physiol. 2007;34(7).
237. Genis L, Dávila D, Fernandez S, Pozo-Rodrigálvarez A, Martínez-Murillo R, Torres-Aleman I. Astrocytes require insulin-like growth factor I to protect neurons against oxidative injury. F1000Res. 2014;3.
238. Reber L, da Silva CA, Frossard N. Stem cell factor and its receptor c-Kit as targets for inflammatory diseases. Vol. 533, European Journal of Pharmacology. 2006.
239. Gagalo I, Rusiecka I, Kocic I. Tyrosine Kinase Inhibitor as a new Therapy for Ischemic Stroke and other Neurologic Diseases: is there any Hope for a Better Outcome? Curr Neuropharmacol. 2015;13(6).
240. Ihle JN. Interleukin-3 and hematopoiesis. Vol. 51, Chemical Immunology. 1992.
241. Itakura A, Miura Y, Hikasa Y, Kiso Y, Matsuda H. Interleukin-3 and stem cell factor modulate cell cycle regulatory factors in mast cells: Negative regulation of p27Kip1 in proliferation of mast cells induced by interleukin-3 but not stem cell factor. In: Experimental Hematology. 2001.
242. Kritas SK, Saggini A, Cerulli G, Caraffa A, Antinolfi P, Pantalone A, et al. Interrelationship between IL-3 and mast cells. Vol. 28, Journal of biological regulators and homeostatic agents. 2014.
243. Weber GF, Chousterman BG, He S, Fenn AM, Nairz M, Anzai A, et al. Interleukin-3 amplifies acute inflammation and is a potential therapeutic target in sepsis. Science (1979). 2015;347(6227).
244. Chavany C, Vicario-Abejón C, Miller G, Jendoubi M. Transgenic mice for interleukin 3 develop motor neuron degeneration associated with autoimmune reaction against spinal cord motor neurons. Proc Natl Acad Sci U S A. 1998;95(19).
245. Gasque P, Singhrao SK, Neal JW, Götze O, Morgan BP. Expression of the receptor for complement C5a (CD88) is up-regulated on reactive astrocytes, microglia, and endothelial cells in the inflamed human central nervous system. American Journal of Pathology. 1997;150(1).
246. Griffin RS, Costigan M, Brenner GJ, Ma CHE, Scholz J, Moss A, et al. Complement induction in spinal cord microglia results in anaphylatoxin C5a-mediated pain hypersensitivity. Journal of Neuroscience. 2007;27(32).
247. Soruri A, Grigat J, Kiafard Z, Zwirner J. Mast cell activation is characterized by upregulation of a functional anaphylatoxin C5a receptor. BMC Immunol. 2008;9.
248. Yuan B, Fu F, Huang S, Lin C, Yang G, Ma K, et al. C5a/C5aR Pathway Plays a Vital Role in Brain Inflammatory Injury via Initiating Fgl-2 in Intracerebral Hemorrhage. Mol Neurobiol. 2017;54(8).
249. Lian H, Yang L, Cole A, Sun L, Chiang ACA, Fowler SW, et al. NFκB-Activated Astroglial Release of Complement C3 Compromises Neuronal Morphology and Function Associated with Alzheimer's Disease. Neuron. 2015;85(1).
250. Lian H, Litvinchuk A, Chiang ACA, Aithmitti N, Jankowsky JL, Zheng H. Astrocyte-microglia cross talk through complement activation modulates amyloid pathology in mouse models of alzheimer's disease. Journal of Neuroscience. 2016;36(2).
251. Burnstock G. Purinergic mechanisms and pain - An update. Vol. 716, European Journal of

Pharmacology. 2013.
252. Osipchuk Y, Cahalan M. Cell-to-cell spread of calcium signals mediated by ATP receptors in mast cells. Nature. 1992;359(6392).
253. Zhang H, Yang H, He S. TNF increases expression of IL-4 and PARs in mast cells. Cellular Physiology and Biochemistry. 2010;26(3).
254. Yuan H, Zhu X, Zhou S, Chen Q, Zhu X, Xue M, et al. Role of mast cell activation in inducing microglial cells to release neurotrophin. J Neurosci Res. 2010;88(6).
255. Knerlich-Lukoschus F, von der Ropp-Brenner B, Lucius R, Mehdorn HM, Held-Feindt J. Spatiotemporal CCR1, CCL3(MIP-1α), CXCR4, CXCL12(SDF-1α) expression patterns in a rat spinal cord injury model of posttraumatic neuropathic pain: Laboratory investigation. J Neurosurg Spine. 2011;14(5).
256. Juremalm M, Hjertson M, Olsson N, Harvima I, Nilsson K, Nilsson G. The chemokine receptor CXCR4 is expressed within the mast cell lineage and its ligand stromal cell-derived factor-1α acts as a mast cell chemotaxin. Eur J Immunol. 2000;30(12).
257. Yan Y, Su J, Zhang Z. The CXCL12/CXCR4/ACKR3 Response Axis in Chronic Neurodegenerative Disorders of the Central Nervous System: Therapeutic Target and Biomarker. Vol. 42, Cellular and Molecular Neurobiology. 2022.
258. Kim DY, Hong GU, Ro JY. Signal pathways in astrocytes activated by cross-talk between of astrocytes and mast cells through CD40-CD40L. J Neuroinflammation. 2011;8.
259. Komiya H, Takeuchi H, Ogawa Y, Hatooka Y, Takahashi K, Katsumoto A, et al. CCR2 is localized in microglia and neurons, as well as infiltrating monocytes, in the lumbar spinal cord of ALS mice. Mol Brain. 2020;13(1).
260. Collington SJ, Hallgren J, Pease JE, Jones TG, Rollins BJ, Westwick J, et al. The Role of the CCL2/CCR2 Axis in Mouse Mast Cell Migration In Vitro and In Vivo. The Journal of Immunology. 2010;184(11).
261. Chen J, Liu X, Zhong Y. Interleukin-17A: The Key Cytokine in Neurodegenerative Diseases. Vol. 12, Frontiers in Aging Neuroscience. 2020.
262. Kolbinger F, Huppertz C, Mir A, Padova F. IL-17A and Multiple Sclerosis: Signaling Pathways, Producing Cells and Target Cells in the Central Nervous System. Curr Drug Targets. 2016;17(16).
263. Rentzos M, Rombos A. The role of IL-15 in central nervous system disorders. Vol. 125, Acta Neurologica Scandinavica. 2012.
264. Jackson NE, Wang HW, Tedla N, McNeil HP, Geczy CL, Collins A, et al. IL-15 induces mast cell migration via a pertussis toxin-sensitive receptor. Eur J Immunol. 2005;35(8).
265. Pan W, Wu X, He Y, Hsuchou H, Huang EYK, Mishra PK, et al. Brain interleukin-15 in neuroinflammation and behavior. Vol. 37, Neuroscience and Biobehavioral Reviews. 2013.
266. Pachter JS, de Vries HE, Fabry Z. The blood-brain barrier and its role in immune privilege in the central nervous system. Vol. 62, Journal of Neuropathology and Experimental Neurology. 2003.
267. Winkler EA, Sengillo JD, Sagare AP, Zhao Z, Ma Q, Zuniga E, et al. Blood-spinal cord barrier disruption contributes to early motor-neuron degeneration in ALS-model mice. Proc Natl Acad Sci U S A. 2014;111(11).
268. Garbuzova-Davis S, Hernandez-Ontiveros DG, Rodrigues MCO, Haller E, Frisina-Deyo A, Mirtyl S, et al. Impaired blood-brain/spinal cord barrier in ALS patients. Brain Res.

2012;1469.
269. Nelissen S, Lemmens E, Geurts N, Kramer P, Maurer M, Hendriks J, et al. The role of mast cells in neuroinflammation. Vol. 125, Acta Neuropathologica. 2013.
270. Lindsberg PJ, Strbian D, Karjalainen-Lindsberg ML. Mast cells as early responders in the regulation of acute blood-brain barrier changes after cerebral ischemia and hemorrhage. Vol. 30, Journal of Cerebral Blood Flow and Metabolism. 2010.
271. Yang Y, Estrada EY, Thompson JF, Liu W, Rosenberg GA. Matrix metalloproteinase-mediated disruption of tight junction proteins in cerebral vessels is reversed by synthetic matrix metalloproteinase inhibitor in focal ischemia in rat. Journal of Cerebral Blood Flow and Metabolism. 2007;27(4).
272. Zhao BQ, Tejima E, Lo EH. Neurovascular proteases in brain injury, hemorrhage and remodeling after stroke. In: Stroke. 2007.
273. Kim YS, Joh TH. Matrix metalloproteinases, new insights into the understanding of neurodegenerative disorders. Biomol Ther (Seoul). 2012;20(2).
274. Mattila OS, Strbian D, Saksi J, Pikkarainen TO, Rantanen V, Tatlisumak T, et al. Cerebral mast cells mediate blood-brain barrier disruption in acute experimental ischemic stroke through perivascular gelatinase activation. Stroke. 2011;42(12).
275. Goldschmidt RC, Hough LB, Glick SD. Rat Brain Mast Cells: Contribution to Brain Histamine Levels. J Neurochem. 1985;44(6).
276. Ito T, Smrž D, Jung MY, Bandara G, Desai A, Smržová Š, et al. Stem Cell Factor Programs the Mast Cell Activation Phenotype. The Journal of Immunology. 2012;188(11).
277. Dubreuil P, Letard S, Ciufolini M, Gros L, Humbert M, Castéran N, et al. Masitinib (AB1010), a potent and selective tyrosine kinase inhibitor targeting KIT. PLoS One. 2009;4(9).
278. Lortholary O, Chandesris MO, Livideanu CB, Paul C, Guillet G, Jassem E, et al. Masitinib for treatment of severely symptomatic indolent systemic mastocytosis: a randomised, placebo-controlled, phase 3 study. The Lancet. 2017;389(10069).
279. Georgin-Lavialle S, Lhermitte L, Suarez F, Yang Y, Letard S, Hanssens K, et al. Mast cell leukemia: Identification of a new c-Kit mutation, dup(501-502), and response to masitinib, a c-Kit tyrosine kinase inhibitor. Eur J Haematol. 2012;89(1).
280. Eisen A. The dying forward hypothesis of als: Tracing its history. Vol. 11, Brain Sciences. 2021.
281. Fischer LR, Culver DG, Tennant P, Davis AA, Wang M, Castellano-Sanchez A, et al. Amyotrophic lateral sclerosis is a distal axonopathy: Evidence in mice and man. Exp Neurol. 2004;185(2).
282. Moloney EB, de Winter F, Verhaagen J. ALS as a distal axonopathy: Molecular mechanisms affecting neuromuscular junction stability in the presymptomatic stages of the disease. Front Neurosci. 2014;(8 JUL).
283. Cashman CR, Höke A. Mechanisms of distal axonal degeneration in peripheral neuropathies. Vol. 596, Neuroscience Letters. 2015.
284. Kennel PF, Finiels F, Revah F, Mallet J. Neuromuscular functicon impairment is not caused by motor neurone loss in FALS mice: An electromyographic study. Neuroreport. 1996;7(8).
285. Gould TW, Buss RR, Vinsant S, Prevette D, Sun W, Knudson CM, et al. Complete dissociation of motor neuron death from motor dysfunction by Bax deletion in a mouse model of ALS. Journal of Neuroscience. 2006;26(34).

286. Hegedus J, Putman CT, Gordon T. Time course of preferential motor unit loss in the SOD1G93A mouse model of amyotrophic lateral sclerosis. Neurobiol Dis. 2007;28(2).
287. Suzuki M, McHugh J, Tork C, Shelley B, Klein SM, Aebischer P, et al. GDNF secreting human neural progenitor cells protect dying motor neurons, but not their projection muscule, in a rat model of familial ALS. PLoS One. 2007;2(8).
288. Rouaux C, Panteleeva I, René F, de Aguilar JLG, Echaniz-Laguna A, Dupuis L, et al. Sodium valproate exerts neuroprotective effects in vivo through CREB-binding protein-dependent mechanisms but does not improve survival in an amyotrophic lateral sclerosis mouse model. Journal of Neuroscience. 2007;27(21).
289. Bilsland LG, Sahai E, Kelly G, Golding M, Greensmith L, Schiavo G. Deficits in axonal transport precede ALS symptoms in vivo. Proc Natl Acad Sci U S A. 2010;107(47).
290. Williamson TL, Cleveland DW. Slowing of axonal transport is a very early event in the toxicity of ALS-linked SOD1 mutants to motor neurons. Nat Neurosci. 1999;2(1).
291. de Vos KJ, Hafezparast M. Neurobiology of axonal transport defects in motor neuron diseases: Opportunities for translational research? Vol. 105, Neurobiology of Disease. 2017.
292. Magrané J, Cortez C, Gan WB, Manfredi G. Abnormal mitochondrial transport and morphology are common pathological denominators in SOD1 and TDP43 ALS mouse models. Hum Mol Genet. 2014;23(6).
293. Salvadores N, Sanhueza M, Manque P, Court FA. Axonal degeneration during aging and its functional role in neurodegenerative disorders. Vol. 11, Frontiers in Neuroscience. 2017.
294. Keller AF, Gravel M, Kriz J. Live imaging of amyotrophic lateral sclerosis pathogenesis: Disease onset is characterized by marked induction of GFAP in schwann cells. Glia. 2009;57(10).
295. Verheijen MHG, Peviani M, Hendricusdottir R, Bell EM, Lammens M, Smit AB, et al. Increased axonal ribosome numbers is an early event in the pathogenesis of amyotrophic lateral sclerosis. PLoS One. 2014;9(1).
296. Wang L, Pytel P, Feltri ML, Wrabetz L, Roos RP. Selective knockdown of mutant SOD1 in Schwann cells ameliorates disease in G85R mutant SOD1 transgenic mice. Neurobiol Dis. 2012;48(1).
297. Kano O, Beers DR, Henkel JS, Appel SH. Peripheral nerve inflammation in als mice: Cause or consequence. Neurology. 2012;78(11).
298. van Dyke JM, Smit-Oistad IM, Macrander C, Krakora D, Meyer MG, Suzuki M. Macrophage-mediated inflammation and glial response in the skeletal muscle of a rat model of familial amyotrophic lateral sclerosis (ALS). Exp Neurol. 2016;277.
299. Devigili G, Üçeyler N, Beck M, Reiners K, Stoll G, Toyka K v., et al. Vasculitis-like neuropathy in amyotrophic lateral sclerosis unresponsive to treatment. Acta Neuropathol. 2011;122(3).
300. Nardo G, Trolese MC, de Vito G, Cecchi R, Riva N, Dina G, et al. Immune response in peripheral axons delays disease progression in SOD1G93A mice. J Neuroinflammation. 2016;13(1).
301. Nardo G, Trolese MC, Verderio M, Mariani A, de Paola M, Riva N, et al. Counteracting roles of MHCI and CD8+ T cells in the peripheral and central nervous system of ALS SOD1G93A mice. Mol Neurodegener. 2018;13(1).

302. Suzuki H, Miura S, Liu YY, Tsuchiya M, Ishii H. Substance P induces degranulation of mast cells and leukocyte adhesion to venular endothelium. Peptides (NY). 1995;16(8).
303. Purcell WM, Atterwill CK. Mast cells in neuroimmune function: Neurotoxicological and neuropharmacological perspectives. Vol. 20, Neurochemical Research. 1995.
304. van der Kleij HP, Bienenstock J. Significance of Conversation between Mast Cells and Nerves. Allergy, Asthma & Clinical Immunology. 2005;1(2).
305. Parada CA, Tambeli CH, Cunha FQ, Ferreira SH. The major role of peripheral release of histamine and 5-hydroxytryptamine in formalin-induced nociception. Neuroscience. 2001;102(4).
306. Zuo Y, Perkins NM, Tracey DJ, Geczy CL. Inflammation and hyperalgesia induced by nerve injury in the rat: A key role of mast cells. Pain. 2003;105(3).
307. Oliveira SM, Drewes CC, Silva CR, Trevisan G, Boschen SL, Moreira CG, et al. Involvement of mast cells in a mouse model of postoperative pain. Eur J Pharmacol. 2011;672(1–3).
308. Cuadros MA, Sepulveda MR, Martin-Oliva D, Marín-Teva JL, Neubrand VE. Microglia and Microglia-Like Cells: Similar but Different. Vol. 16, Frontiers in Cellular Neuroscience. 2022.
309. Cuní-López C, Stewart R, Quek H, White AR. Recent Advances in Microglia Modelling to Address Translational Outcomes in Neurodegenerative Diseases. Cells. 2022 May 17;11(10):1662.
310. Witcher KG, Eiferman DS, Godbout JP. Priming the Inflammatory Pump of the CNS after Traumatic Brain Injury. Vol. 38, Trends in Neurosciences. 2015.
311. Bennett ML, Bennett FC. The influence of environment and origin on brain resident macrophages and implications for therapy. Vol. 23, Nature Neuroscience. 2020.
312. Priller J, Flügel A, Wehner T, Boentert M, Haas CA, Prinz M, et al. Targeting gene-modified hematopoietic cells to the central nervous system: Use of green fluorescent protein uncovers microglial engraftment. Nat Med. 2001;7(12).
313. Ajami B, Bennett JL, Krieger C, McNagny KM, Rossi FMV. Infiltrating monocytes trigger EAE progression, but do not contribute to the resident microglia pool. Nat Neurosci. 2011;14(9).
314. Prinz M, Erny D, Hagemeyer N. Ontogeny and homeostasis of CNS myeloid cells. Vol. 18, Nature Immunology. 2017.
315. Mildner A, Schmidt H, Nitsche M, Merkler D, Hanisch UK, Mack M, et al. Microglia in the adult brain arise from Ly-6ChiCCR2+ monocytes only under defined host conditions. Nat Neurosci. 2007;10(12).
316. Ratajczak MZ, Adamiak M, Plonka M, Abdel-Latif A, Ratajczak J. Mobilization of hematopoietic stem cells as a result of innate immunity-mediated sterile inflammation in the bone marrow microenvironment - The involvement of extracellular nucleotides and purinergic signaling. Vol. 32, Leukemia. 2018.
317. Zlokovic B v. The Blood-Brain Barrier in Health and Chronic Neurodegenerative Disorders. Neuron. 2008;57(2):178–201.
318. Engelhardt B, Ransohoff RM. Capture, crawl, cross: The T cell code to breach the blood-brain barriers. Vol. 33, Trends in Immunology. 2012.
319. Kierdorf K, Katzmarski N, Haas CA, Prinz M. Bone Marrow Cell Recruitment to the Brain in the Absence of Irradiation or Parabiosis Bias. PLoS One. 2013;8(3).
320. Banisadr G, Gosselin RD, Mechighel P, Kitabgi P, Rostène W, Parsadaniantz SM. Highly

regionalized neuronal expression of monocyte chemoattractant protein-1 (MCP-1/CCL2) in rat brain: Evidence for its colocalization with neurotransmitters and neuropeptides. Journal of Comparative Neurology. 2005;489(3).
321. Gómez-Nicola D, Fransen NL, Suzzi S, Hugh Perry V. Regulation of microglial proliferation during chronic neurodegeneration. Journal of Neuroscience. 2013;33(6).
322. Burnstock G. Purine and purinergic receptors. Brain Neurosci Adv. 2018;2.
323. Moll NM, Ransohoff RM. CXCL12 and CXCR4 in bone marrow physiology. Vol. 3, Expert Review of Hematology. 2010.
324. Jobe O, Kim J, Tycksen E, Onkar S, Michael NL, Alving CR, et al. Human primary macrophages derived in vitro from circulating monocytes comprise adherent and non-adherent subsets with differential expression of siglec-1 and CD4 and permissiveness to HIV-1 infection. Front Immunol. 2017;8(OCT).
325. Klinder A, Markhoff J, Jonitz-Heincke A, Sterna P, Salamon A, Bader R. Comparison of different cell culture plates for the enrichment of non-adherent human mononuclear cells. Exp Ther Med. 2019;
326. Hinze A, Stolzing A. Microglia differentiation using a culture system for the expansion of mice non-adherent bone marrow stem cells. Journal of Inflammation (United Kingdom). 2012;9.
327. Jiang Y, Jahagirdar BN, Reinhardt RL, Schwartz RE, Keene CD, Ortiz-Gonzalez XR, et al. Pluripotency of mesenchymal stem cells derived from adult marrow. Nature. 2002;418(6893).
328. Catlett JP, Leftwich JA, Westin EH, Grant S, Huff TF. C-kit expression by CD34+ bone marrow progenitors and inhibition of response to recombinant human interleukin-3 following exposure to c-kit antisense oligonucleotides. Blood. 1991;78(12).
329. Chabot B, Stephenson DA, Chapman VM, Besmer P, Bernstein A. The proto-oncogene c-kit encoding a transmembrane tyrosine kinase receptor maps to the mouse W locus. Nature. 1988;335(6185).
330. Olender L, Thapa R, Gazit R. Isolation of Murine Myeloid Progenitor Populations by CD34/CD150 Surface Markers. Cells. 2022;11(3).
331. Ogawa M, Matsuzaki Y, Nishikawa S, Hayashi SI, Kunisada T, Sudo T, et al. Expression and function of c-kit in hemopoietic progenitor cells. Journal of Experimental Medicine. 1991;174(1).
332. Dahlin JS, Ding Z, Hallgren J. Distinguishing Mast Cell Progenitors from Mature Mast Cells in Mice. Stem Cells Dev. 2015;24(14).
333. Pittoni P, Piconese S, Tripodo C, Colombo MP. Tumor-intrinsic and -extrinsic roles of c-Kit: Mast cells as the primary off-target of tyrosine kinase inhibitors. Vol. 30, Oncogene. 2011.
334. Grimbaldeston MA, Chen CC, Piliponsky AM, Tsai M, Tam SY, Galli SJ. Mast cell-deficient W-sash c-kit mutant kitW-sh/W-sh mice as a model for investigating mast cell biology in vivo. American Journal of Pathology. 2005;167(3).
335. Bauer O, Razin E. Mast cell-nerve interactions. Vol. 15, News in Physiological Sciences. 2000.
336. Kalichman MW, Powell HC, Calcutt NA, Mizisin AP. Mast cell degranulation and blood-nerve barrier permeability in rat sciatic nerve after 7 days of hyperglycemia. Am J Physiol Heart Circ Physiol. 1995;268(2 37-2).

337. Caughey GH. Mast cell proteases as protective and inflammatory mediators. Adv Exp Med Biol. 2011;716.
338. Hiromatsu Y, Toda S. Mast cells and angiogenesis. Vol. 60, Microscopy Research and Technique. 2003.
339. Leon A, Buriani A, Dal Toso R, Fabris M, Romanello S, Aloe L, et al. Mast cells synthesize, store, and release nerve growth factor. Proc Natl Acad Sci U S A. 1994;91(9).
340. Mizisin AP, Weerasuriya A. Homeostatic regulation of the endoneurial microenvironment during development, aging and in response to trauma, disease and toxic insult. Vol. 121, Acta Neuropathologica. 2011.
341. Staser K, Yang FC, Clapp DW. Mast cells and the neurofibroma microenvironment. Vol. 116, Blood. 2010.
342. Lowry KS, Murray SS, McLean CA, Talman P, Mathers S, Lopes EC, et al. A potential role for the p75 low-affinity neurotrophin receptor in spinal motor neuron degeneration in murine and human amyotrophic lateral sclerosis. Amyotrophic Lateral Sclerosis and Other Motor Neuron Disorders. 2001;2(3).
343. Levi-Montalcini R, Skaper SD, Dal Toso R, Petrelli L, Leon A. Nerve growth factor: From neurotrophin to neurokine. Vol. 19, Trends in Neurosciences. 1996.
344. Rodewald HR, Dessing M, Dvorak AM, Galli SJ. Identification of a committed precursor for the mast cell lineage. Science (1979). 1996;271(5250).
345. Zhang S, Zeng X, Yang H, Hu G, He S. Mast cell tryptase induces microglia activation via protease-activated receptor 2 signaling. Cellular Physiology and Biochemistry. 2012;29(5–6).
346. Yamadera M, Fujimura H, Inoue K, Toyooka K, Mori C, Hirano H, et al. Microvascular disturbance with decreased pericyte coverage is prominent in the ventral horn of patients with amyotrophic lateral sclerosis. Amyotroph Lateral Scler Frontotemporal Degener. 2015;16(5–6).
347. Gama Sosa MA, de Gasperi R, Rocher AB, Wang ACJ, Janssen WGM, Flores T, et al. Age-related vascular pathology in transgenic mice expressing presenilin 1-associated familial Alzheimer's disease mutations. American Journal of Pathology. 2010;176(1).
348. Dai H, Korthuis RJ. Mast cell proteases and inflammation. Vol. 8, Drug Discovery Today: Disease Models. 2011.
349. Dell'italia LJ, Collawn JF, Ferrario CM. Multifunctional role of chymase in acute and chronic tissue injury and remodeling. Vol. 122, Circulation Research. 2018.
350. Ashina K, Tsubosaka Y, Nakamura T, Omori K, Kobayashi K, Hori M, et al. Histamine induces vascular hyperpermeability by increasing blood flow and endothelial barrier disruption in vivo. PLoS One. 2015;10(7).
351. Haig DM, Huntley JF, MacKellar A, Newlands GFJ, Inglis L, Sangha R, et al. Effects of stem cell factor (kit-ligand) and interleukin-3 on the growth and serine proteinase expression of rat bone-marrow-derived or serosal mast cells. Blood. 1994 Jan 1;83(1):72–83.
352. Olmos-Alonso A, Schetters STT, Sri S, Askew K, Mancuso R, Vargas-Caballero M, et al. Pharmacological targeting of CSF1R inhibits microglial proliferation and prevents the progression of Alzheimer's-like pathology. Brain. 2016;139(3).
353. Klein D, Patzkó Á, Schreiber D, van Hauwermeiren A, Baier M, Groh J, et al. Targeting the colony stimulating factor 1 receptor alleviates two forms of Charcot-Marie-Tooth disease

in mice. Brain. 2015;138(11).
354. Mora JS, Genge A, Chio A, Estol CJ, Chaverri D, Hernández M, et al. Masitinib as an add-on therapy to riluzole in patients with amyotrophic lateral sclerosis: a randomized clinical trial. Amyotroph Lateral Scler Frontotemporal Degener. 2020;
355. Mora JS, Bradley WG, Chaverri D, Hernández-Barral M, Mascias J, Gamez J, et al. Long-term survival analysis of masitinib in amyotrophic lateral sclerosis. Ther Adv Neurol Disord. 2021;14.
356. Faraco G, Park L, Anrather J, Iadecola C. Brain perivascular macrophages: characterization and functional roles in health and disease. Vol. 95, Journal of Molecular Medicine. 2017.
357. Rossi L, Challen GA, Sirin O, Lin KKY, Goodell MA. Hematopoietic Stem Cell Characterization and Isolation. In: Methods in Molecular Biology. 2011.
358. Berardi AC, Wang A, Levine JD, Lopez P, Scadden DT. Functional isolation and characterization of human hematopoietic stem cells. Science (1979). 1995;267(5194).
359. Weissman IL, Shizuru JA. The origins of the identification and isolation of hematopoietic stem cells, and their capability to induce donor-specific transplantation tolerance and treat autoimmune diseases. Blood. 2008;112(9).
360. Kim E, Hurtz C, Koehrer S, Wang Z, Balasubramanian S, Chang BY, et al. Ibrutinib inhibits pre-BCR+ B-cell acute lymphoblastic leukemia progression by targeting BTK and BLK. Blood. 2017;129(9):1155–65.
361. Rabinovich-Nikitin I, Ezra A, Barbiro B, Rabinovich-Toidman P, Solomon B. Chronic administration of AMD3100 increases survival and alleviates pathology in SOD1G93A mice model of ALS. J Neuroinflammation [Internet]. 2016;13(1):1–11. Available from: http://dx.doi.org/10.1186/s12974-016-0587-6